TECHNISCHE UNIVERSITÄT MÜNCHEN
Department für Chemie
Lehrstuhl für Biotechnologie

Influence of the Hsp90 co-chaperones on client protein activation

Priyanka Sahasrabudhe

Vollständiger Abdruck der von der Fakultät für Chemie der Technischen Universität München zur Erlangung des akademischen Grades eines

Doktors der Naturwissenschaften (Dr. rer. nat.)

genehmigten Dissertation.

Vorsitzende:		Prof. Dr. K. Lang
Prüfer der Dissertation:	1.	Prof. Dr. J. Buchner
	2.	Prof. Dr. M. Sattler
	3.	Prof. Dr. St. Jentsch
		Ludwig-Maximilians-Universität München

Die Dissertation wurde am 21.12.2015 bei der Technischen Universität München eingereicht und durch die Fakultät für Chemie am 04.04.2016 angenommen.

Abstract

In the crowded cellular milieu, molecular chaperones orchestrate the proper folding of proteins and maintain proteostasis. One of the most important and complex chaperone networks in the cell is that of the heat shock protein 90 (Hsp90). Hsp90, initially identified in response to heat stress, is evolutionarily conserved and abundant in the cell. Unlike other chaperones, Hsp90 binds proteins which are in a near-native state and assists in the maturation and activation of specific client proteins. More than 300 Hsp90 client proteins have been identified which belong to various functional classes including nuclear receptors, kinases and transcription factors. The diversity of the client proteins and their roles as key effector proteins, has made Hsp90 a potential target for therapeutic strategies, especially against cancer. For its chaperoning activity, Hsp90 undergoes drastic ATP-dependent cyclic conformational changes. While progressing through the ATPase cycle, Hsp90 associates with a cohort of co-chaperones which are thought to regulate the kinetics of the ATPase activity. Moreover, the Hsp90 machinery works in close collaboration with Hsp70 machinery.

During the last decades, several studies have elucidated the structure and conformational dynamics of Hsp90. Most Hsp90 co-chaperones have been characterized with respect to their domain architecture, their interaction with certain conformations of Hsp90 and their influence on the Hsp90 ATPase activity. Despite this extensive knowledge, the basic mechanism of how Hsp90 can chaperone functionally and structurally distinct client proteins, remains elusive. No specific recognition sequence or motif common to all client proteins has been identified for interaction with Hsp90. The intriguing question, how the large cohort of co-chaperones influence the maturation and activation of client proteins still remains unanswered.

In this work, the effect of Hsp90 co-chaperones on client proteins was systematically analysed using the co-chaperone deletion strains of *S.cerevisiae* (Baker's yeast). The effect of deleting or lowering expression of an essential co-chaperone on client activity, compared to the wild type strain was monitored. The client proteins chosen for the study include steroid hormone receptors (SHRs) and the viral Src kinase. Studying functionally and structurally unrelated client proteins, offered an insight

into which co-chaperones are specific for a protein family. Additionally, studying five different SHRs, provided a comparison of the co-chaperone dependency within one protein family.

The in-depth characterization of the Hsp90 co-chaperone deletion/knock-down strains confirmed that modulating the levels of co-chaperones did not adversely affect the basic cellular processes. Despite a strong homology among some co-chaperones, changes in the expression of one did not lead to compensatory changes in the others. The systematic analysis of Hsp90 client proteins showed that the influence of co-chaperones was post-translational. In spite of being bona fide Hsp90 client proteins, the extent to which they depended on Hsp90 was variable. The client proteins also showed specific co-chaperones requirements for their activation. While Cpr6 and Sba1 were essential for all the SHRs, Sti1 and Cdc37 played a prominent role in v-Src maturation. Most other co-chaperones showed client-specific effects. Surprisingly, deletion of certain co-chaperones also led to the increase in activity of client proteins, suggesting a negative regulatory role. Further characterization of the glucocorticoid receptor (GR) showed that Sti1 deletion affected its conformation and led to a decrease in activity. Intriguingly however, Sti1, which was essential for GR as well as v-Src activation, was dispensable for their stabilized mutants.

Taken together, this work conclusively shows that clients depend on specific co-chaperones for their activation and differences exist even within a closely-related protein family. The co-chaperones, thus act as modulators to adapt the Hsp90 cycle to the requirements of a specific client protein. Taking into account the central importance of Hsp90 in numerous cellular pathways, the specific client-co-chaperone relationships can be viewed as a vital regulatory hub to ensure optimal client activation.

Acknowledgements

Carrying out a research project is never possible by a single person alone. A lot of people have, in some way, contributed and I would like to express my gratitude towards all of them. First and foremost, I would like to thank Prof. Dr. Johannes Buchner for giving me an opportunity to work on an extremely interesting project. All the ups and downs during this four-year journey have taught me a lot at every step. I would like to acknowledge his constant support and encouragement during this time. It helped immensely to keep up my motivation and perseverance, even through the toughest times. I also am obliged to my TAC members, Prof. Dr. Jentsch and Prof. Dr. Itzen for their valuable guidance during this project.

I feel extremely fortunate that at the beginning of my PhD project, Julia Rohrberg introduced me to this topic. Under her friendly guidance, I learnt a lot and her support has truly been instrumental in all this work. I would also like to specially thank Natalia, Alex, Vroni, Hannah and Christoph who were always happy to help and had great advice of offer. Thanks also to the IMPRS graduate program, and everyone in the IMPRS office for all the help for setting up in Munich. Knowing a whole class of graduate students in my year, made me feel at home in Munich immediately.

The Buchner lab has been a fun place to work, thanks to all my lab mates. I would specially like to thank my office mates Frank and Sandrine for the all the fruitful scientific discussions and equally for the countless random conversations which made sharing the office space with them so much fun! On this note, I would also like to thank Patzi, Katrin, Marina, Christine, Sabine, Gordi, Bene and Chrissy for always keeping the mood bright. Thanks to them I enjoyed, and at times, even looked forward to the Mensa break (thankfully the food did not dictate the mood!). A big lab like ours, doesn't run itself. For all the technical help in the lab, I would like to express my gratitude to Martin Haslbeck (Hasi). I would also like to thank Bettina for always being extremely prompt with all the ordering and for EM imaging of the yeast strains. I think I also owe her one for improving my German! I want to thank Chris, Klaus and Katha for their help in analysing the gene-chip data. How can I forget to

thank the BIF people! In addition to their solid economic support and travel grants, I found a great network of friends among the BIF fellows!

The time I did not spend in the lab, was mostly spent in the wonderful company of some amazing people I met in Munich. I would like to thank Nena, my guitar-lesson partner, who has been around all these four years, be it going to IMPRS lectures, or travelling to India! I also want to thank Jaydeep, Aarathi, Prajakta and Urjita for keeping me from ever feeling home-sick. They have been my extended family in Munich. I take this opportunity to specially thank Jaydeep, for being there always! Right from the silliest moments, to even writing this thesis, his constant support and company have made these four years, the best ever.

Last but not the least, a BIG thank you to my parents, who regardless of the distance that separates us, have always been with me and believed in me through all my endeavours.

Contents

1 Introduction

The name ‘protein’ is derived from the Greek word ‘protos’, meaning primary or first rank of importance. Proteins are the most abundant component within a cell and constitute more than half the dry weight of a cell. They have a range of indispensable roles in every cells ranging from catalysing slow reactions in the form of enzymes to forming the structural framework of the cell. For a protein to be active and functional, it is of utmost importance that it is folded correctly into its three-dimensional native structure. Protein folding is thus, one of the most fundamental processes in all living cells and protein misfolding can have adverse effects on physiological processes.

1.1 Protein folding *in vivo*

According to Anfinsen’s principle, the entire information required for folding a protein is contained in its amino acid sequence and folding is therefore a spontaneous process [Anfinsen, 1973]. However, in the crowded environment of the cell, with total cytosolic protein reaching concentrations of 300-400 g/l and up to a volume of 40% occupied by macromolecules, the dynamics of protein folding is largely altered [Ellis & Minton, 2003; Zimmerman & Trach, 1991]. The resultant excluded

volume effect, which on one hand is essential for enhancing the functional interactions between macromolecules, in turn strongly increases the tendency of non-native and structurally flexible proteins to aggregate [Zimmerman & Minton, 1993; Ellis & Minton, 2006]. This phenomenon of 'macromolecular crowding' thus makes protein folding challenging *in vivo*.

During translation the N-terminal end of the polypeptide chain emerges out of the ribosome, while the C-terminal end is yet to be synthesized [Frydman & Hartl, 1996]. Translation itself is a relatively slow process with the rate of about 4-20 amino acids per second. This means that the nascent polypeptide chain emerges slowly from the ribosome tunnel. As against this, the rate at which a protein can fold is much faster ($<$1 sec) [Agashe & Hartl, 2000]. Due to this discrepancy in the translational and folding rates, the newly emerging polypeptide chain can be exposed in a partially folded, aggregation-sensitive state for prolonged periods of time. Since the complete polypeptide chain has not been synthesized, the entire information required for its folding is not available at this stage. Moreover, non-native intra-chain contacts formed during translation could block folding upon completion of synthesis. As a result, nascent polypeptides often require folding assistance before they can reach their native structure. Protein folding involves very small overall changes in energy, typically ranging from 1 to 15 kcal/mol, as a protein progresses from its unfolded state to its native structure [Fersht & Daggett, 2002]. This is the basis of the intrinsic instability of many proteins. It is also due to this small energy difference, that most proteins can undergo drastic conformational changes while carrying out their cellular functions. About 30% of all eukaryotic proteins have large intrinsically disordered regions [Liu *et al.*, 2009]. Due to their inherent flexibility, different disordered regions can bind to a common binding site on an interaction partner. Such capacity for binding diversity plays important roles in both protein-protein interaction networks and gene regulation networks [Dunker *et al.*, 2008]. However, the intrinsic instability or disorder of these proteins can also lead them to unfold and aggregate when exposed to stress. The cell and its crowded milieu are constantly subjected to various types of stresses like heat stress, oxidative stress, viral infection, cytokines, glucose deprivation, or exposure to toxins and certain metals. These 'proteotoxic' stresses can cause proteins to misfold and aggregate as partially folded proteins have a much greater tendency to aggregate in the crowded cellular environment than in isolated dilute solutions *in vitro* [White *et al.*, 2010; Ellis & Minton, 2006]. In addition to stress, the occurrence of random mutations can disrupt the ability of a protein to adopt a

stable fold, leading to serious consequences on the general physiology of the cell and in effect on human health. Many neurodegenerative diseases like Alzheimer's disease, Parkinson's disease and Huntington's disease as well as several metabolic diseases like Diabetes mellitus Type 2, artherosclerosis and even cancer have protein folding defects and aggregation as their underlying cause [Balch *et al.*, 2008; Huang & Stultz, 2009; Díaz-Villanueva *et al.*, 2015].

In order to rescue the cell from deleterious *de novo* folding defects or those induced by stress, every cell has an array of helper proteins called molecular chaperones which are involved in the quality control of proteins in the cells and help to maintain 'proteostasis' [Brandvold & Morimoto, 2015].

1.2 Assisted proteostasis *in vivo*

Molecular chaperones were first discovered as proteins which were synthesized upon heat stress in *Drosophila* larvae, hence they were first termed heat shock proteins (Hsps) [Tissiéres *et al.*, 1974; Ashburner & Bonner, 1979]. Subsequently, it was shown that these proteins are not specifically upregulated only upon elevated temperatures, but also by other stresses like oxidative phosphorylation, inhibiting electron transport and also in response to various amino acid analogues and antibiotics. This led to the finding that these so-called heat shock proteins actually act as molecular chaperones which help the cell deal with its increased burden of abnormally folded proteins [Georgopoulos & Welch, 1993; Richter *et al.*, 2010]. Also, despite being called Hsps, most of the chaperones are constitutively expressed in all cell types, and only upregulated upon stress.

The molecular chaperones are allosteric machines that do not have a single well-defined substrate. Instead, they have a unique feature, which is their ability to promiscuously interact with a wide range of unfolded proteins. [Bukau *et al.*, 1996; Walter & Buchner, 2002]. They maintain proteostasis by chaperoning almost all stages in the life of a protein, right from assisting *de novo* folding, preventing protein aggregation, refolding the misfolded proteins, disaggregating and refolding aggregated proteins or finally by degrading the misfolded proteins which are beyond rescue [Kim *et al.*, 2013; Hartl *et al.*, 2011] (Figure 1.1). In addition to molecular chaperones other protein folding catalysts include enzymes like protein disulfide isomerase (PDI) and other members of the thioredoxin family and peptide-

prolylisomerases (PPIases). PDI catalyses both formation as well as the reduction of disulphide bonds in substrates [Wang & Tsou, 1993; Wang *et al.*, 2015]. PPIases on the other hand, assist in restructuring the client proteins by catalysing the slow rotational motion of peptide bonds preceding a proline residue [Fanghänel & Fischer, 2004; Schiene-Fischer, 2014; Schmidpeter & Schmid, 2015]. Together these chaperones and folding catalysts work in concert with their respective regulator proteins to ensure proper protein folding and maintenance of the proteins in their native functional three-dimensional conformation.

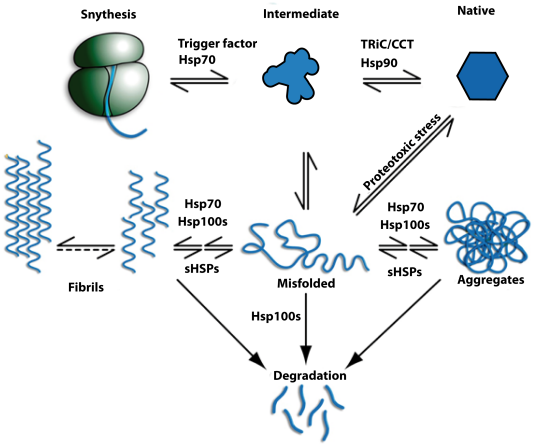

Figure 1.1: Stages in the life of a protein *in vivo*. Right from its emergence from the ribosome, the nascent polypeptide chain requires assistance of molecular chaperones. The nascent polypeptide chain folds via several intermediates to a functional native conformation. In presence of stress, chaperones assist misfolded proteins to refold and also help to disaggregate aggregated proteins.

1.3 Molecular chaperones

The basic principle of chaperones is to transiently bind exposed hydrophobic patches of folding intermediates in order to prevent intra and inter-molecular interactions which might hinder proper folding of the proteins. The chaperones are not a part of the final structures of proteins. The folded proteins are released and the chaperones can be 'recycled' thus providing the non-native proteins new opportunities to productively fold to reach its native state [Buchner, 1996; Bukau & Horwich, 1998; Ellis & Hartl, 1999]. The molecular chaperones work at stoichiometric ratios to decrease the

concentration of non-native proteins and in effect decrease the aggregation potential of folding proteins [Kiefhaber *et al.*, 1991]. The chaperones can be divided into five major and broadly conserved families namely, the small heat shock proteins (sHSPs), Hsp60 or chaperonins, Hsp70, Hsp90 and Hsp100s, where the numbers following 'Hsp' denote their molecular weights.

- 'Holdases' and 'Foldases'

  Chaperones can be functionally divided into 2 groups namely, 'holdases' and 'foldases'. As the names suggest, the 'holdase' chaperones, for example sHsps or the bacterial Trigger Factor, bind to the exposed hydrophobic patches of the non-native protein, thereby preventing aggregation. These chaperones are ATP-independent. However, in order to actively fold a protein to its native structure, the 'foldases' are required. The most prominent 'foldase' chaperone machines include Hsp60, Hsp70 and Hsp90. All these chaperones hydrolyse ATP which fuels their dynamic conformational structural changes required for their chaperoning function[Bukau & Horwich, 1998; Bukau *et al.*, 2000; Frydman, 2001; Hartl & Hayer-Hartl, 2002; Welch, 1991].

- From the ribosome and beyond

  Based on their cellular location and the stage of protein folding they assist, chaperones can also be considered to fall into two groups. The first group consists of the cytosolic chaperones which assist protein folding either co- or post-translationally. The other class of chaperones are those associated with the ribosome which can directly assist the early stages of co-translational folding of the nascent polypeptide [Gloge *et al.*, 2014; Preissler & Deuerling, 2012]. Ribosome-associated chaperones are present both in eukaryotes and prokaryotes, however, co-translational folding already at the ribosome is of utmost importance in eukaryotes as the rate of translation is even slower. In bacteria, the most prominent example of ribosome-associated chaperone is the Trigger Factor. The Trigger Factor interacts with every emerging nascent polypeptide chain and keeps it unfolded and in solution until the rest of the protein is translated or until the Hsp70 machinery starts to fold the protein domains that have exited the ribosomal tunnel. In the eukaryotic system, there is no direct homologue of the Trigger Factor but other ribosome-associated proteins belonging to different protein families exist. In *Saccharomyces cerevisiae*

for instance, there is a ternary complex at the ribosome comprising of two homologues of Hsp70, namely Ssb and Ssz and the Hsp40 protein Zuotin (Zuo)[Scior & Deuerling, 2014; Gautschi *et al.*, 2001]. Moreover, the nascent chain-associated complex (NAC) found in eukaryotes including yeast and mouse plays a role in proteostasis [Kirstein-Miles *et al.*, 2013].

1.4 Small heat shock proteins (sHSPs)

The sHSPs, as the name suggests, are the smallest members of the chaperone machinery. They are most widespread, but are poorly conserved. The sHSPs structurally have a common α-crystallin domain. In principle, the sHSPs are an example of the holdases, as they interact with a large number of partially folded proteins to prevent their aggregation upon stress-induced unfolding. The sHSPs form large dynamic oligomers in the cell, often including 24mers, which has made their structural characterization challenging [van Montfort *et al.*, 2001; Peschek *et al.*, 2013]. While their mode of action is to form soluble complexes with the partially folded proteins, they are also recruited to aggregates upon severe stress [Cashikar *et al.*, 2005; Haslbeck *et al.*, 2005; Liberek *et al.*, 2008]. By associating with the aggregates, the sHSPs alter the structure of the aggregate such that the proteins can then be reversibly refolded by other ATP-dependent chaperones like Hsp70/40 or Hsp100 [Haslbeck *et al.*, 1999]. It has been recently shown that due to their structural flexibility, sHsps can expose distinct binding interfaces and can thus interact with a wide variety of substrates [Mainz *et al.*, 2015]. sHsps are often activated by heat stress or post-translational modifications, which leads to their dissociation into smaller complexes [Haslbeck *et al.*, 2005, 2015]

1.5 Chaperonins or Hsp60

Chaperonins are large double ring chaperones that function by encapsulating non-native proteins (up to 60 kDa) in an ATP-dependent manner to give them a chance to fold in isolation. In bacteria, the most well-studied chaperonin is the GroE machinery. It consists of two heptameric rings which form a large GroEL 'cage' (Hsp60 in mitochondria). The co-chaperone GroES, also a heptameric ring, binds as a lid to close the cavity (Hsp10 in mitochondria) [Horwich, 2013; Skjærven *et al.*, 2015].

The mechanism of action of GroEL-ES has been extensively studied. The apical domains of GroEL have exposed hydrophobic amino-acid residues in the ring centre where the non-native substrate binds. Recent studies have elucidated the structure of GroEL with bound substrate in both open and closed conformation [Clare *et al.*, 2009; Chen *et al.*, 2013]. Closing of this ring by GroES, in the presence of ATP, results in a large conformational change in the GroEL ring that leads to the formation of a cage with a highly hydrophilic, net-negatively-charged inner wall [Xu *et al.*, 1997; Skjaerven *et al.*, 2012]. Encapsulated proteins are free to fold in this isolated environment for the duration of ATP hydrolysis. The substrate is released upon GroES dissociation and the cycle can repeat. In the eukaryotic cytosol the GroE machinery has been replaced by a distant relative called TRiC/CCT complex [Lopez *et al.*, 2015]. In the recent years, extensive structural information has accumulated. Structurally, the TRiC complex consists of two octameric rings. Unlike GroE complex, the TRiC/CCT has a built-in lid to replace the function of GroES [Zhang *et al.*, 2010a; Dekker *et al.*, 2011; Leitner *et al.*, 2012]. Mechanistically, the TRiC reaction is much slower allowing longer times for the substrates to fold [Valpuesta *et al.*, 2002]. The substrate spectrum is also more limited and surprisingly, the TRiC machinery is not upregulated during stress in yeast [Eisen *et al.*, 1998].

1.6 Hsp100s

The Hsp100 family of chaperones consists of AAA+ ATPases which act as powerful 'unfoldases' and 'disaggregases'. The different members of this family either unfold proteins and deliver them to compartmentalized proteases or help to disassemble aggregates, thus giving them a chance to refold. They are powerful ATP-dependent motors which can pull proteins through the central pore of their hexameric ring [Neuwald *et al.*, 1999; Haslberger *et al.*, 2008]. In bacteria, the Hsp100 family includes several members like ClpA, ClpB, ClpC, ClpE, ClpX and ClpY. Similar proteins are also found in mitochondria, plants and yeast (Hsp104) [Glover & Lindquist, 1998; Barends *et al.*, 2010]. ClpX and ClpA unfold proteins which are marked for degradation by pushing them through a central pore lined with tyrosine residues which provides non-specific binding sites for the translocating polypeptide. The unfolded polypeptide is then digested and degraded in the proteolytic chamber of the associated ClpP peptidase [Baker & Sauer, 2012]. Alternatively, ClpB or the yeast

Hsp104 have a unique ability to disaggregate proteins. However, both these proteins cannot recognize aggregated proteins in the absence of Hsp70 [Winkler *et al.*, 2012]. Thus, these proteins work in concert with Hsp70 and its co-factors to disaggregate and refold the aggregated/misfolded proteins [Seyffer *et al.*, 2012; Lee *et al.*, 2013]. Higher eukaryotes (nematodes and mammals) lack cytosolic Hsp100 proteins or any comparable disaggregases [Richter *et al.*, 2010].

1.7 Hsp70

The Hsp70 chaperone is one of the most conserved and central players in protein homoeostasis in the cell. Hsp70 isoforms are present in the cytosol and in organelles like mitochondria, chloroplasts and the endoplasmic reticulum. Hsp70s act on almost all stages of proteostasis. Under physiological conditions, Hsp70s are involved in the *de novo* folding of nascent polypeptides [Deuerling & Bukau, 2004]. Under stress, they are upregulated and they prevent aggregation of unfolded proteins [Tyedmers *et al.*, 2010]. Working down stream of chaperones like Hsp100s and sHsps, Hsp70 can also actively refold misfolded or aggregated proteins [Mayer & Bukau, 2005]. Hsp70 typically consists of a nucleotide binding domain (NBD) and a substrate binding domain (SBD) connected by an interdomain linker. The SBD consists of a β-sandwich subdomain which contains the peptide binding pocket and an α-helical lid. The transition between open and closed conformations of the SBD is central to the chaperoning function of Hsp70. Crystal structures of both the open and closed conformations of DnaK have been solved [Kityk *et al.*, 2012; Zhu *et al.*, 1996]. The SBD of Hsp70 can promiscuously bind all proteins that have an exposed stretch of seven, mainly hydrophobic amino acids in an extended conformation, preferably flanked by positively charged amino acid residues [Zhu *et al.*, 1996; Rüdiger *et al.*, 1997; Marcinowski *et al.*, 2011]. Hsp70s do not work alone in the cell, but interact with a variety of co-chaperones belonging to the J-domain protein (Hsp40) family. The J-domain co-chaperones play a role in targeting Hsp70s to the substrate proteins. The other set of co-chaperones are nucleotide exchange factors. The affinity of Hsp70 for substrates in the SBD is tightly coupled to ATP hydrolysis in the NBD. The allosteric communication between the NBD and the SBD has recently been resolved [Kityk *et al.*, 2015]. In the ADP-bound state, the conformational equilibrium is shifted towards a closed state with the NBD and SBD only connected via the interdomain linker and the substrate tightly enclosed in the substrate binding pocket. Nucleotide exchange factors

then catalyse the dissociation of ADP and ATP can bind subsequently bind the NBD. ATP binding induces a conformational rearrangement of the domains such that the SBDβ domain docks to the NBD and results in the opening of the α-helical SBD lid. This conformation has a low affinity for substrates but high release rates. The substrates associate with the J-domain co-chaperones and bind with high rates to the open conformation of Hsp70. Substrate binding induces the closing of the SBDα and also leads to the dissociation of the docked SBDβ from the NBD. This conformational rearrangement, favours ATP hydrolysis and the cycle can repeat (Figure 1.2).

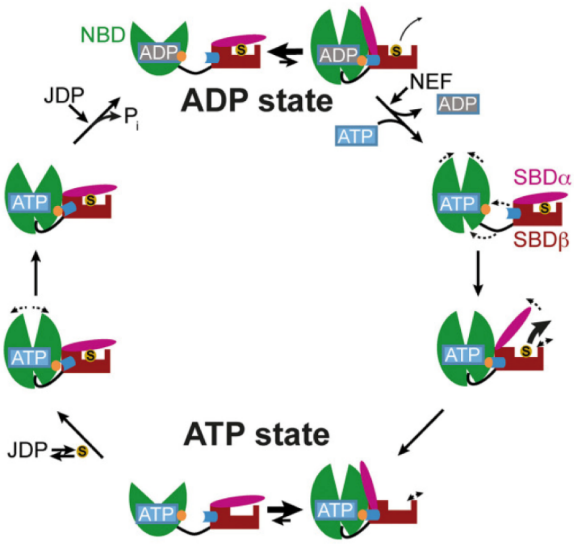

Figure 1.2: Hsp70 conformational cycle. In the ADP state Hsp70 is in equilibrium between the closed state with the substrate tightly bound and the transient open state. NEFs catalyse the exchange of ADP with ATP. ATP binding leads to structural rearrangements and docking of SBD (red) to the NBD (green). The lid of the SBD (magenta) opens. In the ATP state, Hsp70 is in equilibrium between the open state and transient closed state. J-domains recruit substrates and substrate binding leads to further conformational changes. Substrates stimulate ATP hydrolysis and then the cycle can repeat. Figure adopted from [Mayer & Kityk, 2015]

In yeast, the Hsp70 gene family comprises of fourteen genes, of which nine proteins are cytosolic and five are compartment specific. The cytosolic Hsp70s in yeast can be subdivided into 4 subfamilies. The major cytosolic sub-family in yeast is the Hsp70-Ssa (Stress Seventy sub-family A), which consists of 4 members Ssa1-4. The Ssa subfamily is essential in yeast and the expression of at least one component is required for viability [Werner-Washburne *et al.*, 1987; Stone & Craig, 1990]. Consti-

tutively expressed Ssa1 and 2 are 97% identical to each other, while stress inducible Ssa3 and 4 are 87% identical to each other [Sharma *et al.*, 2009]. In addition to the Ssa subfamily, there are two cytosolic components of the Ssb subfamily, namely Ssb1 and Ssb2 which differ in only 4 amino acids. Ssb1 and 2 are involved in binding to the translating ribosomes and nascent polypeptide chains [Peisker *et al.*, 2010]. The third sub-family comprises of Sse1 and 2, of which Sse1 is constitutive, while Sse2 is stress-induced. Expression of at least one member of the Sse subfamily is essential for viability in yeast. Despite being classified as Hsp70s, Sse1 acts as a nucleotide exchange factor for Hsp70 [Dragovic *et al.*, 2006]. The last cytosolic Hsp70 member is the constitutively expressed Ssz1. Ssz1 is a component of the ribosome-associated-complex (RAC) [Gautschi *et al.*, 2001; Huang *et al.*, 2005].

- Hsp40 (J-proteins)

  The Hsp40 family of co-chaperones are very diverse and target Hsp70 to different specific sites and functions. Simplistically, the J-proteins are thought to initially bind the non-native substrate protein, thereby preventing its aggregation and delivering it to Hsp70. Typically, Hsp40 is an elongated V-shaped dimer consisting of a conserved J-domain that activates the Hsp70 ATPase activity [Craig *et al.*, 2006; Hageman & Kampinga, 2009]. The various J-proteins differ significantly in the remainder of their structure [Kampinga & Craig, 2010]. Typically, following the J-domain there is a β-sub-domain that contains a surface exposed substrate binding site. Since Hsp40 interacts with the NBD as well as the CTD of Hsp70, client transfer from Hsp40 to Hsp70 is mediated [Landry, 2003]. The substrates are then delivered to Hsp70 for binding via the polypeptide backbone [Li *et al.*, 2003; Jiang *et al.*, 2007; Rodriguez *et al.*, 2008]. In yeast, Ydj1 is one of the most abundant cytosolic J-protein. While Ydj1 is not essential for viability in yeast, the Ydj1 deletion strain has a severe growth defect [Caplan & Douglas, 1991]. Ydj1 is thought to interact with Ssa1-2 and recruit them to protein folding on ER membranes [Caplan *et al.*, 1992]. Ydj1 also plays well-established roles in driving client proteins from Hsp70 to the Hsp90 machinery [Wegele *et al.*, 2006; Flom *et al.*, 2008].

- Nucleotide exchange factors (NEFs)

  The other set of Hsp70 co-factors are the NEFs. Unlike J-proteins, which have a common functional J-domain, the NEFs are structurally dissimilar. They can be

grouped into 3 large groups, HspBP1-type NEFs, Hsp70-like NEFs, and Bag family-NEFs. NEFs usually bind Hsp70 after ATP hydrolysis and catalyse ADP $\rightarrow$ ATP exchange, resulting in lid opening and substrate release [Schuermann *et al.*, 2008; Polier *et al.*, 2008; Kampinga & Craig, 2010]. Despite their structural differences, all NEFs interact with the ATPase domain of Hsp70.

The Hsp70-like NEF, Sse1, (also classified as Hsp110) [Raviol *et al.*, 2006], is the most abundant NEF in the yeast cytosol. Although Sse1 is not essential for yeast viability, deleting both Sse1 and Ydj1 causes lethality [Shaner *et al.*, 2006]. The deletion of Sse1 leads to a slight growth defect in yeast. Sse1 binds Hsp70 with a high affinity and the crystal structure for the complex has been resolved [Polier *et al.*, 2008; Schuermann *et al.*, 2008]. The crystal structures show that Sse1 is homologous to Hsp70, however it does not employ the nucleotide-dependent allosteric Hsp70 cycle. Instead Sse1 functions as an 'holdase' and binds unfolded proteins thereby preventing their aggregation. Additionally, Sse1 has been implicated to function as a Hsp90 co-chaperone [Liu *et al.*, 1999]. Owing to its role in governing cellular stress responses with Hsp70, it has been recently described as a principle NEF in yeast [Abrams *et al.*, 2014].

The other important NEFs are the Bag-family NEFs and in yeast this family represented by a single member called Snl1 [Sondermann *et al.*, 2002]. Like all members of this family, Snl1 contains a cytosolic Bag-domain that can interact with Hsp70's ATPase domain. Snl1 is tethered to the ER or the nuclear membrane via its amino-terminal transmembrane domain. Deletion of Snl1 does not lead to any growth defect, unlike the Sse1 and Ydj1 deletion. Snl1 is known to interact with ribosomal proteins and plays a role in translation [Verghese & Morano, 2012].

1.8 Hsp90

The Hsp90 molecular chaperone is evolutionarily conserved and highly abundant comprising of about 1-2% of the total cellular proteins [Taipale *et al.*, 2010] under physiological conditions. It is further up-regulated upon stress [Welch & Feramisco, 1982]. Unlike Hsp70 and the chaperonins, which interact with non-native polypeptides, Hsp90 binds partially folded proteins in a near-native state. Moreover, it is an atypical chaperone, as it shows some specificity in the substrates (also known as client proteins) it folds and does not promiscuously bind every non-native protein

[Jakob & Buchner, 1994; Wandinger *et al.*, 2008]. Hsp90 client proteins are key regulators in various cellular processes including cell cycle control, cell survival, hormone signalling and response to cellular stress, making Hsp90 indispensable for the cell. Under stress conditions, Hsp90 binds unstable protein conformations and thus prevents them from aggregation or inactivation [Rutherford & Lindquist, 1998]. Hsp90 also stabilizes proteins with unfavourable mutations, in turn playing a pivotal role in evolutionary processes as mutations are buffered and the manifestation of mutations is facilitated [Jarosz & Lindquist, 2010]. This very feature of Hsp90 is also exploited by cancer cells as Hsp90 buffers oncogenic mutations and stabilizes oncogenic proteins. It is thus regarded essential for cellular transformation and the progression of cancer [Whitesell & Lin, 2012]. On the other hand, Hsp90 also plays a crucial role in cellular defence against cancer by activating the tumor suppressor transcription factor p53 and inhibiting the transcription factor HSF1 [Whitesell & Lindquist, 2009]. Many Hsp90 client proteins are deregulated in cancerous cells [Falsone *et al.*, 2004; Blagosklonny *et al.*, 1996]. All these findings have put Hsp90 in the spotlight of clinical research and understanding its molecular mechanism has become a crucial requirement for the development of better therapeutic strategies.

1.8.1 Hsp90 homologues and localization

Hsp90 is present in almost all life forms (except Archea) and in almost all cellular compartment in eukaryotes. The bacterial Hsp90 (HtpG) is a relatively simple chaperone that is dispensable for life. However, Hsp90 has evolved into one of the most complex and sophisticated chaperone networks and is essential in all eukaryotic cells. Most simple eukaryotes like, *Drosophila* and *C.elegans* have only a single cytosolic Hsp90 [Johnson, 2012]. In higher eukaryotes, predominantly two cytosolic isoforms are present, stress inducible Hsp90α and constitutive Hsp90β [Langer *et al.*, 2003; Taherian *et al.*, 2008; Zuehlke *et al.*, 2015]. Plants express several additional cytosolic isoforms [Kadota & Shirasu, 2012; Breiman, 2014]. Notably *S. cerevisiae* also has two cytosolic isoforms : the inducible Hsp82 and the constitutive Hsc82. The isoforms are 97% identical, but are very differently regulated [Farrelly & Finkelstein, 1984; Borkovich *et al.*, 1989]. Apart from the abundant cytosolic isoforms, a small pool of Hsp90 is also found in the nucleus. It is believed that Hsp90 translocates into the nucleus with the client protein as Hsp90 itself does not harbour any nuclear localization sequence [Pratt *et al.*, 1993]. While intracellular Hsp90 is a key

player in protein homoeostasis, Hsp90 secreted outside the cell (extracellular Hsp90) carries out varied functions like stimulating the immune system [Oura *et al.*, 2011], promoting cell motility in wound healing and cancer cell invasion [Li *et al.*, 2007; Hance *et al.*, 2014]. Apart form this, there are also several organelle-specific Hsp90 isoforms, like TRAP1 in the mitochondria [Felts *et al.*, 2000; Leskovar *et al.*, 2008], Grp94 in the endoplasmic reticulum [Frey *et al.*, 2007; Dollins *et al.*, 2007; Marzec *et al.*, 2012] and Hsp90C in the chloroplasts in plant cells [Trösch *et al.*, 2015]. While in eukaryotes cytosolic Hsp90 requires the assistance of large cohort of helper proteins called co-chaperones, its prokaryotic homologue seems to act on its own. However, the structural organization and the mechanism of the ATPase cycle necessary for the Hsp90 chaperone activity are conserved among cytosolic and organellar species [Richter *et al.*, 2008; Johnson, 2012].

1.8.2 Hsp90 structure and conformational dynamics

Hsp90 exist as a dynamic dimer and the dimerization is essential for its chaperoning activity. The protomer consists of an N-terminal domain (NTD), followed by a flexible charged linker region (CLR), a middle domain (MD), and finally a C-terminal domain (CTD) with a MEEVD motif (Figure 1.3). The NTD is involved in nucleotide binding and hydrolysis. The CLR plays an important role in Hsp90 function as mutations in this region impair client activity and regulation by some co-chaperones [Hainzl *et al.*, 2009; Jahn *et al.*, 2014]. The MD also plays a concerted role in ATP hydrolysis together with the NTD. The CTD is essential for dimerization. All three domains (NTD, MC and CTD) are involved in binding various co-chaperones and clients [Mayer & Le Breton, 2015]. The MEEVD motif of the C-terminal end is an anchor for all the co-chaperones that posses the TPR domain.

In its apo state (nucleotide free state), Hsp90 forms an open V-shaped dimer called 'open conformation'. Upon ATP binding, a series of structural changes ensue. The lid segment of the NTD closes over the bound nucleotide. This leads to the dimerization of the two NTDs via strand exchange [Ali *et al.*, 2006] and formation of the 'Closed 1' state. The flexible loop of the MD then forms contacts with the nucleotide binding pocket of the NTD inducing a twisted compact 'Closed 2' conformation [Huai *et al.*, 2005; Richter *et al.*, 2008] (Figure 1.4).

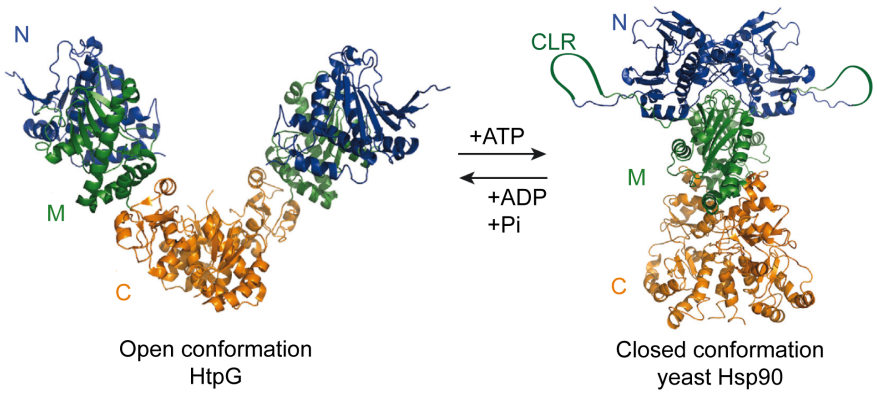

Figure 1.3: Open and closed conformation of Hsp90. Crystal structures of Hsp90 from *E.coli* (HtpG) in the open conformation (left, PDB 2IOQ) and closed nucleotide bound conformation from yeast (right, PDB 2CG9) are shown. The NTD is blue, the MD is green and the CTD is orange. CLR stands for charged linker region connecting NTD and MD.

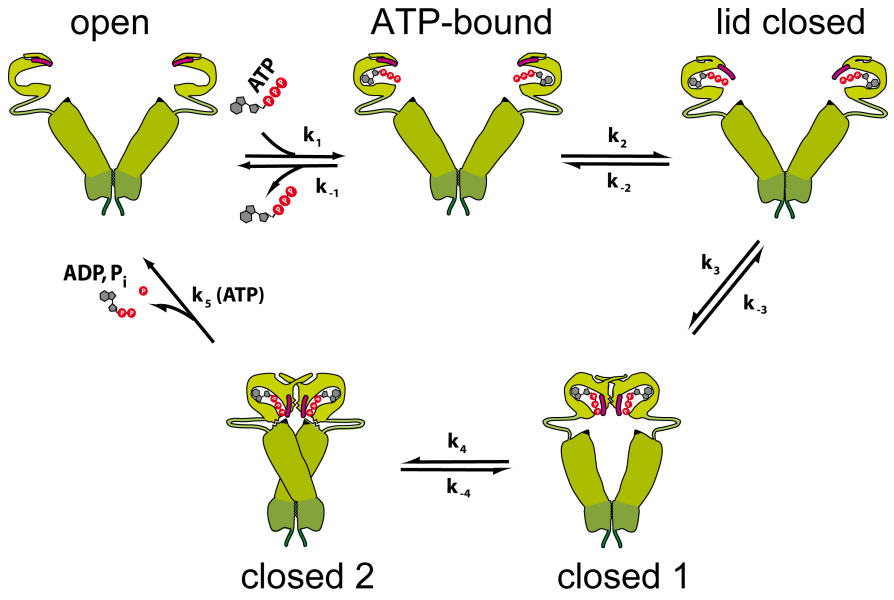

Figure 1.4: Conformational dynamics of Hsp90. ATP binding leads to the closing of the lid segment of the NTD (lid closed). This conformation is the first intermediate in which the lids are closed, but dimerization of the NTDs is yet to occur. The NTDs then dimerize forming the closed 1 conformation, followed by MDs associating with the NTDs. ATP hydrolysis occurs when Hsp90 reaches the closed 2 conformation. ADP and Pi are then released and the N-domain dissociates and the cycle can repeat. Figure adapted from [Li *et al.*, 2013]

The nucleotide binding site is special because ATP is bound in a kinked conformation. The nucleotide binding site in the NTD, together with parts of the MD form the split-ATPase site [Ali *et al.*, 2006; Richter & Buchner, 2011]. After ATP hydrolysis, Hsp90 switches back to the open conformation, the hydrolysed nucleotide is released and the cycle can repeat. The rate limiting step in this process is the N-terminal dimerization and not ATP binding or hydrolysis itself. Altogether, the ATP turnover rate of Hsp90 is extremely slow (1 per minute in yeast and 10 times slower in humans), but the conformational changes during the ATPase activity are conserved from yeast to man [Panaretou *et al.*, 1998; Hessling *et al.*, 2009; Richter *et al.*, 2008]. The CTD also undergoes rapid opening and closing movements exactly out of sync with the NTD, suggesting that the dynamic changes in the NTD are communicated all the way to the CTD [Ratzke *et al.*, 2010]. While the bacterial HtpG conformation is largely dictated by the nucleotide, the conformational dynamics in eukaryotic Hsp90 is complex. Independent of nucleotide binding, yeast Hsp90 can fluctuate between two open and two closed conformations by thermal fluctuations and nucleotide binding only slightly changes the energy barrier within the different conformations. Thus the eukaryotic Hsp90 can be envisioned as a probabilistic protein machine which requires an array of co-chaperones to stabilize specific conformations [Ratzke *et al.*, 2012; Mayer & Le Breton, 2015].

1.8.3 Hsp90 co-chaperones

Eukaryotic Hsp90 is subject to elaborate conformational regulation by more than 20 co-chaperones (identified to date). While some of them have been well-characterized with respective to Hsp90, most of their biological roles still remain enigmatic. The co-chaperones can be grouped into those which modulate the ATPase activity of Hsp90, those involved in recruiting the client proteins to Hsp90, those which co-ordinate the interplay between Hsp90 and other chaperone systems and those which contribute to the Hsp90 chaperoning function through their distinct enzymatic activities [Röhl *et al.*, 2013]. These categories largely overlap making a disparate classification impossible. The co-chaperones involved in client-recruitment generally prefer open Hsp90 conformation, and with some exceptions, slow down the ATPase activity of Hsp90 [Southworth & Agard, 2011; Gaiser *et al.*, 2010; Kadota *et al.*, 2010]. Most of the co-chaperones prefer one of the conformational states of Hsp90 and hence are thought to contribute to driving the dynamic conformational cycle. The largest group

of co-chaperones are the TPR domain containing chaperones. TPR domains are defined by tandem repeats of 34-amino acids which fold into seven α-helices and bind to the -EEVD terminals of both Hsp70 and/or Hsp90 [Smith, 2004] (Figure 1.5).

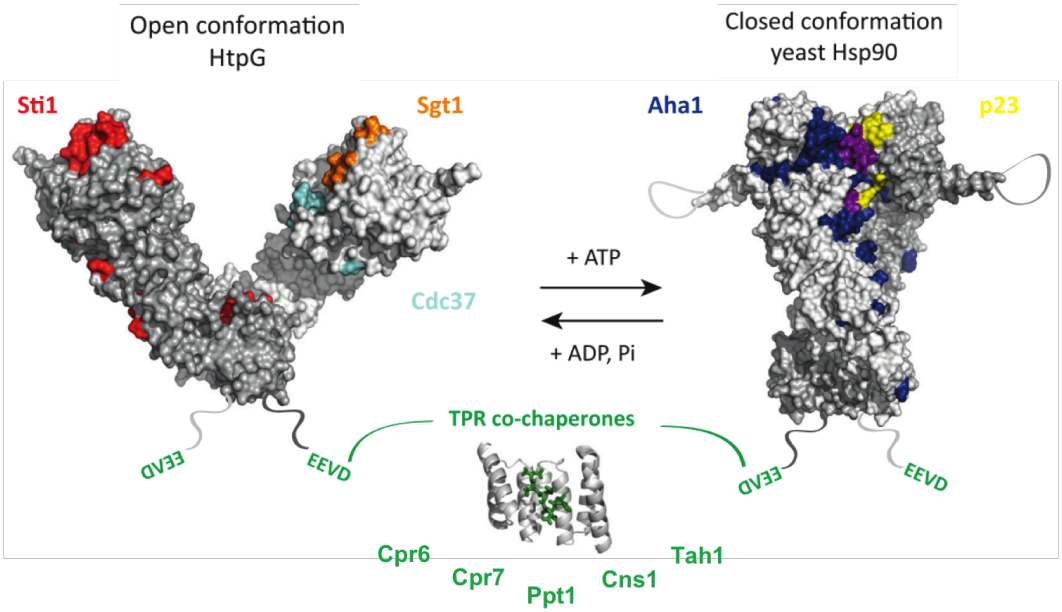

Figure 1.5: Hsp90 co-chaperones prefer distinct conformations of Hsp90. Surface representation of Hsp90 in the closed and open conformation is shown with co-chaperone binding sites coloured. Sti1: red, Sgt1: orange, Cdc37: light blue on the open Hsp90. Aha1: blue, p23/Sba1: yellow, overlapping sites for Aha1 and p23: purple. The TPR domain is shown in the centre in complex with the C-terminal MEEVD motif (green). The TPR co-chaperones are listed in green. Figure adapted from [Röhl *et al.*, 2013].

Table 1.1: Hsp90 co-chaperones

Yeast	Mammals	Hsp90-binding	Function	References
Sti1	Hop1	MEEVD motif, MD, NTD	Connector binds Hsp70 and Hsp90, ATPase inhibitor for Hsp90, stabilizes open state	[Röhl *et al.*, 2015; Alvira *et al.*, 2014; Schmid *et al.*, 2012; Lee *et al.*, 2012; Li *et al.*, 2011]
Aha1	Aha1	NTD MD	Hsp90 ATPase activator	[Meyer *et al.*, 2004; Li *et al.*, 2013; Retzlaff *et al.*, 2010; Rehn & Buchner, 2015]
Hch1		MD (putative)	Hsp90 ATPase activator	[Armstrong *et al.*, 2012]

Table 1.1: Hsp90 co-chaperones

Yeast	Mammals	Hsp90-binding	Function	References
Ppt1	PP5	MEEVD motif	Phosphatase, client activation	[Soroka *et al.*, 2012; Wandinger *et al.*, 2006]
Cpr6 Cpr7	Cyp40	MEEVD motif MEEVD motif	Prolylisomerase, Chaperone activity	[Mayr *et al.*, 2000; Pirkl & Buchner, 2001]
Sba1	p23	NTD, MD	Hsp90-client-complex assembly, client release, Hsp90 ATPase inhibitor	[Karagöz *et al.*, 2011; Richter *et al.*, 2004; Ali *et al.*, 2006; Martinez-Yamout *et al.*, 2006; Rehn & Buchner, 2015]
Tah1,Pih1	Tah1, Pih1	MEEVD motif	Component of the R2TP complex, complex interacts with Hsp90 through Pih1 to mediate assembly	[Eckert *et al.*, 2010; Back *et al.*, 2013; Jiménez *et al.*, 2012]
Cdc37	Cdc37	NTD	Kinase specific co-chaperone, ATPase inhibitor	[Calderwood, 2015; Boczek *et al.*, 2015; Siligardi *et al.*, 2002]
Sgt1	Sgt1	NTD	Part of the ubiquitin ligase complex, adaptor for clients	[Ogi *et al.*, 2015; Eckl *et al.*, 2014; Johnson *et al.*, 2014; Zhang *et al.*, 2008]
Cns1	Cns1	MEEVD motif	Function unknown	[Tenge *et al.*, 2015; Hainzl *et al.*, 2004; Tesic *et al.*, 2003]

- Sti1

  Yeast Sti1 (Stress inducible 1), known as Hop1 (Hsp70 and Hsp90 organising protein) in higher eukaryotes, is one of the best characterized Hsp90 co-chaperone. It is significantly upregulated upon stress [Nicolet & Craig, 1989; Eisen *et al.*, 1998]. Sti1 is a TPR co-chaperone and is composed of three TPR domains and

two aspartate-proline rich domains (DP domains). The protein consists of two modules, the first consisting of TPR1-DP1, followed by the second consisting of TPR2A-TPR2B-DP2. The crystal structure of these domains has been recently solved [Schmid *et al.*, 2012]. TPR1 and TPR2B are responsible for recognizing Hsp70, while TPR2A is specific for Hsp90 [Scheufler *et al.*, 2000; Schmid *et al.*, 2012] (Figure 1.6A). Recent studies further show that Hsp90 regulates the conformation of Sti1. Prior to Hsp90 binding, Sti1 is compact and the TPR2B has a high affinity for Hsp70. Hsp90 binding induces a stretched conformation of Sti1 and binding of Hsp70 switches to TPR1 [Röhl *et al.*, 2015]. The DP domains seem to contribute to substrate activation [Schmid *et al.*, 2012; Southworth & Agard, 2011]. One monomer of Sti1 binding one Hsp90 dimer can completely inhibit the Hsp90 ATPase activity [Lee *et al.*, 2012; Schmid *et al.*, 2012; Li *et al.*, 2012]. The inhibition is achieved by binding of the central element of Sti1, to the C-terminal end of Hsp90 and the Hsp90 middle domain which leads to a stabilization of the open conformation of Hsp90 [Hessling *et al.*, 2009; Southworth & Agard, 2011]. Thus the inhibitory action of Sti1 is not by blocking access to the nucleotide binding site, but rather by restricting the conformational changes of Hsp90 which are required for ATP hydrolysis. Thus Sti1 is thought to be a non-competitive inhibitor of Hsp90 [Richter *et al.*, 2003]. Thus, Sti1/Hop1 physically connects both Hsp70 and Hsp90 machineries by binding both chaperones simultaneously at the TPR domains and further facilitates client transfer to Hsp90 by restricting Hsp90 in an open conformation. The exact mechanism of transferring a client protein from Hsp70 to Hsp90, mediated by the mammalian Sti1 homologue, Hop1 shows that the client is delivered to the opposite side than the Sti1 binding site on the Hsp90 dimer [Alvira *et al.*, 2014]. The conformational flexibility of Sti1 and its parallel interaction with Hsp70 and Hsp90 allow for efficient client transfer. In addition to the structural influence of Hsp90, Sti1 as well as Hop1 are also subjected to inhibitory phosphorylation. In spite of not being essential for viability, Sti1 is still under tight regulation [Röhl *et al.*, 2015].

- Ppt1

  Protein Phosphatase-T is another TPR co-chaperone of Hsp90. The TPR domain of Ppt1 suppresses the phosphatase activity of Ppt1 by blocking the access to its active site. Upon binding to Hsp90 via the TPR domain, Ppt1 is activated and act as a serine-threonine phosphatase that dephosphorylates Hsp90 and also Cdc37 [Vaughan *et al.*, 2008] (Figure 1.6B). This dephosphorylation of Hsp90 is thought

to affect its function and client activation *in vivo*. Ppt1 also regulates Hsp90 by affecting its ATPase and co-chaperone binding activities [Wandinger *et al.*, 2006; Soroka *et al.*, 2012]. Ppt1 is present both in the nucleus and cytoplasm and is mainly expressed during logarithmic phase. In yeast Ppt1 is non-essential for viability but deletion affects the activity of Hsp90 clients. It has recently been suggested that the TPR domain of Ppt1 interacts differently with the CTD of Hsp90 than other TPR co-chaperones and may be involved in more than just binding to Hsp90 [Johnson *et al.*, 2014].

- p23/Sba1

  p23/Sba1 (increased sensitivity to benzoquinone ansamycins) is a small acidic non-TPR protein. Structurally, p23 has a stably folded N-domain, organized as a seven stranded β-sandwich followed by an unstructured C-terminal tail, which could not be crystallized [Weikl *et al.*, 1999; Ali *et al.*, 2006]. p23 acts at a late stage in the Hsp90 conformational cycle. Crystal structures in complex with Hsp90 show that p23 binds in a depression at the interface of the two Hsp90-N domains. Additional interaction site with some residues in the Hsp90-M domain has also been suggested [Ali *et al.*, 2006; Li *et al.*, 2013]. p23 also exerts long-distance conformational changes in the Hsp90-M domain distant from the expected binding site [Martinez-Yamout *et al.*, 2006; Karagöz *et al.*, 2011]. p23 competes with Sti1 for the M-domain binding site and this is important for the progression of the Hsp90 conformational cycle [Li *et al.*, 2011]. For p23-Hsp90 interaction to occur, Hsp90 must bind ATP, its molecular lid must be closed, its NTDs must associate with each other, and its middle domain catalytic loop must dock with the NTD ATP-binding pocket [Ali *et al.*, 2006; Martinez-Yamout *et al.*, 2006] (Figure 1.6C).

  This conformational state is normally achieved transiently before ATP hydrolysis [Richter *et al.*, 2004]. As it traps Hsp90 in an ATP hydrolysis competent, transient state, it inhibits the Hsp90 ATPase by about 50%, while stimulating ATP binding [McLaughlin *et al.*, 2006]. Whether p23 inhibits the ATPase activity by decelerating hydrolysis itself or by impeding the release of ADP and Pi or both is not yet clear [Ali *et al.*, 2006; Karagöz *et al.*, 2011]. p23/Sba1 facilitates the binding and maturation of client proteins by stabilizing the closed, normally transient conformation of Hsp90. The C-terminal unstructured tail of p23 plays an important role in its chaperone activity [Weaver *et al.*, 2000]. It is know that p23/Sba1 is the limiting component for the stability of Hsp90-client protein heterocomplexes [Morishima *et al.*, 2003]. p23 also has Hsp90 independent functions and has been

shown to modulate nuclear receptors and transcription factors [Echtenkamp *et al.*, 2011; Freeman & Yamamoto, 2002; Oxelmark *et al.*, 2006].

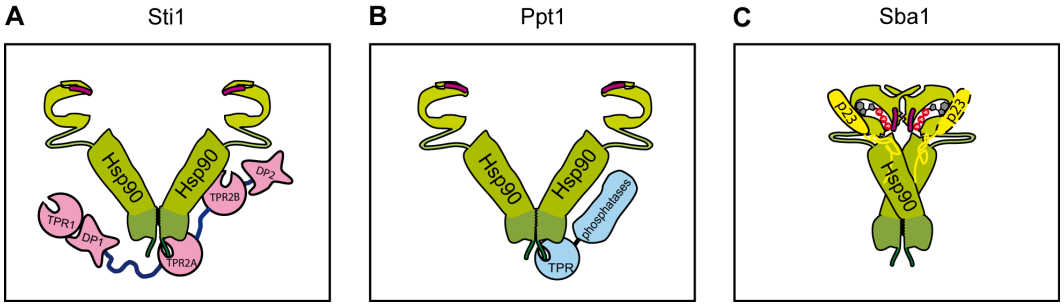

Figure 1.6: Hsp90 co-chaperones prefer distinct conformations of Hsp90. (A) Sti1 prefers and stabilizes the open conformation of Hsp90. Primary interaction site is the C-terminal MEEVD with secondary contacts in the M-domain. (B) Ppt1 also binds Hsp90 via its TPR domain at the C-terminal MEEVD motif. (C) p23/Sba1 binds the closed Hsp90 at the N-domain via its CS (p23-like) motif, and slows down ATP hydrolysis. Figure adapted from [Li *et al.*, 2012].

- Cpr6 and Cpr7

  Cpr6 and Cpr7 of yeast and Cyp40 of mammals are homologous co-chaperones that contain an amino-terminal peptidyl-prolyl isomerase (PPIase) and carboxyl-terminal TPR domain. The PPIase domain catalyses the interconversion of the cis-trans isomerization of peptide bonds prior to proline residues. The TPR domain, on the other hand, mediates the interaction with the C-terminal MEEVD motif of Hsp90 [Fanghänel & Fischer, 2004](Figure 1.7A). In addition to the Hsp90 dependent role, both proteins also have independent chaperone activity [Bose *et al.*, 1996; Freeman & Morimoto, 1996]. Cpr6 and Cpr7 share 38% amino acid identity and 47% sequence homology [Duina *et al.*, 1996]. Despite this, the two proteins differ significantly, both *in vitro* and *in vivo* and the carboxyl-terminal 100 amino acids are critical determinants of their specific functions. [Zuehlke *et al.*, 2013; Tenge *et al.*, 2015]. While both proteins are constitutively expressed, only Cpr6 is upregulated upon stress [Dolinski *et al.*, 1998]. Cpr6 has a stronger PPIase activity, while Cpr7 is a better chaperone, however the physiological implications of these differences are not yet understood [Mayr *et al.*, 2000]. Deletion of Cpr7 in yeast causes retardation of growth, but no growth defects are associated with Cpr6 deletion [Duina *et al.*, 1996]. In the recent years, Ura2, a protein involved in pyrimidine synthesis has been shown to be a substrate for Cpr6. Cpr6 inter-

acted with Ura2 via its TPR domain, even in the absence of Hsp90, while Cpr7 TPR domain did not interact [Zuehlke *et al.*, 2013]. Cpr6 has also been shown to form a complex with Hsp90 and Sti1, thus integrating it in the Hsp90 cycle [Li *et al.*, 2011]. Cpr7, on the other hand, is thought to play a role in modulating the nucleotide-dependent conformational changes of Hsp90 by mediating proper signalling of nucleotide bound state to the C-terminal. It also regulates the interaction of Hsp90 with other co-chaperones like Cpr6 [Zuehlke & Johnson, 2012]. While both co-chaperones interact with the ribosome, it has been postulated that Cpr7 has ribosomal functions in unstressed cells, and the over-expression of stress-inducible Cpr6 may disrupt Cpr7 function by competing for Hsp90 or ribosomes [Tenge *et al.*, 2015]. Thus Cpr6 and Cpr7, despite being homologues, likely perform overlapping but non-redundant tasks in the cell.

- Aha1 and Hch1

  Aha1 stands for Activator of Hsp90 ATPase and was identified as a Hsp90 co-chaperone, based on a homology search of Hch1 (High Copy suppressor of Hsp90 temperature sensitive mutants). Canonical Aha1 is composed of two domains connected by a linker peptide that is 40 amino acids, whereas Hch1 is a single domain corresponding to the Aha1 N terminal domain. The Aha1-N domain shares 36% sequence identity and 50% homology to Hch1. While Aha1 is conserved from yeast to man, Hch1 is only present in lower eukaryotes [Panaretou *et al.*, 2002; Lotz *et al.*, 2003]. Aha1 interacts with Hsp90 in an inverted manner, such that the Aha1 N-terminal domain binds the M-domain of Hsp90 and the Aha1 C-terminal domain binds the NTD of Hsp90 [Meyer *et al.*, 2004; Retzlaff *et al.*, 2010; Koulov *et al.*, 2010] (Figure 1.7B). The Aha1-Hsp90 interaction is salt-dependent and nucleotide independent, however Aha1 binds with a higher affinity to the closed conformation of Hsp90. Aha1 and Hch1 activate the ATPase activity of Hsp90, although the Aha1-N domain and Hch1 alone do so to a lower extent. Isolated Aha1-C domain cannot stimulate the Hsp90 ATPase activity, although it enhances the effect of the Aha1-N domain [Hessling *et al.*, 2009; Retzlaff *et al.*, 2010]. Both Aha1 and Hch1 share a conserved RKxK motif which is involved in the remodelling of the catalytic loop of Hsp90 and facilitates ATP hydrolysis. One full length Aha1 molecule is essential and sufficient for full stimulation of Hsp90 [Retzlaff *et al.*, 2010]. Binding of Aha1 accelerates N-terminal dimerization of Hsp90 and activates ATP hydrolysis in both N-domains of the Hsp90 dimer. Recently it has been suggested that the human homologue of Aha1 has Hsp90-independent chaperone

activity, for which the first 22 amino acids are crucial. These residues are missing in the yeast homologue, which does not have chaperoning activity [Tripathi *et al.*, 2014]. Aha1-client relationships have also suggested a role for Aha1 in promoting disposal of defective proteins by targeting them to degradation [Wang *et al.*, 2006; Tripathi *et al.*, 2014]. Deletion of Hch1, but not Aha1 confers resistance to Hsp90 inhibitors [Armstrong *et al.*, 2012]. Additionally, a mutation in the catalytic loop of Hsp90 specifically impairs Aha1 but not Hch1, suggesting that proteins interact with the Hsp90 catalytic loop in different ways [Horvat *et al.*, 2014]. Thus, Aha1 and Hch1, despite their homology in the N-terminal domain, may have very different roles *in vivo*.

- Tah1 and Pih1

  Tah1 (TPR-containing protein associated with Hsp90) and Pih1 (Protein Interacting with Hsp90) are two further client-specific Hsp90 co-chaperones and have been mainly described in context of chromatin remodelling complexes and small nuclear ribo-nucleoprotein (RNP) maturation [Zhao *et al.*, 2005, 2008]. Tah1 is a TPR co-chaperone, however the TPR domain of Tah1 is unusual. TPR domains typically consist of three TPR motifs and a C-terminal cap helix. The Tah1-TPR domain however, only consists of two TPR motifs and a C-terminal cap helix but can still interact with the C-terminal MEEVD motif of Hsp90 [Jiménez *et al.*, 2012]. The minimal TPR domain of Tah1 is followed by an unstructured region. In case of Pih1, two domains have been identified: the N-terminal Pih1 (32-166) domain and the C-terminal CHORD-SGT1 (CS) domain [Manival *et al.*, 2014]. Pih1 alone is unstable and is degraded from its N-terminus. The aggregation-prone property of Pih1 mainly results from its C-terminal sequence. Pih1 being so unstable, can even be used as a degradation tag in yeast [Jiménez *et al.*, 2012]. The C-terminal region of Tah1 interacts with the C-terminus of Pih1 thereby stabilizing it [Zhao *et al.*, 2008; Jiménez *et al.*, 2012]. Tah1-Pih1 and Hsp90 can form a ternary complex in which Tah1 interacts with the C-terminal MEEVD motif of Hsp90 and the C-terminus of Pih1. Pih1 additionally forms contacts with the M-domain of Hsp90 (Figure 1.7C). Tah1 alone is a weak activator of the Hsp90 ATPase activity. The Tah1-Pih1 complex however, inhibits the ATP hydrolysis of Hsp90 and arrests the Hsp90 cycle [Eckert *et al.*, 2010; Millson *et al.*, 2008]. This step is considered essential to prepare Hsp90 to take over clients involved in RNP assembly. Recent studies have also highlighted the importance of phosphorylation of the human Pih1 in client recruitment to Hsp90 [Pal *et al.*, 2014].

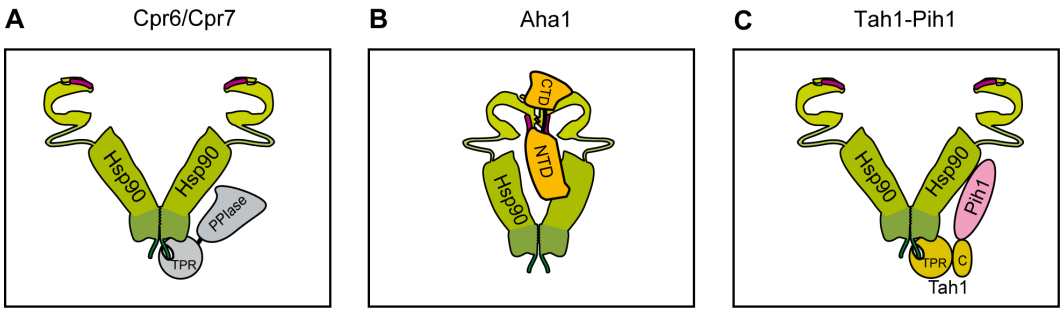

Figure 1.7: Hsp90 co-chaperones prefer distinct conformations of Hsp90. (A) Cpr6 and Cpr7 are TPR co-chaperones that interact with the C-terminal MEEVD motif of Hsp90. (B) Aha1 prefers the closed conformation of Hsp90 and forms contacts to the NTD and the MD of Hsp90 in an inverted manner. (C) Tah1 is a TPR co-chaperone and interacts with the C-terminal MEEVD motif of Hsp90. The C-domain of Tah1 mediates interaction with Pih1. Figure adapted from [Li *et al.*, 2012].

- Cdc37

  Cdc37 (Cell Division Cycle 37 homologue) is a kinase-specific co-chaperone that acts early in the Hsp90 chaperone cycle [Roe *et al.*, 2004; Gaiser *et al.*, 2010]. Similar to Sti1, it stabilizes the open conformation of Hsp90 and inhibits the ATP hydrolysis. Structural studies have shown that Cdc37 binds to surfaces of the Hsp90 N-domain implicated N-terminal dimerization and association with the MD. Thus by precluding N-terminal dimerization and blocking access of the catalytic loop of the middle domain with the ATPase binding pocket, it fixes the ATP lid in an open conformation and prevents closing of the Hsp90 molecule [Roe *et al.*, 2004; Shao *et al.*, 2001; Siligardi *et al.*, 2002; Gaiser *et al.*, 2010] (Figure 1.8A). Notably, Cdc37 does not influence the nucleotide accessibility of Hsp90 [Eckl *et al.*, 2013]. Aha1 and Cdc37 can bind Hsp90 simultaneously, but do not directly interact. On the other hand, Sba1 and Cdc37 are mutually exclusive in Hsp90 binding. Similar to Sti1, Sba1 also competes with Cdc37 to bind to Hsp90 and drives the conformational cycle further [Siligardi *et al.*, 2004; Eckl *et al.*, 2013]. Cdc37 is important for chaperoning kinases and recruits them to the Hsp90 machinery [Taipale *et al.*, 2012]. Early on, Cdc37 was found as a part of the Hsp90-v-Src kinase complex [Dey *et al.*, 1996; Stepanova *et al.*, 1996]. The N-terminal domain of Cdc37 is involved in kinase binding. Its activity is strictly controlled by phosphorylation of its Ser 13 (Ser 14 in yeast), which is important for client processing [Shao *et al.*, 2003; Vaughan *et al.*, 2006]. Recent biophysical studies also show that the phosphorylation induces a compact structure of Cdc37 which might be crucial for its

client recruiting properties [Liu & Landgraf, 2015]. The phosphorylated form of Cdc37 was also shown to essential for the activation of v-Src [Boczek *et al.*, 2015]. Unlike the co-chaperones discussed above, Cdc37 is essential for viability in yeast [Turnbull *et al.*, 2005]. It also functions as a chaperone itself with possible Hsp90-independent functions [Kimura *et al.*, 1997; MacLean & Picard, 2003; Echtenkamp & Freeman, 2012].

- Cns1

  Cns1 (Cyclophilin seven suppressor) was discovered as a suppressor of a severe growth defect caused by deletion of Cpr7 [Marsh *et al.*, 1998]. Similar to Sti1, Cns1 also has three TPR domains and interacts with both Hsp70 and Hsp90 (Figure 1.8B). It shares a weak homology of 24% and sequence identity of 18% with Sti1. However, unlike Sti1 and most other TPR co-chaperones, Cns1 is essential for viability in yeast. It is not upregulated upon stress and, compared to Sti1, it is a poorly expressed protein in yeast [Dolinski *et al.*, 1998; Ghaemmaghami *et al.*, 2003; Kulak *et al.*, 2014]. While it has no effect on the ATPase activity of Hsp90, Cns1 acts as a potent activator of Hsp70 ATP hydrolysis [Hainzl *et al.*, 2004]. Cns1 and Cpr7 also interact with the ribosome, however the functional relevance of this interaction is not completely clear [Tenge *et al.*, 2015]. Genetic interaction studies have shown that overexpression of Cpr7 can suppress temperature sensitivity of Cns1 mutants. Cns1 and Cpr7 are also thought to interact in the absence of Hsp90 [Tesic *et al.*, 2003]. All this support the notion that Cns1 and Cpr7 share an important function *in vivo*, however their cellular functions are not simply redundant but may only partially overlap.

- Sgt1

  Sgt1 (Suppressor of G2 allele of skp1) has been studied intensively in plants [Takahashi *et al.*, 2003; Kadota *et al.*, 2008; Wang *et al.*, 2015]. Sgt1 contains an amino-terminal TPR domain, a CS (CHORD and Sgt1) domain and a conserved Sgt1-specific-carboxy-terminal (SGS) domain. Despite being a TPR co-chaperone, the interaction with Hsp90 does not occur via its TPR domain but through a CS (CHORD and Sgt1) domain which is structurally similar to p23 [Lee *et al.*, 2004; Kadota *et al.*, 2008; Zhang *et al.*, 2008] (Figure 1.8C). The binding site is located in Hsp90-NTD however Sgt1 preferentially binds Hsp90 in the absence of nucleotide. Unlike p23, the interaction of the CS domain with Hsp90 does not affect the lid and has no influence on the ATPase activity of Hsp90 [Catlett & Kaplan, 2006; Botër

et al., 2007]. In plants, Hsp90 and Sgt1 form a ternary complex with another co-chaperone, Rar1, which acts as a co-remodulator in plant immunity [Kadota & Shirasu, 2012]. The CHORD domains of Rar1 bind to the two NTDs of Hsp90 and stabilize the open conformation. Sgt1 can interact with this Rar1-Hsp90 complex and recruit clients. ATP binding can take place in this conformation as the lid of Hsp90-NTD is very flexible [Zhang *et al.*, 2010b; Kadota & Shirasu, 2012; Blacklock & Verkhivker, 2014]. The TPR domain of Sgt1 is involved in recruiting clients. Sgt1 also plays a role in maturation of NLR (nucleotide-binding site and leucine-rich repeat domain) proteins [Austin *et al.*, 2002]. The interaction with the leucine-rich protein repeats is mediated via its SGS domain [Stuttmann *et al.*, 2008]. Sgt1 is essential for viability in yeast. It has been recently shown that the nematode Sgt1 homologue binds Hsp90 in the absence of nucleotides, but more strongly in the presence of ATP, suggesting that Sgt1 might interact with open and closed conformations of Hsp90, albeit with different affinities [Eckl *et al.*, 2014].

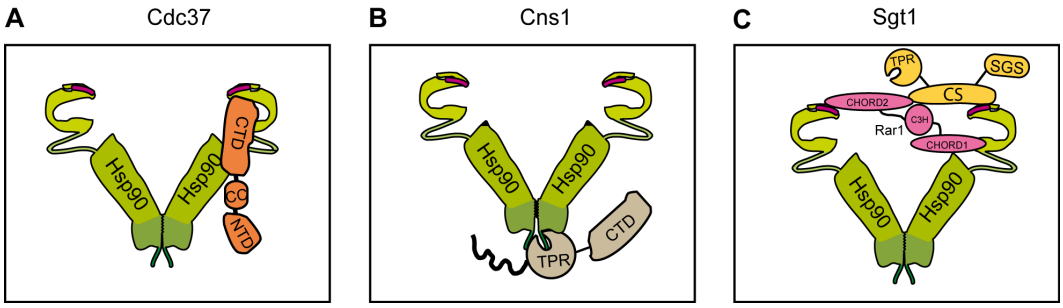

Figure 1.8: Hsp90 co-chaperones prefer distinct conformations of Hsp90. (A)Cdc37 interacts with open Hsp90 via its C-terminal domain. The N-terminal binds kinases. (B) Cns1 is a TPR co-chaperones and interaction to Hsp90 is mediated via the MEEVD motif. The representation of Cns1 is based on unpublished results. (C) Sgt1, despite being a TPR co-chaperone, interacts with Hsp90 at the NTD via its CS domain. The TPR domain binds clients. Figure adapted from [Li *et al.*, 2012].

1.8.4 Post-translational modifications of Hsp90

Hsp90 being an influential chaperone, is under very stringent regulation. In addition to the co-chaperone modulators, a second layer of regulation of the Hsp90 function is provided by post-translational modifications. To date many modifications have been

discovered for Hsp90 including, phosphorylation, acetylation, nitrosylation, SUMOylation, glycosylation and even methylation (reviewed extensively in [Mollapour & Neckers, 2012]). These modifications affect the ATPase activity, co-chaperone binding, conformational dynamics and almost every facet of Hsp90 function. Phosphorylation is the best studied and most frequent modification on Hsp90. Phosphorylation sites localized in all three domains of Hsp90 have been identified so far. Modifications in the CTD of Hsp90, can influence the ATPase activity in the NTD, suggesting that phosphorylation plays a role in long distance communication within the Hsp90 molecule [Retzlaff *et al.*, 2009; Martínez-Ruiz *et al.*, 2005]. Typically, phosphorylation reduces the chaperone function of Hsp90 and slows down the conformational kinetics [Soroka *et al.*, 2012]. Different kinases are involved in phosphorylating Hsp90, some of which even require Hsp90's assistance to fold themselves. Additionally, the Hsp90-Cdc37 complex is also regulated by phosphorylation, imparting directionality to the Hsp90 cycle [Xu *et al.*, 2012]. Phosphorylation of Aha1 promotes its interaction with Hsp90 and have important consequences for Hsp90-dependent chaperoning of client proteins [Dunn *et al.*, 2015]. Mammalian Hsp90 has also been found to be acetylated at many sites, which can influence client maturation and co-chaperone binding [Scroggins *et al.*, 2007; de la Rosa *et al.*, 2014]. Nitrosylation inhibits client activation *in vivo* and ATPase activation *in vitro* [Martínez-Ruiz *et al.*, 2005; Retzlaff *et al.*, 2009]. SUMOylation in the Hsp90-NTD, facilitates the recruitment of Aha1 [Mollapour *et al.*, 2014]. Finally, methylation has also been reported for Hsp90 and is thought to play a role in human carcinogenesis [Donlin *et al.*, 2012; Hamamoto *et al.*, 2014]. Thus PTMs offer further complexity in regulating Hsp90 and act as switch points for allosteric communication.

1.8.5 Hsp90 clients

In addition to the huge cohort of co-chaperones, another feature that sets Hsp90 apart from all other chaperones is its set of substrate proteins. While Hsp90 shows some specificity in its client proteins, to date more than 300 client proteins have been identified for Hsp90 (for an updated list see [Picard, 2015]). Since Hsp90 client proteins belong to diverse functional and structural protein families, it has not been possible to identify any common sequence or domain among them that Hsp90 might recognize. Two criteria common to all the Hsp90 client proteins are, first, they interact with Hsp90 and second, the inhibition of Hsp90 leads to a decrease in client stability and activity. The interaction with the Hsp90 machinery enables

their correct folding, activation, transport and even degradation [Pratt *et al.*, 2006; Picard *et al.*, 1990; Pratt, 1990; Young *et al.*, 2003; Whittier *et al.*, 2004; Wang *et al.*, 2006]. Recent work on Tau and the glucocorticoid receptor have led to the notion that Hsp90 does not require any specific client structure but it binds proteins which have hydrophobic residues scattered over a large surface area [Karagöz *et al.*, 2014; Lorenz *et al.*, 2014; Karagöz & Rüdiger, 2015]. Hsp90 client proteins belong to various functional classes, the most predominant and well-studied ones being nuclear receptors and protein kinases [Joab *et al.*, 1984; Ziemiecki *et al.*, 1986; Smith & Toft, 1992; Xu & Lindquist, 1993; Wayne *et al.*, 2011; Taipale *et al.*, 2012]. Besides these, there are also E3 ligases [Taipale *et al.*, 2012], transcription factors, including the key activator of the heat shock response, HSF1 and the tumor suppressor p53 [Zou *et al.*, 1998; Walerych *et al.*, 2004]. By interacting with its substrate proteins, Hsp90 also plays a key regulatory role in processes such as innate and adapted immune response [Li *et al.*, 2002; Mayor *et al.*, 2007; Proia & Kaufmann, 2015], protein transport and secretion by interacting with components of the Rab GTPase cycle [Chen *et al.*, 2005; Lotz *et al.*, 2008], DNA repair [Pennisi *et al.*, 2015] and RNA processing [Boulon *et al.*, 2008; Zhao *et al.*, 2008; Miyoshi *et al.*, 2010]. These examples just provide a glimpse into the enormous diversity of the Hsp90 client proteins. Due to its far-reaching influence Hsp90 has emerged as a promising target for anti-cancer and anti-fungal therapeutics [Taldone *et al.*, 2014; Veri & Cowen, 2014]. The precise mode of action of Hsp90 and its ability to chaperone such diverse proteins still remains a hot topic of investigation. The intrinsic conformational flexibility of Hsp90 and the 'tool-box' of co-chaperones together with post-translational regulation seems to contribute to the plasticity of Hsp90 in chaperoning its diverse 'clientèle'. The client proteins used in this study are listed in the following section (Table 1.2).

Table 1.2: Hsp90 client proteins used in this work

Class	Name	Abbr.	References
Steroid hormone receptors	Glucocorticoid receptor	GR	[Paul *et al.*, 2014; Lorenz *et al.*, 2014]
	Androgen receptor	AR	[Fang *et al.*, 1996; Rao *et al.*, 2001; Paul *et al.*, 2014]
	Progesterone receptor	PR	[Sun *et al.*, 2012; Paul *et al.*, 2014; Kosano *et al.*, 1998]
	Estradiol receptor	ER	[Oxelmark *et al.*, 2003; Fliss *et al.*, 2000]
	Mineralocorticoid receptor	MR	[Faresse *et al.*, 2010; Paul *et al.*, 2014]

Table 1.2: Hsp90 client proteins used in this work

Class	Name	Abbr.	References
	GR F602S	GR1e	[Bledsoe *et al.*, 2002; Kirschke *et al.*, 2014]
	GR A605V, M752T, V702A, E705G, F602S	GR9a	[Seitz *et al.*, 2010; Lorenz *et al.*, 2014]
Kinases	Viral Src kinase	v-Src	[Xu & Lindquist, 1993; Panaretou *et al.*, 2002; Boczek *et al.*, 2015]
	cellular Src mutants	c-Src3M c-Src3MΔC	[Boczek *et al.*, 2015]

- Steroid hormone receptors (SHRs)

  Steroid hormone receptors are bona fide and the best studied Hsp90 client proteins. These receptors, upon activation by steroid hormones, undergo conformational changes and translocate from the cytosol to the nucleus. In the nucleus they can function as transcription factors which turn on specific target genes, thus affecting development, homoeostasis and metabolism of an organism [Evans, 1988]. The SHRs domain structure consist of an N-terminal variable domain, a DNA-binding domain (DBD) followed by a variable hinge region which connects the DBD to the C-terminal ligand binding domain (LBD) [Kumar & Thompson, 1999] (Figure 1.9). The DBD is highly conserved and is responsible for binding to the specific DNA sequence called hormone response element (HRE) thus enabling the SHRs to act as transcription factors. The LBD, as the name suggests, is involved in hormone binding and is also important in binding to Hsp90.

  The SHRs belonging to the subfamily 3 of nuclear receptors, classified on the basis of their function and mechanism, have been used in this study. [Mangelsdorf *et al.*, 1995]. These include the glucocorticoid receptor (GR),the mineralocorticoid receptor (MR), the estrogen receptor-α (ER), the progesterone receptor (PR) and the androgen receptor (AR). The SHRs require Hsp90 to reach their hormone-activable conformation. In brief, the partially folded SHR is passed on from the Hsp70 to the Hsp90 machinery. Hsp90, together with a large cohort of co-chaperones forms and 'holds' the SHR in their mature conformation compatible for ligand binding. The receptors are predominantly localized in the cytosol and shuttle to the nucleus upon hormone binding (AR and GR). Alternatively, they can be present in the hormone-bound and unbound form in the nucleus (ER and PR). MR without

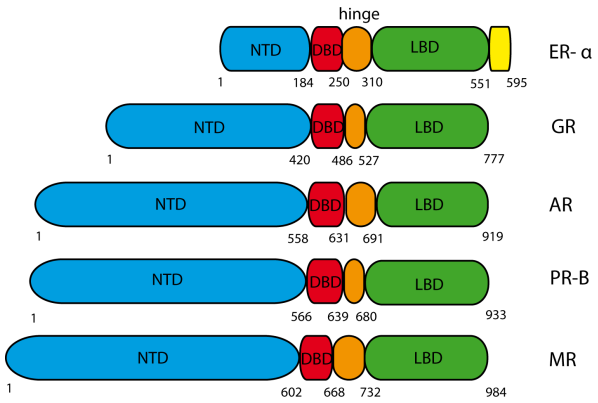

Figure 1.9: Schematic representation of the domain structure of SHRs. Each of the SHRs, have an N-terminal domain (NTD, blue), a DNA-binding domain (DBD, red), a hinge region (orange) and a ligand-binding domain (LBD, green). The NTD and the hinge regions are variable, while the DBD and LBD are conserved among the SHRs. The numbers indicate domain boundaries according to UniProt IDs: ER-P03372, GR-P04150, AR-P10275, PR-B-P06401 and MR-P08235.

bound-hormone is present in equal amount in the cytosol and nucleus [Echeverria & Picard, 2010]. The import in the nucleus is mediated by the nuclear localization signal (NLS) located in the variable region and the LBD [Picard *et al.*, 1990; Picard & Yamamoto, 1987; Zhou *et al.*, 1994]. The NLS is hidden by bound chaperones and is exposed only upon hormone binding. Evolutionarily, GR and MR show the highest sequence homology, followed by PR, AR and ER with decreasing homology [Mangelsdorf *et al.*, 1995].

During the last decades several distinct complexes with SHRs, Hsp90 and co-chaperones have been shown [Smith, 1993; Scherrer *et al.*, 1992; Pratt, 1992; Lorenz *et al.*, 2014]. The Hsp90 chaperone cycle has been best described for GR and PR. According to reconstitution experiments, a SHR must pass through three different complexes. SHR first binds Hsp40 which recruits it to Hsp70. This forms the 'early complex'. Sti1/Hop1 binds to Hsp70 and Hsp90 simultaneously. It stabilizes the open conformation of Hsp90 and inhibits its ATPase activity, thus enabling the transfer of the SHR from Hsp70 to Hsp90. While this mechanism has been established for GR, it is not clear whether all SHRs are transferred in this way. This forms the 'intermediate' complex [Cintron & Toft, 2006]. Recent work using sophisticated biophysical methods like FRET, aUC and NMR have shown that the other TPR site of Hsp90 can be occupied by PPIases, leading to an 'asymmetric complex' [Southworth & Agard, 2011; Lorenz *et al.*, 2014; Mayer & Le Breton,

2015; Ratajczak *et al.*, 2015]. The association of p23 and ATP in the next step leads to the closing of Hsp90 and the dissociation of Hsp70 and Hsp40 and Sti1 forming the 'late complex'. Another PPIase or TPR co-chaperone can then bind the free MEEVD domain. Drastic conformational changes of Hsp90 from the open to the compact conformation then ensue and ATP is hydrolysed. After ATP hydrolysis, p23 and the PPIases are released and the cycle can repeat. A general schematic representation of the Hsp90 cycle for SHRs is shown in Figure 1.10.

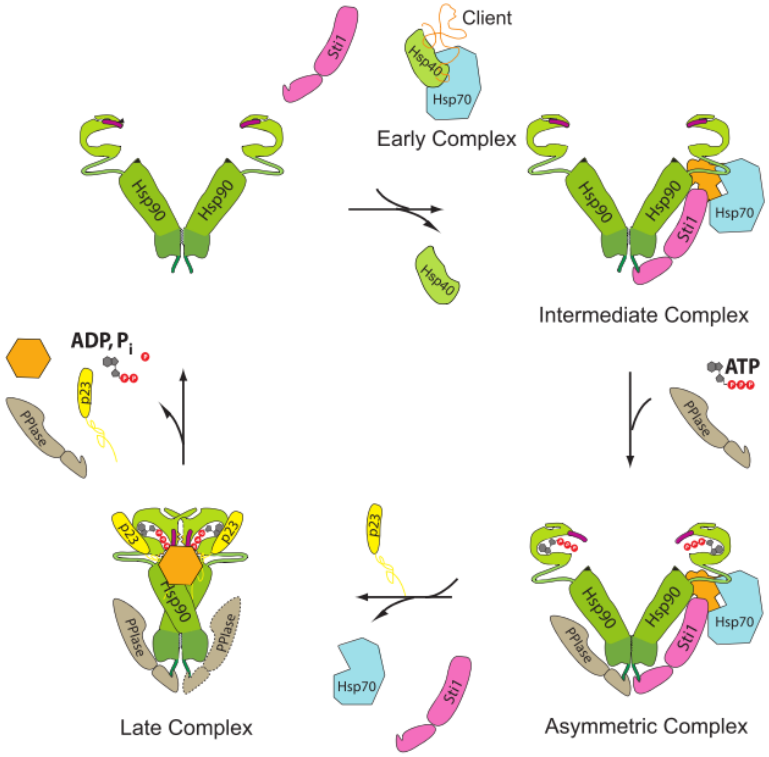

Figure 1.10: Hsp90 cycle for SHRs. A simplistic model for the Hsp90 chaperone cycle for SHRs is shown. Figure adopted from [Li *et al.*, 2013]

The mammalian PPIases FKBP52, FKBP51 and CyP40 are found to some degree in all receptor complexes [Barent *et al.*, 1998; Ratajczak *et al.*, 2015], but they seem to be selected by specific client proteins. FKBP51 preferentially interacts with PR, GR and MR while CyP40 is found in complex with ER [Davies & Sánchez, 2005; Riggs *et al.*, 2007, 2003; Tranguch *et al.*, 2005]. FKBP52 leads to an increase in hormone binding affinity by GR, but this function is not essential for GR activation [Pratt & Toft, 2003]. The function of the co-chaperones in the SHR complexes is thus not well understood and this open area of investigation is the basis of this work.

- v-Src

  v-Src is a viral kinase belonging to the Src kinase family of non-receptor tyrosine kinases, which play an important role in many signal transduction pathways. It is the first identified and one of the most stringent Hsp90 client proteins [Brugge *et al.*, 1981]. Additionally, v-Src is also the first identified oncogene [Rous, 1911]. Infection of chicken with the Rous sarcoma virus triggers malignant tumors of connective tissue, which is due to the constitutive activity of v-Src. The human homologue of this viral kinase is called cellular Src kinase (c-Src), with which it shares 98% homology [Stéhelin & Graf, 1978]. c-Src is normally inactive in the cells and can be activated by phosphorylation under certain conditions. Unlike its viral homologue, c-Src is dependent on Hsp90 only in its nascent state and dissociates quickly after kinase folding is achieved [Xu *et al.*, 1999]. It has therefore been classified as non-client protein of Hsp90. v-Src on the other hand, stably binds Hsp90 and stringently depends on Hsp90 for its activation [Brugge, 1986; Xu & Lindquist, 1993; Xu *et al.*, 1999]. c-Src is quite resistant to chemical as well as thermal denaturation, contrary to v-Src which is already unstable at body temperature [Boczek *et al.*, 2015].

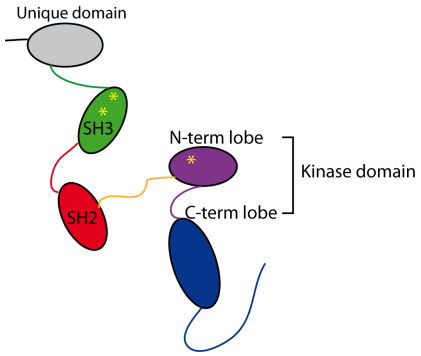

Figure 1.11: Schematic representation of the domain structure of Src kinases. The N-terminal unique domain is shown in grey. SH3 in green, SH2 in red. The kinase domain N-terminal lobe is shown in purple, while the C-terminal lobe is blue. A long C-terminal extension is also denoted which is missing in c-Src3MΔC. Yellow (*) denote the mutations in the c-Src constructs. Two are in the SH3 and one in the kinase domain. Figure adapted from [Boczek *et al.*, 2015].

Src kinases consist of a unique domain followed by SH3 and SH2 domains and a flexible linker which connects the SH2 domain with a highly conserved kinase domain (Figure 1.11). c-Src has an additional stretch at its C-terminus that includes a tyrosine at position 527, whose phosphorylation status regulates its kinase activ-

ity [Cooper *et al.*, 1986]. v-Src differs from c-Src by several point mutations and is missing the C-terminal "regulatory" stretch. Due to these differences, v-Src cannot be down regulated and is constantly active leading to its pathological effects [Reynolds *et al.*, 1987; Takeya & Hanafusa, 1983]. c-Src can be turned into v-Src by introducing point mutations and deleting the C-terminal, and several of these mutants have been linked to cancer progression and metastasis in humans [Kato *et al.*, 1986; Miyazaki *et al.*, 1999] Despite the close homology, v-Src and c-Src show a completely different model for chaperone dependence. This hints towards stability and conformation of the client being important for substrate recognition by Hsp90 [Citri *et al.*, 2006; Hikri *et al.*, 2009; Boczek *et al.*, 2015]. The co-chaperone Cdc37 was always found in a complex with Hsp90 and v-Src, as well as other kinases [Stancato *et al.*, 1994; Stepanova *et al.*, 1996]. Therefore Cdc37 is referred to as a kinase specific co-chaperone [Mandal *et al.*, 2007]. As mentioned previously, Cdc37 is thought to recruit kinases to Hsp90 [Boczek *et al.*, 2015]. The phosphatase PP5 (yeast Ppt1) associates with the Hsp90-kinase-Cdc37 ternary complex and regulates the phosphorylation states of Cdc37 [Vaughan *et al.*, 2008].

1.9 The Hsp70-Hsp90 cycle

Summarizing the state-of-the-art knowledge that we have about Hsp90 machinery and its modes of regulation, a dynamic conformational Hsp90 cycle fuelled by ATP hydrolysis can be assembled (Figure 1.12). Based on our understanding it is apparent that Hsp70 must act earlier than Hsp90 as it has a high affinity for short hydrophobic stretches [Karagöz & Rüdiger, 2015; Mayer, 2013]. 'Connector' co-chaperones like Sti1 can act as a scaffold for the client transfer to occur. However, given the fact that Sti1 is not essential for viability in yeast and its role has been mainly defined in context of GR and v-Src, there could be alternative client transfer pathways in the cell [Alvira *et al.*, 2014; Lotz *et al.*, 2003]. Moreover, in spite of the universal presence of co-chaperones, there isn't a single one preserved in all species [Johnson & Brown, 2009].

It is apparent from the model that the current picture of the Hsp90 system is far from complete. While some of the co-chaperones have been characterized as client-recruiters, or Hsp90 modulators, most of them have not been "fitted" in the Hsp90 chaperone cycle. While some co-chaperones bind the same domain of Hsp90 or bind different Hsp90 conformations, sterical overlap and competition for binding

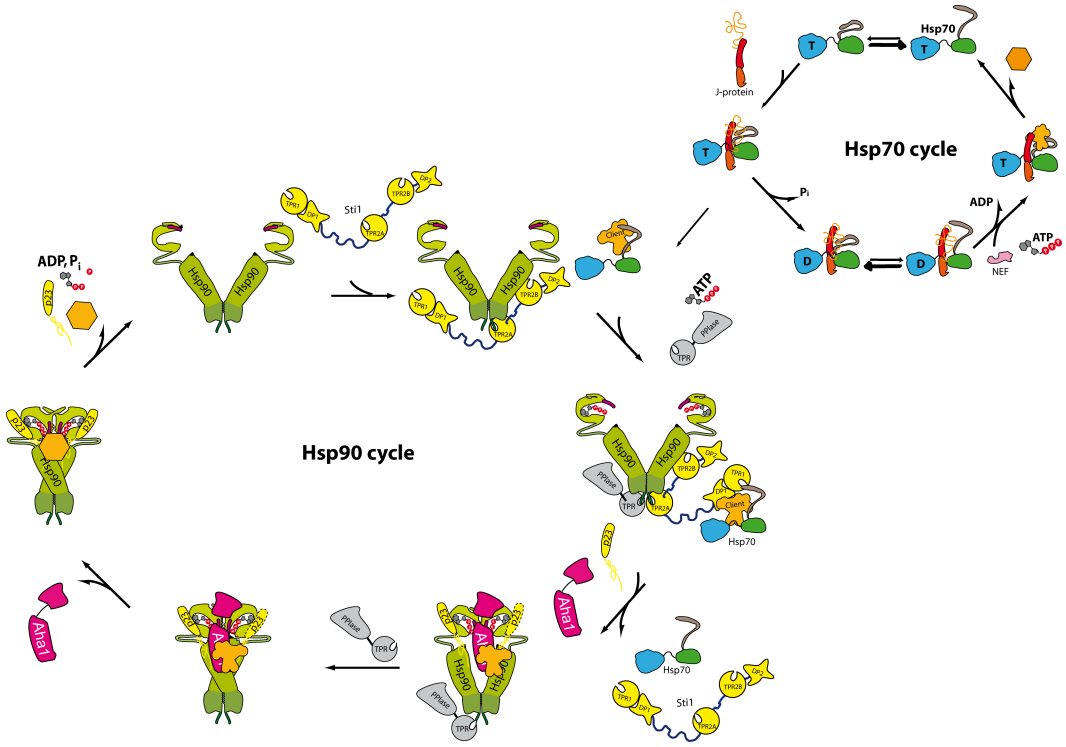

Figure 1.12: Hsp70-Hsp90 chaperone cycle. Newly synthesized and/or partially folded proteins are delivered to Hsp70 in complex with Hsp40 (Ydj1). Hsp70 machinery can process non-client proteins on its own (Hsp70 cycle). Hsp90-client proteins like GR are transferred from the Hsp70 to the Hsp90 machinery through the adaptor protein Sti1. For the progression of the cycle, Aha1 (magenta) and PPIase (grey) synergistically lead to the exit of Sti1 and form an asymmetric chaperone complex. Aha1 accelerates the N-terminal dimerization of Hsp90. Binding of p23/Sba1 replaces Aha1 and stabilizes a fully closed Hsp90 conformation. Upon ATP hydrolysis, p23 is released and the cycle repeats. Figure adapted from [Li *et al.*, 2012, 2013; Mayer & Le Breton, 2015].

sites restricts the combinations of co-chaperones that can bind to Hsp90 at the same time [Siligardi *et al.*, 2004; Harst *et al.*, 2005]. For instance, Hsp90 forms ternary complexes with Aha1 and Cpr6, but not Aha1 and Cpr7 [Li *et al.*, 2013], suggesting that only certain co-chaperone combinations may form. The exact role and contribution of the co-chaperones in client maturation is not completely clear. The emerging picture is that the Hsp70-Hsp90 chaperone cycle is largely dictated by the client protein. In other words, the co-chaperones seem to customize the Hsp90 cycle to fit the requirements of the client proteins (reviewed in [Li *et al.*, 2013]). Thus, despite major contributions in deciphering the molecular mechanism of Hsp90, a thorough understanding of the role of co-chaperones for client maturation remains enigmatic.

1.10 Objectives

The aim of this work is to deepen our understanding of the Hsp90 machinery, especially the role of co-chaperones in the client activation process. Extensive research over the past decades has uncovered the central importance of Hsp90 in numerous cellular pathways. The diversity of the client proteins has made Hsp90 a potential target for many therapeutic strategies [Taldone *et al.*, 2014]. However, several key questions remain unanswered. For instance, how does Hsp90 recognize its client proteins? How can Hsp90 chaperone such a wide diversity of clients and yet have some specificity unlike the promiscuous Hsp70? And most importantly, how does the large repertoire of Hsp90 co-chaperones contribute to the activation of client proteins. While a lot is known about the modulation of Hsp90's conformational dynamics by co-chaperones, the client side of the story is still relatively unexplored.

In this work, we asked two main questions, first, are the client proteins dependent on specific Hsp90 co-chaperones for their maturation? And second, if yes, then how are the co-chaperones affecting this process? To this end, we used *Saccharomyces cerevisiae* to systematically study several bona fide Hsp90 clients in co-chaperone deletion strains. The Hsp90 system is conserved between yeast and man (see Table 1.1). Thus, we chose to study the chaperone activity of Hsp90 and its co-chaperones in a simple cellular context while maintaining homologous interactions within the chaperone complexes. Most Hsp90 co-chaperones are not essential for viability in yeast. Therefore the respective deletion strains are excellent tools to study the influence of the co-chaperones on the activation and/or maturation of a specific client proteins *in vivo*. For studying the essential co-chaperones, other 'knock-down' strategies were used. Over the last decades, scattered information has been generated for several of these client-co-chaperone dependencies in different background yeast strains. However, a comprehensive analysis of these proteins is largely missing. The objective of this work is to investigate well-known Hsp90 client proteins in a single background yeast strain in order to get a thorough knowledge of how the Hsp90 chaperone machinery is customized to serve different client proteins in a similar environment. Among the client proteins chosen for this study, are also five members of the SHR family. This gives us an opportunity to observe the similarities and differences in the chaperone requirements within a single family as well as among different protein classes. Based on the systematic screen of client-co-chaperone dependencies, the molecular action of some client-co-chaperone pairs is further investigated in depth.

2 Materials and methods

2.1 Materials

2.1.1 Chemicals

Chemicals	Origin
2-Mercaptoethanol	Sigma-Aldrich (St. Louis, USA)
2-Nitrophenyl β-D-galactopyranoside (ONPG)	Sigma-Aldrich (St. Louis, USA)
2-Propanol	Roth (Karlsruhe, Germany)
4-(2-hydroxyethyl)-1-piperazine ethanesulfonic acid (HEPES) Pufferan®	Roth (Karlsruhe, Germany)
5'-Fluoroacetic acid (5'-FOA)	Fermentas (St. Leon-Rot, Deutschland)
Acetic acid glacial	Roth (Karlsruhe, Germany)
Acrylamide/Bis solution, 19:1 (40% w/v)	Serva (Heidelberg, Germany)
Adenosine 5'-diphosphate (ADP) disodium salt hydrate	Roche (Mannheim, Germany)
Adenosine 5'-triphosphate (ATP) disodium salt hydrate	Roche (Mannheim, Germany)

Chemicals	Origin
Adenosine 5'-(β,γ-imido)triphosphate (AMPPnP) lithium salt hydrate	Roche (Mannheim, Germany)
Adenosine-5'-o-(3-thio-triphosphate) (ATPγS) lithium salt hydrate	Roche (Mannheim, Germany)
Agar Agar SERVA Kobel powder research grade	Serva (Heidelberg, Germany)
Agarose SERVA research grade	Serva (Heidelberg, Germany)
Amino acids	Sigma-Aldrich (St. Louis, USA)
Ammonium persulfate (APS)	Roth (Karlsruhe, Germany)
Ampicillin sodium salt	Roth (Karlsruhe, Germany)
Bacto^{TM} Peptone Enzymatic Digest of protein	Becton, Dickinson & Company (Sparks, USA)
Bromophenol blue sodium salt	Merck (Darmstadt, Germany)
Coomassie SERVA blue research grade	Serva (Heidelberg, Germany)
D(+)-Glucose monohydrate	Merck (Darmstadt, Germany)
Deoxycorticosterone (DOC)	Sigma-Aldrich (St. Louis, USA)
Deoxyribonucleotidetriphosphate (dNTPs)	Roche (Mannheim, Germany)
Dithiothreitol (DTT)	Roth (Karlsruhe, Germany)
di-Sodium hydrogen phosphate dihydrate	Merck (Darmstadt, Germany)
Difco^{TM} Yeast Nitrogen Base w/o Amino Acids	Becton, Dickinson & Company (Sparks, USA)
Dimethylsulfoxid (DMSO)	Merck (Darmstadt, Germany)
Dipotassium phosphate trihydrate	Merck (Darmstadt, Germany)
DNA Stain G	Serva (Heidelberg, Germany)
Dodecylsulfate-Na-salt research grade (SDS)	Serva (Heidelberg, Germany)
Ethanol	Roth (Karlsruhe, Germany)
G418-Sulphate, Geneticin	GibcoBRL (Karlsruhe, Deutschland)
Galactose	Merck (Darmstadt, Deutschland)
Geldanamycin	
Glucose	Merck (Darmstadt, Deutschland)
Glycerine	Roth (Karlsruhe, Germany)
Hydrochloric acid	Roth (Karlsruhe, Germany)
Imidazole	Sigma-Aldrich (St. Louis, USA)
Isopropyl-β-D-thiogalactopyranoside (IPTG)	AppliChem (Darmstadt, Germany)
Kanamycin Sulfate 750 U/mg	Serva (Heidelberg, Germany)

Chemicals	Origin
LB-Medium Powder	Serva (Heidelberg, Germany)
Lithium acetate	Roth (Karlsruhe, Germany)
Magnesium chloride hexahydrate	Merck (Darmstadt, Germany)
Magnesium sulphate	Merck (Darmstadt, Germany)
Methanol	Roth (Karlsruhe, Germany)
Milk powder blotting grade	Roth (Karlsruhe, Germany)
N'N'N'N'-Tetramethylethylenediamine (TEMED)	Roth (Karlsruhe, Germany)
Nicotineamide adenine dinucleotide (NADH)	Roche (Mannheim, Germany)
Orange G	Sigma-Aldrich (St. Louis, USA)
Phosphoenolpyruvate (PEP)	Roche (Mannheim, Germany)
Phosphoric acid	Merck (Darmstadt, Germany)
Polyethylene glycol (PEG) 4000 for synthesis	Merck (Darmstadt, Germany)
Polyethylene-exorbitant-monolaureate (Tween-20)	Merck (Darmstadt, Germany)
Ponceau staining solution	Serva (Heidelberg, Germany)
Potassium chloride	Roth (Karlsruhe, Germany)
Potassium dihydrogen phosphate	Merck (Darmstadt, Germany)
Protease Inhibitor mix HP, FY, G	Serva (Heidelberg, Germany)
Radicicol	Sigma-Aldrich (St. Louis, USA)
Raffinose	Merck (Darmstadt, Germany)
Salmon sperm DNA	Sigma-Aldrich (St. Louis, USA)
Sodium chloride	Merck (Darmstadt, Germany)
Sodium dihydrogen phosphate monohydrate	Merck (Darmstadt, Germany)
Sodium hydroxide	Merck (Darmstadt, Germany)
Titriplex® (EDTA)	Merck (Darmstadt, Germany)
Tris-(hydroxymethyl)-aminomethane, TRIS, Pufferan®	Roth (Karlsruhe, Germany)
Triton X-100	Merck (Darmstadt, Germany)
Urea	Merck (Darmstadt, Germany)
Xylene-cyanol blue	Roth (Karlsruhe, Germany)
Yeast Extract	Merck (Darmstadt, Germany)
Yeast Nitrogen Base (YNB)	Difco (Detroit, USA)
YPD Broth	Roth (Karlsruhe, Germany)

Chemicals	Origin
β-Estradiol	Sigma-Aldrich (St. Louis, USA)
Hormones	
11- deoxycorticosterone (DOC)	Sigma-Aldrich (St. Louis, USA)
Aldosterone	Sigma-Aldrich (St. Louis, USA)
Estradiol	Sigma-Aldrich (St. Louis, USA)
Progesterone	Sigma-Aldrich (St. Louis, USA)
Dihydroxy-testosterone	Sigma-Aldrich (St. Louis, USA)

2.1.2 Laboratory equipment and consumables

Laboratory equipment	Manufacturer
Autoclaves and Laboratory ovens	
Autoclave	Memmert (Büchenbach, Germany)
60° oven	Binder (Tuttlingen, Germany)
Sanoclav	Wolf (Bad Überkingen-Hausen, Germany)
Blotting devices	
Chromatography paper 3 mm Chr	GE Healthcare (Chalfont St. Giles, UK)
ImageQuant LAS 4000	GE Healthcare (Chalfont St. Giles, UK)
Roti® -PVDF, pore size 0.25 μm	Roth (Karlsruhe, Germany)
Semi-dry blotting chambers	Biometra (Göttingen, Germany)
Western Bright™ ECL-Spray	Advansta (Menlo Park, USA)
Centrifuges and rotors	
Analytical ultracentrifuge Optima XL-A	Beckman (Krefeld, Germany)
Avanti J25 and J26 XP	Beckman Coulter (Brea, USA)
JA-10, JA-25.50 rotors	Beckman (Krefeld, Germany)
Heraeus Fresco 17	Heraeus (Hanau, Germany)
Mikro 20, Universal 16R/320R, Rotina 420R	Hettich Zentrifugen (Tuttlingen, Germany)
Tabletop centrifuge 5415C	Eppendorf (Köln, Germany)
Chromatography systems	
Äkta FPLC; UPC906; P920	GE Healthcare (Chalfont St. Giles, UK)

Laboratory equipment	Manufacturer
Superloop™	GE Healthcare (Chalfont St. Giles, UK)
Columns for Chromatography	
HAT 2.5 ml	GE Healthcare (Chalfont St. Giles, UK)
His MultiTrap FF 5 ml	GE Healthcare (Chalfont St. Giles, UK)
Resource-Q 6 ml	GE Healthcare (Chalfont St. Giles, UK)
16/60 Superdex 75 pg 120 ml	GE Healthcare (Chalfont St. Giles, UK)
16/60 Superdex 200 pg 120 ml	GE Healthcare (Chalfont St. Giles, UK)
SDS-electrophoresis devices	
Mighty Small dual gel caster	GE Healthcare (Chalfont St. Giles, UK)
TB1 Thermoblock	Biometra (Göttingen, Germany)
Mighty Small II SE/SE260 chambers	GE Healthcare (Chalfont St. Giles, UK)
Hamilton syringes	Hamilton (Switzerland)
Electrophoresis power supplies	
EPs 601, 1001, 3500	GE Healthcare (Chalfont St. Giles, UK)
PCR cyclers	
MJ Mini Personal Thermocycler	Bio Rad (Hercules, USA)
Primus	MWG Biotech (Ebersberg, Germany)
Gel documentation systems	
Bio-Doc IITM gel documentation system	Biometra (Göttingen, Germany)
ImageQuant 4000	GE Healthcare (Chalfont St. Giles, UK)
pH-meter	
pH electrode Multi Cal®	WTW (Weilheim, Germany)
Pipettes and accessories	
Automatic multi-channel pipette (200 μl)	VWR International (Darmstadt, Germany)
Pasteur pipettes (230 mm)	VWR International (Darmstadt, Germany)
Pipetboy	
Pipetman® (10, 20, 200 and 1000 μl)	Gilson (Middleton, USA)
MagRack 6	GE Healthcare (Chalfont St. Giles, UK)
Refrigerators and ice machines	
Economy, Premium, Comfort	Liebherr (Bulle, Switzerland)

Laboratory equipment	Manufacturer
Ice machine	Ziegra Eismaschinen (Hannover, Germany)
Refrigerator	Bosch (Gerlingen, Germany)
Ultra low temperature freezer	New Brunswick Scientific (Enfield, USA)
Freezer −80°C	Sanyo (San Diego, USA)
Scales	
SI-4002	Denver Instrument (New York, USA)
Universal, BL310, BP1215	Saratorius (Göttingen, Germany)
Shaking and mixing devices	
Certomat® RM	Sartorius (Göttingen, Germany)
Magnetic stirrer with heating MR 3001	Heidolph (Schwabach, Germany)
Polymax 1040/2040	Heidolph (Schwabach, Germany)
Reax control vortexer	Heidolph (Schwabach, Germany)
Roller mixer Stuart™ SRT6D	Stuart Equipment (USA)
Thermomixer compact/comfort	Eppendorf (Hamburg, Germany)
Tube mixer	New Brunswick Scientific (Enfield, USA)
Variomag Monoshake (96-well)	H+P Labortechnik (Oberschleißheim,Germany)
Vortex MS2	IKA (Wilmington, USA)
Incubators	
Incubators	New Brunswick Scientific (Enfield, USA)
Water bath Haake F6-K	Haake (Karlsruhe, Germany)
Absorption spectrophotometers	
Cary 50/100 Bio UV-Vis	Varian (Palo Alto, USA)
Nano Drop® ND-1000	Peqlab (Erlangen, Germany)
Sunrise absorbance reader	Tecan (Salzburg, Austria)
Genios Microplate reader	Tecan (Salzburg, Austria)
Ultraspec 1100 pro	GE Healthcare (Chalfont St. Giles, UK)
Cell disruption machines	
Basic Z cell disruption system	Constant systems (Warwick, UK)
Silent crusher M	Heidolph (Schwabach, Germany)
Swing mill MM400	Retsch® (Haan, Germany)

Laboratory equipment	Manufacturer
Consumables	
Cellulose acetate filter (pore size: 0.45 μm)	Sartorius (Göttingen, Germany)
Concentrator Amicon® (MWCO: 10, 30 kDa)	Merck (Darmstadt, Germany
Dialyse Membrane Spectra/Por Dialysis (MWCO: 6-8000 Da)	SpectrumLabs (Breda, Netherlands)
Eppendorf reaction tubes (0,25 ; 1,5; 2 ml)	Eppendorf AG (Hamburg, Germany)
Glass pearls and balls	Roth (Karlsruhe, Germany)
Mega Block 96-Well, 1.2 ml, PP	Sarstedt (Newton, USA)
Micro assay plate, chimney 96 well	Greiner Bio-one (Frickenhauesn, Germany)
Ni-Sepharose™ HP Beads	GE Healthcare (Chalfont St. Giles, UK)
Petri dishes	Greiner Bio-one (Frickenhauesn, Germany)
pH-indicator	Merck (Darmstadt, Germany)
Plastic cuvettes (10 x 4 x 45 mm)	Sarstedt (Newton, USA)
Quartz cuvettes (10 mm)	Hellma®
Tissue culture plate, 96-well, flat bottom with lid	Sarstedt (Newton, USA)

2.1.3 Antibodies

Antibodies	Source
Rabbit polyclonal antibodies against yeast proteins	
Hsp82, Sti1, Ppt1, Sba1	Pineda Antibody Services, Berlin
Cpr6, Aha1, Hch1, Tah1	Pineda Antibody Services, Berlin
Cpr7	Jill Johnson
Tah1	W.Houry, University of Toronto, Canada
Pih1	W.Houry, University of Toronto, Canada
Rabbit polyclonal antibodies against SHRs	
GR (P-20) sc-1002	Santa Cruz Biotechnologies, (Santa Cruz USA)

Antibodies	Source
PR (H-190) sc-7208	Santa Cruz Biotechnologies, (Santa Cruz USA)
AR (H-280): sc-13062	Santa Cruz Biotechnologies, (Santa Cruz USA)
MCR (H-300):sc-11412	Santa Cruz Biotechnologies, (Santa Cruz USA)
ERα (MC-20):sc-542	Santa Cruz Biotechnologies, (Santa Cruz USA)
huGR (N499)	Keith Yamamoto, University of California, San Francisco, CA
GR	Pineda Antibody Services, Berlin
MR	Pineda Antibody Services, Berlin
ER	Pineda Antibody Services, Berlin
Others mouse antibodies	
Monoclonal PGK	Invitrogen (Karlsruhe, Germany)
Monoclonal Phosphotyrosine (clone 4G10)	Millipore (Bedford, USA)
Polyclonal GFP	Roche
Monoclonal HA clone HA-7	Sigma
Monoclonal avian-Src EC10	Millipore (Bedford, USA)
Secondary monoclonal antibodies	
anti-mouse-POD conjugate	Sigma (St. Louis, USA)
anti-rabbit-POD conjugate	Sigma (St. Louis, USA)
Pierce^{TM} Anti-HA Magnetic Beads	Pierce Biotechnology (Rockford, USA)

2.1.4 Enzymes, standards and kits

Name	Source
Alkaline Phosphatase	Roche (Mannheim, Germany)
Pfu-DNA-Polymerase	Promega (Mannheim, Germany)
Pwo-DNA-Polymerase	Roche (Mannheim, Germany)
GoTaq® DNA polymerase	Promega (Madison, USA)
Phusion® High-Fidelity DNA Polymerase	NEB (Frankfurt, Germany)
T4 DNA Ligase	Promega (Madison, USA)

Name	Source
T4 DNA Polymerase	NEB (Frankfurt, Germany)
Q5® High-Fidelity DNA Polymerase	NEB (Frankfurt, Germany)
Restriction enzymes	Promega (Madison, USA)
DNA-Standard peqGOLD 1 kb with Orange G	Peqlab (Erlangen, Germany)
Pre-stained protein marker IV	Peqlab (Erlangen, Germany)
DNase	AppliChem (Darmstadt, Germany)
Salmon sperm DNA	Roche (Mannheim, Germany)
Lyticase from Anthrobacter luteus	Sigma-Aldrich (St. Louis, USA)
Lactate dehydrogenase (LDH) from rabbit muscle	Roche (Mannheim, Germany)
Pyruvate kinase (PK)	Roche (Mannheim, Germany)
Proteinase K	Sigma-Aldrich (St. Louis, USA)
Wizard® Plus SV Minipreps DNA Purification System	Promega (Madison, USA)
Wizard® SV Gel and PCR Clean-Up System	Promega (Madison, USA)
Site-Directed Mutagenesis Kit	Stratagene (La Jolla, USA)

2.1.5 Oligonucleotides

Primer name	Sequence
GRE-Fwd	gatccagaacaaaatgttctg
GRE-rev	cagaacattttgttctggatc
FLAG-huGR-BamHI-Fwd	gatcgtggatccgattacaaggatgacgacgataagatggactccaaagaatc
huGR-XhoI-Rev	gatctgctcgagtcacttttgatgaaacagaagttttttgatatttcc
FLAG-huAR-BamHI-Fwd	gatcgtggatccgattacaaggatgacgacgataagatggaagtgcagttagg
huAR-XhoI-Rev	gatctgctcgagtcactgggtgtggaaatagatgggc
FLAG-huPR-BamHI-Fwd	gatcgtggatccgattacaaggatgacgacgataagatgagccggtccgggtg
huPR-XhoI-Rev	gatctgctcgagtcacttttttatgaaagagaaggggtttcacc
FLAG-huER-BamHI-Fwd	gatcgtggatccgattacaaggatgacgacgataagatgaccctccacacc
huER-XhoI-Rev	gatctgctcgagtcagaccgtggcagggaaaccctc

Primer name	Sequence
FLAG-ratMR-SpeI-Fwd	gatcgtactagtgattacaaggatgacgacgataagatggaaaccaaaggc
ratMR-EcoRV-Rev	gatcgtgatatctcactttctgtgaaagtaaaggggtttgg
3xFLAG-GR-BamHI-f	gatcgtggatccatggactacaaagaccatgacggtgattataaagatcatgatatcgattacaaggatgacgatgacaagagcggcatggactccaaagaatc
Strep-GR-BamHI-f	gatcgtggatccatgtggagccacccgcagttcgaaaaaagcggcatggactccaaagaatc
HA-GR-BamHI-f	gatcgtggatccatgtacccatacgatgttccagattacgctagcggcatggactccaaagaatc
6His-GR-BamHI-f	gatcgtggatccatgggcagcagccatcatcatcatcatcacagcaggcggcatggactccaaagaatc
c-Myc-GR-BamHI-f	gatcgtggatccatggaacaaaaacttatttctgaagaagatctgaggcggcatggactccaaagaatc
HA-AR-BamHI-f	gatcgtggatccatgtacccatacgatgttccagattacgctagcggcatggaagtgcagttagg
HA-ER-BamHI-f	gatcgtggatccatgtacccatacgatgttccagattacgctagcggcatgaccatgaccctc
HA-PR-SpeI-f	gtagctactagtatgtacccatacgatgttccagattacgctagcggcatgagccggtccgggtg
HA-MR-SpeI-f	gatcgtactagtatgtacccatacgatgttccagattacgctagcggcatggaaaccaaaggc
HA-v-Src-BamHI-f	gatcgtggatccatgtacccatacgatgttccagattacgctagcggcatggctagcatgggg
v-Src-XhoI-r	gatctgctcgagctactcagcgacctccaacacacaagc
Aha1term-XhoI-r	gatctgctcgagcgcggatgccgtacagaactac
v-Src-Bem-HAFwd	gattacgctagcggcatggctagcatggggagc
v-Src-Bem-HArev	tggaacatcgtatgggtacatggatccactagttctagaatccg
GR-RTPCR fwd	cagtgtgcttgctcaggagagggg
GR-RTPCR rev	ggtgctttggtctgtggtatacaatttcacattgcc
eGFP-RTPCR fwd	gcggcattttgccttcctgtttttgctcaccc
eGFP-RTPCR rev	ggtatggcttcattcagctccgg
Tah1Fwd-FLIC	cagagaacagattggtggatccatgagccaatttgaaaagcag
Tah1Rev-FLIC	cagtggtggtggtggtggtgctcgagtcaggaccggtcgtatcc
Pih1Fwd-FLIC	cagagaacagattggtggatccatggccgatttcttattgag
Pih1Rev-FLIC	cagtggtggtggtggtggtgctcgagttatatatatatatatagtgtgcgttctttg
P-5'-bluntBamHI-HAFwd	gatcatgtacccatacgatgttccagattacgctagcggc
P-5'-bluntBamHI-HARev	gatcgccgctagcgtaatctggaacatcgtatgggtacat
colPCR-ARrev	ctgagtcatcctcgtccgg
colPCR-GRrev	gcttgcctgacagtaaactgtgcc
colPCR-PRrev	ggaagtcgctatagagaggg

2.1.6 Plasmids

2.1.6.1 Bacterial plasmids

Vector	Insert	Source
pET28a	Hsp82	Hessling, TU München
pET28a	Aha1	Richter, TU München
pRSETa	Cpr6	Prodromou, University of Sussex, UK
pET28a	Ppt1	Soroka, TU München
pET28a	Hch1	Li, TU München
pRSETa	Cpr7	Li, TU München
pETSUMO	Tah1	This work
pETSUMO	Pih1	This work
pETHalo	rMR-LBD-WT	This work
pETHalo	rMR-LBD-C805S	This work

2.1.6.2 Yeast plasmids

Vector	Insert	Source
Plasmid name	Description	Source
p415GPD	Empty vector	LGC Standards GmbH (Wesel, Germany)
pRS313	Empty vector	LGC Standards GmbH (Wesel, Germany)
p413GPD	Empty vector	LGC Standards GmbH (Wesel, Germany)
p413GPD human GR	GR-Expression plasmid, GPD-Promoter	Schmid, TU München
p413GPD human AR	AR-Expression plasmid, GPD-Promoter	Schmid, TU München
p413GPD rat MR	MR-Expression plasmid, GPD-Promoter	Schmid, TU München
p413GPD human ER	ER-Expression plasmid, GPD-Promoter	Schmid, TU München

Vector	Insert	Source
p413GPD human PR	PR-Expression plasmid, GPD-Promoter	Schmid, TU München
p413GPD human HA-GR	HA-GR-Expression plasmid, GPD-Promoter	This work
p413GPD human HA- AR	HA-AR-Expression plasmid, GPD-Promoter	This work
p413GPD rat HA-MR	HA-MR-Expression plasmid, GPD-Promoter	This work
p413GPD human HA-ER	HA-ER-Expression plasmid, GPD-Promoter	This work
p413GPD human HA-PR	HA-PR-Expression plasmid, GPD-Promoter	This work
p413GPD human FLAG-GR	FLAG-GR-Expression plasmid, GPD-Promoter	This work
p413GPD human FLAG-AR	FLAG-AR-Expression plasmid, GPD-Promoter	This work
p413GPD rat FLAG-MR	FLAG-MR-Expression plasmid, GPD-Promoter	This work
p413GPD human FLAG-ER	FLAG-ER-Expression plasmid, GPD-Promoter	This work
p413GPD human FLAG-PR	FLAG-PR-Expression plasmid, GPD-Promoter	This work
p413GPD human His-GR	His-GR-Expression plasmid, GPD-Promoter	This work
p413GPD human Strep-GR	Strep-GR-Expression plasmid, GPD-Promoter	This work
p413GPD human c-Myc-GR	c-Myc-GR-Expression plasmid, GPD-Promoter	This work
p413GPD human GFP-GR	GFP-GR-Expression plasmid, GPD-Promoter	This work
p413Gal1 human GR	GR-Expression plasmid, galactose inducible Promoter	This work
pUCΔSS-26X	β-Galactosidase-Reporter plasmid for GR, MR, PR, AR	J.F. Louvion
pΔsERE	β-Galactosidase-Reporter plasmid for ER	B. Freeman, University of Illinios, USA

Vector	Insert	Source
p413Gal1 v-Src WT	v-Src-Expression plasmid, galactose inducible Promoter	Boczek, TU München
p413Gal1 v-Src 3M	v-Src 3M-Expression plasmid, galactose inducible Promoter	Boczek, TU München
p413Gal1 v-Src 3M delta C	v-Src 3M delta C-Expression plasmid, galactose inducible Promoter	Boczek TU München
p413Gal1 c-Src WT	c-Src-Expression plasmid, galactose inducible Promoter	Boczek, TU München
p426GPDβGal	β-Galactosidase-Expression plasmid, GPD-Promoter	Schmid, TU München

2.1.7 Media

2.1.7.1 Bacterial media

Medium	Constituents	Concentration
LB medium	LB	20 g/l
dYT	NaCl	5 g/l
	Yeast Extract	10 g/l
	Tryptone/Peptone	16 g/l
Additives	Ampicillin	200 μg /ml in ddH_2O
	Kanamycin	75 μg /ml in ddH_2O
for plates	Bacto-Agar	2% w/v
Auto-induction medium (1 L)		
958 ml ZY	tryptone	1%
	yeast extract	0.5%
20 ml 50 x M	Na_2HPO_4	25 mM

Medium	Constituents	Concentration
	KH_2HPO_4	25 mM
	NH_4Cl	50 mM
	Na_2SO_4	5 mM
20 ml 50 x 5052	Glycerol	0.5%
	Glucose	0.05%
	α-Lactose	0.2%
2 ml 1 M $MgSO_4$	$MgSO_4$	2 mM
0.2 ml 1000 x trace elements	trace elements	0.2 x

2.1.7.2 Yeast media

Medium	Constituents	Concentration
YPD-medium	YPD	50 g/l
Minimal medium (CSM)	YNB	6.7 g/l
	Selective amino acid mix	0.87 g/l
	Glucose/ Galactose/ Raffinose	20 g/l
Selective amino acid mix	Adenine	0.5 g/l
	Arginine	2 g/l
	Aspartate	2 g/l
	Histidine	2 g/l
	Leucine	10 g/l
	Lysine	2 g/l
	Methionine	2 g/l
	Phenylalanine	2 g/l
	Threonine	2 g/l
	Tryptophan	2 g/l
	Tyrosine	2 g/l
	Uracil	2 g/l
Additives:	G418-Sulfate	200 mg/l
	5-FOA	1 g/l
for making YPD/ CSM plates	Bacto-Agar	2% w/v

Medium	Constituents	Concentration
PLATE-Solution	Sterile 45 % PEG 400	90 ml
	1 M LiOAc	10 ml
	1 M Tris-HCl (pH 7,5)	1 ml
	0,5 M EDTA	0.2 ml

2.1.8 Buffers

Name	Composition
SDS-polyacrylamide electrophoresis	
Lämmli sample buffer (5x)	300 mM Tris/HCl, pH 6.8
	10 % (w/v) SDS
	50 %(v/v) Glycerine
	0.05 % (w/v) Bromophenol blue
	5 % (v/v) β-Mercaptoethanol
Separating gel buffer (4x)	1.5 M Tris/HCl, pH 8.8
	0.8 % (w/v) SDS
Stacking gel buffer (2x)	250 mM Tris/HCl, pH 6.8
	0.4 % (w/v) SDS
SDS-PAGE running buffer (10x)	250 mM Tris, pH 8.0
	1% (w/v) SDS
	2 M Glycine
Coomassie staining	
Fairbanks A	25 % (w/v) Coomassie Brilliant Blue R 250
	25 % (v/v) Ethanol
	8 % (v/v) Acetic acid
Fairbanks D	25 % (v/v) Ethanol
	8 % (v/v) Acetic acid

Name	Composition
Western blotting	
Western blot transfer buffer	50 mM Tris/HCl, pH 7.5 40 mM Glycine 0.04% (w/v) SDS 20% (v/v) Methanol
PBS (10x)	40 mM KH_2PO_4 160 mM Na_2HPO_4 1.15 M NaCl
PBS-T	1x PBS 0.1 % (w/v) Tween
Stripping buffer	62.5 mM Tris/HCl, pH 6.7 100 mM β-Mercaptoethanol 2% (w/v) SDS
β-Galactosidase assay	
Sodium Phosphate buffer	82 mM Na_2HPO_4, pH 7.5 12 mM NaH_2PO_4
Before lysis add	0.1% SDS
ONPG	4 mg/ml in Sodium phosphate buffer
Yeast lysis	
Native lysis buffer	10 mM Tris/HCl, pH 8.5 50 mM NaCl 5 mM EDTA 15 mM $MgCl_2$
Denaturing lysis buffer	8 M Urea 5% SDS 40 mM Tris/HCl, pH 7.5 0.1 mM EDTA

Name	Composition
Protein purification	
Hsp82 and co-chaperones	
Ni-NTA buffer A	50 mM Na_2HPO$_4$, pH 7.8 300 mM NaCl 20 mM Imidazole
Ni-NTA buffer B	50 mM Na$_2$HPO$_4$ 300 mM NaCl 300 mM Imidazole NaOH/H$_3$PO$_4$, pH 7.8
Res-Q buffer 1	40 mM HEPES, pH 7.5 20 mM KCl 1 mM EDTA 1 mM DTT
Res-Q buffer 1	40 mM HEPES, pH 7.5 1 M KCl 1 mM EDTA 1 mM DTT
HAT buffer 1	20 mM K-phosphate, pH 7.5 1 mM DTT
HAT buffer 2	500 mM K-phosphate, pH 7.5 1 mM DTT
SEC buffer Hsp90	40 mM HEPES, pH 7.5 150 mM KCl 5 mM MgCl$_2$ 1 mM DTT
SEC buffer co-chaperones	40 mM HEPES, pH 8 300 mM KCl 1 mM DTT
rMR-LBD	

Name	Composition
MR-Ni-NTA-A buffer	50 mM Tris/HCl, pH 8.0 200 mM NaCl 10 mM Imidazole 2 mM β-Mercaptoethanol 10% Glycerol
MR-Ni-NTA-B buffer	50 mM Tris/HCl, pH 8.0 200 mM NaCl 500 mM Imidazole 2 mM β-Mercaptoethanol 10% Glycerol
TEV-dialysis buffer	50 mM Tris/HCl, pH 8.0 50 mM NaCl 0.5% CHAPS 2 mM β-Mercaptoethanol 10% Glycerol 50 μM corticosterone
MR-SEC buffer	20 mM Tris/HCl, pH 8.0 200 mM NaCl 5 mM DTT 10% Glycerol 1 μM corticosterone
Labelling-dialysis buffer	20 mM HEPES 150 mM KCl 0.04% (w/v) CHAPS
aUC	
Sample preparation buffer	20 mM KCl 5 mM $MgCl_2$ 5 mM DTT
ATPase assay	
ATPase assay buffer	50 mM HEPES/KOH pH 7.5 150 mM KCl

Name	Composition
ATPase premix (2x)	10 mM $MgCl_2$ 4328 ml ATPase assay buffer 240 μl PEP 48 μl NADH 12 μl PK 44 μl LDH

2.1.9 Computer software and programmes

Name	Source
Adobe Reader 8.0	Adobe Inc. (San Jose, USA)
Adobe Illustrator CS4	Adobe Inc. (San Jose, USA)
Adobe Photoshop CS4	Adobe Inc. (San Jose, USA)
BioEdit	Ibis Biosciences (Carlsbad, USA)
Image J	Wayne Rasband (NIH, Bethesda, USA)
LaTeX	Leslie Lamport (LPPL)
Mendeley	Elsevier (Amsterdam, Netherlands)
Microsoft Office 2007	Microsoft (Unterschleißheim, Germany)
Origin 8, 8.6	OriginLab (Northampton, USA)
Sedfit	Peter Schuck (NIH, Bethesda, USA)
Xfluor^{TM}	Tecan (Salzburg, Austria)

2.2 Molecular biological methods

The Polymerase Chain Reaction (PCR) amplified open reading frames (ORFs) were purified using gel extraction or PCR purification kits and were specifically cut using restriction enzymes. DNA was again purified using gel extraction. The purified DNA fragment was then ligated into the respective vector, which was also excised using the same restriction enzymes. Details of the procedure are outlined below.

2.2.1 Polymerase Chain Reaction (PCR)

For cloning different constructs, different polymerases namely, Phusion® High-Fidelity DNA Polymerase, *Pfu* DNA Polymerase, GoTaq® DNA polymerase were used and the buffer and protocols were adjusted according to manufacturer's instructions. PCR products were separated by gel electrophoresis and the band of the right size was excised out of agarose gels and purified using a gel extraction kit.

2.2.2 Restriction digestion

The entire purified PCR product or 5 μg plasmid DNA was specifically cleaved using restriction enzymes. 1 μl of each enzyme was used in a 100 μl final reaction volume. Restriction digestion was usually done overnight at 37°C.

2.2.3 Purification of DNA fragments: Gel extraction

The restriction digested DNA fragments were separated on preparative 1% agarose gels. Gel slices containing the DNA of the required size were cut out from Stain G stained gels under the UV lamp. The DNA was extracted from the gels using the Wizard® SV Gel and PCR Clean-Up System according to the manufacturer's instructions.

2.2.4 Conventional ligation and transformation

The ligation ratios used were 1:3 or 1:6 (vector to insert). The vector and insert were mixed in a 1.5 ml tube and heated to 50°C for 10 seconds to break secondary DNA structures and immediately kept on ice. 1 μl 10x T4 Ligase buffer, 1 μl ATP and 1 μl T4 DNA ligase were added to the DNA and the final volume of the reaction was adjusted to 10 μl. The ligation reaction was incubated overnight at 20°C followed by transformation into chemically competent *E. coli* cells (Section 2.2.7).

2.2.5 One-step sequence and ligation-independent cloning (SLIC)

Primers for PCR were constructed using the NEBuilder® Assembly Tool. PCR product and vector were digested using suitable restriction enzymes and gel purified as described above. 100 ng digested vector was mixed with 40 ng PCR insert, together with NEB Buffer 2, BSA, and T4 Polymerase (NEB) in a 10 μl reaction. The reaction

was incubated at room temperature for 2.5 min and put on ice for 10 min to stop the polymerase reaction. 2 μl of this mix was transformed into XL1 blue competent *E. coli* cells.

2.2.6 Blunt end Mutagenesis

For Aha1 and Hch1 loop mutants, blunt end mutagenesis was done. Primers coding for the change in the amino acids for the swapped loop-domains were used for PCR. The PCR product was gel purified and phosphorylated using polynucleotide kinase (PNK) at 37°C for 1 h. Ligation was done to close the blunt ends. After inactivating the enzymes at 65°C, the original template DNA was digested with Dpn1. The mixture was then transformed into MACH1/XL1Blu chemically competent *E. coli*.

2.2.7 Transformation

Chemically competent BL21 Star DE3/ Mach1/XL1Blu *E. coli* cells were thawed on ice. For transformation 200 μl *E. coli* was mixed with approximately the ligation reaction (10 μl) or 100 ng plasmid for re-transformation and the mixture was incubated on ice for 30 min. Following incubation the cells were exposed to a heat shock at 42°C for 45 seconds and were again incubated on ice for 2 min. 1 ml LB medium was added to the cells and incubation was done at 37°C for 50-60 min with agitation at 900 rpm. The cells were subsequently plated on LB-agar plates supplemented with antibiotic (construct specific).

2.2.8 DNA plasmid purification

Single colonies were picked from LB-agar plates supplemented with antibiotic (construct specific) to inoculate 5 ml LB supplemented with 200 μg/ml ampicillin or 75 μg/ml kanamycin. Cultures were grown overnight at 37°C with constant shaking. 4 ml of the culture was harvested by centrifugation at 13000 rpm (11,600 g) for 1 min at room temperature using a table-top centrifuge. The plasmid DNA was purified using the Wizard® Plus SV Minipreps DNA Purification System following the manufacturer's instructions for the purification of high-copy number plasmids. Concentration of nucleic acids was measured using Thermo Scientific NanoDrop™ 1000 Spectrophotometer reading at 260 nm (1 AU at OD_{260} = 50 μg of double-stranded DNA).

2.2.9 DNA sequencing

The cloned plasmids were sent for sequencing to GATC Biotech or Eurofins Genomics to ensure the correctness of the sequence and absence of mutations. The primer used for sequencing was directly ordered from at the sequencing company. 50-100 ng/μl DNA was sent in a volume of 15-20 μl for sequencing.

2.2.10 RNA isolation from yeast and RT-PCR with SYBR Green kit

Total RNA was isolated from all the yeast strains expressing plasmid-borne GR or enhanced green fluorescent protein (eGFP) using the Promega SV total RNA isolation system according to manufacturer's instructions. Single step RT-PCR was performed using the Agilent technologies SYBR green master mix. The primers for RT-PCR were designed to amplify the ORF of either GR or eGFP.

2.3 Yeast biology Methods

2.3.1 Yeast cultures and maintenance

All the yeast strains purchased from EUROSCARF were stored as glycerol stocks at -80^{o}C. Prior to using a strain in liquid medium, the cells were freshly plated from the glycerol stocks onto YPD plates and incubated at 30^{o}C for 1-2 days. Yeast strains transformed with specific auxotrophic vectors were stored on auxotrophy specific minimal media plates. For experimental analyses, cells were first inoculated into liquid medium, grown ON and then refreshed and allowed to reach log phase (OD_{600} = 1-2) unless specified otherwise. All strains were grown at 30^{o}C in a rotating wheel or with constant shaking.

2.3.2 Growth curves

Overnight cultures grown in YPD were diluted to OD_{600} = 0.01 in a 100-well plate and growth curves were recorded at 600 nm using Bioscreen C MBR at 30^{o}C for 2 days. Additionally, overnight cultures were serially diluted from OD_{600} = 2 and spotted on an YPD plate and grown at 30^{o}C for 2 days.

2.3.3 Temperature ramp

BY4741 yeast strains were grown overnight into stationary phase. The cultures were diluted to OD_{600} = 0.5 and 3 μl of each strain was spotted multiple times on YPD plates. The plate was incubated for 2 days on a temperature ramp from 30°C to 42°C.

2.3.4 Scanning Electron microscopy (SEM)

SEM was done to image yeast cells and compare their morphology to the WT strain. Overnight cultures of the strains were refreshed in YPD and allowed to re-enter late logarithmic to early stationary phase with constant shaking at 30°C. SEM was performed by Bettina Richter with a JEOL 5900 LV microscope (JEOL, Eching, Germany).

2.3.5 Transformation using modified lithium acetate protocol

The protocol used for transforming yeast was modified from [Elble, 1992]. Briefly, freshly streaked colonies were inoculated in YPD and allowed to grow overnight into stationary phase. 200 μl overnight culture was centrifuged for 15 seconds and mixed with 0.67 μl single stranded salmon sperm DNA. 1 μg of the vector to be transformed was added followed by 150 μl PLATE mix (Table 2.1.7) and 6 μl 1 M DTT. The reaction was vortexed briefly after adding each component and incubated at room temperature overnight. Heat shock was performed at 42°C for 30 min and the reaction was allowed to cool. The transformed yeast cells were plated on specific minimal media plates and incubated at 30°C for 2 days.

2.3.6 Yeast colony PCR

A single yeast colony was resuspended in 20 μl Lyticase and incubated at 37°C for 20 min to digest the cell wall. Lyticase was inactivated by incubating the mixture at 95°C for a further 20 min. PCR premix was prepared consisting of forward and reverse primers, dNTPs, GoTaq® polymerase and 5x Green GoTaq® Reaction buffer. 1 μl of the template DNA was used to set up 25 μl PCR reactions. The PCR products were verified on agarose gels.

2.3.7 Harvesting yeast cells

2.3.7.1 Alkali lysis (pellet soluble fractionation)

Samples for western blotting, unless mentioned otherwise, were prepared according to the alkali lysis protocol by [Kushnirov, 2000]. In brief, OD_{600} = 5 of log phase yeast cells were harvested, washed and resuspended in 200 μl of water. 200 μl 0.2 M NaOH was added and incubated at room temperature for 3 min. The cells were pelleted at 13000 g for 1 min and supernatant was discarded. The pellet was resuspended in 100 μl 1x Lämmli sample buffer and boiled at 95°C for 10 min. The sample was again centrifuged to separate the soluble fraction and pellet. The pellet was dissolved in the urea buffer (Table 2.1.8) and further boiled with Lämmli sample buffer for 10 min.

2.3.7.2 Native lysis

OD_{600} = 30 of log phase yeast cells was harvested, washed and resuspended in cold native lysis buffer (Table 2.1.8). Cell lysis was done using glass beads in a bead mill. The lysates were then centrifuged at 14000 g for 10 min to remove unlysed cells and debris. The supernatant was transferred and used for further experiments like pull downs and limited proteolysis.

2.3.8 Activity Assays

2.3.8.1 Beta-galactosidase reporter assay for steroid hormone receptors (SHRs)

SHRs act as transcriptional factors and can bind to a specific promoter sequence to switch on the transcription of the genes coded downstream. Using this principle, two yeast vectors were constructed; one for the expression of the SHR and the other vector harbouring a specific promoter sequence coded upstream of a beta-galactosidase gene (Figure 2.1). Upon induction with hormone, the SHR binds its specific promoter sequence and initiates the transcription of the beta-galactosidase gene. The amount of this enzyme produced is measured directly by monitoring the enzymatic breakdown of its substrate ONPG to o-nitrophenol which is yellow and can be monitored spectrophotometrically. Activity assays for SHRs were performed in 96-well plates. Yeast strains harbouring expression and reporter plasmids were grown overnight at 30°C in deep 96-well plates. The cultures were diluted 1:10 and induced with 10 μM hormone (11- deoxycorticosterone (DOC) for GR, dihydroxy-testosterone for AR,

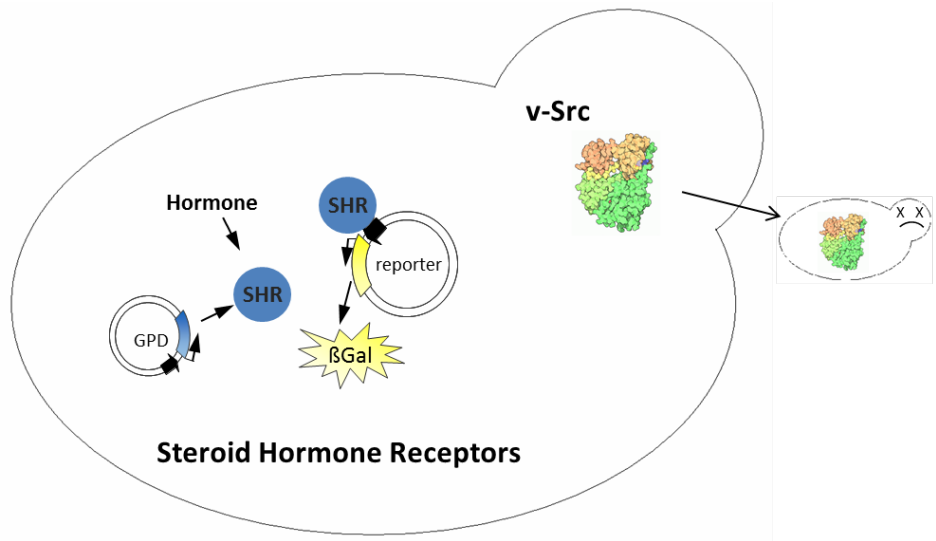

Figure 2.1: Principle of the activity assays. The figure shows the representation of the beta-Galactoside reporter assay for transcription factors, survival assay for phosphotyrosine kinase v-Src

estradiol for ER, progesterone for PR and aldosterone for MR) Incubation was continued overnight in 96-deep well plates with shaking. Unless mentioned otherwise, yeast strains were always cultivated at 30°C. 50-100 μl of the induced culture was centrifuged directly in a 96-well plate. The cell lysis/permeabilisation was done by incubating the cell pellet with 150 μl β-Gal lysis buffer with constant shaking for 15 min at 900 rpm. The reaction was started by adding 50 μl ONPG (4 mg/ml) per well and the development of yellow colour was measured spectrophotometrically at 420 nm wavelength for 30 min. For normalization, the optical density (OD) of the yeast cultures was determined at 600 nm wavelength. The same assay was also performed with log phase cells. Overnight cultures were diluted 1:10 in 5 ml medium and induced for 6 h. 200 μl log phase induced cultures (OD_{600} = 1.2) were harvested in a 96-well plate and the assay was performed as described earlier. No differences were seen between log and stationary phase measurements.

Typically, all the β-gal activity of the strains was measured together with the WT strain on the same 96-well plate. The assays for each SHR were carried out in triplicates, at least three times. The final figures obtained for all the assays are pooled from three or more individual triplicate measurements. To account for the numerical differences contributed by the buffer and ONPG on different days, the entire data sets were normalized. In order to do this normalization, first, an average of the entire data set (one 96-well plate) was calculated. The averages of different measurements

were then scaled with respect to one of them. All the data points within one measurement were then multiplied by this scaling factor. Hence the different measurement were numerically comparable. Finally, all the data points for each strain were pooled and an average and a standard deviation was calculated. Similar procedure was followed for every SHR reporter assay.

2.3.8.2 Survival assay for v-Src and phosphotyrosine blots

Cells transformed with the p413Gal1 plasmid expressing v-Src or c-Src mutants under the control of the Gal1 promoter were grown at 30°C in minimal medium containing 2% raffinose to stationary phase. To induce Src expression, cells were spotted onto an agar plate with minimal medium containing 2% galactose. Therefore, cells were serially diluted and 3 μl were spotted. As a growth control cells were also spotted onto an agar plate containing 2% glucose. The read-out of this assay is negative, i.e. if v-Src is active, it is toxic to yeast and the cells are no longer viable. The yeast strains can grow if v-Src is inactive. The phosphotyrosine activity of v-Src and c-Src mutants was investigated by western blot. Cells were grown overnight in minimal medium containing 2% raffinose. The expression was similarly induced by transferring the cells to minimal medium with 2% galactose for 4 h. OD_{600} = 5 of cells were harvested, lysed using alkali lysis method and induced and uninduced samples were compared on western blot.

2.3.9 Radioactivity incorporation to study translational efficiency

Yeast strains grown overnight were refreshed to OD_{600} = 0.1 and allowed to grow into logarithmic phase at 30°C in a thermomixer. At OD_{600} = 0.8, the cells were washed and resuspended into selective medium lacking methionine and incubated for 30 min at 30°C. 'Hot' S^{35}-Methionine was then added to the cultures and incubated further for 30 min. The cells were then washed and resuspended in selective medium containing cold methionine. Samples were prepared using the alkali lysis protocol and subjected to SDS-PAGE. The gels were analysed using a Typhoon™ 9200 multimode scanner.

2.3.10 Monitoring autophagy

Overnight cultures growing in YPD were refreshed and allowed grow into logarithmic phase. OD_{600} = 1 cells were harvested and samples were prepared by TCA precipi-

tation for SDS-PAGE analysis followed by western blot. The remaining culture was washed and resuspended in YNB lacking all amino acids to induce N_2 starvation and hence autophagy for 2 h. Sample preparation was done by TCA precipitation. Ape1, which is a marker for autophagy was used to ascertain that the autophagy mechanism in all the yeast strains was undisturbed.

2.3.11 Pull downs

Yeast expressing HA-tagged GR or empty control plasmid were grown to an OD_{600} = 1-2 in selective media. All subsequent manipulations were done at 4°C. OD_{600} = 30 of cells were harvested by centrifugation and lysed under native conditions (Section 2.3.7.2). Protein concentrations were normalized to the WT and 0.05% Tween-20 was added to the lysates. 750-800 μl of the lysate was incubated with 20 μl pre-equilibrated anti-HA magnetic beads for 30 min at room temperature. Beads were washed thrice with 300 μl wash buffer (native lysis buffer + 0.05% Tween-20) and finally with ddH_2O. The beads were boiled directly in 1x Lämmli solution without β-mercaptoethanol for 5 min at 95°C. The beads were then removed and the samples were boiled again after addition of 4% β-mercaptoethanol. Immunoprecipitates were separated on 7.5% and 12.5% gels and GR and the co-chaperones were detected by western blotting.

2.3.12 Limited proteolysis

In order to perform limited proteolysis, the yeast lysates were first subjected to pull-downs as described above. Each pull down reaction was used for one concentration of Proteinase K. In brief, incubation with anti-HA magnetic beads for 30 min at room temperature was followed by washing beads as described. 20 μl lysis buffer was added to the beads followed by Proteinase K (0.1 $\mu g/\mu l$ - 2 $\mu g/\mu l$) Proteolysis was done on ice for 10 min. The reaction was stopped by adding 2 mM PMSF, followed by boiling the beads in 2x Lämmli sample buffer at 95°C for 5 min, first without β-mercaptoethanol, and then 5 min after adding 4% β-mercaptoethanol on removal of beads. Entire samples were loaded into Serva™ Electrophoresis 4-12% gradient gels. GR fragments were detected with western blotting.

2.3.13 Transcriptional analyses of △Cpr6, △Cpr7, △Hch1 and △Aha1 using gene-chips

In order to compare the transcriptional profiles i.e. mRNA levels of all genes in the Cpr6, Cpr7 and Hch1 deletion strains, gene-chip analyses were performed. Overnight cultures in YPD medium were refreshed in 50 ml YPD and maintained in logarithmic phase for 2 days. The cells were then harvested, washed with sterile cold PBS and flash-frozen and stored at -80°C. The frozen yeast pellets were then sent and the gene-chip analyses were performed at The Centre of Excellence for Fluorescent Bioanalysis in Regensburg (KFB-Regensburg). The signal strengths obtained from these analyses were converted using the MAS5 algorithm to expression levels (MAS5 normalization algorithm developed by Affymetrix [Affymetrix, 2002]). Two independent samples were sent and analysed for each strain. The mean values of all genes of the deletion strains were normalized to the mean values of the genes from the WT. The genes that exhibited at least a 2-fold difference to the WT were analysed. The first 100 genes up- or down-regulated were clustered and a network was obtained. Cellular function and process were assigned to the genes clustering together using GO Slim Mapper of the Saccharomyces Genome Database.

2.4 Protein biochemistry methods

2.4.1 Recombinant protein expression and purification

2.4.1.1 yHsp82 and the co-chaperones

- **Expression**

  During the course of this work several proteins were expressed and purified. These include, Hsp82, yPpt1, yCpr6, yCpr7, yHch1, yAha1, yTah1, and yPih1. The *E.coli* strain BL21codon+(DE3) was transformed with the pET28a expression plasmids for His-yHsp82, His-Cpr6, His-Aha1, His-Hch1, pRSETA expression plasmid for His-Cpr7 and pETSUMO expression plasmids for yTah1 and yPih1. The transformation protocol is described above. A single transformant colony was inoculated into 150 ml of LB medium with the desired antibiotic (100 μg/ml Ampicillin or 75 μg/ml of Kanamycin) and incubated overnight at 37°C. 35 ml of this overnight culture was then used to inoculate every 2 L flask. Except Hsp82, which was expressed in dYT medium, all other co-chaperones

were expressed in 8 L of LB medium. Induction was done using 1 mM IPTG for 4 h at 37°C. The cells were harvested by centrifugation at 6000 rpm using the JA10 rotor, resuspended in 60 ml Ni-NTA buffer A (Table 2.1.8) supplemented with protease inhibitor HP (1 vial) and stored at −80°C.

- **Cell lysis**

  The cells were thawed and a few crystals of DNase was added to the cell suspension. Lysis was done using a cell disruption apparatus at high pressure of 1.8 kbar and the lysate was centrifuged to clear debris for 40 min at 20000 rpm at 4°C in the JA 25.5 rotor.

- **Purification**

  Since all the proteins were His-tagged, the first step was Ni-affinity chromatography column using the His-Trap FF column. Prior to loading the lysate, the column was equilibrated using 5 column volumes (CV) of water, followed by Ni-NTA buffer B and finally Ni-NTA buffer A. (All columns were equilibrated similarly before use and stored in 20% Ethanol after use.) The lysate was loaded at a flow rate of 4 ml/min and eluted using 60% buffer B. After the Ni-column, the elute fractions were pooled, diluted 1:10 in Resource Q buffer 1 to reduce the salt concentration, and loaded on to a Resource Q ion-exchange column. yAha1 was an exception to this procedure, and was re-run on a Ni-NTA column instead of the Resource Q column. Depending on the pI of the protein being purified, it either bound the column or was collected as flow through. Elution of the bound proteins was done using a continuous salt gradient of Resource Q buffer 2. Note: the pH of the ion-exchange buffers was adjusted according to the pI of the protein of interest. Generally, the pH of the buffer was adjusted to be at least 0.5 to 1 pH above the pI of the protein of interest while using an anion exchanger (Resource Q). The protein would thus be negatively charged in this buffer and would bind to the anion exchange resin of the column. After these first two columns, the purification protocol deviated slightly depending on the protein being purified. For the SUMO tagged yTah1 and yPih1, the tag was cleaved off using SUMO protease Ulp1 in 5 L of dialysis buffer overnight at 4°C. After this digestion step, the protein was again run over a Ni-NTA column to separate the SUMO-His tag. The untagged Tah1 or Pih1 fractions were pooled. For Hsp82, the protein fractions from the Resource Q column were pooled and dialysed in 5 L of HAT dialysis buffer for 1 h at

4°C twice. The protein was then loaded onto a HAT column. The last step of purification for proteins was size exclusion chromatography (SEC). The protein fractions were concentrated to 5-10 ml using a centricon of the required molecular weight cut-off (3K, 10K or 30K MWCO). Depending on the molecular weight and the expected yield of the protein, Superdex 75 or 200 pg HiLoad 16/60 or 26/60 were used for SEC. The final protein fractions were analysed by SDS-PAGE followed by Coomassie staining to ascertain purity. yAha1 and yHch1 were dialysed into a low salt buffer, yPpt1 was dialysed into a glycine rich buffer for stability (Wandinger et al, 2002). The proteins were finally concentrated, flash-frozen in liquid nitrogen in small aliquots and stored at -80°C.

2.4.1.2 Mineralocorticoid receptor-Ligand binding domain of rat (ratMR-LBD)

- **Expression**

  BL21(DE3) *E.coli* were transformed with the pETHalo-ratMR-LBD expression vector. A colony was inoculated in 5 ml of LB supplemented with 75 μg /ml Kanamycin and 2% Glucose. 2 L auto-induction medium was inoculated using 2 ml of the overnight culture and Kanamycin. The culture was allowed to grow at 37°C for 4 h. The flask was then cooled down to approximately 17°C for 1 h and the expression of ratMR-LBD was induced by adding 50 μM of corticosterone and incubated at 17°C overnight. The cells were then harvested and the pellets resuspended in MR-Ni-NTA buffer A were frozen at -80°C as described before.

- **Purification of ratMR-LBD**

  Prior to cell lysis, the cells were thawed and 2 M urea was added for extracting MR-LBD from the cells. Cell lysis was done as described above using the French press. The lysate was first run over a pre-equilibrated His-Trap FF column using a urea gradient to remove the urea and finally have the protein in the normal MR-Ni-NTA buffer A. Elution was done using 100% MR-Ni-NTA buffer B. The fractions of the protein peak were pooled, diluted 1:1 in MR-dialysis buffer and subjected to TEV protease digestion during dialysis to cleave off the Halo-His tag. The protein was then run on a His-Trap column again to separate from the Halo-His tag. Since concentrating the protein at this stage led to severe losses due to aggregation and also formation of higher oligomers, the protein was instead run on the SEC in 8 loops of 5 ml each. All buffers were supplemented with 50 μM corticosterone, while the last SEC buffer was with

1 μM corticosterone. Finally, the monomer peak (corresponding to 65-80 ml) was concentrated, flash frozen in liquid nitrogen and stored at -80°C

2.4.2 Labelling of rMR-LBD with Atto488

3 μg ratMR-LBD was centrifuged at 14000 g at 4°C to remove all aggregates. It was dialysed in 5 L of labelling-dialysis buffer overnight. The protein was again centrifuged and concentration was measured. (almost 50% loss of protein due to aggregation was observed at this step). The fluorescent label Atto488 was added to the protein in a 1:2 (protein : label) molar ratio and incubated with shaking for 55 min at room temperature. The reaction was stopped by adding 5 mM DTT and immediately was put on ice. The protein was again centrifuged and dialysed first in 5 L of labelling-dialysis buffer for 2-3 h and then in fresh 5 L of labelling-dialysis buffer overnight at 4°C to get rid of the excess label. The concentration (Section 2.4.3.3) of the labelled protein and its labelling efficiency was calculated using the following formulas.

$$[M] = \frac{A_{280} - (A_{501} \times 0.1) \times dilution\ factor}{\varepsilon_{protein}} \tag{2.1}$$

$$[Dol] = \frac{A_{501} \times dilution\ factor}{\varepsilon_{Atto488} \times [P]\ Molar} \tag{2.2}$$

2.4.3 Protein concentration measurement

To measure the concentration of proteins three different approaches were used. Both the Bradford and BCA methods were used to measure the relative concentrations of total proteins in yeast lysates.

2.4.3.1 Bradford assay

The total protein concentrations were measured using the Bradford reagent. 10 μl of the lysate was added into 200 μl of the Bradford reagent in a 96-well plate and mixed. Three wells were used as blank with lysis buffer and Bradford reagent. The absorbance was measured in a Cary50 plate reader at 595 nm wavelength.

2.4.3.2 BCA assay

The Pierce™ BCA Protein Assay Kit from Thermo Scientific was used for measuring total protein concentration. The BCA working reagent was prepared by mixing together 50 parts of the BCA Reagent A with 1 part of BCA Reagent B. In a 96-well plate, 25 μl lysate/ protein solution was mixed with 200 μl of BCA working reagent and incubated at 37°C for 10-15 min. The absorbance was then measured at 562 nm using the Cary50 plate reader.

2.4.3.3 UV absorption spectroscopy

UV spectroscopy was used to determine the absolute concentration of purified proteins. During purification, the absorbance at 280 nm was measured using the Protein280 program on the NanoDrop™. This however was done only to estimate the concentration of the protein and does not give a reliable exact value. In order to measure the concentration of the protein accurately, the Cary50 or Cary100 spectrophotometers were used. In brief, the protein concentrations can be measured using the 'Scan' mode, scanning through 200 nm to 300 nm wavelength. The peak intensity at 280 nm was considered for calculation. Prior to measuring the protein concentration a baseline was obtained with the buffer alone. The proteins were generally diluted 1:25 or 1:13 to measure the absorbance at 280 nm. The concentrations were determined using the Lambert-Beer's law (Equation 2.3). The following Table 2.4.3.3 enlists the extinction co-efficient (assuming all cysteines are reduced) of all the proteins used for calculating concentration. The extinction co-efficients were calculated using the Expasy-ProtParam tool based on the amino acid sequence of the protein.

$$c = \frac{A}{\varepsilon \cdot d} \tag{2.3}$$

Key :
c = concentration
A = absorbance
ε = extinction co-efficient
d = path length

Table 2.12: Extinction co-efficients

Protein	Extinction co-efficient (ε)
Hsp82	57300
Sti1	53750
Ppt1	34840
Sba1	29910
Cpr6	20860
Cpr7	40145
Aha1	50545
Hch1	20970
Tah1	10555
Pih1	37525
Cdc37	25900
Cns1	29130
Sgt1	59360
rMR-LBD	38390

2.4.4 SDS-PAGE

Protein samples were resolved by reducing Sodium dodecylsulfate-polyacrylamide gel electrophoresis (SDS-PAGE) as described by [Laemmli *et al.*, 1970]. The samples were prepared as described for individual experiments in the Lämmli buffer and boiled at 95°C. 10-25 μl samples were loaded into the wells. The gels were run for with a constant current of 35 mA per gel for approximately 50 min in a MightySmall™ gel electrophoresis chamber with 1x SDS-buffer. Commercial gradient gels purchased from Serva™ were run for 70 min. Proteins bands were visualized by staining the gels with Coomassie stain or by western blot.

2.4.5 Coomassie staining

This method of detecting protein bands on a SDS gel, was described by Fairbanks [Fairbanks *et al.*, 1971]. The gel was first disassembled from the glass plates and briefly washed with ddH_2O. It was then completely immersed in the Coomassie staining solution and briefly heated up in the microwave, to fasten the staining process. After shaking the gel in the staining solution for 5 min, gel was again washed with

water and finally immersed in the Fairbanks D solution to destain it. To hasten the destaining process, the gel was again heated up briefly in the the destaining solution and a tissue paper was placed on the gel to absorb the excess stain. After destaining, the protein bands resolved according to their molecular weight can be visualized. The detection limit for this method is about 50 ng of protein.

2.4.6 Western Blot

The transfer of proteins to the PVDF membrane was achieved by western blotting using the semi-dry method. After SDS-PAGE, the gels were were washed in the western blot transfer buffer briefly. The PVDF membrane was activated by soaking it in methanol for 10-30 seconds. The membrane was then washed with water and soaked into the transfer buffer. Three pieces of Whatmann paper, followed by the activated PVDF membrane, the gel and finally three more Whatmann papers soaked in the transfer buffer were placed in a stack. The air bubbles within this stack were carefully removed without disturbing the assembly. The transfer was done using the Biometra semi-dry blotting chamber for 90-120 min at 72 mA per blot. The blots were then soaked in 5% milk in PBS-T overnight at 4°C. Prior to developing the blots, the blot was briefly washed in 1x PBS-T buffer and incubated with the primary antibody (Table 2.1.3) for 1 h at room temperature. The blot was then washed with PBS-T thrice for 15 min. The secondary antibody was then added in 1% milk in PBS-T for 1 h at room temperature. Finally the blots were again washed thrice for 15 min. To develop the blot, Advansta WesternBright ECL Spray was sprayed evenly over the entire blot. The chemiluminescent signal was recorded using the ImageQuant LAS 4000.

2.4.7 Stripping western blots

The blot was heated up for 10 sec in 10 ml stripping buffer in a microwave. Subsequently, 70 μl β-mercaptoethanol were added and the blot was incubated on a platform shaker for 10 min at room temperature. After washing the blot thoroughly with water, immunoblotting was repeated as described above with another primary antibody.

2.4.8 ATPase assays

This assay measures the rate of ATP hydrolysis by a coupled enzymatic reaction. In the first step, ATP is hydrolysed to ADP by the ATPase under investigation. In the second step, ATP is regenerated from ADP and phosphoenolpyruvate (PEP) in a reaction catalysed by pyruvate kinase (PK). The second product, pyruvate, is subsequently reduced to lactate by lactate dehydrogenase (LDH) using NADH as a co-substrate. The kinetics of NADH consumption are monitored by absorbance spectroscopy at 340 nm.

$$ATP + H_2O \rightarrow ADP + Pi \tag{2.4}$$

$$PEP + ADP \rightarrow Pyruvate + ATP \tag{2.5}$$

$$Pyruvate + NADH/H^+ \rightarrow Lactate + NAD^+ \tag{2.6}$$

For measuring the ATPase activity of Hsp82 alone or in presence of co-chaperones, first the concentration of the proteins was determined spectrophotometrically as described (Section 2.4.3.3). In a typical ATPase measurement, 2 μM Hsp82 was used. The amount of co-chaperones or client varied according to the purpose of the measurement. 147 μl reactions were set up and a baseline was recorded at 340 nm for 5 min. The ATPase reaction was then started by adding 3 μl of 100 mM ATP in ATPase assay buffer. The rate of NADH consumption was recorded at 340 nm until the signal dropped to 0.4 absorbance units. The background ATPase activity contributed by contaminants, if any, was measured by adding 100 μM radicicol, which inhibits the Hsp82 ATPase activity completely. The final ATPase activity was calculated by subtracting the background ATPase activity, if any.

2.4.9 Analytical ultracentrifugation

Analytical ultracentrifugation is a method to characterize the behaviour of proteins in solution. The principle of this method is based on monitoring the sedimentation of macromolecules such as proteins in solution under the influence of strong centrifugal forces.The aUC measurements were made in the analytical ultracentrifuge Optima XL-A, which is equipped with both a fluorescence detector (UV), as well as visible absorption optics. aUC runs were typically performed with 300 μl of a 400 nM rMR-LBD-Atto488 or hGR-LBD-Atto488 and 6 μM Hsp82, unless mentioned otherwise. The co-chaperones added to the samples were always in 1:1 molar ratio of Hsp82. 2 mM nucleotides (ATP, ADP, ATPγS and AMPPnP) were added to samples where indicated. For competitive binding with unlabelled client protein, 4 μM

rMR-LBD was used. The runs were performed in an AN50-TI rotor at 42000 rpm at 20°C. Sedimentation was monitored at 480 nm and evaluation was done using the Sedfit program. Additionally, rMR-LBD was also confirmed to be monomeric by measuring the sedimentation at 280 nm. The measurements and analysis for analytical ultracentrifugation were carried out by Katrin Back and Daniel Rutz.

3 Results

3.1 Characterization of co-chaperone deletion strains

The Hsp90 chaperone network is evolutionarily conserved, making yeast a good model organism to investigate the principle aspects of its dynamics. Most Hsp90 co-chaperones are not essential for viability in yeast. Therefore the respective deletion strains are excellent tools to study the influence of the co-chaperones on the activation and/or maturation of a specific client protein *in vivo*. However, before using the different strains to study the activity and protein levels of different Hsp90 clients, it was necessary to validate that the strains were WT-like and that the deletion of a certain co-chaperone did not cause systemic defects. To this end, first the growth and morphological characteristics of the co-chaperone deletion strains were studied and compared to the WT. Furthermore, the basic cellular processes like transcription and translation were also monitored for defects. The principle aim of this thorough characterization was to rule out intrinsic defects in the strains and to ascertain that the effects that are observed on the Hsp90 clients are specific and direct.

3.1.1 Growth characteristics

Monitoring the growth rates of all the co-chaperone deletion strains show that they were similar to the WT. There were two exceptions to this. Cpr7 deletion is known to have a growth defect [Duina *et al.*, 1996]. Additionally, the Pih1 deletion strain also showed a slight retardation in growth as compared to the WT (Figure 3.1A). Cdc37, Cns1 and Sgt1 are essential for viability in yeast. Therefore, knock-down strains of these co-chaperones were used in this work. The knock-down was mild without any obvious growth defects in the strains. The same results were obtained by spotting the yeast strains in a serial dilution on YPD plates (Figure 3.1B).

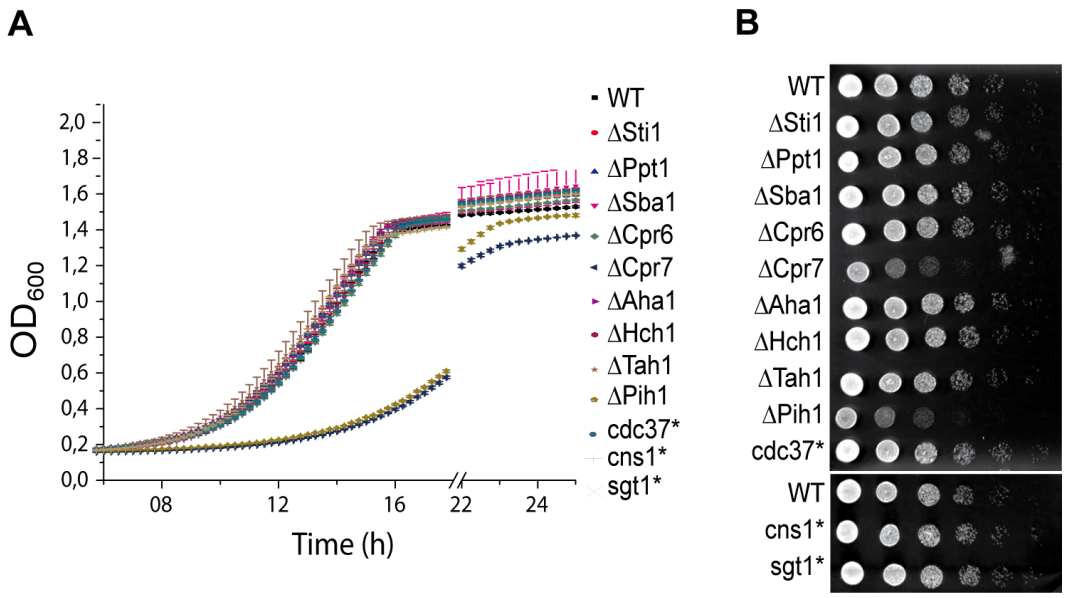

Figure 3.1: Growth characteristics. (A) Growth curves were recorded in the Bioscreen C Microplate reader. Equal starting OD_{600} was used and the cells were grown in a 100-well plate at 30°C with constant shaking for 2 days. (B) OD_{600}=2 cells were serially diluted and 3 μl of each dilution was spotted on YPD plates and allowed to grow at 30°C for 2 days. Co-chaperone deletion strains are denoted by (Δ), while knock-down strains are denoted by (*).

3.1.2 Temperature sensitivity

Mutating or deleting a protein might render the cells sensitive to elevated temperatures or other stresses. As chaperones play an important role during stress, we exposed all the strains to a range of temperatures from 30°C, (optimal temperature

for yeast growth), up to 42°C (severe heat stress/ heat shock). The results of the spot test show that the deletion of Hsp90 co-chaperones did not lead to a temperature-sensitive phenotype (Figure 3.2). The Cpr7 and Pih1 deletion strains again grew slower than the rest, affirming our findings in the growth assays. However, even these strains were not temperature-sensitive.

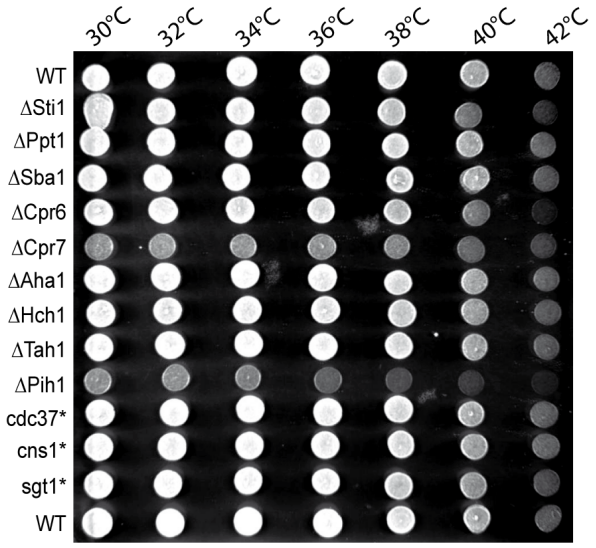

Figure 3.2: Temperature sensitivity of the deletion strains. Stationary phase cells were diluted to OD_{600}=2 and 3 μl were spotted out such that each spot would be exposed to increasing temperatures of the temperature ramp. The temperature gradient was adjusted from 29°C to 43°C. The plates were incubated for 2 days.

3.1.3 Morphology

Following the growth characteristics, log-phase cells were visualized using the Scanning Electron Microscope. The aim was to compare the deletion strains to the WT strain. Sample preparation and imaging was done by Bettina Richter as described earlier [Haslbeck *et al.*, 2004]. The results show that the shape of the cells is WT-like, with no cell-wall damages or other aberrations. There are some differences with respect to the size of the strains, especially in case of Pih1 deletion strain, where the cells appear smaller than the WT cells. In case of Tah1, the magnification used is 5000x instead of 3000x used for the others, and hence they appear to be bigger than the other strains (Figure 3.3). Thus general morphology and cell-wall characteristics of the cells remains unaffected, albeit the slight differences in cell size in some deletion strains.

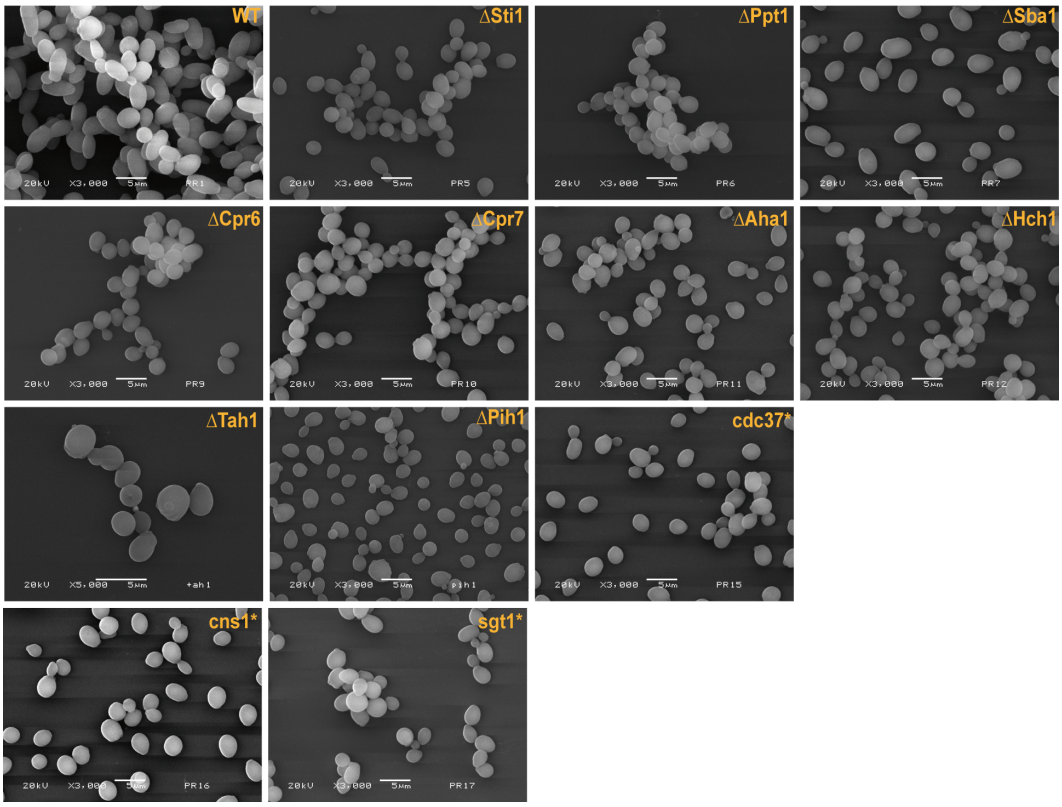

Figure 3.3: Morphology of the yeast strains. Yeast cultures were grown in YPD medium and maintained in the log phase. Images were obtained by SEM. The scale bar represents 5 μm . The magnification used was 3000x all except the Tah1 deletion strain (5000x).

3.1.4 Co-chaperone levels in deletion strains

After a basic characterization of the yeast strains, the next question was whether the deletion of one co-chaperone led to an up/down-regulation of other co-chaperones or Hsp90 itself. This was especially relevant as some Hsp90 co-chaperones have structural homologues like Aha1 and Hch1 or Cpr6 and Cpr7. Additionally, Cpr7 and Cns1 for example, are known to interact and have complementary functions [Tesic *et al.*, 2003]. The co-chaperone levels were first checked in stationary phase cells. No obvious up/down regulation of any co-chaperone was observed (data not shown). However, since all experimental procedures have been performed with log-phase cells, this investigation was also carried out in logarithmic cells. Figure 3.4 shows that none of the co-chaperones under investigation showed significant changes in the deletion strains.

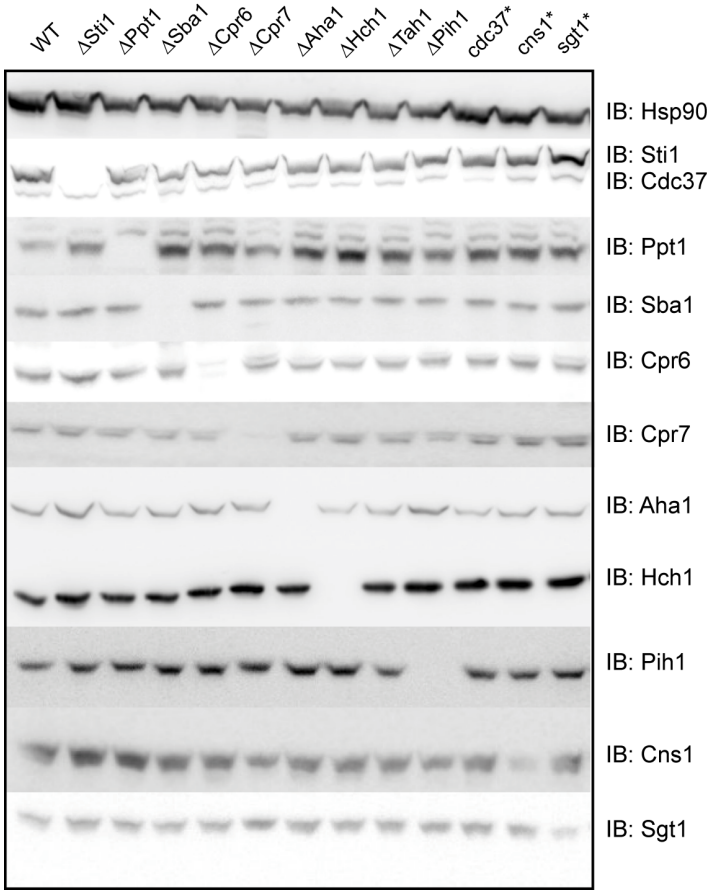

Figure 3.4: Co-chaperone levels in the deletion and knock-down strains. Lysates were prepared from all the strains in the log phase and equal amounts were loaded onto 12.5% SDS gels. Using specific antibodies, each of the co-chaperone was detected in all the strains.

3.1.5 Transcription

To study the exogenously expressed client proteins, it was pre-emptive to ascertain that the deletion strains have no defects in their innate transcriptional machinery. Using RT-PCR, the mRNA levels of GFP, a non-client protein as well as GR, a bona fide Hsp90 client protein were quantified. The mRNA levels in both cases were WT-like (Figure 3.5), ruling out any defects in transcription in the deletion strains. Additionally, the amount of GR mRNA do not vary in the different strains suggesting that the co-chaperones do not influence GR on a transcriptional level.

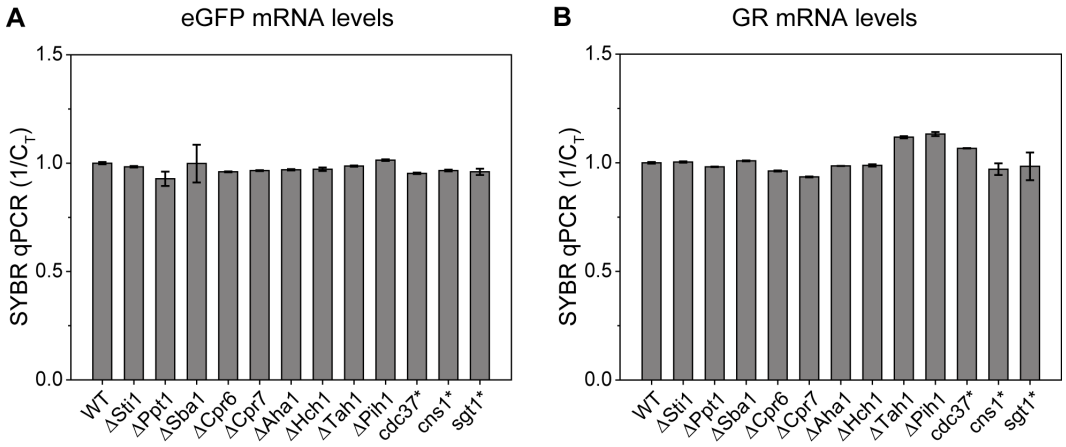

Figure 3.5: Transcription. The SYBR green kit was used for RT-PCR. Total RNA isolation from strains expressing either eGFP (A) or GR (B) was followed by a two-step SYBR green reaction. The fluorescence was measured in triplicates using a RT-PCR cycler. The inverse ratio of the threshold signal is plotted for all strains.

3.1.6 Translation

The translational machinery of the cell was monitored by quantifying the incorporation of radio-labelled methionine (S^{35}-Met) within 30 min. All strains took up methionine to a similar extent, without any significant deviations from the WT level (Figure 3.6A) . The entire lanes on the radio-labelled gel were quantified and compared to the WT level normalized to 100 % (Figure 3.6B). The results show that comparable amounts of protein are produced in all deletion strains during the “pulse-labelling phase”, thus affirming a functional translational machinery.

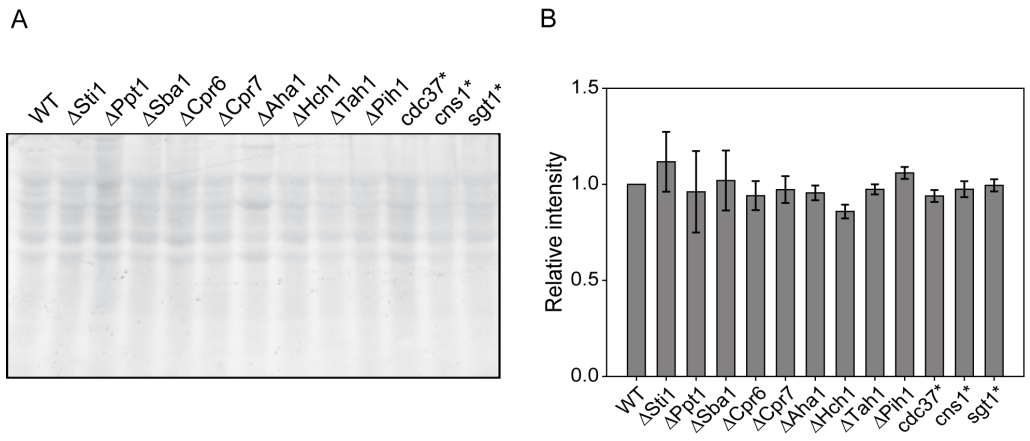

Figure 3.6: Translation. Log phase yeast cultures were switched to a medium supplemented with S^{35}-Met for 30 min at 30°C. The cells were then switched back to "cold" methionine and lysates were prepared for SDS-PAGE. (A) The gel was analysed using a Typhoon 4000 scanner. (B) Entire lanes were quantified with ImageJ. WT intensity was normalized to 1 and the remaining lanes were normalized accordingly.

3.1.7 Protein folding

One of the main functions of chaperones is to assist protein folding. For the Hsp90 machinery, this function is conserved for the Hsp90 client proteins. As a result, the folding of non-client proteins was assessed in the co-chaperone deletion strains. Using two separate approaches, it was confirmed that the yeast strains do not have any defects in folding non-client proteins. Thus any effects on client proteins would be specific to that client-co-chaperone pair. eGFP expressed under the GPD promoter was visualized under the microscope and its cytosolic distribution in the deletion strains was qualitatively compared to the WT. All the strains show similar GFP fluorescence and distribution (Figure 3.7). Additionally, for a functional and quantitative analysis, β-galactosidase was constitutively expressed in all the strains and its activity was monitored using the β-gal assay (Figure 3.8). WT and all the co-chaperone deletion strains exhibit similar β-galactosidase activity, suggesting that it is properly folded and functional.

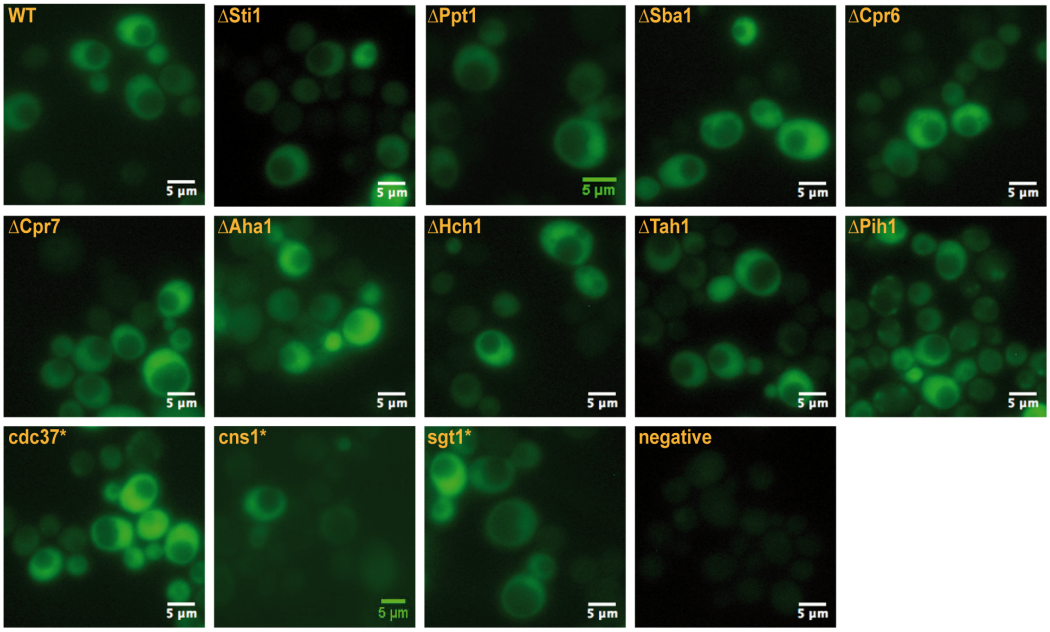

Figure 3.7: eGFP fluorescence in the deletion strains. eGFP was constitutively expressed in all the strains. Log phase cells were used for microscopy using the Zeiss Axiovert 200, inverted fluorescence microscope. 63x oil-immersion objective was used. The scale bar represents 5 μm

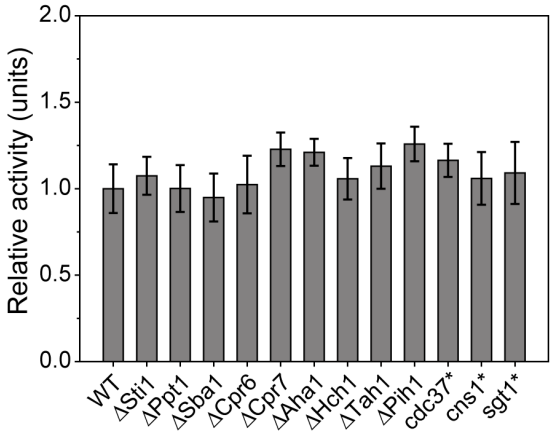

Figure 3.8: Activity of β-gal in the deletion strains. β-galactosidase was expressed in all strains under the GPD promoter. The activity of β-gal was recorded spectrophotometrically at 405 nm for 20 min. The slope of the kinetic was calculated and normalized with the OD_{600}. The measurements were done thrice each time in triplicates and the results were pooled.

3.1.8 Autophagy

Autophagy can be studied in yeast by monitoring the processing of aminopeptidase 1 (Ape1). Ape1 is a resident hydrolase in the vacuole lumen. It is initially synthesized as prApe1, a cytosolic precursor containing an N-terminal propeptide. This precursor is transported into the vacuole by the components of the autophagy machinery, and the N-terminal propeptide is cleaved. This shift in the molecular mass can be detected by SDS-PAGE and Ape1 can be used to monitor specific autophagy [Klionsky *et al.*, 2007]. The complete processing of Ape1 in all the strains demonstrated that autophagy was unaffected in all of them and was comparable to the WT (Figure 3.9). The double band in the Ppt1 deletion strain might be due to over expression of Ape1 in this strain, but the processivity is not affected and autophagy is functional.

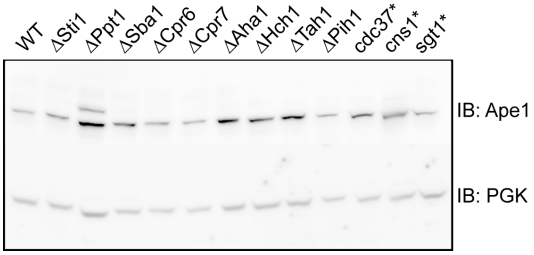

Figure 3.9: Autophagy. Processing of the autophagy marker Ape1 was monitored by exposing the cells to N_2 starvation for 2 h. Equal OD_{600} of cells was used to prepare lysates and analysed by western blot.

Thus, taken together the co-chaperone deletions do not affect transcription, translation and degradation in general. Additionally, the Hsp90 chaperone network does not change upon deletion of one of its component. This already provides a hint that the co-chaperones have specific functions in the cell.

3.2 Influence of the Hsp90 co-chaperones on SHRs

The in-depth characterization done in the previous section ascertained that the Hsp90 co-chaperone deletion strains do not show any obvious defects. Thus, they can be used to monitor the activation and behaviour of various classes of Hsp90 client proteins and their dependence on the Hsp90 co-chaperones. Among the client proteins chosen in this study, the most important ones are the steroid hormone receptors (SHRs). Being transcription factors, their activity can be monitored using β-galactosidase-based reporter assays (β-gal assays). The SHRs were constitutively expressed in yeast. Additionally, the strains were also transformed with a reporter plasmid harbouring a SHR-specific hormone response element (HRE) coded upstream of the β-galactosidase gene. The activity of β-gal directly correlates to the amount of active SHR (Figure 2.1). Of the five SHRs, GR, AR, MR and PR recognize the same response element and have the same reporter plasmid [Beato *et al.*, 1989; Nelson *et al.*, 1999]. ER, on the other hand, recognizes a different DNA sequence and needed a different reporter plasmid [Klein-Hitpaß *et al.*, 1986].

The SHRs used in this study are mammalian proteins. Hence it was first necessary to confirm that these proteins depend on yeast Hsp90 for their activation and maturation. Hsp90 can be specifically inhibited using radicicol which blocks the ATPase cycle and thus the functionality of Hsp90. The WT yeast strain was treated with increasing concentrations of radicicol to inhibit Hsp90 and the effect on the activity of the SHRs was monitored using the β-gal assay. In agreement with the literature, the SHR activities decreased with increasing radicicol concentrations (Figure 3.10A-E). The activity of β-galactosidase alone on the other hand, expressed constitutively in the cell under the GPD promoter, stayed constant (Figure 3.10F). Thus the mammalian SHRs depend on the yeast Hsp90 machinery when expressed exogenously in yeast. The results also validate that β-galactosidase is not an Hsp90 client protein and hence can be used as a reporter to specifically monitor SHR activity.

Within the SHR family, the five receptors show a different response to Hsp90 inhibition. GR, MR and PR respond strongly to Hsp90 inhibition and lose 50% of their activity with just 0.5 to 1 μM radicicol. This shows that these proteins are stringent Hsp90 clients and constantly require the assistance of the Hsp90 machinery for their maturation. On the other hand, AR and, more so, ER seem to depend less stringently on Hsp90 as they show a 50% reduction in their activity only after using 10 μM or more radicicol (Figure 3.10).

Studying all the SHRs, in parallel, in the same yeast parental strain and same

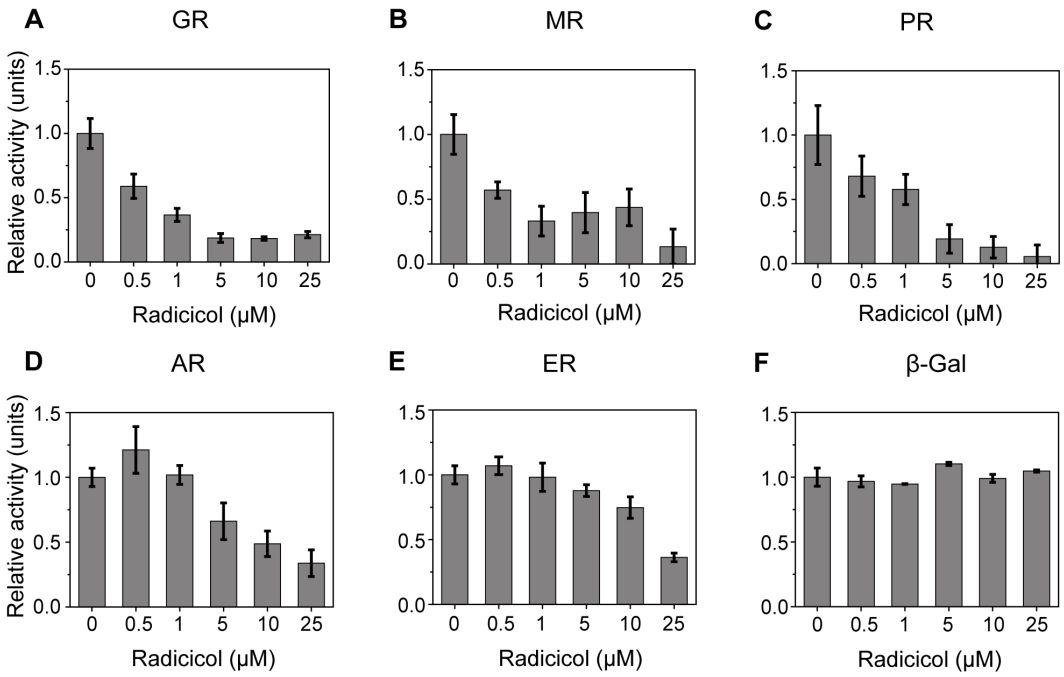

Figure 3.10: Hsp90 dependence of SHRs. Increasing concentrations of the Hsp90 inhibitor radicicol were added to the yeast cultures expressing SHRs or β-galactosidase alone. The activity of β-gal was recorded spectrophotometrically at 405 nm for 20 min. The slope of the kinetic was calculated and normalized with the OD_{600}.

experimental conditions has two advantages. First, the comparison between SHRs will shed light on the differences in the maturation of proteins belonging to the same family. Second, studying stringent and less stringent client protein within a family will help to elucidate the role of co-chaperones on the client proteins.

3.2.1 β-galactosidase activity assay for SHRs

To determine the effect of a specific co-chaperone on a given client, the activities of all the SHRs were measured in each co-chaperone deletion/knock-down strain. The activity was then compared to the WT strain, which was normalized to 1.

- GR

  GR is one of the best studied SHRs. In agreement with the literature [Chang *et al.*, 1997], GR activity is compromised in the Sti1 deletion strain. Additionally, the knock-down of Sgt1 adversely affects GR activity. Unlike the observations by [Duina *et al.*, 1996], Cpr6 deletion led to a decrease in GR activity, while Cpr7 deletion had no influence. Surprisingly, deletion of Ppt1, Aha1 and Hch1, and the knock-down of Cns1, led to an increase in the GR activity. Tah1, and Pih1 deletion and Cdc37 knock-down did not influence GR activity compared to the WT strain. Taken together, the results suggest that the activity of GR is modulated by several Hsp90 co-chaperones and their influence can be either positive or negative (Figure 3.11).

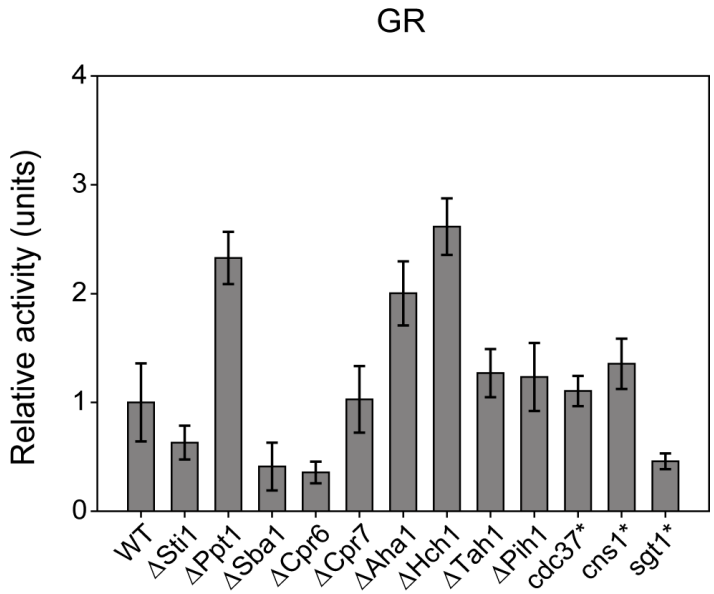

Figure 3.11: Influence of Hsp90 co-chaperones on GR activity. GR was expressed in all strains under the GPD promoter. Absorbance at 405 nm was recorded for for 20 min to determine the β-gal activity. The slope of the kinetic was calculated and normalized with the OD_{600}. The measurements were at least done thrice, each time in triplicates and the results were pooled.

- MR

  MR was studied similarly. The first striking difference to GR was that MR is not dependent on Sti1, for its activity as Sti1 deletion had no effect. Similar to GR, Sba1, Cpr6 deletion and Sgt1 knock-down adversely affected MR activity. Aha1 and Hch1 deletion again led to an increase in MR activity, suggesting a negative regulatory role for these homologous co-chaperones for both GR and MR. Ppt1, Cpr7, Tah1, Pih1 had Cdc37, Cns1 did not affect MR activity (Figure 3.12).

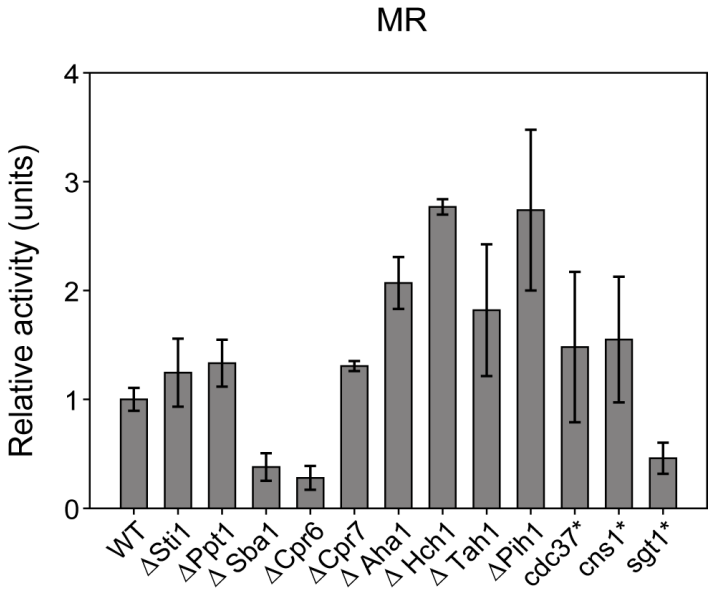

Figure 3.12: Influence of Hsp90 co-chaperones on MR activity. MR was expressed in all strains under the GPD promoter, together with its reporter plasmid. The activity of β-gal was determined as described previously. The measurements were at least done thrice, each time in triplicates and the results were pooled.

- PR

  In the case of PR, Sba1, Cpr6 and Sgt1 again seem to be important for its activity, but Sti1 is not. Surprisingly, knock-down of Cdc37, which is known to be a kinase specific co-chaperone, led to a decrease in PR activity. Like GR, deleting Ppt1, Aha1, and knocking down Cns1 led to an increase in PR activity. Thus except for the Sti1 and Cdc37 effects, PR behaves similarly to GR with regards to its co-chaperone dependence (Figure 3.13).

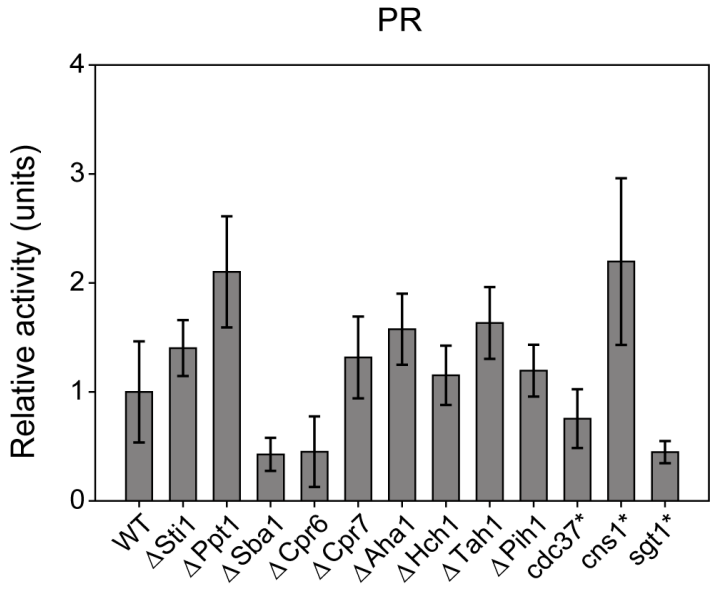

Figure 3.13: Influence of Hsp90 co-chaperones on PR activity. PR was expressed in all strains under the GPD promoter, together with its reporter plasmid. The activity of β-gal was determined as described previously. The measurements were at least done thrice, each time in triplicates and the results were pooled.

- AR

  Deletion of both Sti1 and Ppt1 led to an increase in the activity of AR. Additionally, unlike the other SHRs, deleting Cpr7, Tah1 and Pih1 also led to an increase in the AR activity. Similar to all the SHRs, Sba1 and Cpr6 seem to play an important role in AR activation, however knocking down Sgt1 does not affect AR unlike the other receptors. Taken together, the picture suggests that AR is mostly negatively regulated by the Hsp90 machinery and differs significantly than GR, MR and PR in its co-chaperone requirement (Figure 3.14).

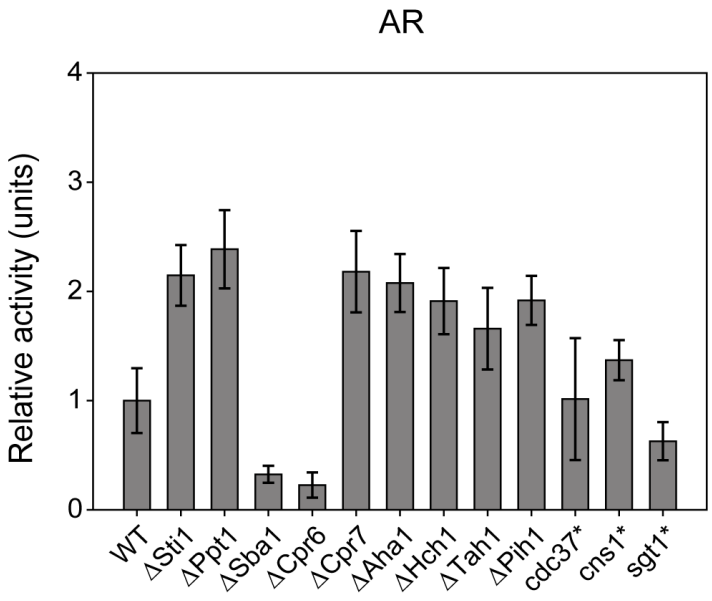

Figure 3.14: Influence of Hsp90 co-chaperones on AR activity. AR was expressed in all strains under the GPD promoter, together with its reporter plasmid. The activity of β-gal was determined as described previously. The measurements were at least done thrice, each time in triplicates and the results were pooled.

- ER

  ER was least dependent on Hsp90 as shown in Figure 3.10E. It fits well that compared to the other SHRs, ER activity is affected by very few co-chaperones. Like observed for the other SHRs, Sba1 and Cpr6 deletion led to a decrease in ER activity, while Cns1 knock-down, led to an increase in ER activity. The effect of knocking down Cns1 on ER activity was even more pronounced than that observed for PR. Other Hsp90 co-chaperones did not influence ER activity. This observation strengthens the notion that ER is not stringently Hsp90 dependent and requires only minor assistance from the Hsp90 system (Figure 3.15).

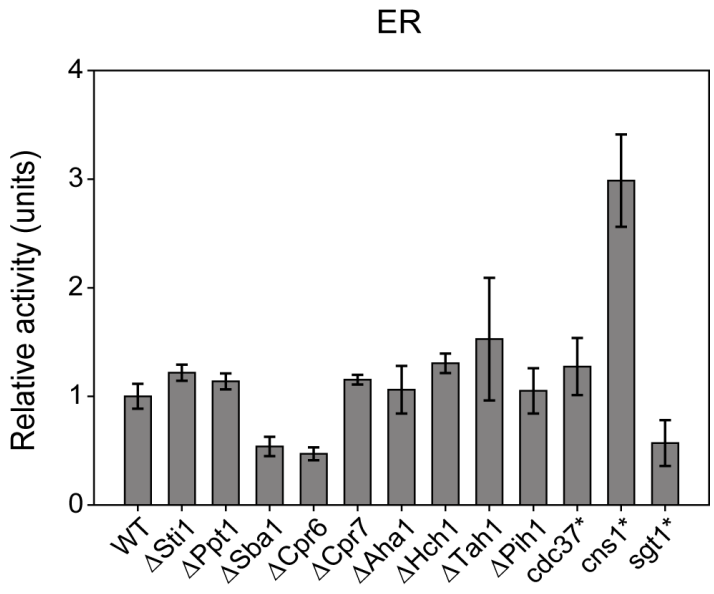

Figure 3.15: Influence of Hsp90 co-chaperones on ER activity. ER was expressed in all strains under the GPD promoter, together with its reporter plasmid. The activity of β-gal was determined as described previously. The measurements were at least done thrice, each time in triplicates and the results were pooled.

3.2.2 Effect of temperature on the co-chaperone dependencies of SHRs

During heat stress, the assistance of co-chaperones may become even more vital for the cell. Moreover, among the Hsp90 co-chaperones, Sti1 and Cpr6 are stress-inducible. It was thus interesting to study the behaviour of the SHRs and their co-chaperone dependence at various temperatures. The optimum temperature used for yeast growth during all the experimental procedures was 30°C. The effect of co-chaperone deletions on SHR activity were carried out also at 20°C and 25°C, and at 37°C to test the effects under heat stress. Comparing the activity of GR in the WT strain at all the four temperatures shows that the activity increases with temperature. In this respect, MR behaved similar to GR (Figure 3.16).

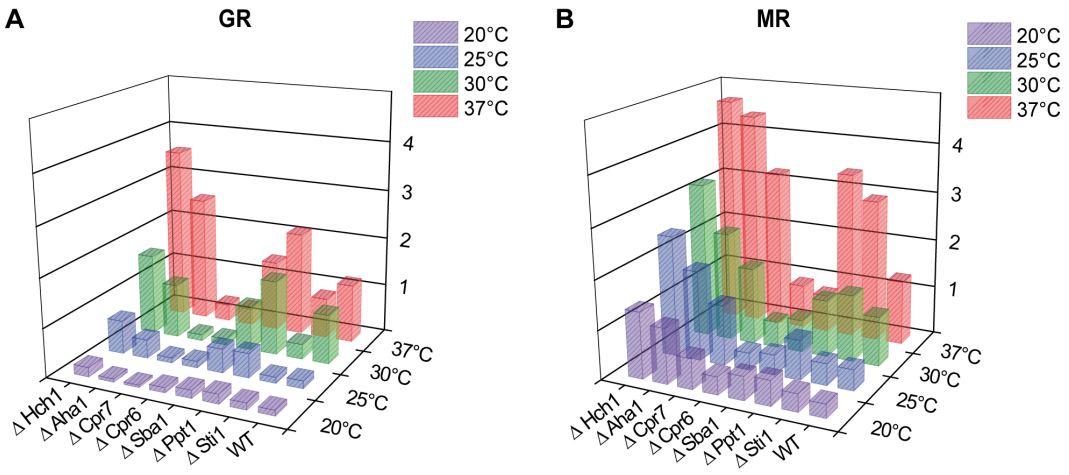

Figure 3.16: Effect of temperature on GR and MR co-chaperone dependency. β-gal assays were repeated for GR and MR at 20°C, 25°C, 30°C (optimal) and 37°C (heat stress). The activity of GR and MR at 30°C was normalized to 1 and the activities in the WT strain at the other temperatures were normalized accordingly. The activity of each SHR in the deletion strains normalized to the WT at each respective temperature.

Surprisingly, PR, AR and ER were no longer active at 37°C (Figure 3.17 and 3.18). In the case of AR, the highest activity was observed at 25°C. Despite these differences, when the activity of a client protein in all the deletion strains was compared to the WT at the same temperature, the trend in client-co-chaperone dependence was still conserved. The results thus show that the client-co-chaperone dependencies are quite robust over a wide temperature range and are not altered under heat stress.

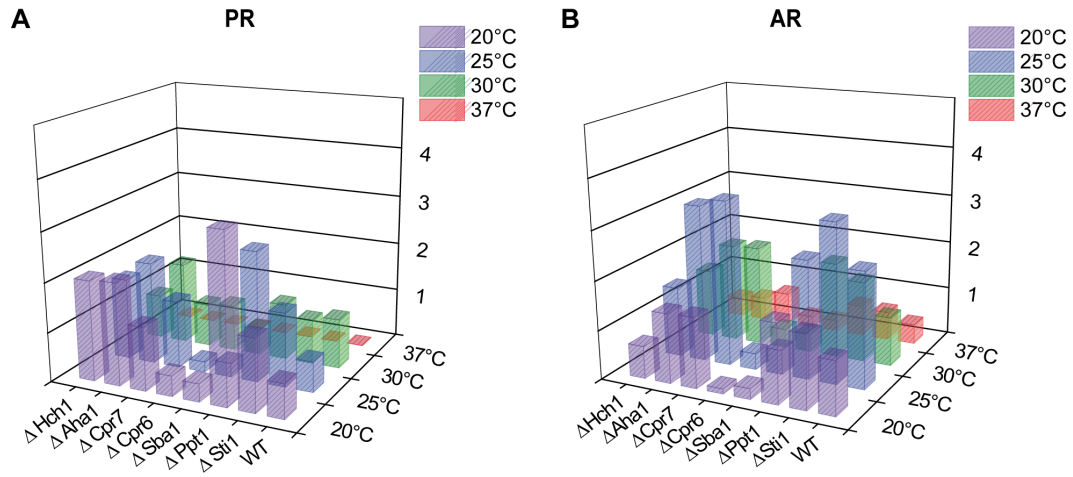

Figure 3.17: Effect of temperature on PR and AR co-chaperone dependency. β-gal assays were repeated at 20°C, 25°C, 30°C and 37°C. Normalization was done similar to Figure 3.16. The activity of each SHR in the deletion strains normalized to the WT at each respective temperature

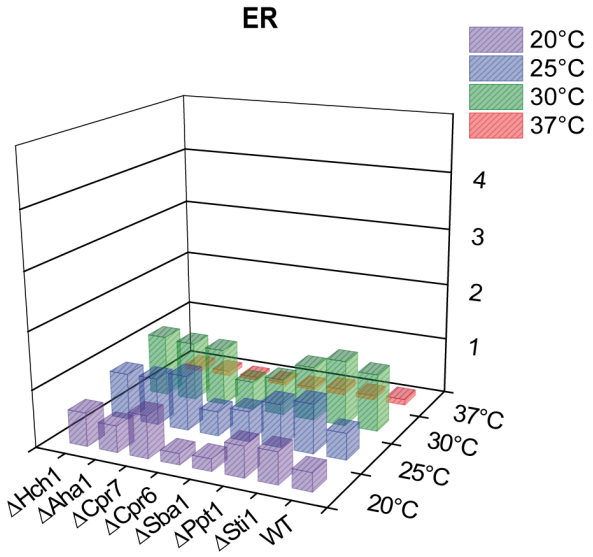

Figure 3.18: Effect of temperature on ER co-chaperone dependency. β-gal assays were repeated at 20°C, 25°C, 30°C and 37°C. Normalization was done similar to Figure 3.16. The activity of each SHR in the deletion strains normalized to the WT at each respective temperature

3.2.3 Tagging SHRs

The activity of the SHRs at different temperatures show that they have specific, robust co-chaperone requirements. In order to investigate the protein levels of the SHRs and

to further investigate the SHR-co-chaperone relationship, it was essential to visualize these proteins by western blot. However, the bottle neck in this endeavour was the lack of good commercial antibodies directed against the SHRs. Thus, to circumvent this problem, the SHRs were initially tagged using the FLAG tag. However, a single FLAG tag (DYKDDDDK) has a sequence similar to the charged linker region of Hsp90. This led to the cross-reactivity of the anti-Hsp90 antibody and unspecific detection of the Hsp90 and the SHRs (82 kDa and 100 kDa). As a result, the SHRs were tagged at the N-terminal end with a HA-tag.

GR, MR and ER were selected to be HA-tagged and analysed further. In order to investigate whether tagging the SHRs at the N-terminus alters their activities, β-gal assays described above were repeated using the tagged variants. The results show that GR and HA-GR show no significant differences with respect to their co-chaperone dependencies (Figure 3.19).

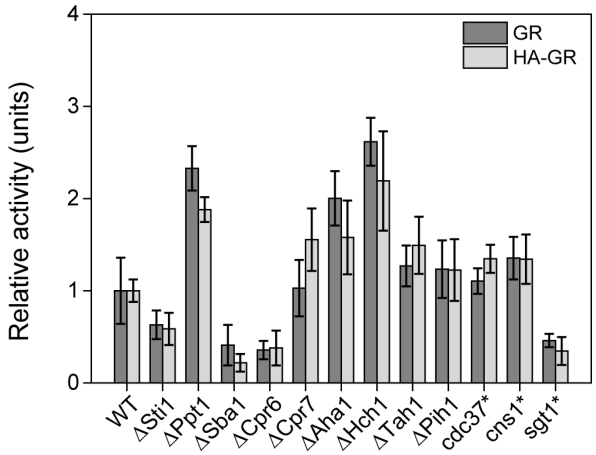

Figure 3.19: HA-GR and GR have similar co-chaperone requirement. β-gal assays were performed with strains expressing N-terminally HA tagged GR. The activity in WT was normalized to 1 and the remaining activities were normalized according to this. The data was pooled from 3 or more separate experiments with biological triplicates in each experiment. For comparison, the pooled data of untagged GR was reused.

For MR, the N-terminal HA-tag altered its chaperone dependency with respect to the Sba1 and Cpr6 deletion strains. Surprisingly, the HA-MR activity did not decrease in these strains, like observed for the untagged MR (Figure 3.20).

Finally, for ER, which is the least Hsp90 dependent SHR, the differences between HA-ER and ER were the most prominent. As shown in Figure 3.15, ER had lower activity in Sba1, Cpr6 and Sgt1 deletion strains. It also showed higher activity in the

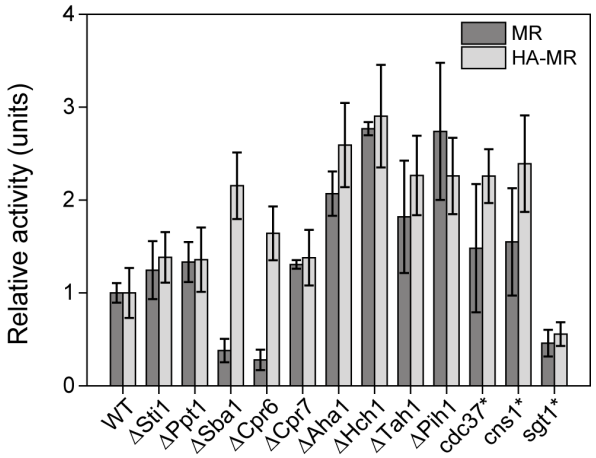

Figure 3.20: HA-MR and MR co-chaperone dependencies. β-gal assays were performed with strains expressing N-terminally HA tagged MR. The measurements were done thrice each time in triplicates and the results were pooled. For comparison, the pooled data of untagged MR was reused.

Cns1 knock-down strain. For HA-ER however, all of these effects no longer held true. Unexpectedly, the HA-ER behaved WT-like in all the deletion strains (Figure 3.21).

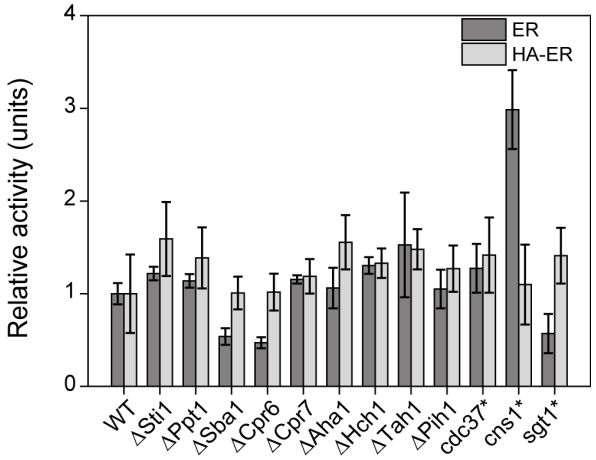

Figure 3.21: HA-ER and ER co-chaperone dependencies. β-gal assays were performed with strains expressing N-terminally HA tagged ER. The measurements were done thrice each time in triplicates and the results were pooled. For comparison, the pooled data of untagged ER was reused.

3.2.4 Effect of the growth phase of yeast on the client-co-chaperone dependencies

In all the β-gal assays elaborated upon above, stationary phase cells were used. For yeast experiments, it is typical to use logarithmically growing cultures. It was therefore essential to analyse whether the growth state of the yeast affected the activity assay read-out. This is especially of interest for the three knock-down strains, as the knock-down effect using dAMP (decreased abundance by mRNA perturbation) was most prominent in the logarithmic phase when the cells were actively growing and reproducing. To this end, the β-gal assays were repeated with yeast grown and maintained in the logarithmic phase. The results show no significant differences in the activity of GR (chosen for test) measured during the log and stationary phase (Figure 3.22). Thus, as a matter of convenience, the assays were uniformly done in the stationary phase.

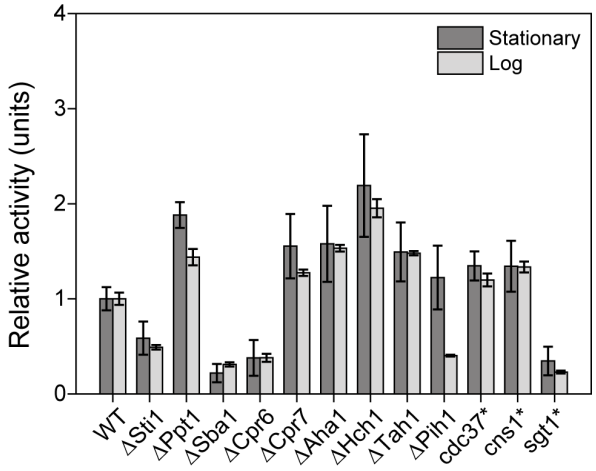

Figure 3.22: GR activity is not influenced by the growth phase of yeast. HA-GR was constitutively expressed in all strains, together with its reporter plasmid. In the stationary phase, the cells were cultured overnight and induction with hormone was done for 20 h. For log phase measurements, the cells were maintained at OD_{600}=1-2 during the entire assay. Hormone induction time was reduced to 4 h. The measurements were done thrice, each time in triplicates and the results were pooled.

3.2.5 Data analysis of the β-gal reporter assays

Every β-galactosidase reporter assay was performed using three separate transformed colonies (biological replicates) in a 96-well plate as described in Section 2.3.8.1. Figure 3.23A gives an example of the raw data measured during a β-gal assay. The kinetic reaction measured for 20 min was plotted and the linear part of the curve was used to calculate the slope. The slopes were normalized using OD_{600} measured for respective well. The total protein concentrations can also be used to normalize the activity measurements. Either method of optimization did not influence the final result. Hence as a matter of convenience, OD_{600} was used. Figure 3.23B is a representative of the numerous β-gal assays measured in this work. It can be seen that the β-gal activity (slope/OD_{600}) obtained for three separate colonies are consistent without showing any major deviations. It is also noteworthy that the lysis buffer does not completely lyse the cells, but only permeabilizes them. This ensures that differences in lysis efficiencies between different strains, if any, do not affect the activity measurements.

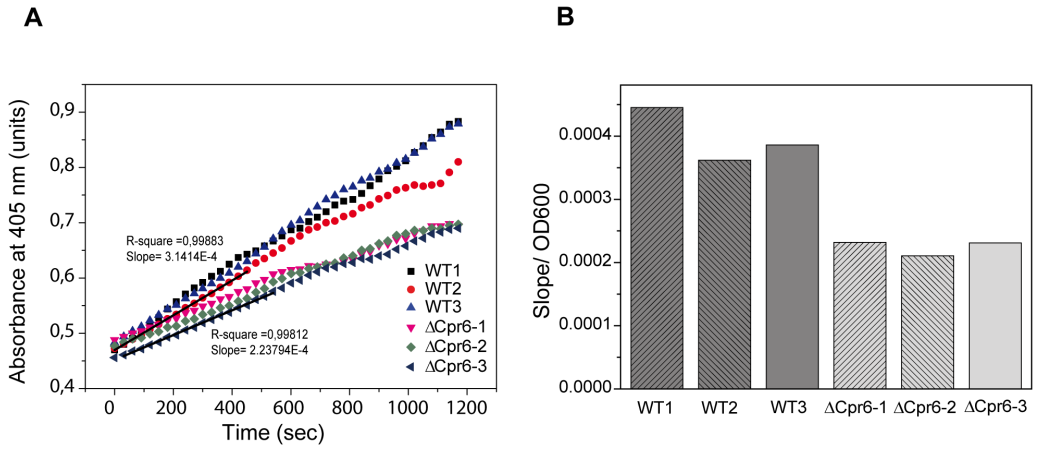

Figure 3.23: Data analysis of the β-gal assays. (A) β-gal assays measured in triplicate for WT and Cpr6 deletion strain are shown. In each case, the linear part of the curve was used to calculate the slope. The R^2 value was greater than 0.98. For the final calculation an average of the three slopes for each strain was used. (B) The slope were normalized with the OD_{600} measured in the same plate-reader.

3.2.6 Protein levels of GR

Since GR and HA-GR behaved similarly in the activity assay, the next step was to investigate whether the differences in the activity correlate to the changes in the steady-state GR levels in different deletion strains.

In order to get reproducible and quantifiable blots, several optimization steps were required. Different loading volumes were tested for the lysates. For HA-GR, 10 μl gave the best results. Initially, individual lysates from different strains expressing the HA-GR were loaded on one gel. However this led to considerable variation in multiple experiments. Hence, in order to get reliable results and reproducibility, lysates made from three different transformants were loaded onto the same gel to get a more direct comparison. It was also observed that the blots looked much better and were more reproducible using logarithmic phase yeast cultures and hence for all the blots, sample were made from yeast grown to an OD_{600}=1-1.2. The lysis was done using the alkali lysis method (Section 2.3.7.1). The blots show that HA-GR levels differ in some deletion strains but mostly are WT-like (Figure 3.24).

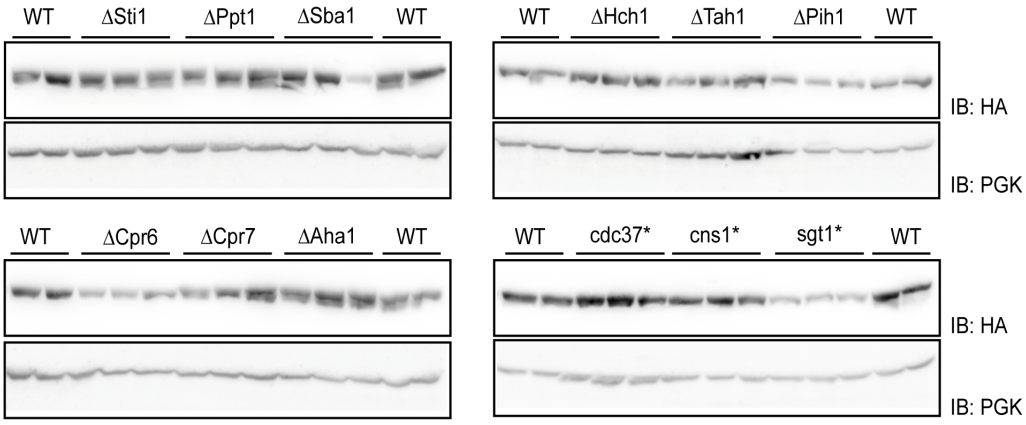

Figure 3.24: Steady-state levels of HA-GR. Three separate log phase cultures were used for preparing samples using the alkali lysis method. Anti-HA monoclonal antibody was used to detect HA-GR. PGK was used as a loading control.

Quantifying the signal using ImageJ and normalizing it with the PGK signal in the respective lane gave the relative amount of GR in a given deletion strain. The HA-GR level in the WT was considered as 1. The quantification showed that most of the co-chaperones deletion strains including Sti1, Ppt1, Cpr7, Hch1 and the Cns1 knock-down strain have comparable HA-GR levels like the WT. Cpr6, Tah1, Cdc37 and Sgt1 deletion/knock-down strains on the other hand, have lower steady-state HA-GR.The Aha1 deletion strain had more HA-GR than the WT. Despite having triplicates on a

single blot, there were some variations among the three samples like Sba1 and Pih1 deletion strains (Figure 3.24).

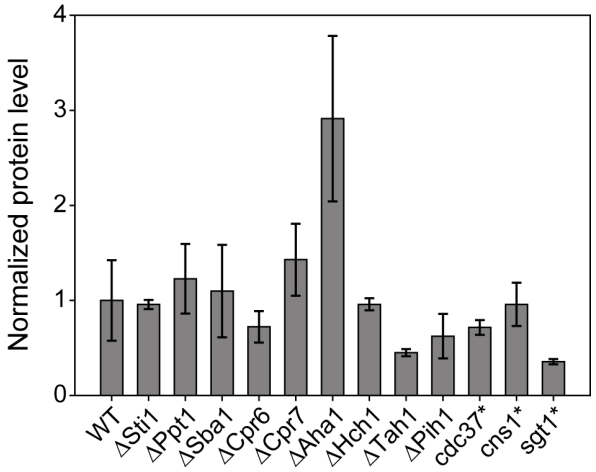

Figure 3.25: Quantification of the steady-state levels of HA-GR. Triplicate-blots like in Figure 3.24 were quantified using ImageJ. The HA-GR band intensities were normalized with the PGK signal in the respective lane. Quantifications from five independent experiments were pooled to obtain the final values and error bars.

In order to analyse the HA-GR levels in further details, the pellet fractions obtained in the alkali lysis method were solubilized using a urea buffer and also analysed by western blot. Figure 3.26 is a representative blot which shows that a significant amount of HA-GR was present in the pellet fraction. This fraction of GR was SDS-insoluble and was likely aggregated in the cells. Solubilizing these aggregates was possible using 8 M urea. The PGK control confirmed that the pellet fraction did not have a contribution of unlysed cells, as PGK, a soluble cytosolic protein, was present only in the supernatant fraction.

Total HA-GR levels were calculated by adding the pellet and supernatant signals. The total HA-GR level (Figure 3.27) in the strains were comparable to the soluble fraction calculated above. Additionally, the distributions of HA-GR in the supernatant and the pellet fraction for each strain were in a similar range (Figure 3.28). Approximately 60-70% of the total HA-GR was soluble, while 30-40% was in the pellet fractions. The Sgt1 knock-down strain was an exception to this with almost 90% of HA-GR in the soluble fraction.

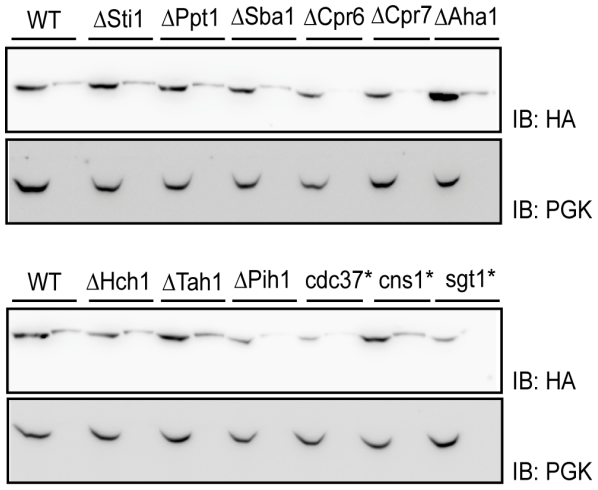

Figure 3.26: Cellular fractionation of HA-GR. HA-GR expressing yeast cultures were lysed according to the alkali lysis method. The pellet fraction was then solubilized in 8 M urea and boiled in equal amounts of Lämmli buffer. Equal volumes of both supernatant and pellet fraction were loaded on SDS-gels. The PGK signal was used to normalize both supernatant and pellet HA-GR signal.

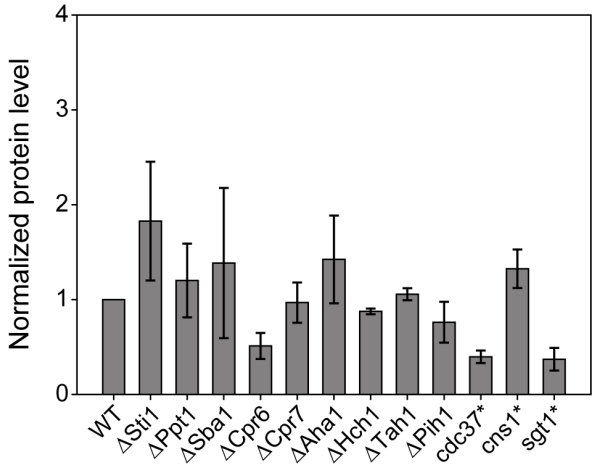

Figure 3.27: Quantification of total HA-GR levels. Normalized HA-GR band intensities quantified using Image J were added to calculate total HA-GR levels in the cell. The WT amount was considered as 1 and remaining strains were normalized accordingly. Data from three individual experiments was pooled to calculate the mean and error.

Soluble fractions from three independent experiments and the triplicates on the same blot measured before were all pooled to obtain a final quantification of HA-GR steady-state levels in all the yeast strains . The HA-GR level was lower than WT in the

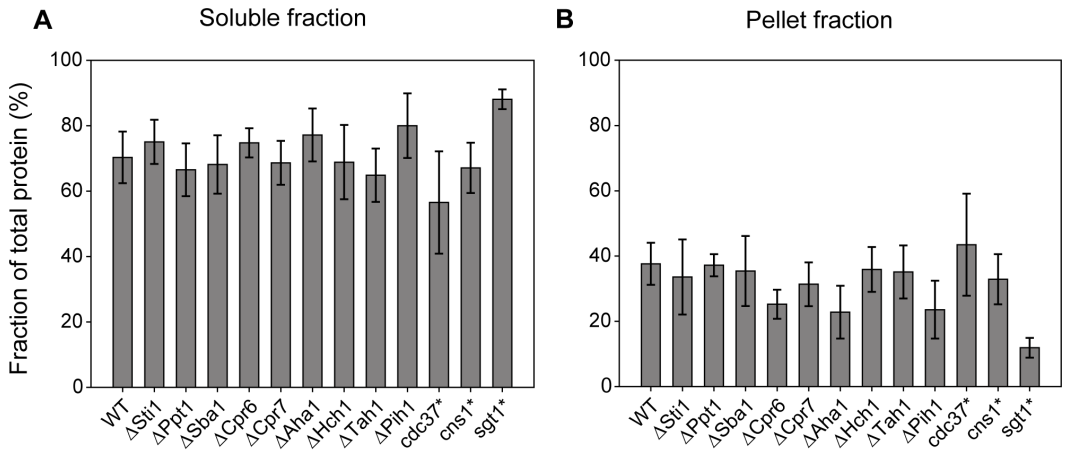

Figure 3.28: Distribution of HA-GR in the supernatant and pellet fraction. Total HA-GR levels were calculated by adding the individual supernatant and pellet normalized intensities. The percentage of the total that is contributed by the supernatant signal is termed as "soluble fraction" (A) and that contributed by the pellet is termed as "pellet fraction"(B). Total HA-GR value in the WT was considered as 100% and the signal of the deletion strains was normalized with respect to the WT.

Cpr6 deletion strain and the Sgt1 knock-down strain. These results correlate perfectly with the decreased activity of the SHRs in this strain (Figure 3.29). Similarly, the increased activity of GR in the Aha1 deletion strain correlates with a higher HA-GR protein level in this strain. However, the same is not true for the Hch1 deletion strain. In some cases, the activity and the protein level did not correlate directly. The Cdc37 knock-down strain had lower levels of HA-GR compared to the WT, but the activity of HA-GR in this strain was WT-like. In the case of Ppt1, Hch1, Tah1 and Pih1 deletion strains, the GR activity was WT-like or slightly higher, however the protein levels were in most cases lower than that in the WT strain. Intriguingly, the HA-GR level in the Sti1 and the Sba1 deletion strains were WT-like, however GR was less active in these strains. Thus, the activity and protein levels do not correlate directly in most cases, pointing towards a more complex regulation and influence of the co-chaperones on GR activity.

3.2.7 Influence of Sti1 deletion on the conformation of HA-GR

Based on the activity protein-level correlation of HA-GR, it was interesting to see that in the case of Sti1, the decreased activity did not correlate with the HA-GR levels.

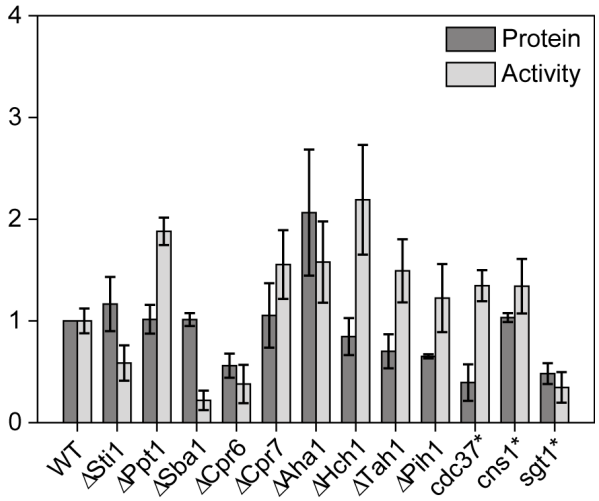

Figure 3.29: Correlation of the activity and protein levels of GR. β-gal activity from Figure 3.11 are compared to the relative soluble HA-GR amount in all the strains.

This suggested that in spite of having WT-like level of HA-GR in the Sti1 deletion strain, the protein was not activated to the same extent. To investigate whether GR expressed in the Sti1 deletion strain is in a different conformation as compared to GR expressed in the WT strain, limited proteolysis for performed. In brief, HA-GR from both WT and Sti1 deletion strain was immunoprecipitated using anti-HA beads. Using increasing concentration of Proteinase K, HA-GR was digested on the beads and analysed by western blot. As a comparison, HA-GR expressed in the Cpr7 deletion strain was also treated similarly.

Figure 3.30A shows that the full length HA-GR (approximately 100 kDa) decreases with increasing Proteinase K concentration. Already at a concentration of 0.1 μg/ml, HA-GR in the Sti1 deletion strain was more susceptible to Proteinase K digestion than in the WT strain, confirming the hypothesis that HA-GR is in a different conformation, in this strain. The lower panel shows a quantification of the 100 kDa HA-GR band. As a control, HA-GR expressed in the Cpr7 deletion strain on the other hand had similar susceptibility to Proteinase K digestion like in the WT strain (Figure 3.30B).

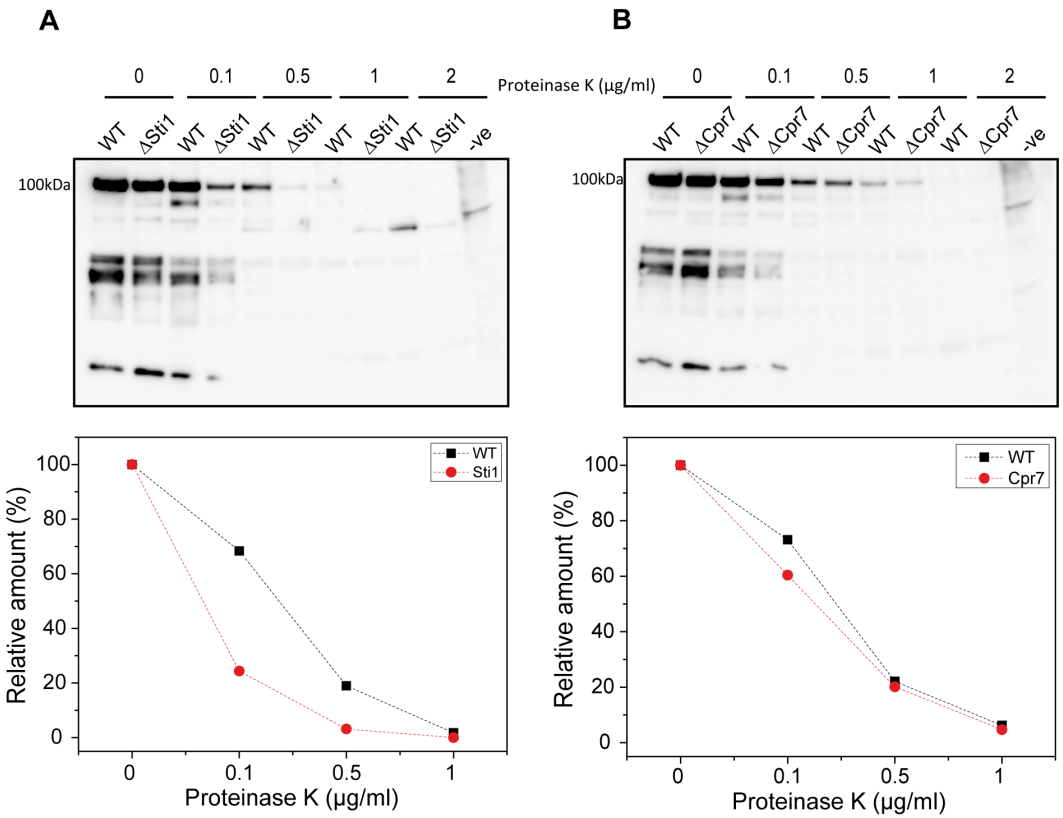

Figure 3.30: Sti1 deletion influences the conformation of GR. OD_{600}=30 cells were lysed in a native buffer without protease inhibitors. Following pull-down using anti-HA beads, HA-GR was subjected to limited proteolysis with increasing Proteinase K concentrations. (A) WT-ΔSti1 comparison; (B) WT-ΔCpr7 comparison. An anti-HA monoclonal antibody (Sigma anti-HA clone HA-7) was used to detect the HA-GR (upper panels). The full-length GR band was quantified by ImageJ (lower panels). The HA-GR level in the WT was normalized to 100%.

3.2.8 Influence of the Hsp90 machinery on stabilized GR mutants

Based on their Hsp90 dependence, the SHRs could be differentiated as stringent and less stringent clients. Furthermore, the less stringent clients like ER also showed fewer Hsp90 co-chaperone requirements. After studying the co-chaperone requirements of GR, it was then interesting to investigate whether stabilized mutants of GR, show any differences to GR-WT with respect to their co-chaperone dependencies. For this purpose, two different stabilized mutants were used: GR-F602S [Bledsoe *et al.*, 2002], referred to as GR1e and GR-A605V, M752T, V702A, E705G, F602S, referred to as GR9a in this study [Seitz *et al.*, 2010]. GR1e possesses a single point

mutation, while GR9a has 5 stabilizing mutations. It has been recently shown that both stabilized mutants are much more active than GR-WT when expressed in yeast [Lorenz *et al.*, 2014]. The authors also show that the two mutants are still dependent on Hsp90, albeit less stringently than the GR-WT. Analysis of the co-chaperone dependence of GR1e shows that it is very similar to GR-WT (Figure 3.31A). Minor differences were observed in terms of fold changes in activity in the Ppt1, Aha1 and Hch1 deletion strains, demonstrating that the changes in activity do not deviate from the WT strain as much as for GR-WT. The trend of co-chaperone dependency however, was the same for GR-WT and GR-1e.

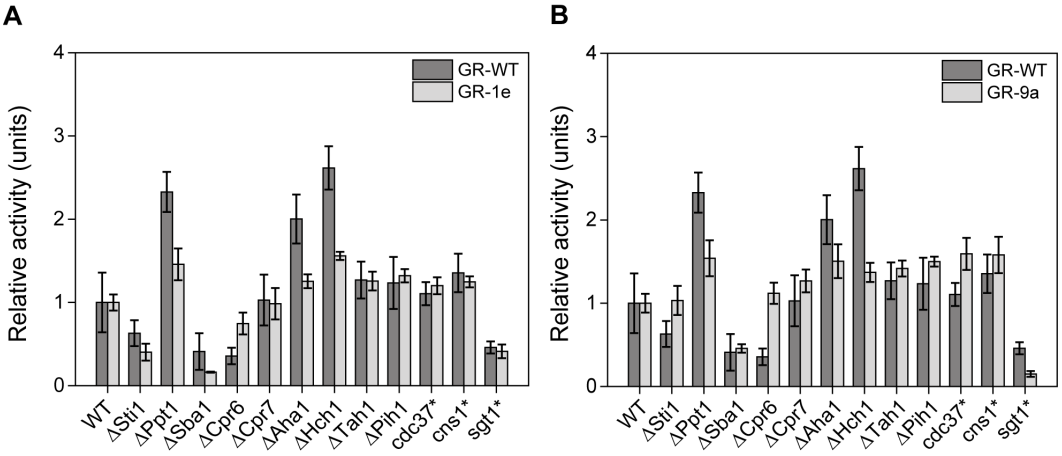

Figure 3.31: Co-chaperone dependency of stabilized GR mutants. GR-1e and GR-9a were constitutively expressed in the strains similar to GR-WT. β-gal assays were performed as described previously. The activity of each construct in the WT strain was normalized to 1 for comparison.

In the case of GR9a, which is further stabilized and also the least dependent on Hsp90 among the three, significant differences in the co-chaperone dependency were observed. One striking effect was that GR9a did not depend on Sti1 and Cpr6 (both co-chaperones essential for GR-WT activation as shown in Figure 3.11). Surprisingly however, GR9a still showed decreased activity in the Sba1 deletion and Sgt1 knockdown strain (Figure 3.31B). Thus stabilization of GR through these mutations seems to alleviates the requirement of Sti1 and Cpr6 in its maturation, suggesting a role of these co-chaperones in stabilizing GR.

3.2.9 Protein levels of GR stabilized mutants

After performing activity assays for the two mutants, their steady-state protein levels were analysed in all the strains. Figure 3.32 shows GR-WT, GR-1e and GR-9a levels with their respective PGK loading controls. The GR-WT and GR-1e protein levels show a similar trend across the deletion strains, corroborating the finding that GR-1e behaves like the GR-WT in the activity assays. On the other hand, the protein level of GR-9a was almost constant in all the deletion strains. It is noteworthy that in the Cpr6 deletion strain, GR-WT and GR-1e levels were lower compared to the WT strain, but the same is not true for GR-9a. In accordance with the activity data, GR-9a shows decreased protein abundance in the Sgt1 knock-down strain. In the Sba1 deletion strain surprisingly, the activity of GR-9a mutant was less than in the WT strain, similar to GR-WT. However, the GR-9a protein levels are comparable to those in the WT strain suggesting that the GR-9a is stable in the Sba1 deletion strain but less active.

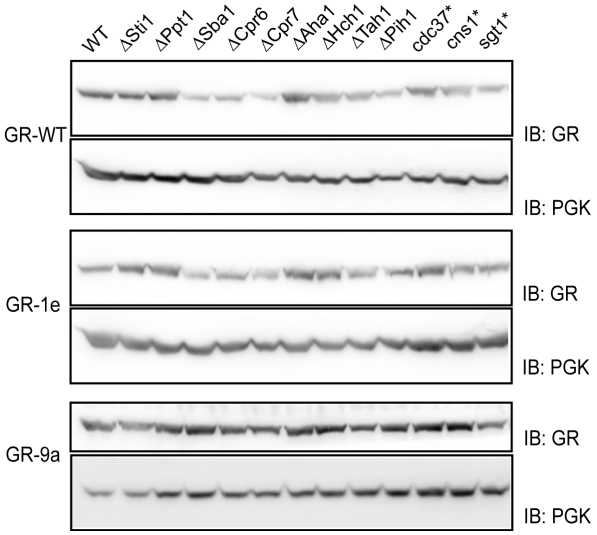

Figure 3.32: Steady-state levels of GR mutants. Log phase cultures constitutively expressing GR-WT, GR-1e and GR-9a were used for preparing samples using the alkali lysis method. Anti-GR polyclonal antibody (anti-GR N499, a kind gift from B.Freeman) was used to detect GR-WT and mutants. PGK was used as a loading control.

3.2.10 Dose response curves for GR and the stabilized mutants

In order to dissect the results obtained in the activity assays and to further validate the phenotype observed for the GR-9a mutant, dose response curves were recorded

for GR-WT and GR-9a with hormone (DOC) concentrations varying from 1 nM to 200 μM . The β-gal activity increases with increasing hormone concentration used for induction. As shown previously, the GR-9a mutant was approximately 8 fold more active than GR-WT. As a result, while GR-9a reached saturation after 50 μM DOC, GR-WT did not. The dose response curves can give a measure for both ligand potency (ligand binding capacity) as well as ligand efficacy (maximum amount of activation possible). However, since the GR-WT curves did not reach saturation, the effects of the deletion strains on efficacy for GR-WT cannot be observed.

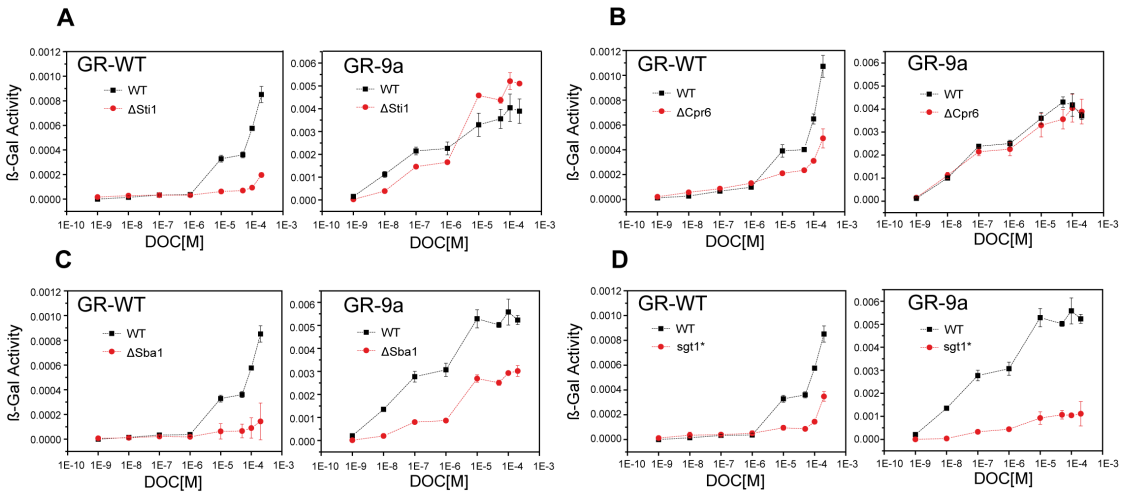

Figure 3.33: Dose response curves-I. β-gal assays were performed with increasing concentration of DOC (1 nM to 200 μM). The black curve depicts the activity of GR in the WT strain, while the red curve stands for the deletion/knock-down strain. Each measurement was done in triplicates.

The curves validate the results obtained in the earlier β-gal assays. Due to a wider range of hormone concentration tested, the effects of co-chaperone deletions/knock-downs could be observed unambiguously. Figure 3.33A-B shows that GR-9a activity is not lowered in the Sti1 and Cpr6 deletion strains while GR-WT has a pronounced lower activity in these strains compared to the WT. The mutant protein also shows a similar ligand potency and ligand efficacy as the WT strain. Despite its stabilization and a greater Hsp90-independence, GR-9a activity dropped in the Sba1 deletion and Sgt1 knock-down strain. In both these cases, GR-9a shows a lower hormone potency as well as a lower efficacy (Figure 3.33C-D).

In the case of the Ppt1, Aha1 and Hch1 deletion strains, GR-WT has slightly higher activity than in the WT-strain. GR-9a has higher activity in the Ppt1 and Aha1 deletion strain, but not in the Hch1 deletion strain. Moreover, in the Ppt1 strain, GR-9a

seems to have a better ligand efficacy than the WT strain (Figure 3.34A-C). Finally, the remaining deletion strains including Cpr7, Tah1, Pih1 and Cdc37 and Cns1 knock-down strains do not show any differences in the activity of both clients compared to the WT strain (Figure 3.34D and 3.35A-D).

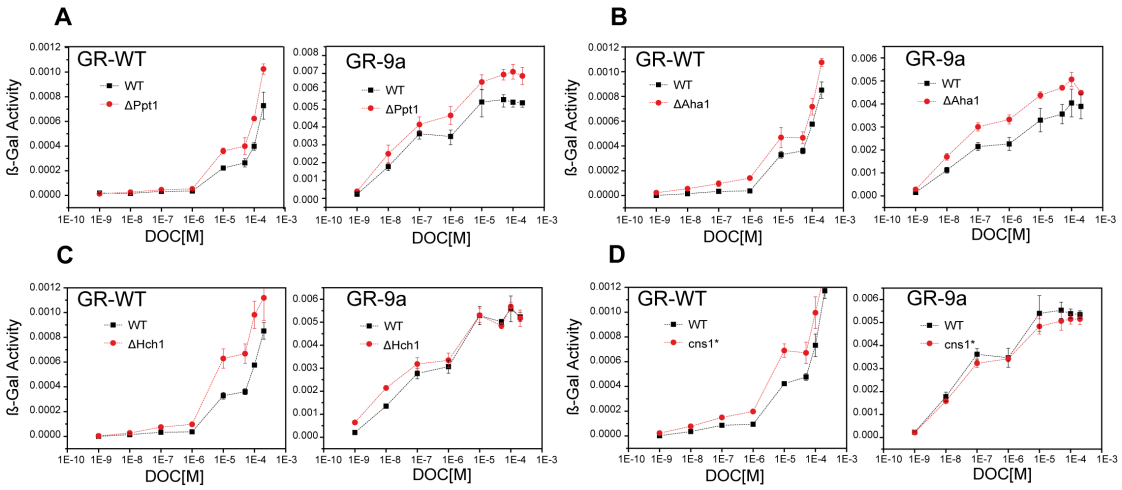

Figure 3.34: Dose response curves-II. β-gal assays were done as described before. WT: black, deletion strain: red. Each measurement was done in triplicates.

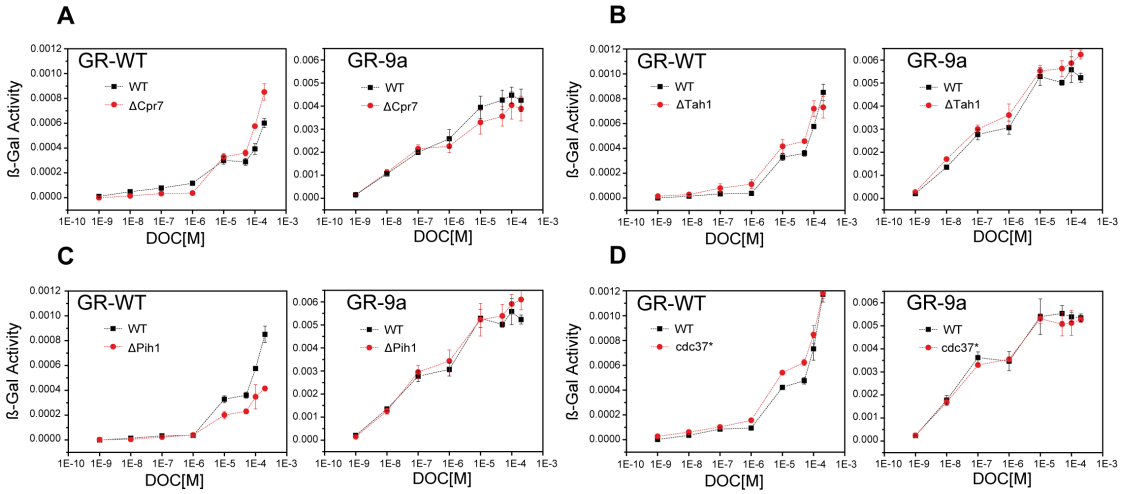

Figure 3.35: Dose response curves-III. β-gal assays were done as described before. WT: black, deletion strain: red. Each measurement was done in triplicates.

3.3 Influence of the Hsp90 co-chaperones on Src kinase variants

The results from the steroid hormone receptors lead to a notion that Hsp90 client proteins require the assistance of specific co-chaperones and these requirements are dictated by the respective client protein. To investigate whether this phenomenon is specific just for SHRs, a viral kinase (v-Src), strongly dependent on Hsp90 was studied next. v-Src is constitutively active and unspecifically phosphorylates proteins, imparting toxicity and cell death in yeast. The activity of v-Src thus can be directly studied in yeast based on a survival test. Moreover, since v-Src is a phosphotyrosine kinase and yeast lack endogenous phosphotyrosine kinases, the activity of v-Src can be monitored specifically by western blot [Brugge, 1986]. The mammalian cellular kinase (c-Src) is not a Hsp90 client, however certain mutants of c-Src need the assistance of the Hsp90 machinery for their maturation. Thus, we employed two such c-Src mutants, namely c-Src3M and c-Src3MΔC that are more similar to v-Src, but less toxic to yeast [Boczek *et al.*, 2015]. It has been shown that v-Src and these Src mutants depend on yeast Hsp90 for their activation. v-Src, as expected, is most strongly Hsp90-dependent, followed by the c-Src3MΔC and c-Src3M mutants [Boczek *et al.*, 2015].

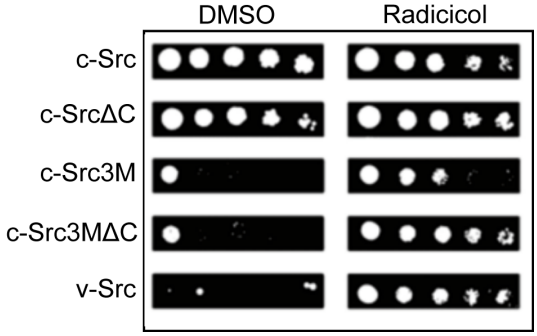

Figure 3.36: Hsp90 dependence of SHRs. c-Src, c-Src mutants and v-Src were spotted on selective media plates with DMSO or the Hsp90 inhibitor radicicol. For v-Src and the c-Src mutants, active proteins impart toxicity to the cell. If the cells are viable, the client protein is inactive. Figure adopted from [Boczek *et al.*, 2015]

The activity of v-Src and both the c-Src mutants was first directly compared on a phosphotyrosine blot (Figure 3.37). The blot shows that as expected, v-Src is the most active among the three, closely followed by c-Src3MΔC. c-Src3M showed the lowest phosphotyrosine activity. Additionally, it should be noted that in the unin-

duced samples, where no Src kinase was expressed, no phosphotyrosine activity was detected.

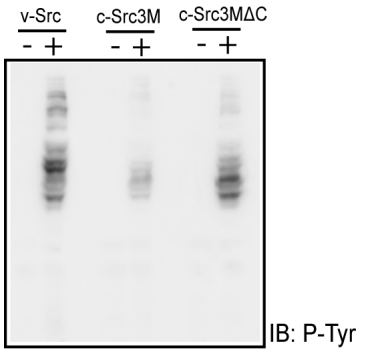

Figure 3.37: Phosphotyrosine activity of v-Src and Src mutants. Expression of v-Src and c-Src mutants was induced under the Gal1 promoter for 6 h (+). In parallel, uninduced samples were grown in selective medium with Raffinose (−). Samples were prepared by the alkali lysis method and analysed by western blot. Equal OD_{600} of cells was used for sample preparation.

3.3.1 v-Src

v-Src is a stringent Hsp90 client. It has been shown that the 'connector' co-chaperone Sti1 and the 'kinase specific' co-chaperone Cdc37 are essential for the maturation of v-Src [Chang *et al.*, 1997; Mandal *et al.*, 2007]. The results from the survival test confirm that exogenously expressed v-Src is toxic to yeast cells. In the WT strain, where v-Src is fully functional, no cell growth is observed (Figure 3.38A). The same is the case for most of the co-chaperone deletion strains. In agreement with the literature, the Sti1 deletion strain can grow in spite of v-Src induction, thus validating the role of Sti1 in v-Src maturation. The Cdc37 dAMP strain, did not grow upon v-Src induction. The probable reason for this effect is that in this strain, the levels of Cdc37 are slightly lower than the WT levels (mRNA amount typically reduced two- to ten-fold [Schuldiner *et al.*, 2005]). The reduced levels of functional full-length Cdc37, unlike the mutant Cdc37 used in earlier studies [Dey *et al.*, 1996; Fliss *et al.*, 1997], is probably sufficient to fold and activate v-Src to some extent. Since v-Src is extremely active in the cells, even a few v-Src functional molecules may be sufficient to impart toxicity to the yeast cells. The survival assays can only show which co-chaperones are required for v-Src maturation. However, if certain co-chaperone act as negative regulators of v-Src activity, such that deleting these co-chaperones would

lead to an increase in v-Src activity, then this information would be lost in this assay as the read-out would still be cell death.

Hence, in order to have a better understanding of v-Src activity, a more sophisticated approach was to monitor its phosphotyrosine activity (Figure 3.38B). The phosphotyrosine blots show that uninduced yeast cells do not show significant phosphotyrosine signal. The entire phosphotyrosine signal thus corresponds to specific v-Src activity. v-Src is active in all strains, as seen in the survival assay. The Sti1 deletion strain shows significantly lower phosphotyrosine levels as compared to the WT, validating the survival results and those published previously [Chang *et al.*, 1997]. Additionally, a slightly lower v-Src activity can be seen in the Cdc37 knock-down strains. Blotting for the levels for v-Src, it can be seen that the steady-state levels of v-Src are lower in the Sti1 deletion strain but are comparable to the WT in the Cdc37 knock-down strain. This suggests that Sti1 and Cdc37 might have different modes of action in assisting the maturation of v-Src. The phosphotyrosine blots also show a slight decrease in the signal for the Sba1 deletion strain which is again in agreement with literature [Fang *et al.*, 1998]. Surprisingly a lower phosphotyrosine activity was also observed in the Sgt1 knock-down strain. These effects however could not be resolved on the survival assay. Both the Sba1 deletion and the Sgt1 knock-down strains also show slightly lower v-Src steady-state levels. Compared to the WT, Cpr7, Hch1, Tah1 and Pih1 show a slight increase in their signal intensities, suggesting that v-Src might be more active in the absence of these co-chaperones.

3.3.2 c-Src3MΔC

c-Src3MΔC is similar to v-Src and depends on Hsp90 for its maturation. The C-terminal regulatory domain of c-Src is truncated in this construct, making it constitutively active. Additionally, three residues in the kinase domain have been mutated making it unstable and Hsp90-dependent. However, albeit these changes c-Src3MΔC is not as active and lethal as v-Src suggesting that additional factors must be responsible for the constitutive hyper-active nature of v-Src. Using the Src mutants offers a "resolution window" to study the chaperone dependence of the Src kinases owing to their decreased toxicity. The survival assays show that Sti1 and Cdc37 play an important role in the activation of c-Src3MΔC (Figure 3.39A). The phosphotyrosine blots validate that the Sti1 deletion strain and the Cdc37 knock-down strains show decreased c-Src3MΔC activity. Like in the case of v-Src, the Sgt1 knock-down also had decreased c-Src3MΔC activity, while Hch1, Tah1, Pih1 showed slightly higher

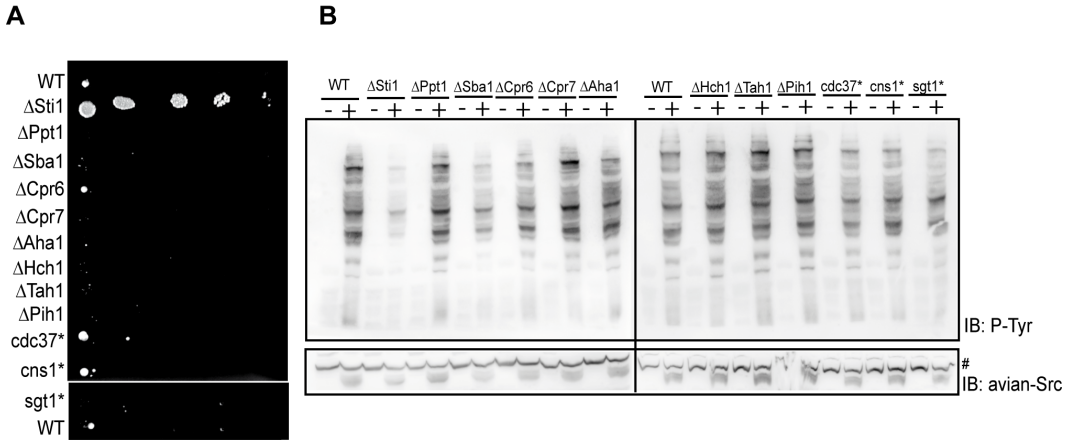

Figure 3.38: Influence of the Hsp90 co-chaperones on v-Src. (A) $OD_{600}=2$ of yeast cells were serially diluted and plated. Growth of yeast indicates inactive v-Src kinase demonstrating the dependence of the kinase on that particular co-chaperone. (B) Phosphotyrosine blots show the activity of v-Src expressed under the Gal1 promoter. v-Src induction (+) was done in galactose medium for 6 h. Uninduced cultures (−) were grown in raffinose medium. (#) : unspecific band, serves as loading control

c-Src3MΔC activity. Surprisingly, the Sba1 deletion strain no longer showed a lower activity for c-Src3MΔC, contrary to the observation for v-Src (Figure 3.39B).

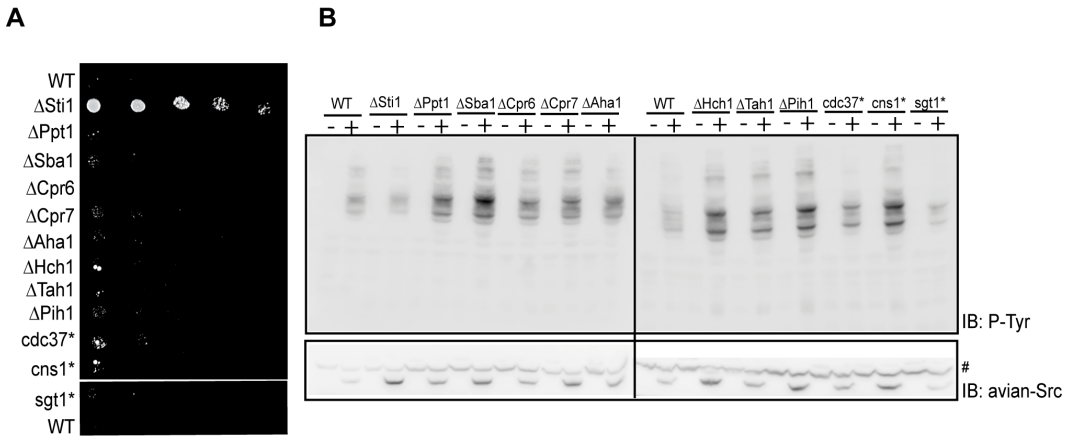

Figure 3.39: Influence of the Hsp90 co-chaperones on c-Src3MΔC. (A) Similar to the assays for v-Src, spot tests were done for c-Src3MΔC. Cell survival indicates inactive c-Src3MΔC. (B) Phosphotyrosine blots for samples expressing c-Src3MΔC (+) and uninduced cultures (−). (#) : unspecific band, serves as loading control

3.3.3 c-Src3M

c-Src3M is more similar to c-Src than v-Src. It has very low phosphotyrosine activity and is not very toxic to yeast. Comparing the three Src kinases in this study, it is also the least dependent on Hsp90. In the survival assay all the strains were able to grow even on galactose plates (Figure 3.40A) and thus is was difficult to comment on the co-chaperone dependence of c-Src3M just based on this assay. Based on the phosphotyrosine blots, the Cdc37 and Sgt1 knock-down strains show a significant decrease in c-Src3M activity. Thus, these co-chaperones are important for c-Src3M maturation, as expected. Surprisingly, the Sti1 deletion strain does not exhibit reduced c-Src3M activity, suggesting that Sti1 requirement in the maturation of this mutant might be alleviated(Figure 3.40B). It should be noted that compared to the phosphotyrosine blots for v-Src, the induced/uninduced signal ratio was lower in this case. In other words, more unspecific background signal was detected in the raffinose grown cultures. Since the general activity of this kinase was very low, the exposure times for the blots had to be increased and hence the higher background signal.

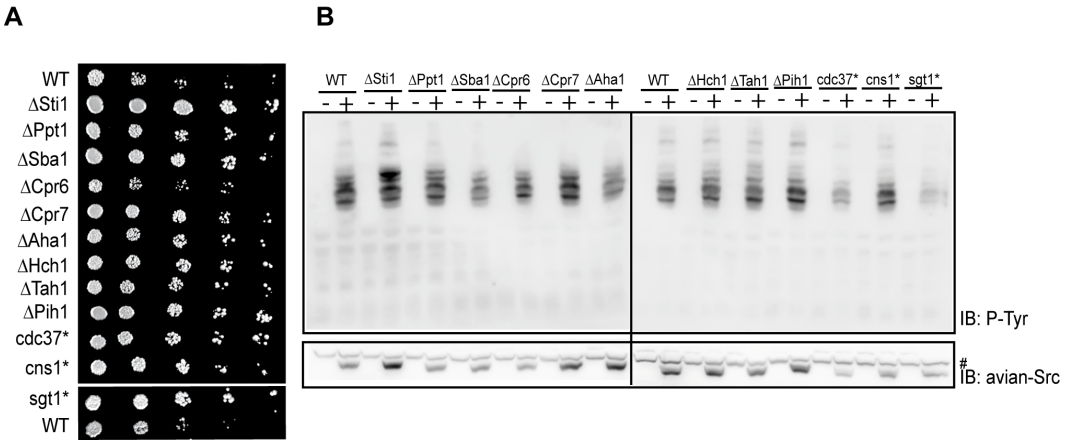

Figure 3.40: Influence of the Hsp90 co-chaperones on c-Src3M. (A) Survival assay for c-Src3M as described earlier. (B) Phosphotyrosine blots showing cultures expressing c-Src3M (+) and uninduced cultures (−).(#) : unspecific band, serves as loading control.

3.3.4 Effect of temperature on the co-chaperone dependency of v-Src

Similar to the SHRs, the effect of temperature on the co-chaperone requirement of v-Src was studied. To this end, survival assays were performed at 25°C (lower than

optimum) and 37°C (heat stress). It was observed that the strains grew slower at 25°C, however they showed a similar trend to the results at 30°C shown earlier (Figure 3.38). The Sti1 deletion strain expressing v-Src grew better than the WT strain at both temperatures. Surprisingly, all the strains were viable at 37°C, suggesting that v-Src was no longer active at this temperature. Given the intrinsic instability of v-Src [Boczek *et al.*, 2015], it is possible that the exogenously expressed protein was not stable at 37°C (Figure 3.41).

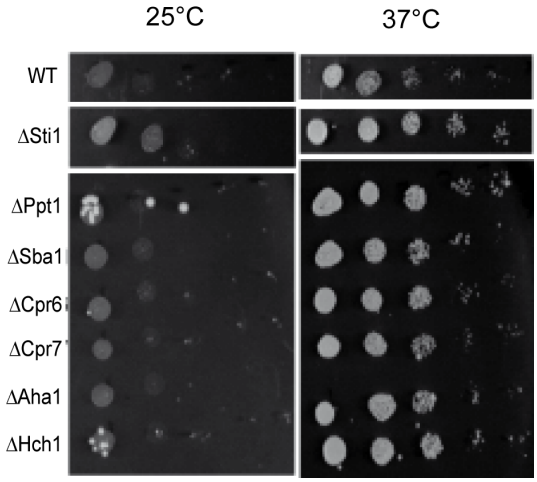

Figure 3.41: Influence of the Hsp90 co-chaperones on c-Src3M. Survival assays were performed as described previously, and plates were incubated at 25°C or 37°C, respectively, for 2 days.

3.4 Influence of the Hsp70 machinery on Hsp90 client proteins

In order to study the influence of some components of the Hsp70 machinery on Hsp90 client proteins, we studied three deletion strains of Hsp70 co-chaperones. Ydj1 is one of the most important J-proteins in yeast. The Ydj1 deletion strain has a growth defect [Caplan & Douglas, 1991] and also exhibits a temperature-sensitive phenotype when grown at 37°C [Caplan *et al.*, 1992]. Sse1 is a member of the Hsp100 family and activates the ATPase activity of Hsp70 [Raviol *et al.*, 2006]. Finally Snl1, a homologue of the mammalian Bag1, acts as a nucleotide exchange factor for Hsp70 [Sondermann *et al.*, 2002]. Each of the SHRs and v-Src were expressed in these deletion strains and their activity was compared to the WT strain.

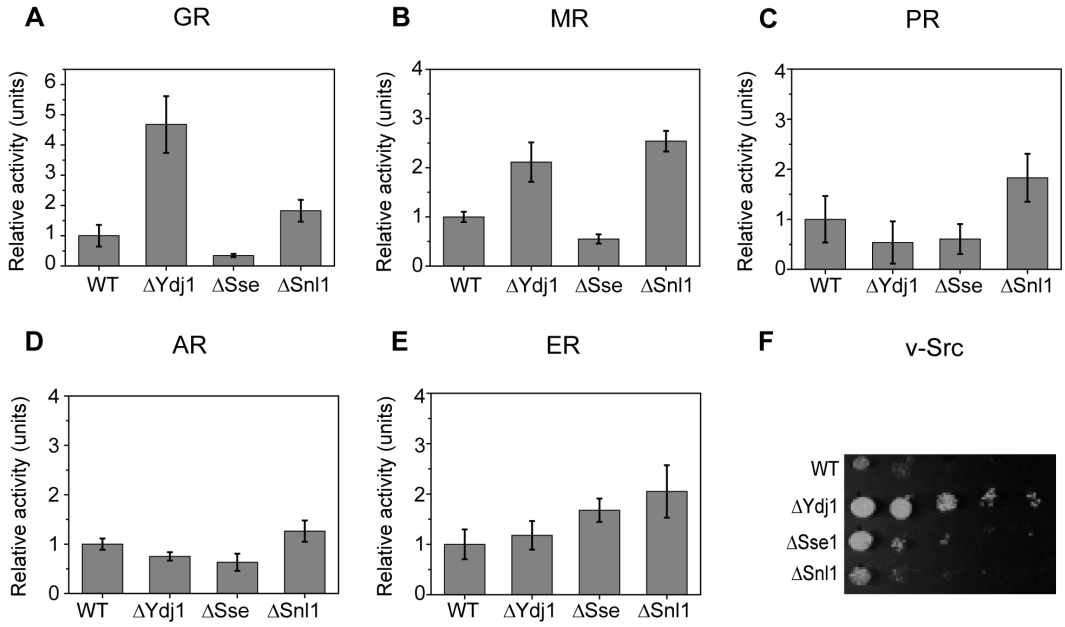

Figure 3.42: Influence of the Hsp70 co-chaperones. (A-E) β-gal assays were measured for all five SHRs in the Hsp70 co-chaperone deletion strains. The activity in the WT strain was considered 1. (F) Survival assays for the effect of Hsp70 co-chaperones on v-Src activity as described previously.

The results show that GR and MR behave similarly and have increased activity in the absence of Ydj1 and Snl1. Deletion of Sse1 on the other hand led to a decrease in GR and MR activity, suggesting a positive role for Sse1 in GR and MR maturation (Figure 3.42A-B). PR and ER also showed higher activity in the Snl1 deletion strain, but not in the Ydj1 strain (Figure 3.42C and E). AR activity on the other hand was not significantly influenced in any of the deletion strains (Figure 3.42D). In the case of v-Src, Ydj1 and to some extent Sse1, seem to be important for v-Src maturation. Snl1 deletion did not influence v-Src activity adversely (Figure 3.42F).

3.5 Transcriptome mapping by gene-chip analysis

To investigate the deletion strains in further details, their transcriptional profiles were studied. To this end, transcriptome mapping of the Cpr6, Cpr7 and Hch1 deletion strains was performed using gene-chip analysis at the Kompetenzzentrum für Fluoreszente Bioanalytik, Regensburg, Germany. Two independent cultures of each deletion strains and the WT strain were maintained in log-phase for two days. The cell-pellets were then flash frozen and sent to Regensburg for further analysis. The gene-chip analysis and data processing was performed by the bioinformaticians. For normalization of the gene-chip data, the MAS5 normalization algorithm developed by Affymetrix [Affymetrix, 2002] was used.

3.5.1 Transcriptional analysis of the $\triangle$Cpr6 strain

Cpr6 is a TPR co-chaperone homologous to Cpr7. It was thus of interest to analyse whether deleting Cpr6 led to any changes in the expression of other TPR co-chaperones, including Cpr7. To this end, the mAS5-algorithm data obtained for the Cpr6 deletion strain was compared to that of the WT strain. As expected, Cpr6 was absent in the deletion strain. Additionally, both Hsp90 isoforms in yeast as well as all the Hsp90 co-chaperones, including Cpr7, did not show deviation in mRNA levels between WT and Cpr6 deletion strain (Figure 3.43). In addition to the Hsp90 system, the Hsp70 machinery, together with nucleotide exchange factors and J-proteins like Ydj1 were not affected (Figure 3.44A). Finally, other chaperone machineries like chaperonins and their modulators, Hsp100s and sHsps were also not affected in this strain (Figure 3.44B). Taken together, the data shows that deleting Cpr6 does not lead to any deviations in the remaining chaperone machinery of the cell. Moreover,

none of the other TPR co-chaperones were upregulated to compensate for the absence of Cpr6.

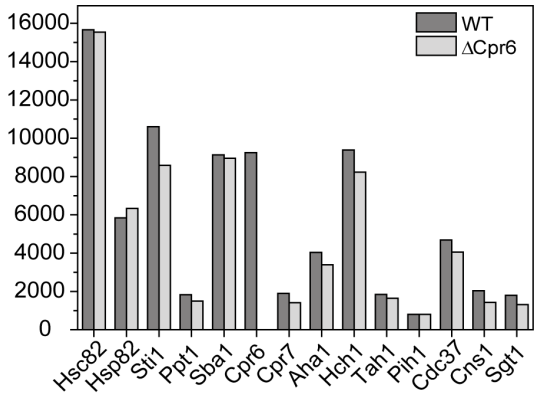

Figure 3.43: Influence of Cpr6 deletion on the Hsp90 machinery. mAS5 values obtained for components of the Hsp90 machinery in the Cpr6 deletion strain were compared with the WT strain.

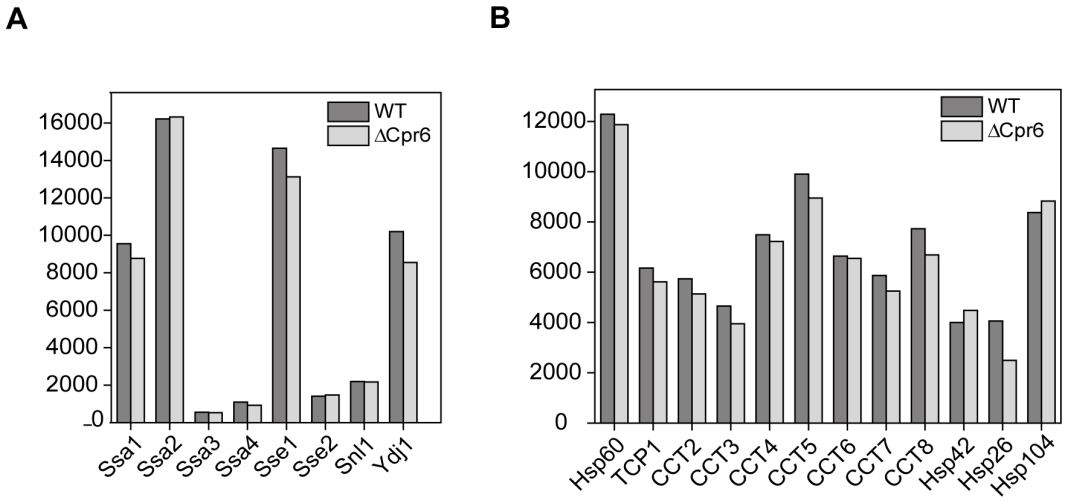

Figure 3.44: Influence of Cpr6 deletion on various chaperone machineries. (A) Comparison of the mAS5 values for components of the Hsp70 machinery. Ssa1-4: isoforms of Hsp70 in yeast, Sse1-2, Snl1 and Ydj1: Hsp70 co-chaperones. (B) Comparison of the mAS5 values for components of other chaperone machineries. TCP1, CCT2-8: modulators of chaperonin Hsp60; Hsp42 and Hsp26: sHsps.

3.5.1.1 Changes in the gene expression in the Cpr6 deletion strain

To further investigate the changes in gene expression in the Cpr6 deletion strain apart from the chaperone machinery, the $\log_2$ values of the mAS5 data of the WT strain were then compared to the $\log_2$ values of Cpr6 deletion strain, and the fold difference was calculated. The first hundred up- or down-regulated hits were selected and clustered based on co-regulation patterns from co-expression databases. The bioinformatic analysis showed that in the Cpr6 deletion strain, 71 genes showed a two-fold or greater up/down regulation as compared to the WT strain. These 71 genes were a part of the genes selected for assembling the network. Most of the genes selected could be assembled into an interconnected network. The network of genes showing lower expression in the Cpr6 strain as compared to the WT are shown in Figure 3.45. It was evident from the network analysis that transcripts related to iron metabolism (ARN1, ARN2, FRE5, TIS11, FIT1 and SIT1) were down-regulated in the Cpr6 deletion strain. Additionally, another larger cluster of genes was identified which belongs to genes involved in the anaerobic metabolism in yeast. Compared to the WT, these transcripts showed reduced expression.

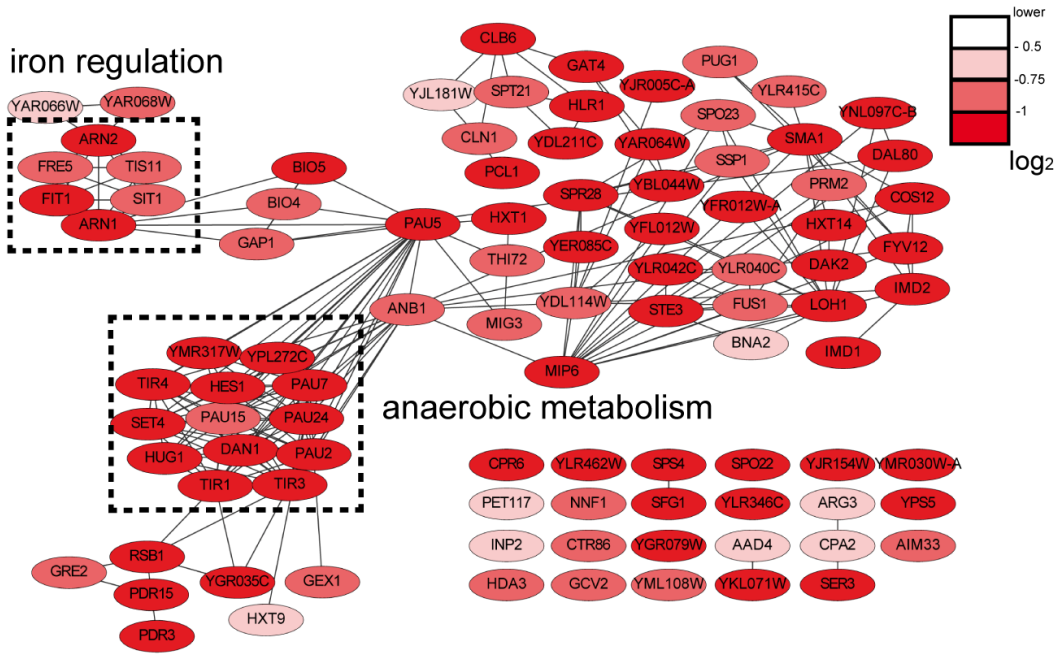

Figure 3.45: Network of genes down-regulated in the Cpr6 deletion strain. Genes are coloured in accordance to their log differences with the WT strain. 100% red: $-1 > \log_2(x)$; light red: $-0.75 > \log_2(x) > -1$; pink: $-0.5 > \log_2(x) > -0.75$. Black dotted boxes highlight clusters according to cellular pathways.

Clustering the genes which had increased expression compared to the WT strains, led to the generation of another interconnected network (Figure 3.46). The network shows that transcripts related to phosphate metabolism (PHO family, SPL2, VTC3 and 4, and PHM6) were upregulated in the Cpr6 strain in comparison to the WT. Moreover, another large cluster of genes was evident. Functionally characterizing the individual components of this cluster, it could be seen that most of these transcripts were found to be upregulated under heat shock or stress conditions. A majority of the members of this cluster are membrane proteins which localize to the plasma membrane, endoplasmic reticulum or the mitochondrial inter-membrane space. Some components of this cluster also are known to be upregulated in response to glucose starvation, stationary phase and DNA replication stress. Intriguingly, a function or metabolic pathway common to all the genes in this cluster could not be identified and requires further bioinformatic investigation.

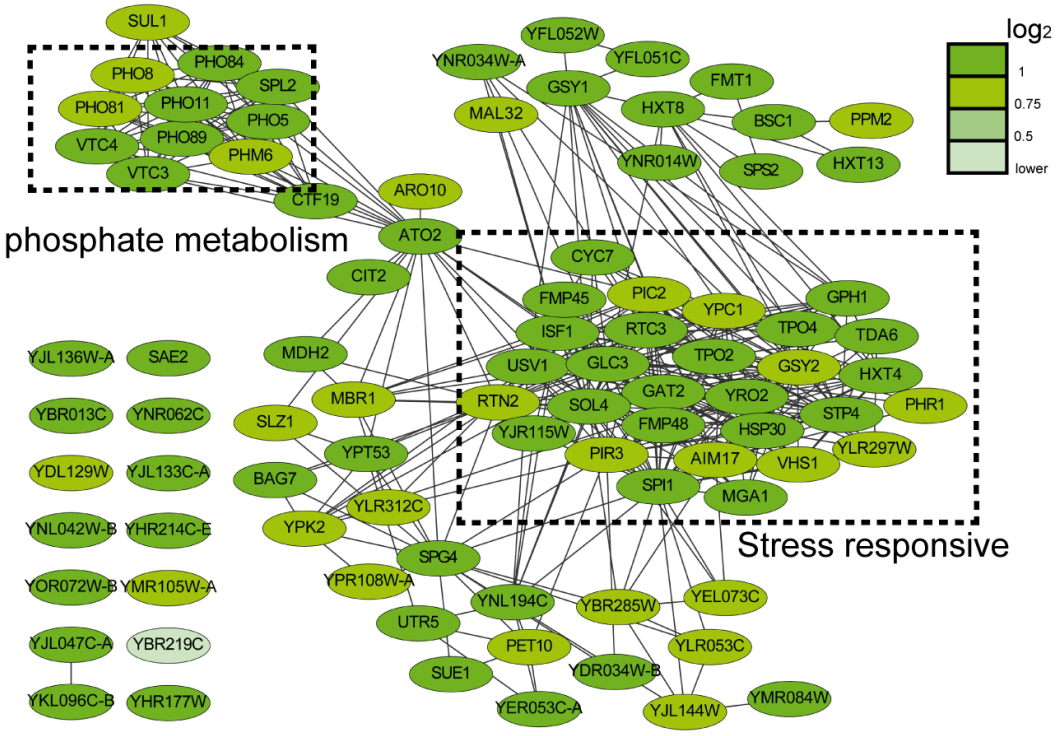

Figure 3.46: Network of genes up-regulated in the Cpr6 deletion strain. Genes are coloured in accordance to their log differences with the WT strain. 100% green: $\log_2(x) > 1$; 75% green: $1 > \log_2(x) > 0.75$; 50% green: $0.75 > \log_2(x) > 0.5$; 25% green: $0.5 > \log_2(x)$. Black dotted boxes highlight clusters according to cellular pathways.

3.5.2 Transcriptional analysis of the ΔCpr7 strain

Similar to Cpr6, the Cpr7 deletion strain was validated by the missing Cpr7 mRNA. Additionally, none of the components of the Hsp90 machinery were perturbed upon deleting Cpr7 (Figure 3.47). Other chaperone machineries in the cell, like the Hsp70, sHsps, chaperonins and Hsp100s were all at levels comparable to the WT (Figure 3.48A-B). Thus, like Cpr6, Cpr7 deletion did not lead to any significant modification of the chaperone machinery in the cell.

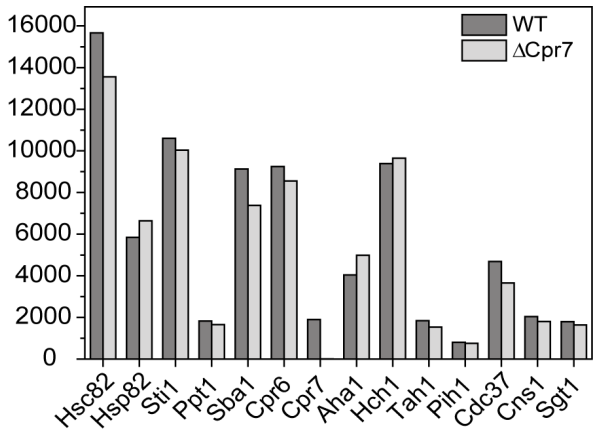

Figure 3.47: Influence of Cpr7 deletion on the Hsp90 machinery. mAS5 values obtained for components of the Hsp90 machinery in the Cpr7 deletion strain were compared with the WT strain.

3.5.2.1 Changes in the gene expression in the Cpr7 deletion strain

The transcriptional profile of the Cpr7 deletion strain was compared next to the WT strain. Again the first hundred genes in either direction were selected. Of these 200 genes, 120 genes showed more than 2 fold deviation from the WT transcripts. Network analysis of the down regulated genes showed similar clustering to the Cpr6 deletion strain. The Cpr7 deletion strain also showed a reduced expression (compared to the WT) of genes involved in iron metabolism as well as anaerobic growth (Figure 3.49).

Analysing the genes with increased expression in the Cpr7 deletion strain showed that in this case, most of the genes formed one large cluster, similar to the stress responsive cluster up-regulated in the Cpr6 deletion strain. Most of the members in this cluster are common to both the Cpr6 and Cpr7 deletion strains. The Cpr7

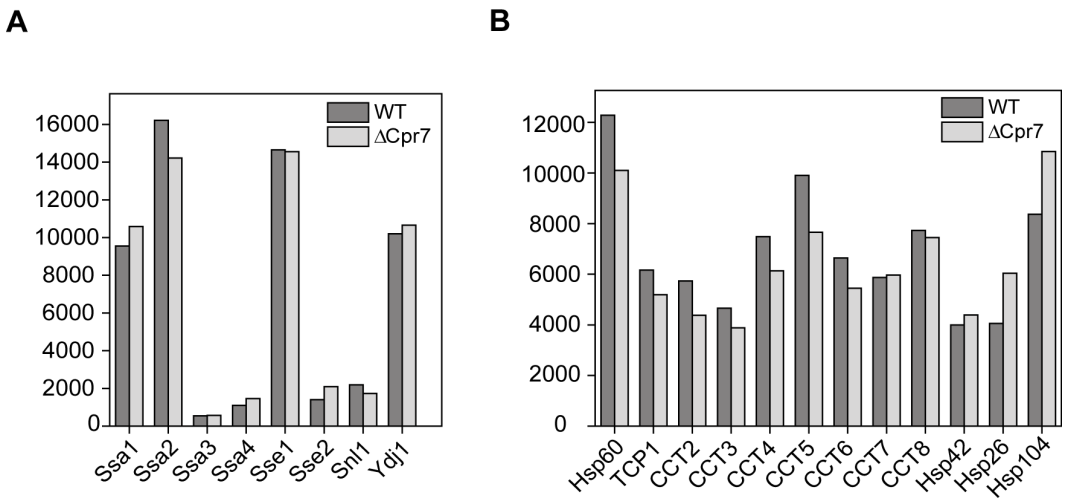

Figure 3.48: Influence of Cpr7 deletion on various chaperone machineries. (A) Comparison of the mAS5 values for components of the Hsp70 machinery. (B) Comparison of the mAS5 values for components of other chaperone machineries.

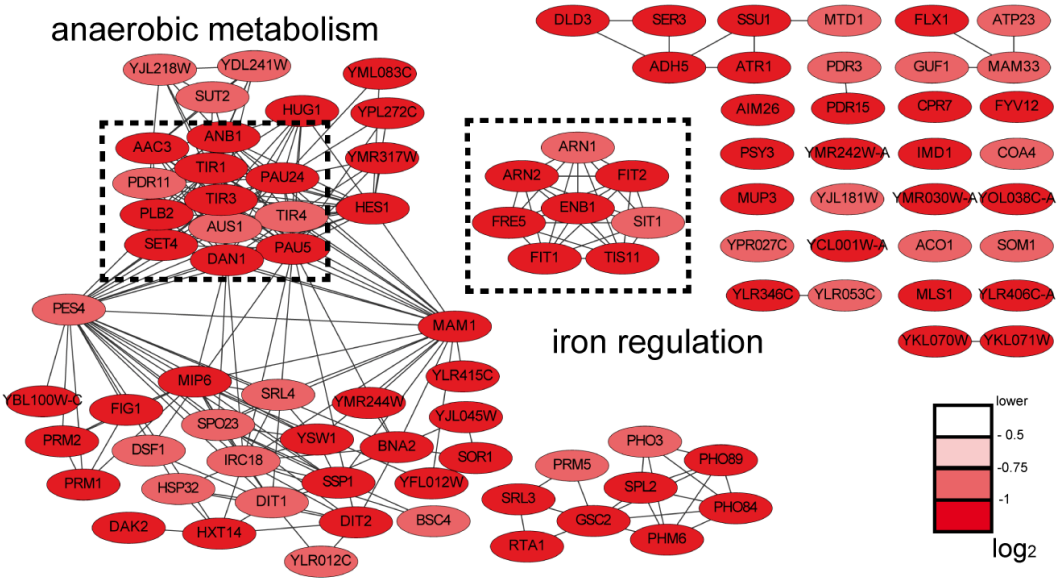

Figure 3.49: Network of genes down-regulated in Cpr7 deletion strain. The same colour code as Figure 3.45 is used. Black dotted boxes highlight clusters according to cellular pathways.

deletion strain did not show any up-regulation of the phosphate metabolism like in case of Cpr6 (Figure 3.50).

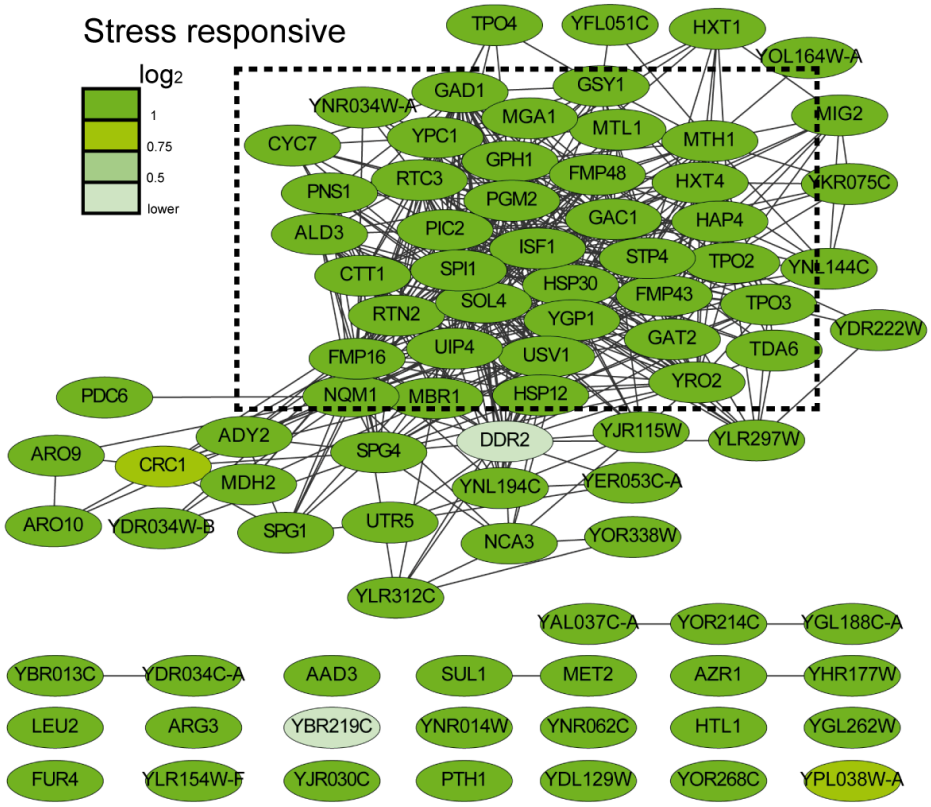

Figure 3.50: Network of genes up-regulated in Cpr7 deletion strain. The same colour code as Figure 3.46 is used. Black dotted boxes highlight clusters according to cellular pathways.

3.5.3 Transcriptional analysis of the ΔHch1 strain

Hch1 is homologous to the N-domain of Aha1. However, deleting this co-chaperone also did not lead to differences in the mRNA levels of any other components of the Hsp90 machinery. Not even the homologous Aha1 showed any deviation from the WT levels (Figure 3.51). Other chaperone machineries in the cell, like the Hsp70, chaperonins and Hsp100s and sHsps were all at levels comparable to the WT strain (Figure 3.52A-B).

3.5.3.1 Changes in the gene expression in the Hch1 deletion strain

Similar to Cpr6 and Cpr7, the transcriptional profile of the Hch1 deletion strain was also compared to the WT strain. In the case of Hch1 deletion strain, only 38 genes showed more than 2 fold deviation from the WT. The network formed from genes showing reduced expression in the Hch1 deletion strain looked significantly different

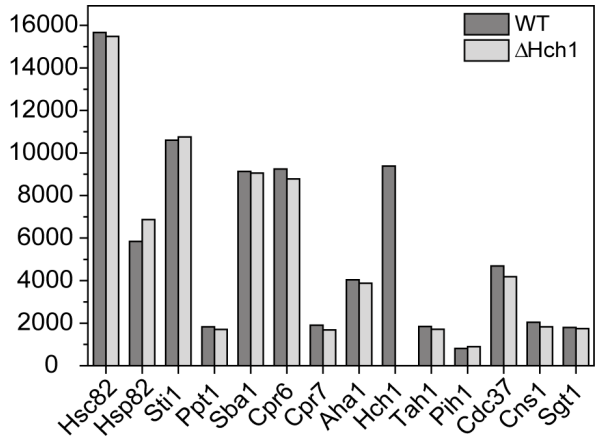

Figure 3.51: Influence of Hch1 deletion on the Hsp90 machinery. mAS5 values obtained for components of the Hsp90 machinery in the Hch1 deletion strain were compared with the WT strain.

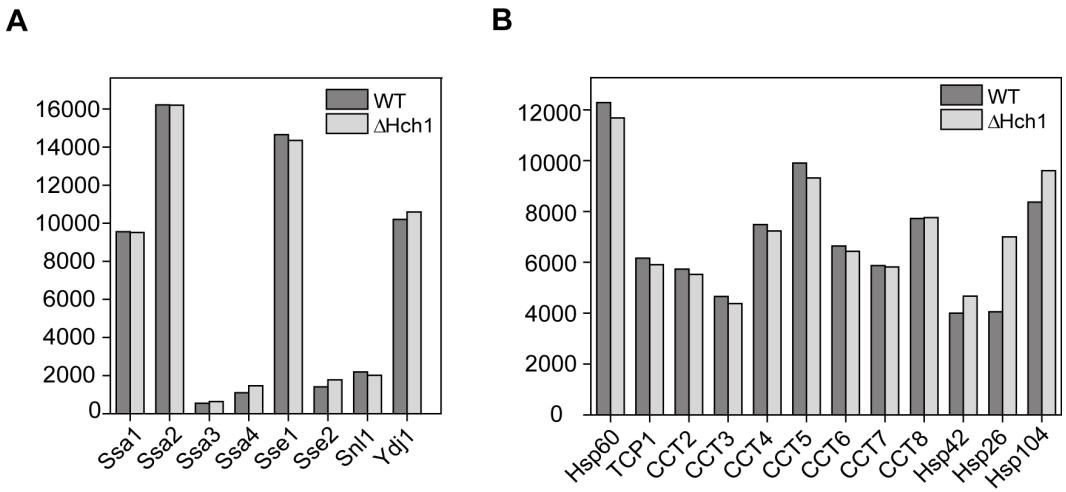

Figure 3.52: Influence of Hch1 deletion on various chaperone machineries. (A) Comparison of the mAS5 values for components of the Hsp70 machinery. (B) Comparison of the mAS5 values for components of other chaperone machineries.

than the down-regulated networks shown above. In case of the Hch1 deletion strain, a few genes (PAU5, 15, 24, HES1, DAN1, TIR3 and 4) belonging to the large anaerobic metabolism clusters were observed again (Figure 3.53). It should be noted that the anaerobic metabolism cluster in the Hch1 deletion strain is much smaller than in the Cpr6 and Cpr7 deletion strain. The Hch1 deletion strain did not show a down regulation of genes involved in iron regulation. Intriguingly, another tightly bound cluster was observed in the Hch1 network. The genes in this cluster are involved in

serine/glycine biosynthesis (SER1, 3, 33), histidine biosynthesis (HIS3, 5, 7), purine biosynthesis (ADE2, 4, 8) as well as fatty acid biosynthesis (CEM1). Additionally, SHM2, involved in generating precursors for amino acids, purines as well as fatty acid synthesis was found in this cluster suggesting a common link between these metabolic processes.

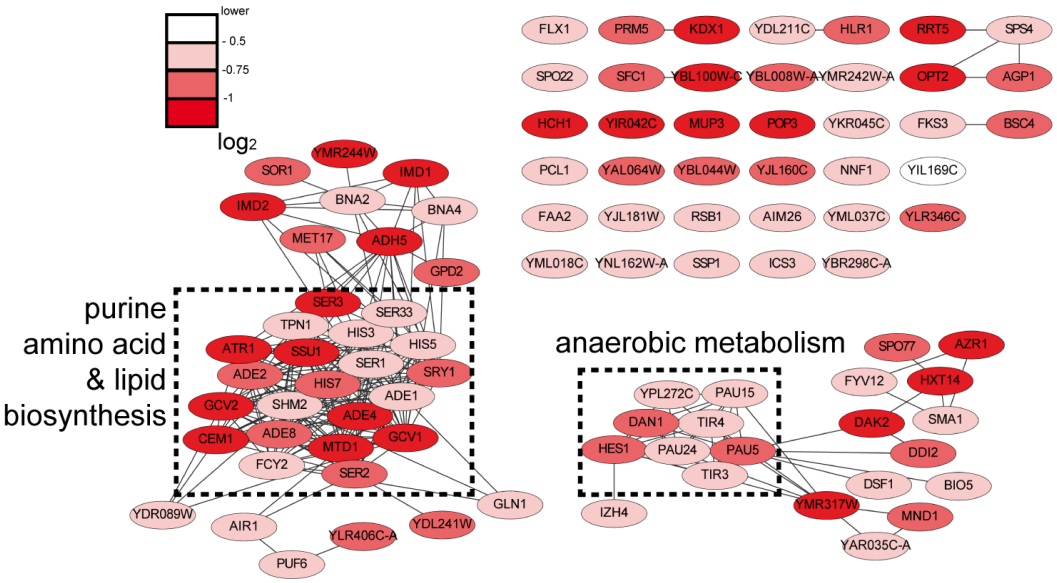

Figure 3.53: Network of genes down-regulated in Hch1 deletion strain. The same colour code as Figure 3.45 is used. Black dotted boxes highlight clusters according to cellular pathways.

The up-regulated genes in the Hch1 deletion strain compared to the WT strain, formed three different clusters (Figure 3.54). The stress responsive cluster observed in the Cpr6 and Cpr7 deletion strain profiles was again observed in the Hch1 deletion strain. Additionally, similar to the Cpr6 deletion strain, genes involved in phosphate metabolism were also upregulated. Unlike the up-regulation networks for Cpr6 and Cpr7, the Hch1 network showed another small cluster. The genes in this cluster are involved in mating and respond to pheromones (PRM6, FUS1, ASG7). Others play a role in facilitating cell adhesion during mating (AGA1, FIG1). The reason for the up-regulation of these genes in the Hch1 deletion strain is unclear.

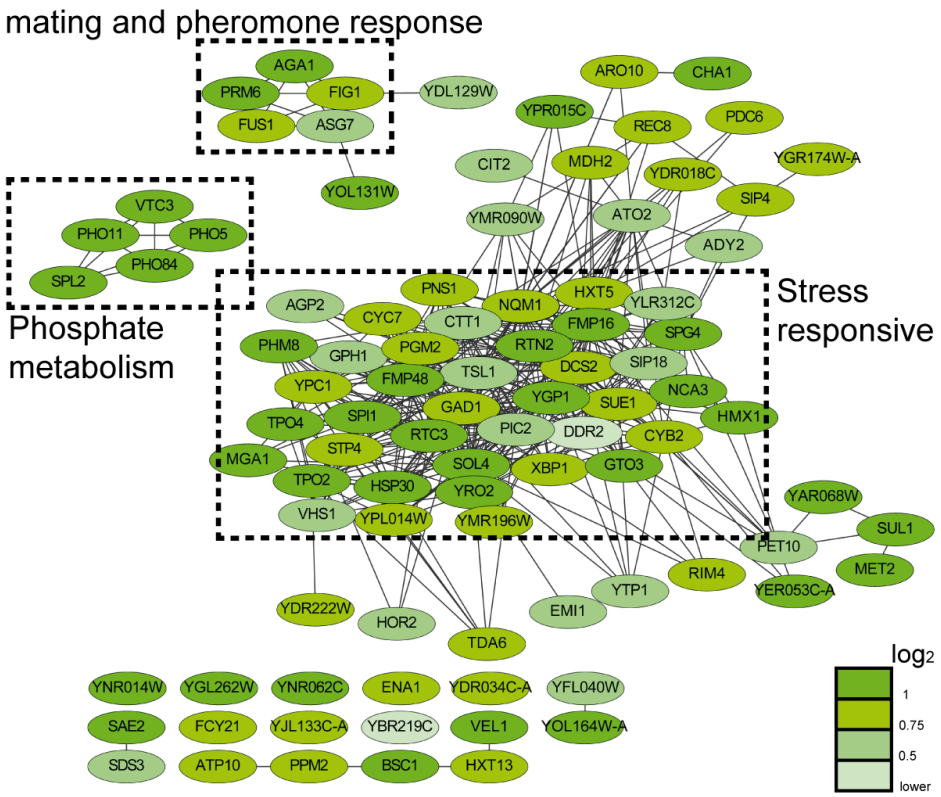

Figure 3.54: Network of genes up-regulated in Hch1 deletion strain. The same colour code as Figure 3.46 is used. Additionally, black dotted boxes highlight clusters according to cellular pathways.

3.6 Quantification of Hsp90 co-chaperones in yeast

The multi-component Hsp90 system in yeast is very tightly regulated. While Hsp90 is abundantly expressed in the cell, there is a considerable variation in the co-chaperones. Four different high-throughput studies have been published to date, each employing a different technique for quantifying the proteome of yeast. The method used to calculate the protein abundance in all these studies differ with respect to the tag on the protein (TAP, GFP) and the high-throughput technique employed (high-throughput microscopy, mass spectrometry and flow cytometry) [Ghaemmaghami *et al.*, 2003; Chong *et al.*, 2015; Newman *et al.*, 2006; Kulak *et al.*, 2014].

In order to estimate the number of endogenously expressed, untagged co-chaperones per cell, the lysates from the WT BY4741 yeast strain were prepared. First the OD_{600} of the log phase cultures was measured and the cells were counted. Every $OD_{600}=5$ of cells were lysed in 100 μl Lämmli sample buffer. Comparing the cells counted and

the final lysate volume, the cells/μl lysate was calculated. Figure 3.55 shows that in most of the experiments, the cells/lysate volume (μl) was maintained constant. This served as a good control for the final calculation. Three experiments (no. 2, 14 and 17), where the cells/lysate showed a significant deviation from the rest, were not considered for further calculations.

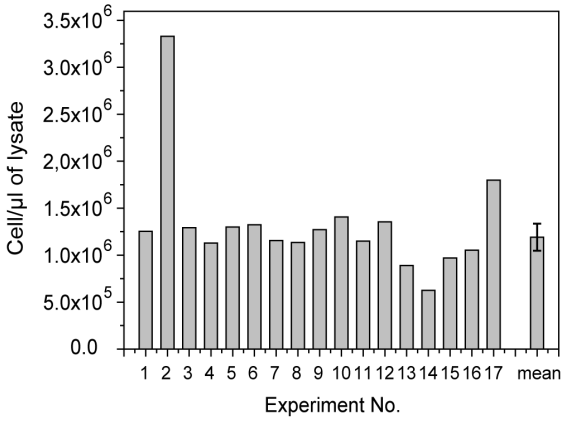

Figure 3.55: Distribution of cells/μl of lysate. Logarithmic WT cultures were diluted and the cells were counted using a Neubauer chamber. OD_{600} was measured and the cells were lysed in Lämmli buffer following alkali lysis (100 μl sample buffer per OD_{600}=5). For every experiment, the cells/μl of lysate was calculated.

The lysate was loaded in triplicates (3-5 dilutions each) on a gel together with a purified co-chaperone of known concentrations. A standard curve was generated using the purified co-chaperone signal and the concentration of the protein in the lysate was calculated. In all cases the R^2 value of the slope of the standard curve used was greater than 0.95. Based on the cell number, the molecules/cell for every co-chaperone were estimated. The results show a representative blot for each co-chaperone (Figure 3.56A). Hsp82 was the most abundant protein in the Hsp90 machinery as expected. However, the Hsp82 molecules/cell are about three-fold less than that predicted previously [Ghaemmaghami *et al.*, 2003]. Surprisingly, Cpr6 and Sba1, closely followed by Sti1 were also abundant in the cell (Figure 3.56B). Cpr7 is less abundant in the cell compared to Cpr6. Hch1, the yeast specific homologue of Aha1 is also much less abundant in comparison to Aha1. Surprisingly, the essential co-chaperones namely, Cdc37, Cns1 and Sgt1 are among the least abundant components of the Hsp90 machinery. Table 3.1 shows the molecules per cell for the Hsp90 co-chaperones and offers a comparison to the values published earlier.

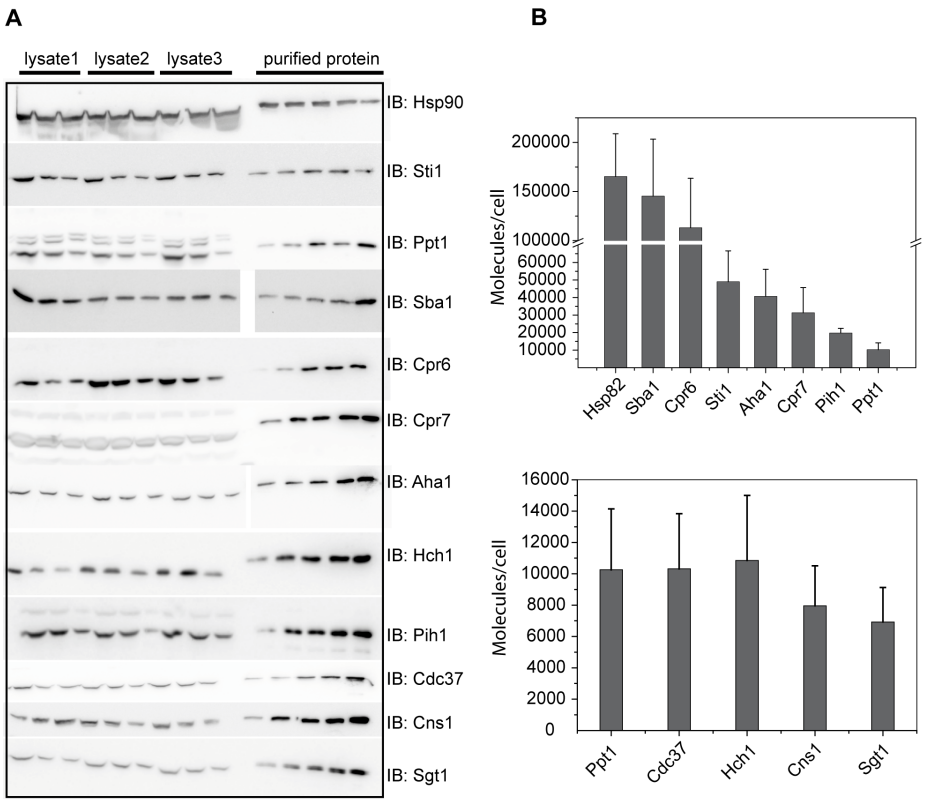

Figure 3.56: Quantification of the Hsp90 co-chaperones. (A) A representative blot for Hsp90 and each co-chaperone is shown. Three separate lysates were loaded in 3 dilutions each. On the right, increasing concentrations of purified protein was loaded to generate a standard curve. The amount of a given protein in the lysate was calculated based on the equation obtained for the standard curve. (B) The band intensities were quantified using Image J. The concentration of the protein in the lysate was determined based upon the standard curve generated from same blot. Finally an average over all the experiments was calculated for each co-chaperone and Hsp90, with error bars. Upper panel shows the abundantly expressed components of the Hsp90 machinery, while lower panel shows the less abundant ones. Ppt1 is shown in both, for comparison.

Table 3.1: Comparison of the quantification of co-chaperones

Protein	**This work**	**Ghaemmaghami**[1]	**Chong**[2]	**Newman**[3]	**Kulak**[4]
Hsp82	147483	445000	4167	6395	10044
Sba1	137741	33700	1590	2017	28577
Cpr6	112387	18600	645	1053	33801
Sti1	49011	67600	2593	3997	52260
Aha1	40690	13900	662	813	17266
Cpr7	31326	3230	117	154	1610
Pih1	20246	2610	ND	ND	841
Ppt1	10260	6990	273	314	4688
Cdc37	10242	10200	406	449	10034
Hch1	10191	8530	799	912	28484
Cns1	7170	672	199	274	3705
Sgt1	6925	1340	78	ND	1666
Tah1	ND	1660	134	76	ND

(1) [Ghaemmaghami *et al.*, 2003]
(2) [Chong *et al.*, 2015]
(3) [Newman *et al.*, 2006]
(4) [Kulak *et al.*, 2014]

4
Discussion

The Hsp90 molecular chaperone, together with its large cohort of co-chaperones, forms a very sophisticated, tightly regulated chaperone machinery in the cell. The conformational dynamics of Hsp90, the modulation of its essential ATPase activity by various co-chaperones, post-translational modifications and finally the influence of the client itself, make Hsp90 a highly dynamic molecular chaperone. These multiple layers of modulation enable Hsp90 to chaperone over 300 client proteins. Hsp90 client proteins belong to different functional classes including transcription factors and kinases and play an important role in various cellular pathways. As a result, Hsp90 takes centre stage in maintaining homeostasis in the cell. Extensive research over the past decades has uncovered the central importance of Hsp90 in numerous cellular pathways. The diversity of the client proteins has made Hsp90 a potential target for many therapeutic strategies, especially against cancer [Taldone *et al.*, 2014]. Biochemical and biophysical methods have elucidated the structure and the regulatory mechanism of Hsp90, including its interaction with co-chaperones and the conformational dynamics coupled to ATP hydrolysis. While reconstitution and *in vitro* studies have helped in dissecting the Hsp90 cycle, the client side of the story has always been under-represented. It is still not clear what qualifies a protein to be a Hsp90 client. No specific recognition sequence or motif, common among the client

proteins has been identified for interaction with Hsp90. How the co-chaperones influence client maturation also remains enigmatic. This prompted us to investigate the roles of the Hsp90 co-chaperones with respect to client proteins.

4.1 Characterization of co-chaperone deletion strains

Evolutionarily, the Hsp90 system has become more complex from bacteria to lower eukaryotes to finally mammalian cells [Johnson, 2012]. Despite this, the Hsp90 chaperone network is largely conserved between yeast and man. This made it possible to study well-known mammalian client proteins in a relatively simpler context using *Saccharomyces cerevisiae*, while still maintaining the client-co-chaperone complexes. Yeast, being a simple eukaryotic, single cell organism, encompasses all the benefits of working with eukaryotic cells (like cellular organisation, post-translational modifications, secretory system) and, at the same time, has a simplified genome and proteome. The entire genome of yeast has been sequenced and performing genetic manipulations in yeast is relatively easy as compared to the mammalian system. In the case of Hsp90 and its co-chaperones, using yeast has an added advantage. Most of the Hsp90 co-chaperones in yeast are not essential for viability. Thus it is possible to directly study the effect of deleting a co-chaperone on the activity of Hsp90 client proteins. Among the co-chaperones, three are essential for viability and hence could only be knocked down. The dAMP technique was used to achieve this. The diploid strains from the dAMP library generated by the Weissman group [Breslow *et al.*, 2008] (Thermo Scientific Open Biosystems) were sporulated and haploids were picked showing the desired knock-down of the essential co-chaperones.

Deleting a certain protein completely can sometimes have secondary effects on the cell. Thus, in order to ensure that the effects of deleting the co-chaperone on a particular Hsp90 client protein were specific, a thorough characterization of the deletion strains was essential. The general characterization showed that apart from the Cpr7 and Pih1 deletion strain, none of the other strains showed any growth defect. The growth defect of the Cpr7 strain has been observed previously [Duina *et al.*, 1996]. In the case of Pih1, it has been shown to have a growth defect at 37°C, but not at 22°C [Paci *et al.*, 2012]. The growth curves measured in this work were recorded at 30°C. Moreover, the effect of Pih1 deletion on general growth characteristics of yeast could be strain-specific, as the studies performed earlier were done using the W303 background strain, while BY4741 was used in this study. The differences between

these strains with respect to cell size, membrane potential and tolerance to alkali metals have been described earlier [Petrezselyova *et al.*, 2010]. Thus, a different response to Pih1 deletion might be plausible. After studying the growth characteristics of all the strains, we studied the morphology of the cells. Pih1 cells appeared to be slightly smaller than the WT. All remaining strains had WT-like morphology, suggesting that the 'cellular infrastructure' of the strains was not influenced, including the slow growing Cpr7 deletion strain.

During the course of this work, we studied exogenously expressed (plasmid-borne) client proteins in these strains. The activity and the steady-state protein levels in the deletion strain were compared to that in the WT. For this, it was first essential to ascertain that the effects on the client proteins are not influenced by any dysfunctional cellular process. We tested the cellular machineries involved in protein production and maintenance. We first monitored transcription of a non-client protein eGFP and observed that the amount of eGFP-mRNA is comparable in all the strains. Secondly, the rate of overall translation monitored by the incorporation of radio-labelled methionine was also WT-like in all strains. Folding of two different non-client proteins, eGFP and β-Galactosidase showed that protein folding was not compromised in any of the strains. Moreover, constitutively expressed β-Gal showed WT-like activity in all the deletion/knock-down strains. This was an important control showing that β-Gal activity itself is not influenced in any of the deletion strains. Used in the reporter assay, β-Gal can thus function as an unbiased reporter protein which is not Hsp90-dependent. Finally, the complete processing of an autophagy marker ascertained a functional autophagy system in all strains. These exhaustive control experiments establish that the co-chaperone deletion strains as well as the three knock-down strains are fully functional, without any obvious defects in the cellular processes studied. To complete this characterization, the proteasomal degradation in all the strains needs to be monitored using ubiquitin-β-galactosidase fusion protein [Bachmair *et al.*, 1986]. This chimeric protein is recognized by the proteasomal machinery is degraded via the ubiquitin-proteasomal system (UPS).

To investigate whether deleting a co-chaperone influences the expression of other components of Hsp90 machinery, the protein levels of each of the co-chaperones was analysed by western blot. The blots showed that none of the co-chaperone deletions/knock-downs led to the up- or down-regulation of the other co-chaperones or Hsp90 itself. This was an important finding as it suggests that the co-chaperone functions might not be redundant. Deleting one, does not lead to any compensatory changes in the other co-chaperone levels. This was especially interesting in the case

of the two pairs of homologous Hsp90 co-chaperones in yeast. Cpr6 and Cpr7 share 38% amino acid identity and have peptidyl-prolyl isomerase activity. Deleting either did not lead to an up-regulation in the levels of the other. Both these PPIases have been suggested to differ in their *in vivo* functions [Mayr *et al.*, 2000], and the non-compensatory behaviour also points towards their functions being non-related and non-redundant. Similarly, Aha1 and its N-domain homologue Hch1 also show no changes upon deleting either co-chaperone. Furthermore, transcriptional gene-chip analysis was done for all four of these deletion strains to compare and contrast the effects of the deletion. The transcript levels also confirm our protein data that none of the components of the Hsp90 machinery is affected in these deletion strains. Moreover, none of the components of other chaperone machineries shows any deviation from their respective WT-transcript levels in these strains.

Based on this thorough characterization of the deletion strains, it can be concluded that the strains in each case lack the respective co-chaperone, but this deficiency does not adversely affect any of the innate cellular processes. Thus, these strains are an excellent tool to study the influence of these co-chaperones specifically on various Hsp90 client proteins.

4.2 Influence of the Hsp90 co-chaperones on clients

During this work, the first question asked was whether Hsp90 client proteins have specific requirements of co-chaperones for their maturation and activation. To answer this question, Hsp90 client proteins belonging to two main functional classes were selected. The first class of proteins are nuclear receptors which can function as transcription factors in response to ligand binding. Within this class, 5 different steroid hormone receptors (SHRs) were investigated. Each of these steroid hormone receptors was found to be dependent on the yeast Hsp90 when expressed exogenously in yeast. The second most important class of Hsp90 clients are the kinases. As a representative of kinases, the stringently Hsp90-dependent v-Src was studied. Studying these functionally and structurally distinct client proteins was beneficial to highlight the differences between different classes of client proteins. Additionally, studying all five SHRs served to examine the difference and similarities within a closely related protein family. RT-PCR showed that the mRNA levels of GR were similar in all the deletion/knock-downs strains. Thus the effect of co-chaperones on client proteins is post-translational. The results obtained from the β-Gal assays

for SHRs and survival assays and phosphotyrosine blots for v-Src are summarized in Figure 4.1.

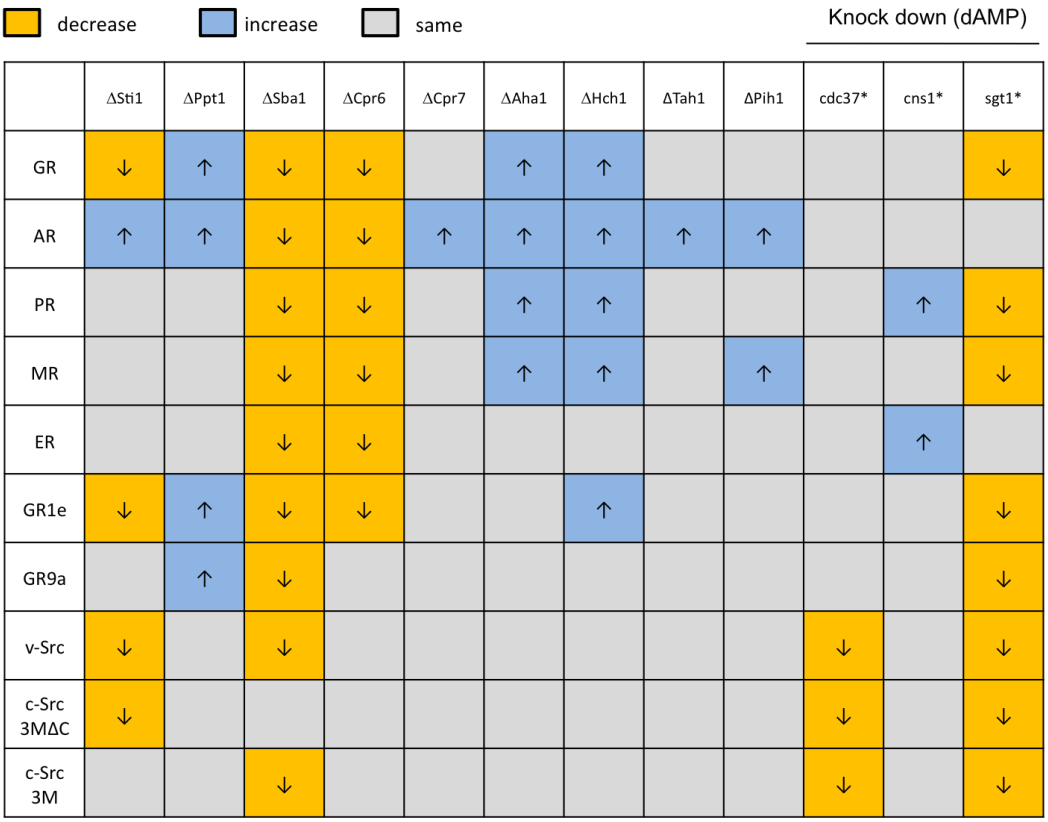

Figure 4.1: Client co-chaperone dependencies. Arranged in the rows are the different client proteins and their variants. The co-chaperone deletion strains are arranged in columns. A decrease in client activity, compared to the WT, in a certain co-chaperone deletion/ knock-down strain is shown in yellow (↓). Relative increase in activity is highlighted in blue (↑). Grey squares indicate WT-like activity in the respective strains.

- SHRs

  An overview of the matrix shows that the client proteins respond differently to the deletion of co-chaperones. Within the SHRs family, several notable differences can be seen. The most extensively studied client, GR, shows a decrease in activity in the Sti1-, Sba1- and Cpr6-deletion strain as well as in the Sgt1 knock-down strain. The results for Sti1 and Sba1 have been reported previously [Chang *et al.*, 1997; Freeman *et al.*, 2000] and serve as a positive control for the experimental setup used in this work. Cpr6 and Sgt1 additionally, also seem to be essential for GR

maturation. Surprisingly, it has been reported earlier that GR activity decreases upon Cpr7 deletion but not upon Cpr6 deletion [Duina *et al.*, 1998], however a significant decrease of GR activity in the Cpr7 deletion strain was not observed. The dose response curves obtained using a range of hormone concentrations, also indicate that GR behaved similarly in the WT and the Cpr7 deletion strain (Figure 3.35A). Thus in our hands, GR activity did not seem to be dependent on Cpr7. Cpr6 on the other hand, seems to be crucial for GR activation. In the recent years, it has been shown that in the absence of clients, Cpr6, Sti1, and Hsp90 form an asymmetric intermediate complex that is essential for further progression of the Hsp90 cycle [Li *et al.*, 2011]. Additionally, this complex can process the GR-LBD more efficiently, suggesting that the two co-chaperones might influence the conformation of Hsp90 such that it can bind GR [Lorenz *et al.*, 2014]. These results go hand in hand with the finding that Cpr6 seems to play a crucial role for GR maturation *in vivo*.

Surprisingly, deletion of Ppt1, Aha1 and Hch1 led to an increase in the activity of GR. The absence of Aha1 or Hch1 has been reported to lead to a decrease in GR activity *in vivo* [Harst *et al.*, 2005]. The authors also suggest that Aha1 might improve the efficiency of Hsp90 in chaperoning the client. However, a recent study has shown that Aha1 competes with GR-LBD *in vitro* for interaction with Hsp90 [Lorenz *et al.*, 2014]. The increase in activity in the absence of Aha1 that we observe, might be due to an increased interaction with Hsp90, due to lack of competition. Aha1, is thought to play a negative regulatory role in CFTR processing (another Hsp90 client), targeting it to degradation [Wang *et al.*, 2006]. Thus, the absence of Aha1 might lead to the stabilization of the client protein, and hence increased activity in comparison to the WT. Aha1 and Hch1, do not compensate for this effect when the other co-chaperone is missing, suggesting that their influence of GR-Hsp90 interaction might be different. Contrary to earlier reports [Wandinger *et al.*, 2006], GR was more active in the Ppt1 deletion strain. The reason for this is unclear. Extensive studies have shown that the phosphorylation of Hsp90 on different sites have differential effects on specific client proteins [Mollapour *et al.*, 2011]. The authors showed that the T22E phosphomimetic mutant of yHsp90, led to an increase in GR activity. In case of the Ppt1 deletion strain, it can be postulated that the absence of this phosphatase might shift the equilibrium to a phosphorylated conformation of Hsp90, which specifically leads to an increase in the GR activity. In order to test this hypothesis, the phosphorylation pattern of Hsp90 in the Ppt1 deletion strain can be compared to that in the WT strain by

mass spectrometry. Any differences could then be followed up to test their effect on client processing. The other co-chaperones tested did not influence GR activity, suggesting that they might not be crucial in GR processing. The matrix shows that co-chaperone like Cpr6 and Sba1 seem to be important for SHR processing. All the SHRs showed a decrease of activity in these deletion strains. Similarly, Sgt1 knock-down influenced GR, MR, PR activity, but both AR and ER showed WT-like activity in this strain. Sgt1 has been studied extensively in plants and is thought to be important for plant immunity [Kadota & Shirasu, 2012]. Additionally, the TPR domain of Sgt1 is involved in binding to NLR proteins [Austin *et al.*, 2002]. However, the role of Sgt1 in processing steroid hormone receptors has not been studied before. The significant decrease in activity of GR, MR and PR, but not AR and ER in the Sgt1 knock-down strain suggests a specific role of Sgt1 in the activation of the SHRs. Further characterization of this effect, supplemented by *in vitro* studies of Sgt1 on SHR-Hsp90 interactions would be interesting. Cpr6, Sba1 (decreased SHR activity in null strains), Aha1 and Hch1 (increased SHR activity in null strains) seem to have an important role in SHR maturation as these effects were conserved among the 5 members. On the other hand, each SHR diverges slightly in their co-chaperone requirement, highlighting the differential co-chaperone requirement even within a protein family. For instance, Sti1 seems to be essential for GR activity, but does not influence the activity of other SHRs. AR activity increases in most of the deletion strains, suggesting that the presence of these co-chaperones might have a negative regulatory effect on AR processing. MR showed increased activity in the Pih1 deletion strain, but not in the Tah1 deletion strain. Additionally, Cns1 knock-down led to increase in the activity of PR and ER, but not the other SHRs.

Evolutionarily, GR and MR are among the closest related SHRs [Mangelsdorf *et al.*, 1995]. Both these SHRs however, show considerable differences to each other with respect to the co-chaperone requirements. It is thus interesting to study these two proteins in further details and also *in vitro*. To this end, a stabilized mutant of MR-LBD has been purified and preliminary experiments already show certain differences to the GR-LBD. MR-LBD did not significantly modulate the ATPase activity of Hsp90, as opposed to GR-LBD, which has an inhibitory effect [Lorenz *et al.*, 2014]. Moreover, analytical ultracentrifugation showed that MR-LBD did not bind efficiently to the yHsp90, in the presence or absence of nucleotides (unpublished data). Complex formation with Hsp90 could be observed only in the presence of Sba1, Cpr6 as well as Sgt1, which fits well to the *in vivo* data suggesting that these co-chaperones are important for MR activity (data not shown).

GR-LBD on the other hand forms a stable complex with Hsp90, even in the absence of co-chaperones [Lorenz *et al.*, 2014]. It is noteworthy that ER, the least Hsp90 dependent SHR and also evolutionarily the farthest member of family, did not have an extensive co-chaperone requirement. Thus, taken together, the β-gal assay results confirm that SHRs have differential co-chaperone dependencies and differences exist even within a closely related protein family.

- v-Src and c-Src mutants

  The Src kinase variants were studied using two different assays. In the first assay, the toxicity of v-Src to yeast cell was used as a read-out for v-Src activity (cell death implied active v-Src). Additionally, since yeast lack endogenous phosphotyrosine kinases, the phosphotyrosine activity of Src kinase variants could be monitored by western blot. In the case of v-Src, the phosphotyrosine activity in the Sti1 deletion strain was less than the WT, as expected [Chang *et al.*, 1997]. Additionally, the Cdc37 knock-down strain showed a lower v-Src phosphotyrosine activity in agreement with earlier reports [Stancato *et al.*, 1994; Mandal *et al.*, 2007]. The Cdc37 dAMP strain used in this work however, did not grow upon v-Src induction, despite the lower phosphotyrosine activity of v-Src. Western blot analysis 3.4 shows that Cdc37 is mildly knocked down in the dAMP strain. On the other hand, previous studies showing a complete inactivation of v-Src in absence of functional Cdc37, have employed Cdc37 mutants. These Cdc37 mutants can sustain viability, but do not partake in the processing of v-Src [Dey *et al.*, 1996; Fliss *et al.*, 1997]. The dAMP strain used here has reduced levels of functional full-length Cdc37 (Figure 3.4), which is probably sufficient to fold and activate v-Src to some extent. Since v-Src is extremely active in the cells, even a few v-Src functional molecules may be sufficient to impart toxicity to the yeast cells. Finally, phosphotyrosine blots also show lower v-Src activity in the Sba1 deletion strain, in agreement with previous reports [Fang *et al.*, 1998], as well as in the Sgt1 knock-down strain. However, the effect in the survival tests was not observed. The survival assays can only show which co-chaperones are essential in folding v-Src. The negative regulatory role of co-chaperones, if any, cannot be resolved using the survival assays. To this end, the phosphotyrosine blots could show if v-Src is more active in some deletion strain than in the WT. Hch1, Tah1, and Pih1 show a slight increase in v-Src phosphotyrosine activity, however as the effect was not very prominent and unambiguous, it has not been included in the matrix. In addition to v-Src, two Hsp90 dependent c-Src mutants were analysed similarly. The benefit in studying the c-Src mutants,

is that they are less active and hence less toxic to yeast. Thus the readout in the survival assays is not directly life or death. c-Src3MΔC, which is similar to v-Src, also requires Sti1, Cdc37 and Sgt1. The cells expressing c-Src3MΔC grow better in the Cdc37 knock-down strain as compared to the WT. The reason for this is that c-Src3MΔC is less active and hence less toxic than v-Src. The knock-down of Cdc37, led to an even further decrease in c-Src3MΔC activity, thus allowing the cells to grow better than the WT strain. Surprisingly, the decrease in phosphotyrosine activity in the Sba1 deletion strain was no longer observed for this mutant. In the case of c-Src3M, which is the least active and also least dependent on Hsp90, survival assays were not very informative as c-Src3M is not very toxic. The phosphotyrosine blots surprisingly showed that this mutant no longer showed decreased activity in the Sti1 deletion strain.

In summary, the results suggest that, Cdc37 is important for kinases. Since the knock-down of Cdc37 did not have an effect on SHR activity, it seems to be kinase specific. Surprisingly, Sgt1 knock-down affected both SHRs and Src kinase variants. Similar to its effect on the SHR activity, Sgt1 has not been studied in context of v-Src. Our results suggest a wider role for Sgt1, more than its involvement in immunity and NLR protein processing. To dissect the role of Sgt1 on SHRs and the Src kinase variants, it would be interesting to study whether Sgt1 influences their conformation. Furthermore, Sgt1 has been shown to interact with an ubiquitin E3-ligase [Kitagawa *et al.*, 1999] and is thought to mediate the degradation of proteins involved in plant immunity [Sangster & Queitsch, 2005]. It would be worthwhile to study whether this role of Sgt1 can also be extended for SHRs and v-Src. Additionally, using purified SHR-LBDs as well as the kinase domain of v-Src, interaction with Sgt1 can be monitored. The influence of Sgt1 on the Hsp90-client complex can also be studied. This 'global' effect of Sgt1 is thus interesting and begs further investigation.

The activity assays for the different client proteins thus validate their differential co-chaperone requirements. It has been proposed recently [Li *et al.*, 2013] that instead of one common Hsp90 cycle for chaperoning clients, there might be several client-specific Hsp90 cycles. The wide array of co-chaperones, coupled to the structural dynamics and post-translational modifications of Hsp90, customize it to serve the needs of the client proteins. The activity assays performed in this work, after a thorough characterization of the strains used, forms a solid matrix of client-specific effects which can be used as a profound base for further investigation of specific

client-co-chaperone pairs.

4.3 Analysis of the client-co-chaperone dependencies

The client-co-chaperone relationship was not influenced by temperature changes or by the growth phase of yeast. This asserted that these dependencies are robust, even during stress conditions. Based on these results, the next question was to compare whether the activity correlated to the levels of the client proteins. For this purpose, GR was N-terminally HA tagged. Unfortunately, tagging ER and MR at the N-terminus led to unexpected problems as the tagged variants differed from their untagged forms with respect to co-chaperone dependencies. Tagging can lead to stabilization of the tagged protein, however this mostly applies to big tags like SUMO, MBP and GST [Costa *et al.*, 2014]. It is unclear how a single HA-tag at the N-terminus influences MR and ER, but nor GR. As shown in Figure 1.9, the N-terminal regions of the SHRs are the least conserved and thus tagging at this end might have differential effects. In would be interesting to investigate whether HA-ER still depends on Hsp90 as it no longer showed any co-chaperone dependence. N-terminal tagging of MR and ER influenced their activities in the deletion strains and the lack of proper commercial antibodies hindered their detection on western blots. To find a solution for this problem and to reliably detect these SHRs, the ligand binding domains of the respective proteins were purified and antibodies were generated in rabbits. In the preliminary tests both antibodies detected MR and ER expressed in yeast lysates specifically (unpublished data).

Since HA-GR showed the same co-chaperone dependency as untagged GR, the protein levels of HA-GR were compared with the activity in different strains. The correlation in most cases was not direct, (i.e. the protein level and the activity did not change in the same order and direction) indicating a complex influence of the co-chaperones on the client proteins. Based on this activity-protein correlation, several deletion strains showed interesting effects: Sti1 and Sba1 deletion led to decreased GR activity despite having WT-like protein levels. Sti1 is involved in the transfer of GR from the Hsp70 to Hsp90 machinery and Hsp70 inhibits the hormone binding of GR by partially unfolding it [Kirschke *et al.*, 2014]. Thus, it could be reasoned that deletion of Sti1 might push the equilibrium toward the Hsp70-GR complex and render GR less capable of hormone binding and hence less activable. The limited proteolysis experiment shows that GR is in a different conformation in the Sti1 deletion

strain as it was more sensitive to Proteinase K digestion. This different conformation could be that of Hsp70-bound GR, which cannot bind hormone and is partially unfolded. By performing pull-down experiments, it would be possible to investigate whether more GR is in complex with Hsp70 in the Sti1 deletion strain, compared to the WT. To conclusively prove whether GR in the Sti1 deletion strain has lowered ligand potency, dose response curves with increasing hormone concentrations were performed. However, since saturation could not be reached, even upto 200 μM , ligand potency and efficacy could not be judged. It would be interesting to test whether GR in the Sba1 deletion strain also shows altered conformation, which might explain its lowered activity. The activity-protein correlation also showed Cpr6 and Sgt1 strains have lower activity as there are lower GR levels in this strain. In this context, it is not clear yet whether less GR is produced in this strain, or whether GR is unstable and degraded faster than in the WT strain. Moreover, Cpr6 seems essential for the activation of all the SHRs and Sba1 and Sgt1 influenced not only most of the SHRs, but also the Src kinases. For deciphering the role of these three co-chaperones, the protein-activity correlations for the other SHRs and kinases would be instrumental. In case of kinases, the phosphotyrosine activity correlated qualitatively to the protein levels of the Src kinase.

The activity and protein level correlations can be used to envision the role of co-chaperones for specific client proteins. Figure 4.2 shows a flow chart that puts together all the activity and protein level possibilities and shows further experimental directions to consider in each case. For instance, in the cases where the protein levels are WT-like, but activity is lower, studying the conformation of the client protein by limited proteolysis could explain whether the co-chaperone influences its conformation. Additionally, the influence of the missing co-chaperone on client localization and client aggregation could also be informative. In another scenario, where the client protein is more active and has higher levels than the WT, it would be instrumental to study whether the protein is stabilized and not degraded. It is unclear yet, what might cause WT-like levels of GR to be more active in certain deletion strains. In such cases, a negative regulatory role of co-chaperones could be envisioned, which might allow the client to be more active in the absence the co-chaperones. The advantage of constructing such a flow chart is that it will help to streamline further experiments to explain specific client-co-chaperone relationships.

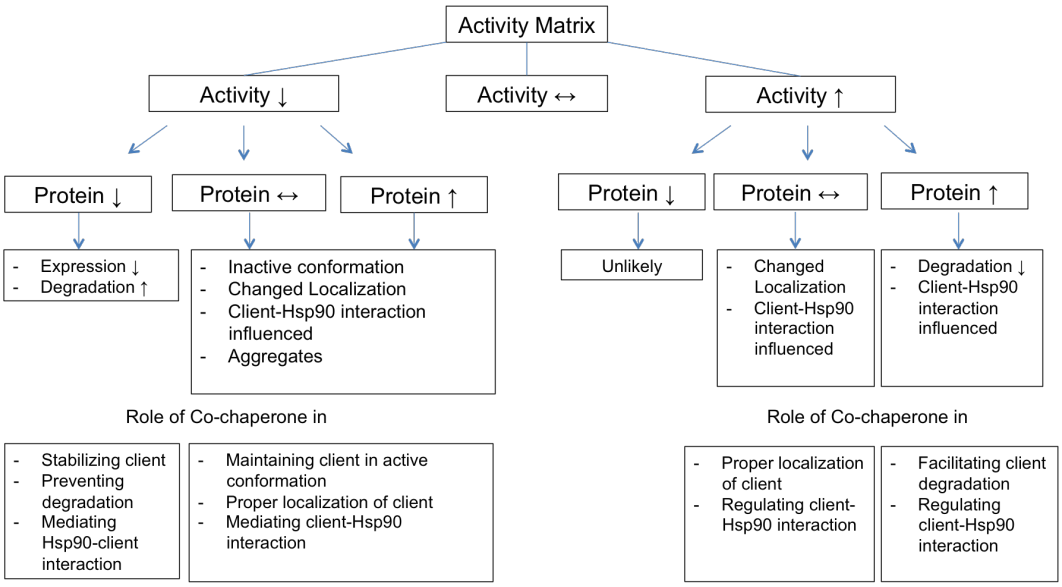

Figure 4.2: Flowchart for characterizing the client-co-chaperone relationship *in vivo*. Key: (↑) : increase; (↓) : decrease; (⟷): same. 'Protein' stands for level of the client estimated by quantifying western blots. All comparisons are done with the WT strain.

4.3.1 Stabilized mutants

In addition to the SHRs, two stabilized GR mutants were studied similarly. The activity assays for these mutants show that GR1e, with a single stabilizing mutation is similar to GR-WT, whereas GR-9a, with 5 stabilizing mutations is more co-chaperone-independent. Interestingly for GR-9a, Sti1 as well as Cpr6 deletion did not influence its activity. Notably, GR-9a still requires Sba1 and Sgt1 for its activity, and shows a slight increase in activity in the Hch1 deletion strain like GR-WT. The dose response curves showed that in these strains both ligand potency (affinity for the ligand) as well as the ligand efficacy (maximum activation reached) were influenced. Together with v-Src, two c-Src mutants were also studied. c-Src3MΔC behaves similar to v-Src, but is less active. The stability of this mutant however is comparable to v-Src. c-Src3M, on the other hand, still has the C-terminal end of c-Src and hence is more stable [Boczek *et al.*, 2015].

Stabilized GR mutants as well as the c-Src3M were less dependent on Hsp90 [Lorenz *et al.*, 2014; Boczek *et al.*, 2015]. The activity assay results affirm that lowered dependence on Hsp90 implies fewer co-chaperone requirements. ER, which was not stringently Hsp90-dependent, also fits this observation. Intriguingly, c-Src3M as

well as GR-9a, both abrogate their dependence on Sti1. While Sti1 was essential for both GR-WT and v-Src, the stable variants no longer need Sti1. This hints towards Sti1 playing an important role in stabilizing these client proteins. Sti1 is thought to be a connector co-chaperone for the Hsp70 and Hsp90 cycles and inhibits the Hsp90 ATPase activity by stabilizing the open conformation [Röhl *et al.*, 2015]. Acting as a scaffold, Sti1 facilitates client transfer from Hsp70 to Hsp90. However, Sti1 was not essential for all the SHRs. This suggests that Sti1 might be specific for GR and v-Src. More so, Sti1 is not essential for viability in yeast. All this together hints towards there being other mechanisms for client transfer between Hsp70 and Hsp90. The finding that stabilized variants no longer depend on Sti1, hints towards the possibility that this co-chaperone might influence on the conformation of GR and v-Src. The limited proteolysis experiment showed that GR expressed in the Sti1 deletion strain has an altered conformation. Similarly, it would be interesting to perform limited proteolysis on the GR-9a as well as c-Src3M mutants in this strain.

An alternative possibility, could be that Sti1 is just a scaffold and the difference between GR and GR-9a and v-Src and c-Src3M could already be at the level of Hsp70 and its co-chaperones. For this, it would be imperative to analyse whether these client mutants depend on Hsp70 as their WT counterparts. If client transfer from Hsp70 to Hsp90 is not essential in this case, then the influence of Sti1 might be abrogated. Further work in this direction will certainly be instrumental in understanding the Hsp70-90 client transfer.

The work in this thesis, proves conclusively that Hsp90 client proteins depend on specific co-chaperones for their activation. The work done on SHRs highlights the differences in the co-chaperone requirement within a protein family. While some co-chaperones are essential for an entire family of proteins, other are client-specific. The systematic activity assays performed for six different client proteins and their mutants provides a solid ground-work to select client-co-chaperone pairs which could be of interest for further investigation. Moreover, Sgt1, an essential co-chaperone in yeast, which was hitherto studied extensively in plants, might have a wider role in Hsp90 client-activation. The results also suggest that Sti1 plays an important role for GR and v-Src, which is no longer necessary for their stabilized version. Despite being established as a connector co-chaperone for Hsp70 and Hsp90, Sti1 was not required for all the clients studied, pointing towards alternate client transfer mechanisms. Taken together, the work here elaborates upon the underlying complexity of the Hsp90 system and proposes that the co-chaperones might be one of the key players in modulating Hsp90 such that it can chaperone a wide array of client proteins.

References

ABRAMS, J.L., VERGHESE, J., GIBNEY, P.A. & MORANO, K.A. (2014). Hierarchical functional specificity of cytosolic heat shock protein 70 (hsp70) nucleotide exchange factors in yeast. *Journal of Biological Chemistry*, **289**, 13155–13167. 11

AFFYMETRIX, I. (2002). Statistical algorithms description document. *Technical paper*. 62, 110

AGASHE, V.R. & HARTL, F.U. (2000). Roles of molecular chaperones in cytoplasmic protein folding. In *Seminars in cell & developmental biology*, vol. 11, 15–25, Elsevier. 2

ALI, M.M., ROE, S.M., VAUGHAN, C.K., MEYER, P., PANARETOU, B., PIPER, P.W., PRODROMOU, C. & PEARL, L.H. (2006). Crystal structure of an hsp90–nucleotide–p23/sba1 closed chaperone complex. *Nature*, **440**, 1013–1017. 13, 15, 17, 19

ALVIRA, S., CUÉLLAR, J., RÖHL, A., YAMAMOTO, S., ITOH, H., ALFONSO, C., RIVAS, G., BUCHNER, J. & VALPUESTA, J.M. (2014). Structural characterization of the substrate transfer mechanism in hsp70/hsp90 folding machinery mediated by hop. *Nature Communications*, **5**. 16, 18, 32

ANFINSEN, C.B. (1973). Principles that govern the folding of protein chains. *Science*, **181**, 223–230. 1

ARMSTRONG, H., WOLMARANS, A., MERCIER, R., MAI, B. & LAPOINTE, P. (2012). The Co-Chaperone Hch1 Regulates Hsp90 Function Differently than Its Homologue Aha1 and Confers Sensitivity to Yeast to the Hsp90 Inhibitor NVP-AUY922. *PLoS ONE*, **7**. 16, 22

ASHBURNER, M. & BONNER, J.J. (1979). The induction of gene activity in drosophila by heat shock. *Cell*, **17**, 241–254. 3

AUSTIN, R., MASCHERA, B., WALKER, A., FAIRBAIRN, L., MELDRUM, E., FARROW, S. & UINGS, I. (2002). Mometasone furoate is a less specific glucocorticoid than fluticasone propionate. *European Respiratory Journal*, **20**, 1386–1392. 25, 129

BACHMAIR, A., FINLEY, D. & VARSHAVSKY, A. (1986). In vivo half-life of a protein is a function of its amino-terminal residue. *Science*, **234**, 179–186. 125

BACK, R., DOMINGUEZ, C., ROTHÉ, B., BOBO, C., BEAUFILS, C., MORÉRA, S., MEYER, P., CHARPENTIER, B., BRANLANT, C., ALLAIN, F.H.T. *et al.* (2013). High-resolution structural analysis shows how tah1 tethers hsp90 to the r2tp complex. *Structure*, **21**, 1834–1847. 17

BAKER, T.A. & SAUER, R.T. (2012). Clpxp, an atp-powered unfolding and protein-degradation machine. *Biochimica et Biophysica Acta (BBA)-Molecular Cell Research*, **1823**, 15–28. 7

BALCH, W.E., MORIMOTO, R.I., DILLIN, A. & KELLY, J.W. (2008). Adapting proteostasis for disease intervention. *science*, **319**, 916–919. 3

BARENDS, T.R., WERBECK, N.D. & REINSTEIN, J. (2010). Disaggregases in 4 dimensions. *Current opinion in structural biology*, **20**, 46–53. 7

BARENT, R.L., NAIR, S.C., CARR, D.C., RUAN, Y., RIMERMAN, R.A., FULTON, J., ZHANG, Y. & SMITH,

D.F. (1998). Analysis of fkbp51/fkbp52 chimeras and mutants for hsp90 binding and association with progesterone receptor complexes. *Molecular endocrinology*, **12**, 342–354. 30

BEATO, M., CHALEPAKIS, G., SCHAUER, M. & SLATER, E.P. (1989). Dna regulatory elements for steroid hormones. *Journal of steroid biochemistry*, **32**, 737–747. 80

BLACKLOCK, K. & VERKHIVKER, G.M. (2014). Allosteric regulation of the hsp90 dynamics and stability by client recruiter cochaperones: protein structure network modeling. *PLoS ONE*. 25

BLAGOSKLONNY, M.V., TORETSKY, J., BOHEN, S. & NECKERS, L. (1996). Mutant conformation of p53 translated in vitro or in vivo requires functional hsp90. *Proceedings of the National Academy of Sciences*, **93**, 8379–8383. 12

BLEDSOE, R.K., MONTANA, V.G., STANLEY, T.B., DELVES, C.J., APOLITO, C.J., MCKEE, D.D., CONSLER, T.G., PARKS, D.J., STEWART, E.L., WILLSON, T.M. *et al.* (2002). Crystal structure of the glucocorticoid receptor ligand binding domain reveals a novel mode of receptor dimerization and coactivator recognition. *Cell*, **110**, 93–105. 27, 98

BOCZEK, E.E., REEFSCHLÄGER, L.G., DEHLING, M., STRULLER, T.J., HÄUSLER, E., SEIDL, A., KAILA, V.R. & BUCHNER, J. (2015). Conformational processing of oncogenic v-src kinase by the molecular chaperone hsp90. *Proceedings of the National Academy of Sciences*, **112**, E3189–E3198. 17, 24, 28, 31, 32, 103, 108, 134

BORKOVICH, K., FARRELLY, F., FINKELSTEIN, D., TAULIEN, J. & LINDQUIST, S. (1989). hsp82 is an essential protein that is required in higher concentrations for growth of cells at higher temperatures. *Molecular and Cellular Biology*, **9**, 3919–3930. 12

BOSE, S., WEIKL, T., BÜGL, H. & BUCHNER, J. (1996). Chaperone function of hsp90-associated proteins. *Science*, **274**, 1715–1717. 20

BOTËR, M., AMIGUES, B., PEART, J., BREUER, C., KADOTA, Y., CASAIS, C., MOORE, G., KLEANTHOUS, C., OCHSENBEIN, F., SHIRASU, K. *et al.* (2007). Structural and functional analysis of sgt1 reveals that its interaction with hsp90 is required for the accumulation of rx, an r protein involved in plant immunity. *The Plant Cell*, **19**, 3791–3804. 24

BOULON, S., MARMIER-GOURRIER, N., PRADET-BALADE, B., WURTH, L., VERHEGGEN, C., JÁDY, B.E., ROTHÉ, B., PESCIA, C., ROBERT, M.C., KISS, T. *et al.* (2008). The hsp90 chaperone controls the biogenesis of l7ae rnps through conserved machinery. *The Journal of cell biology*, **180**, 579–595. 27

BRANDVOLD, K.R. & MORIMOTO, R.I. (2015). The chemical biology of molecular chaperones-implications for modulation of proteostasis. *Journal of molecular biology*. 3

BREIMAN, A. (2014). Plant hsp90 and its co-chaperones. *Current Protein and Peptide Science*, **15**, 232–244. 12

BRESLOW, D.K., CAMERON, D.M., COLLINS, S.R., SCHULDINER, M., STEWART-ORNSTEIN, J., NEWMAN, H.W., BRAUN, S., MADHANI, H.D., KROGAN, N.J. & WEISSMAN, J.S. (2008). A comprehensive strategy enabling high-resolution functional analysis of the yeast genome. *Nature methods*, **5**, 711–718. 124

BRUGGE, J. (1986). Interaction of the rous sarcoma virus protein pp60 src with the cellular proteins pp50 and pp90. In *Retroviruses 4*, 1–22, Springer. 31, 103

BRUGGE, J.S., ERIKSON, E. & ERIKSON, R. (1981). The specific interaction of the rous sarcoma virus transforming protein, pp60 src, with two cellular proteins. *Cell*, **25**, 363–372. 31

BUCHNER, J. (1996). Supervising the fold: functional principles of molecular chaperones. *The FASEB Journal*, **10**, 10–19. 4

BUKAU, B. & HORWICH, A.L. (1998). The hsp70 and hsp60 chaperone machines. *Cell*, **92**, 351–366. 4, 5

BUKAU, B., HESTERKAMP, T. & LUIRINK, J. (1996). Growing up in a dangerous environment: a network of multiple targeting and folding pathways for nascent polypeptides in the cytosol. *Trends in cell biology*, **6**, 480–486. 3

BUKAU, B., DEUERLING, E., PFUND, C. & CRAIG, E.A. (2000). Getting newly synthesized proteins into shape. *Cell*, **101**, 119–122. 5

CALDERWOOD, S.K. (2015). Cdc37 as a co-chaperone to hsp90. In *The Networking of Chaperones by Co-chaperones*, 103–112, Springer. 17

CAPLAN, A.J. & DOUGLAS, M.G. (1991). Characterization of ydj1: a yeast homologue of the bacterial dnaj protein. *The Journal of cell biology*, **114**, 609–621. 10, 109

CAPLAN, A.J., CYR, D.M. & DOUGLAS, M.G. (1992). Ydj1p facilitates polypeptide translocation across different intracellular membranes by a conserved mechanism. *Cell*, **71**, 1143–1155. 10, 109

CASHIKAR, A.G., DUENNWALD, M. & LINDQUIST, S.L. (2005). A chaperone pathway in protein disaggregation hsp26 alters the nature of protein aggregates to facilitate reactivation by hsp104. *Journal of Biological Chemistry*, **280**, 23869–23875. 6

CATLETT, M.G. & KAPLAN, K.B. (2006). Sgt1p is a unique co-chaperone that acts as a client adaptor to link hsp90 to skp1p. *Journal of Biological Chemistry*, **281**, 33739–33748. 24

CHANG, H., NATHAN, D.F. & LINDQUIST, S. (1997). In vivo analysis of the hsp90 cochaperone sti1 (p60). *Molecular and cellular biology*, **17**, 318–325. 82, 104, 105, 127, 130

CHEN, C.Y., SAKISAKA, T. & BALCH, W.E. (2005). Use of hsp90 inhibitors to disrupt gdi-dependent rab recycling. *Methods in enzymology*, **403**, 339–347. 27

CHEN, D.H., MADAN, D., WEAVER, J., LIN, Z., SCHRÖDER, G.F., CHIU, W. & RYE, H.S. (2013). Visualizing groel/es in the act of encapsulating a folding protein. *Cell*, **153**, 1354–1365. 7

CHONG, Y.T., KOH, J.L., FRIESEN, H., DUFFY, K., COX, M.J., MOSES, A., MOFFAT, J., BOONE, C. & ANDREWS, B.J. (2015). Yeast proteome dynamics from single cell imaging and automated analysis. *Cell*, **161**, 1413–1424. 119, 122

CINTRON, N.S. & TOFT, D. (2006). Defining the requirements for hsp40 and hsp70 in the hsp90 chaperone pathway. *Journal of Biological Chemistry*, **281**, 26235–26244. 29

CITRI, A., HARARI, D., SHOCHAT, G., RAMAKRISHNAN, P., GAN, J., EISENSTEIN, M., KIMCHI, A., WALLACH, D., PIETROKOVSKI, S. & YARDEN, Y. (2006). Hsp90 recognizes a common surface on client kinases. *Journal of Biological Chemistry*. 32

CLARE, D.K., BAKKES, P., VAN HEERIKHUIZEN, H., VAN DER VIES, S. & SAIBIL, H.R. (2009). Chaperonin complex with a newly folded protein encapsulated in the folding chamber. *Nature*, **457**, 107–110. 7

COOPER, J.A., GOULD, K.L., CARTWRIGHT, C.A. & HUNTER, T. (1986). Tyr527 is phosphorylated in pp60c-src: implications for regulation. *Science*, **231**, 1431–1434. 31

COSTA, S., ALMEIDA, A., CASTRO, A. & DOMINGUES, L. (2014). Fusion tags for protein solubility, purification and immunogenicity in escherichia coli: the novel fh8 system. *Frontiers in microbiology*, **5**. 132

CRAIG, E., HUANG, P., ARON, R. & ANDREW, A. (2006). The diverse roles of j-proteins, the obligate hsp70 co-chaperone. 10

DAVIES, T.H. & SÁNCHEZ, E.R. (2005). Fkbp52. *The international journal of biochemistry & cell biol-*

ogy, **37**, 42–47. 30

DE LA ROSA, D.A., JIMENEZ-CANINO, R., LORENZO-DIAZ, F. & GIRALDEZ, T. (2014). Hsp90 acetylation regulates mineralocorticoid receptor subcellular dynamics and aldosterone-induced promoter transactivation (1097.15). *The FASEB Journal*, **28**, 1097–15. 26

DEKKER, C., ROE, S.M., MCCORMACK, E.A., BEURON, F., PEARL, L.H. & WILLISON, K.R. (2011). The crystal structure of yeast cct reveals intrinsic asymmetry of eukaryotic cytosolic chaperonins. *The EMBO journal*, **30**, 3078–3090. 7

DEUERLING, E. & BUKAU, B. (2004). Chaperone-assisted folding of newly synthesized proteins in the cytosol. *Critical reviews in biochemistry and molecular biology*, **39**, 261–277. 8

DEY, B., LIGHTBODY, J.J. & BOSCHELLI, F. (1996). Cdc37 is required for p60v-src activity in yeast. *Molecular biology of the cell*, **7**, 1405–1417. 23, 104, 130

DÍAZ-VILLANUEVA, J.F., DÍAZ-MOLINA, R. & GARCÍA-GONZÁLEZ, V. (2015). Protein folding and mechanisms of proteostasis. *International journal of molecular sciences*, **16**, 17193–17230. 3

DOLINSKI, K.J., CARDENAS, M.E. & HEITMAN, J. (1998). Cns1 encodes an essential p60/sti1 homolog in saccharomyces cerevisiae that suppresses cyclophilin 40 mutations and interacts with hsp90. *Molecular and cellular biology*, **18**, 7344–7352. 20, 24

DOLLINS, D.E., WARREN, J.J., IMMORMINO, R.M. & GEWIRTH, D.T. (2007). Structures of grp94-nucleotide complexes reveal mechanistic differences between the hsp90 chaperones. *Molecular cell*, **28**, 41–56. 13

DONLIN, L.T., ANDRESEN, C., JUST, S., RUDENSKY, E., PAPPAS, C.T., KRUGER, M., JACOBS, E.Y., UNGER, A., ZIESENISS, A., DOBENECKER, M.W. *et al.* (2012). Smyd2 controls cytoplasmic lysine methylation of hsp90 and myofilament organization. *Genes & development*, **26**, 114–119. 26

DRAGOVIC, Z., BROADLEY, S.A., SHOMURA, Y., BRACHER, A. & HARTL, F.U. (2006). Molecular chaperones of the hsp110 family act as nucleotide exchange factors of hsp70s. *The EMBO journal*, **25**, 2519–2528. 10

DUINA, A.A., CHANG, H.C.J., MARSH, J.A., LINDQUIST, S. & GABER, R.F. (1996). A cyclophilin function in hsp90-dependent signal transduction. *Science*, **274**, 1713–1715. 20, 72, 82, 124

DUINA, A.A., MARSH, J.A., KURTZ, R.B., CHANG, H.C.J., LINDQUIST, S. & GABER, R.F. (1998). The peptidyl-prolyl isomerase domain of the cyp-40 cyclophilin homolog cpr7 is not required to support growth or glucocorticoid receptor activity in saccharomyces cerevisiae. *Journal of Biological Chemistry*, **273**, 10819–10822. 128

DUNKER, A.K., SILMAN, I., UVERSKY, V.N. & SUSSMAN, J.L. (2008). Function and structure of inherently disordered proteins. *Current opinion in structural biology*, **18**, 756–764. 2

DUNN, D.M., WOODFORD, M.R., TRUMAN, A.W., JENSEN, S.M., SCHULMAN, J., CAZA, T., REMILLARD, T.C., LOISELLE, D., WOLFGEHER, D., BLAGG, B.S. *et al.* (2015). c-abl mediated tyrosine phosphorylation of aha1 activates its co-chaperone function in cancer cells. *Cell reports*, **12**, 1006–1018. 26

ECHEVERRIA, P.C. & PICARD, D. (2010). Molecular chaperones, essential partners of steroid hormone receptors for activity and mobility. *Biochimica et Biophysica Acta (BBA)-Molecular Cell Research*, **1803**, 641–649. 28

ECHTENKAMP, F.J. & FREEMAN, B.C. (2012). Expanding the cellular molecular chaperone network through the ubiquitous cochaperones. *Biochimica et Biophysica Acta (BBA)-Molecular Cell Research*, **1823**, 668–673. 24

ECHTENKAMP, F.J., ZELIN, E., OXELMARK, E., WOO, J.I., ANDREWS, B.J., GARABEDIAN, M. & FREEMAN, B.C. (2011). Global functional map of the p23 molecular chaperone reveals an extensive cellular network. *Molecular cell*, **43**, 229–241. 20

ECKERT, K., SALIOU, J.M., MONLEZUN, L., VIGOUROUX, A., ATMANE, N., CAILLAT, C., QUEVILLON-CHÉRUEL, S., MADIONA, K., NICAISE, M., LAZEREG, S. *et al.* (2010). The pih1-tah1 cochaperone complex inhibits hsp90 molecular chaperone atpase activity. *Journal of Biological Chemistry*, **285**, 31304–31312. 17, 22

ECKL, J.M., RUTZ, D.A., HASLBECK, V., ZIERER, B.K., REINSTEIN, J. & RICHTER, K. (2013). Cdc37 (cell division cycle 37) restricts hsp90 (heat shock protein 90) motility by interaction with n-terminal and middle domain binding sites. *Journal of Biological Chemistry*, **288**, 16032–16042. 23

ECKL, J.M., DRAZIC, A., RUTZ, D.A. & RICHTER, K. (2014). Nematode sgt1-homologue d1054. 3 binds open and closed conformations of hsp90 via distinct binding sites. *Biochemistry*, **53**, 2505–2514. 17, 25

EISEN, M.B., SPELLMAN, P.T., BROWN, P.O. & BOTSTEIN, D. (1998). Cluster analysis and display of genome-wide expression patterns. *Proceedings of the National Academy of Sciences*, **95**, 14863–14868. 7, 17

ELBLE, R. (1992). A simple and efficient procedure for transformation of yeasts. *Biotechniques*, **13**, 18. 57

ELLIS, R.J. & HARTL, F.U. (1999). Principles of protein folding in the cellular environment. *Current opinion in structural biology*, **9**, 102–110. 4

ELLIS, R.J. & MINTON, A.P. (2003). Cell biology: join the crowd. *Nature*, **425**, 27–28. 1

ELLIS, R.J. & MINTON, A.P. (2006). Protein aggregation in crowded environments. *Journal of Biological Chemistry*, **387**. 2

EVANS, R.M. (1988). The steroid and thyroid hormone receptor superfamily. *Science*, **240**, 889–895. 28

FAIRBANKS, G., STECK, T.L. & WALLACH, D.F.H. (1971). Electrophoretic analysis of the major polypeptides of the human erythrocyte membrane. *Biochemistry*, **10**, 2606–2617, pMID: 4326772. 67

FALSONE, S.F., LEPTIHN, S., OSTERAUER, A., HASLBECK, M. & BUCHNER, J. (2004). Oncogenic mutations reduce the stability of src kinase. *Journal of molecular biology*, **344**, 281–291. 12

FANG, Y., FLISS, A.E., ROBINS, D.M. & CAPLAN, A.J. (1996). Hsp90 regulates androgen receptor hormone binding affinity in vivo. *Journal of Biological Chemistry*, **271**, 28697–28702. 27

FANG, Y., FLISS, A.E., RAO, J. & CAPLAN, A.J. (1998). Sba1 encodes a yeast hsp90 cochaperone that is homologous to vertebrate p23 proteins. *Molecular and cellular biology*, **18**, 3727–3734. 105, 130

FANGHÄNEL, J. & FISCHER, G. (2004). Insights into the catalytic mechanism of peptidyl prolyl cis/trans isomerases. *Frontiers in bioscience: a journal and virtual library*, **9**, 3453–3478. 4, 20

FARESSE, N., RUFFIEUX-DAIDIE, D., SALAMIN, M., GOMEZ-SANCHEZ, C.E. & STAUB, O. (2010). Mineralocorticoid receptor degradation is promoted by hsp90 inhibition and the ubiquitin-protein ligase chip. *American Journal of Physiology-Renal Physiology*, **299**, F1462–F1472. 27

FARRELLY, F.W. & FINKELSTEIN, D.B. (1984). Complete sequence of the heat shock-inducible hsp90 gene of saccharomyces cerevisiae. *Journal of Biological Chemistry*, **259**, 5745–5751. 12

FELTS, S.J., OWEN, B.A., NGUYEN, P., TREPEL, J., DONNER, D.B. & TOFT, D.O. (2000). The hsp90-

related protein trap1 is a mitochondrial protein with distinct functional properties. *Journal of Biological Chemistry*, **275**, 3305–3312. 13

FERSHT, A.R. & DAGGETT, V. (2002). Protein folding and unfolding at atomic resolution. *Cell*, **108**, 573–582. 2

FLISS, A.E., FANG, Y., BOSCHELLI, F. & CAPLAN, A.J. (1997). Differential in vivo regulation of steroid hormone receptor activation by cdc37p. *Molecular biology of the cell*, **8**, 2501–2509. 104, 130

FLISS, A.E., BENZENO, S., RAO, J. & CAPLAN, A.J. (2000). Control of estrogen receptor ligand binding by hsp90. *The Journal of steroid biochemistry and molecular biology*, **72**, 223–230. 27

FLOM, G.A., LEMIESZEK, M., FORTUNATO, E.A. & JOHNSON, J.L. (2008). Farnesylation of ydj1 is required for in vivo interaction with hsp90 client proteins. *Molecular biology of the cell*, **19**, 5249–5258. 10

FREEMAN, B.C. & MORIMOTO, R.I. (1996). The human cytosolic molecular chaperones hsp90, hsp70 (hsc70) and hdj-1 have distinct roles in recognition of a non-native protein and protein refolding. *The EMBO Journal*, **15**, 2969. 20

FREEMAN, B.C. & YAMAMOTO, K.R. (2002). Disassembly of transcriptional regulatory complexes by molecular chaperones. *Science*, **296**, 2232–2235. 20

FREEMAN, B.C., FELTS, S.J., TOFT, D.O. & YAMAMOTO, K.R. (2000). The p23 molecular chaperones act at a late step in intracellular receptor action to differentially affect ligand efficacies. *Genes & development*, **14**, 422–434. 127

FREY, S., LESKOVAR, A., REINSTEIN, J. & BUCHNER, J. (2007). The atpase cycle of the endoplasmic chaperone grp94. *Journal of Biological Chemistry*, **282**, 35612–35620. 13

FRYDMAN, J. (2001). Folding of newly translated proteins in vivo: the role of molecular chaperones. *Annual review of biochemistry*, **70**, 603–647. 5

FRYDMAN, J. & HARTL, F.U. (1996). Principles of chaperone-assisted protein folding: differences between in vitro and in vivo mechanisms. *Science*, **272**, 1497–1502. 2

GAISER, A.M., KRETZSCHMAR, A. & RICHTER, K. (2010). Cdc37-hsp90 complexes are responsive to nucleotide-induced conformational changes and binding of further cofactors. *Journal of Biological Chemistry*, **285**, 40921–40932. 15, 23

GAUTSCHI, M., LILIE, H., FÜNFSCHILLING, U., MUN, A., ROSS, S., LITHGOW, T., RÜCKNAGEL, P. & ROSPERT, S. (2001). Rac, a stable ribosome-associated complex in yeast formed by the dnak-dnaj homologs ssz1p and zuotin. *Proceedings of the National Academy of Sciences*, **98**, 3762–3767. 6, 10

GEORGOPOULOS, C. & WELCH, W. (1993). Role of the major heat shock proteins as molecular chaperones. *Annual review of cell biology*, **9**, 601–634. 3

GHAEMMAGHAMI, S., HUH, W.K., BOWER, K., HOWSON, R.W., BELLE, A., DEPHOURE, N., O'SHEA, E.K. & WEISSMAN, J.S. (2003). Global analysis of protein expression in yeast. *Nature*, **425**, 737–741. 24, 119, 120, 122

GLOGE, F., BECKER, A.H., KRAMER, G. & BUKAU, B. (2014). Co-translational mechanisms of protein maturation. *Current opinion in structural biology*, **24**, 24–33. 5

GLOVER, J.R. & LINDQUIST, S. (1998). Hsp104, hsp70, and hsp40: a novel chaperone system that rescues previously aggregated proteins. *Cell*, **94**, 73–82. 7

HAGEMAN, J. & KAMPINGA, H.H. (2009). Computational analysis of the human hsph/hspa/dnaj family and cloning of a human hsph/hspa/dnaj expression library. *Cell Stress and Chaperones*, **14**, 1–21. 10

HAINZL, O., WEGELE, H., RICHTER, K. & BUCHNER, J. (2004). Cns1 is an activator of the ssa1 atpase activity. *Journal of Biological Chemistry*, **279**, 23267–23273. 17, 24

HAINZL, O., LAPINA, M.C., BUCHNER, J. & RICHTER, K. (2009). The charged linker region is an important regulator of hsp90 function. *Journal of Biological Chemistry*, **284**, 22559–22567. 13

HAMAMOTO, R., TOYOKAWA, G., NAKAKIDO, M., UEDA, K. & NAKAMURA, Y. (2014). Smyd2-dependent hsp90 methylation promotes cancer cell proliferation by regulating the chaperone complex formation. *Cancer letters*, **351**, 126–133. 26

HANCE, M.W., NOLAN, K.D. & ISAACS, J.S. (2014). The double-edged sword: conserved functions of extracellular hsp90 in wound healing and cancer. *Cancers*, **6**, 1065–1097. 13

HARST, A., LIN, H. & OBERMANN, W. (2005). Aha1 competes with hop, p50 and p23 for binding to the molecular chaperone hsp90 and contributes to kinase and hormone receptor activation. *Biochem. J*, **387**, 789–796. 33, 128

HARTL, F.U. & HAYER-HARTL, M. (2002). Molecular chaperones in the cytosol: from nascent chain to folded protein. *Science*, **295**, 1852–1858. 5

HARTL, F.U., BRACHER, A. & HAYER-HARTL, M. (2011). Molecular chaperones in protein folding and proteostasis. *Nature*, **475**, 324–332. 3

HASLBECK, M., WALKE, S., STROMER, T., EHRNSPERGER, M., WHITE, H.E., CHEN, S., SAIBIL, H.R. & BUCHNER, J. (1999). Hsp26: a temperature-regulated chaperone. *The EMBO Journal*, **18**, 6744–6751. 6

HASLBECK, M., BRAUN, N., STROMER, T., RICHTER, B., MODEL, N., WEINKAUF, S. & BUCHNER, J. (2004). Hsp42 is the general small heat shock protein in the cytosol of saccharomyces cerevisiae. *The EMBO journal*, **23**, 638–649. 73

HASLBECK, M., FRANZMANN, T., WEINFURTNER, D. & BUCHNER, J. (2005). Some like it hot: the structure and function of small heat-shock proteins. *Nature structural & molecular biology*, **12**, 842–846. 6

HASLBECK, M., WEINKAUF, S. & BUCHNER, J. (2015). Regulation of the chaperone function of small hsps. In *The Big Book on Small Heat Shock Proteins*, 155–178, Springer. 6

HASLBERGER, T., ZDANOWICZ, A., BRAND, I., KIRSTEIN, J., TURGAY, K., MOGK, A. & BUKAU, B. (2008). Protein disaggregation by the aaa+ chaperone clpb involves partial threading of looped polypeptide segments. *Nature structural & molecular biology*, **15**, 641–650. 7

HESSLING, M., RICHTER, K. & BUCHNER, J. (2009). Dissection of the atp-induced conformational cycle of the molecular chaperone hsp90. *Nature structural & molecular biology*, **16**, 287–293. 15, 18, 21

HIKRI, E., SHPUNGIN, S. & NIR, U. (2009). Hsp90 and a tyrosine embedded in the hsp90 recognition loop are required for the fer tyrosine kinase activity. *Cellular signalling*, **21**, 588–596. 32

HORVAT, N.K., ARMSTRONG, H., LEE, B.L., MERCIER, R., WOLMARANS, A., KNOWLES, J., SPYRACOPOULOS, L. & LAPOINTE, P. (2014). A mutation in the catalytic loop of hsp90 specifically impairs atpase stimulation by aha1p, but not hch1p. *Journal of molecular biology*, **426**, 2379–2392. 22

HORWICH, A.L. (2013). Chaperonin-mediated protein folding. *Journal of Biological Chemistry*, **288**, 23622–23632. 6

HUAI, Q., WANG, H., LIU, Y., KIM, H.Y., TOFT, D. & KE, H. (2005). Structures of the n-terminal and middle domains of e. coli hsp90 and conformation changes upon adp binding. *Structure*, **13**, 579–590. 13

HUANG, A. & STULTZ, C.M. (2009). Finding order within disorder: elucidating the structure of proteins associated with neurodegenerative disease. *Future medicinal chemistry*, **1**, 467–482. 3

HUANG, P., GAUTSCHI, M., WALTER, W., ROSPERT, S. & CRAIG, E.A. (2005). The hsp70 ssz1 modulates the function of the ribosome-associated j-protein zuo1. *Nature structural & molecular biology*, **12**, 497–504. 10

JAHN, M., REHN, A., PELZ, B., HELLENKAMP, B., RICHTER, K., RIEF, M., BUCHNER, J. & HUGEL, T. (2014). The charged linker of the molecular chaperone hsp90 modulates domain contacts and biological function. *Proceedings of the National Academy of Sciences*, **111**, 17881–17886. 13

JAKOB, U. & BUCHNER, J. (1994). Assisting spontaneity: the role of hsp90 and small hsps as molecular chaperones. *Trends in biochemical sciences*, **19**, 205–211. 12

JAROSZ, D.F. & LINDQUIST, S. (2010). Hsp90 and environmental stress transform the adaptive value of natural genetic variation. *Science*, **330**, 1820–1824. 12

JIANG, J., MAES, E.G., TAYLOR, A.B., WANG, L., HINCK, A.P., LAFER, E.M. & SOUSA, R. (2007). Structural basis of j cochaperone binding and regulation of hsp70. *Molecular cell*, **28**, 422–433. 10

JIMÉNEZ, B., UGWU, F., ZHAO, R., ORTÍ, L., MAKHNEVYCH, T., PINEDA-LUCENA, A. & HOURY, W.A. (2012). Structure of minimal tetratricopeptide repeat domain protein tah1 reveals mechanism of its interaction with pih1 and hsp90. *Journal of Biological Chemistry*, **287**, 5698–5709. 17, 22

JOAB, I., RADANYI, C., RENOIR, M., BUCHOU, T., CATELLI, M.G., BINART, N., MESTER, J. & BAULIEU, E.E. (1984). Common non-hormone binding component in non-transformed chick oviduct receptors of four steroid hormones. *Nature*. 27

JOHNSON, J.L. (2012). Evolution and function of diverse hsp90 homologs and cochaperone proteins. *Biochimica et Biophysica Acta (BBA)-Molecular Cell Research*, **1823**, 607–613. 12, 13, 124

JOHNSON, J.L. & BROWN, C. (2009). Plasticity of the hsp90 chaperone machine in divergent eukaryotic organisms. *Cell Stress and Chaperones*, **14**, 83–94. 32

JOHNSON, J.L., ZUEHLKE, A.D., TENGE, V.R. & LANGWORTHY, J.C. (2014). Mutation of essential hsp90 co-chaperones sgt1 or cns1 renders yeast hypersensitive to overexpression of other co-chaperones. *Current genetics*, **60**, 265–276. 17, 19

KADOTA, Y. & SHIRASU, K. (2012). The hsp90 complex of plants. *Biochimica et Biophysica Acta (BBA)-Molecular Cell Research*, **1823**, 689–697. 12, 25, 129

KADOTA, Y., AMIGUES, B., DUCASSOU, L., MADAOUI, H., OCHSENBEIN, F., GUEROIS, R. & SHIRASU, K. (2008). Structural and functional analysis of sgt1–hsp90 core complex required for innate immunity in plants. *EMBO reports*, **9**, 1209–1215. 24

KADOTA, Y., SHIRASU, K. & GUEROIS, R. (2010). Nlr sensors meet at the sgt1–hsp90 crossroad. *Trends in biochemical sciences*, **35**, 199–207. 15

KAMPINGA, H.H. & CRAIG, E.A. (2010). The hsp70 chaperone machinery: J proteins as drivers of functional specificity. *Nature reviews Molecular cell biology*, **11**, 579–592. 10, 11

KARAGÖZ, G.E. & RÜDIGER, S.G. (2015). Hsp90 interaction with clients. *Trends in biochemical sciences*, **40**, 117–125. 27, 32

KARAGÖZ, G.E., DUARTE, A.M., IPPEL, H., UETRECHT, C., SINNIGE, T., VAN ROSMALEN, M., HAUSMANN, J., HECK, A.J., BOELENS, R. & RÜDIGER, S.G. (2011). N-terminal domain of human hsp90 triggers binding to the cochaperone p23. *Proceedings of the National Academy of Sciences*, **108**, 580–585. 17, 19

KARAGÖZ, G.E., DUARTE, A.M., AKOURY, E., IPPEL, H., BIERNAT, J., LUENGO, T.M., RADLI, M., DI-

DENKO, T., NORDHUES, B.A., VEPRINTSEV, D.B. *et al.* (2014). Hsp90-tau complex reveals molecular basis for specificity in chaperone action. *Cell*, **156**, 963–974. 27

KATO, J., TAKEYA, T., GRANDORI, C., IBA, H., LEVY, J. & HANAFUSA, H. (1986). Amino acid substitutions sufficient to convert the nontransforming p60c-src protein to a transforming protein. *Molecular and cellular biology*, **6**, 4155–4160. 32

KIEFHABER, T., RUDOLPH, R., KOHLER, H.H. & BUCHNER, J. (1991). Protein aggregation in vitro and in vivo: a quantitative model of the kinetic competition between folding and aggregation. *Nature Biotechnology*, **9**, 825–829. 5

KIM, Y.E., HIPP, M.S., BRACHER, A., HAYER-HARTL, M. & ULRICH HARTL, F. (2013). Molecular chaperone functions in protein folding and proteostasis. *Annual review of biochemistry*, **82**, 323–355. 3

KIMURA, Y., RUTHERFORD, S.L., MIYATA, Y., YAHARA, I., FREEMAN, B.C., YUE, L., MORIMOTO, R.I. & LINDQUIST, S. (1997). Cdc37 is a molecular chaperone with specific functions in signal transduction. *Genes & development*, **11**, 1775–1785. 24

KIRSCHKE, E., GOSWAMI, D., SOUTHWORTH, D., GRIFFIN, P.R. & AGARD, D.A. (2014). Glucocorticoid receptor function regulated by coordinated action of the hsp90 and hsp70 chaperone cycles. *Cell*, **157**, 1685–1697. 27, 132

KIRSTEIN-MILES, J., SCIOR, A., DEUERLING, E. & MORIMOTO, R.I. (2013). The nascent polypeptide-associated complex is a key regulator of proteostasis. *The EMBO journal*, **32**, 1451–1468. 6

KITAGAWA, K., SKOWYRA, D., ELLEDGE, S.J., HARPER, J.W. & HIETER, P. (1999). Sgt1 encodes an essential component of the yeast kinetochore assembly pathway and a novel subunit of the scf ubiquitin ligase complex. *Molecular cell*, **4**, 21–33. 131

KITYK, R., KOPP, J., SINNING, I. & MAYER, M.P. (2012). Structure and dynamics of the atp-bound open conformation of hsp70 chaperones. *Molecular cell*, **48**, 863–874. 8

KITYK, R., VOGEL, M., SCHLECHT, R., BUKAU, B. & MAYER, M.P. (2015). Pathways of allosteric regulation in hsp70 chaperones. *Nature communications*, **6**. 8

KLEIN-HITPASS, L., SCHORPP, M., WAGNER, U. & RYFFEL, G.U. (1986). An estrogen-responsive element derived from the 5' flanking region of the xenopus vitellogenin a2 gene functions in transfected human cells. *Cell*, **46**, 1053–1061. 80

KLIONSKY, D.J., CUERVO, A.M. & SEGLEN, P.O. (2007). Methods for monitoring autophagy from yeast to human. *Autophagy*, **3**, 181–206. 79

KOSANO, H., STENSGARD, B., CHARLESWORTH, M.C., MCMAHON, N. & TOFT, D. (1998). The assembly of progesterone receptor-hsp90 complexes using purified proteins. *Journal of Biological Chemistry*, **273**, 32973–32979. 27

KOULOV, A.V., LAPOINTE, P., LU, B., RAZVI, A., COPPINGER, J., DONG, M.Q., MATTESON, J., LAISTER, R., ARROWSMITH, C., YATES, J.R. *et al.* (2010). Biological and structural basis for aha1 regulation of hsp90 atpase activity in maintaining proteostasis in the human disease cystic fibrosis. *Molecular biology of the cell*, **21**, 871–884. 21

KULAK, N.A., PICHLER, G., PARON, I., NAGARAJ, N. & MANN, M. (2014). Minimal, encapsulated proteomic-sample processing applied to copy-number estimation in eukaryotic cells. *Nature methods*, **11**, 319–324. 24, 119, 122

KUMAR, R. & THOMPSON, E.B. (1999). The structure of the nuclear hormone receptors. *Steroids*, **64**, 310–319. 28

KUSHNIROV, V.V. (2000). Rapid and reliable protein extraction from yeast. *Yeast*, **16**, 857–860. 58

LAEMMLI, U.K. *et al.* (1970). Cleavage of structural proteins during the assembly of the head of bacteriophage t4. *nature*, **227**, 680–685. 67

LANDRY, S.J. (2003). Structure and energetics of an allele-specific genetic interaction between dnaj and dnak: correlation of nuclear magnetic resonance chemical shift perturbations in the j-domain of hsp40/dnaj with binding affinity for the atpase domain of hsp70/dnak. *Biochemistry*, **42**, 4926–4936. 10

LANGER, T., ROSMUS, S. & FASOLD, H. (2003). Intracellular localization of the 90 kda heat shock protein (hsp90α) determined by expression of a egfp–hsp90α-fusion protein in unstressed and heat stressed 3t3 cells. *Cell biology international*, **27**, 47–52. 12

LEE, C.T., GRAF, C., MAYER, F.J., RICHTER, S.M. & MAYER, M.P. (2012). Dynamics of the regulation of hsp90 by the co-chaperone sti1. *The EMBO journal*, **31**, 1518–1528. 16, 18

LEE, J., KIM, J.H., BITER, A.B., SIELAFF, B., LEE, S. & TSAI, F.T. (2013). Heat shock protein (hsp) 70 is an activator of the hsp104 motor. *Proceedings of the National Academy of Sciences*, **110**, 8513–8518. 8

LEE, Y.T., JACOB, J., MICHOWSKI, W., NOWOTNY, M., KUZNICKI, J. & CHAZIN, W.J. (2004). Human sgt1 binds hsp90 through the chord-sgt1 domain and not the tetratricopeptide repeat domain. *Journal of Biological Chemistry*, **279**, 16511–16517. 24

LEITNER, A., JOACHIMIAK, L.A., BRACHER, A., MÖNKEMEYER, L., WALZTHOENI, T., CHEN, B., PECHMANN, S., HOLMES, S., CONG, Y., MA, B. *et al.* (2012). The molecular architecture of the eukaryotic chaperonin tric/cct. *Structure*, **20**, 814–825. 7

LESKOVAR, A., WEGELE, H., WERBECK, N.D., BUCHNER, J. & REINSTEIN, J. (2008). The atpase cycle of the mitochondrial hsp90 analog trap1. *Journal of Biological Chemistry*, **283**, 11677–11688. 13

LI, J., QIAN, X. & SHA, B. (2003). The crystal structure of the yeast hsp40 ydj1 complexed with its peptide substrate. *Structure*, **11**, 1475–1483. 10

LI, J., RICHTER, K. & BUCHNER, J. (2011). Mixed hsp90–cochaperone complexes are important for the progression of the reaction cycle. *Nature structural & molecular biology*, **18**, 61–66. 16, 19, 21, 128

LI, J., SOROKA, J. & BUCHNER, J. (2012). The hsp90 chaperone machinery: conformational dynamics and regulation by co-chaperones. *Biochimica et Biophysica Acta (BBA)-Molecular Cell Research*, **1823**, 624–635. 18, 20, 23, 25, 33

LI, J., RICHTER, K., REINSTEIN, J. & BUCHNER, J. (2013). Integration of the accelerator Aha1 in the Hsp90 co-chaperone cycle. *Nature structural & molecular biology*, **20**, 326–31. 14, 16, 19, 30, 33, 131

LI, W., LI, Y., GUAN, S., FAN, J., CHENG, C.F., BRIGHT, A.M., CHINN, C., CHEN, M. & WOODLEY, D.T. (2007). Extracellular heat shock protein-90α: linking hypoxia to skin cell motility and wound healing. *The EMBO journal*, **26**, 1221–1233. 13

LI, Z., MENORET, A. & SRIVASTAVA, P. (2002). Roles of heat-shock proteins in antigen presentation and cross-presentation. *Current opinion in immunology*, **14**, 45–51. 27

LIBEREK, K., LEWANDOWSKA, A. & ZIĘTKIEWICZ, S. (2008). Chaperones in control of protein disaggregation. *The EMBO journal*, **27**, 328–335. 6

LIU, J., FAEDER, J.R. & CAMACHO, C.J. (2009). Toward a quantitative theory of intrinsically disordered proteins and their function. *Proceedings of the National Academy of Sciences*, **106**, 19819–

19823. 2

LIU, W. & LANDGRAF, R. (2015). Phosphorylated and unphosphorylated serine 13 of cdc37 stabilize distinct interactions between its client and hsp90 binding domains. *Biochemistry*, **54**, 1493–1504. 24

LIU, X.D., MORANO, K.A. & THIELE, D.J. (1999). The yeast hsp110 family member, sse1, is an hsp90 cochaperone. *Journal of Biological Chemistry*, **274**, 26654–26660. 11

LOPEZ, T., DALTON, K. & FRYDMAN, J. (2015). The mechanism and function of group ii chaperonins. *Journal of molecular biology*. 7

LORENZ, O.R., FREIBURGER, L., RUTZ, D.A., KRAUSE, M., ZIERER, B.K., ALVIRA, S., CUÉLLAR, J., VALPUESTA, J.M., MADL, T., SATTLER, M. *et al.* (2014). Modulation of the hsp90 chaperone cycle by a stringent client protein. *Molecular cell*, **53**, 941–953. 27, 28, 29, 99, 128, 129, 130, 134

LOTZ, G.P., LIN, H., HARST, A. & OBERMANN, W.M. (2003). Aha1 binds to the middle domain of hsp90, contributes to client protein activation, and stimulates the atpase activity of the molecular chaperone. *Journal of Biological Chemistry*, **278**, 17228–17235. 21, 32

LOTZ, G.P., BRYCHZY, A., HEINZ, S. & OBERMANN, W.M. (2008). A novel hsp90 chaperone complex regulates intracellular vesicle transport. *Journal of cell science*, **121**, 717–723. 27

MACLEAN, M. & PICARD, D. (2003). Cdc37 goes beyond hsp90 and kinases. *Cell stress & chaperones*, **8**, 114. 24

MAINZ, A., PESCHEK, J., STAVROPOULOU, M., BACK, K.C., BARDIAUX, B., ASAMI, S., PRADE, E., PETERS, C., WEINKAUF, S., BUCHNER, J. *et al.* (2015). The chaperone [alpha] b-crystallin uses different interfaces to capture an amorphous and an amyloid client. *Nature structural & molecular biology*, **22**, 898–905. 6

MANDAL, A.K., LEE, P., CHEN, J.A., NILLEGODA, N., HELLER, A., DISTASIO, S., OEN, H., VICTOR, J., NAIR, D.M., BRODSKY, J.L. *et al.* (2007). Cdc37 has distinct roles in protein kinase quality control that protect nascent chains from degradation and promote posttranslational maturation. *The Journal of cell biology*, **176**, 319–328. 32, 104, 130

MANGELSDORF, D.J., THUMMEL, C., BEATO, M., HERRLICH, P., SCHÜTZ, G., UMESONO, K., BLUMBERG, B., KASTNER, P., MARK, M., CHAMBON, P. *et al.* (1995). The nuclear receptor superfamily: the second decade. *Cell*, **83**, 835–839. 28, 29, 129

MANIVAL, X., JACQUEMIN, C., CHARPENTIER, B. & QUINTERNET, M. (2014). 1h, 15n and 13c resonance assignments of the yeast pih1 and tah1 c-terminal domains complex. *Biomolecular NMR assignments*, **9**, 71–73. 22

MARCINOWSKI, M., HÖLLER, M., FEIGE, M.J., BAEREND, D., LAMB, D.C. & BUCHNER, J. (2011). Substrate discrimination of the chaperone bip by autonomous and cochaperone-regulated conformational transitions. *Nature structural & molecular biology*, **18**, 150–158. 8

MARSH, J.A., KALTON, H.M. & GABER, R.F. (1998). Cns1 is an essential protein associated with the hsp90 chaperone complex in saccharomyces cerevisiae that can restore cyclophilin 40-dependent functions in cpr7δcells. *Molecular and cellular biology*, **18**, 7353–7359. 24

MARTÍNEZ-RUIZ, A., VILLANUEVA, L., DE ORDUÑA, C.G., LÓPEZ-FERRER, D., HIGUERAS, M.Á., TARÍN, C., RODRÍGUEZ-CRESPO, I., VÁZQUEZ, J. & LAMAS, S. (2005). S-nitrosylation of hsp90 promotes the inhibition of its atpase and endothelial nitric oxide synthase regulatory activities. *Proceedings of the National Academy of Sciences of the United States of America*, **102**, 8525–8530. 26

MARTINEZ-YAMOUT, M.A., VENKITAKRISHNAN, R.P., PREECE, N.E., KROON, G., WRIGHT, P.E. &

DYSON, H.J. (2006). Localization of sites of interaction between p23 and hsp90 in solution. *Journal of Biological Chemistry*, **281**, 14457–14464. 17, 19

MARZEC, M., ELETTO, D. & ARGON, Y. (2012). Grp94: An hsp90-like protein specialized for protein folding and quality control in the endoplasmic reticulum. *Biochimica et Biophysica Acta (BBA)-Molecular Cell Research*, **1823**, 774–787. 13

MAYER, M. & BUKAU, B. (2005). Hsp70 chaperones: cellular functions and molecular mechanism. *Cellular and molecular life sciences*, **62**, 670–684. 8

MAYER, M.P. (2013). Hsp70 chaperone dynamics and molecular mechanism. *Trends in biochemical sciences*, **38**, 507–514. 32

MAYER, M.P. & KITYK, R. (2015). Insights into the molecular mechanism of allostery in hsp70s. *Frontiers in molecular biosciences*, **2**. 9

MAYER, M.P. & LE BRETON, L. (2015). Hsp90: Breaking the symmetry. *Molecular cell*, **58**, 8–20. 13, 15, 29, 33

MAYOR, A., MARTINON, F., DE SMEDT, T., PÉTRILLI, V. & TSCHOPP, J. (2007). A crucial function of sgt1 and hsp90 in inflammasome activity links mammalian and plant innate immune responses. *Nature immunology*, **8**, 497–503. 27

MAYR, C., RICHTER, K., LILIE, H. & BUCHNER, J. (2000). Cpr6 and cpr7, two closely related hsp90-associated immunophilins from saccharomyces cerevisiae, differ in their functional properties. *Journal of Biological Chemistry*, **275**, 34140–34146. 17, 20, 126

MCLAUGHLIN, S.H., SOBOTT, F., YAO, Z.P., ZHANG, W., NIELSEN, P.R., GROSSMANN, J.G., LAUE, E.D., ROBINSON, C.V. & JACKSON, S.E. (2006). The co-chaperone p23 arrests the hsp90 atpase cycle to trap client proteins. *Journal of molecular biology*, **356**, 746–758. 19

MEYER, P., PRODROMOU, C., LIAO, C., HU, B., ROE, S.M., VAUGHAN, C.K., VLASIC, I., PANARETOU, B., PIPER, P.W. & PEARL, L.H. (2004). Structural basis for recruitment of the ATPase activator Aha1 to the Hsp90 chaperone machinery. *The EMBO journal*, **23**, 1402–1410. 16, 21

MILLSON, S., VAUGHAN, C., ZHAI, C., ALI, M., PANARETOU, B., PIPER, P., PEARL, L. & PRODROMOU, C. (2008). Chaperone ligand-discrimination by the tpr-domain protein tah1. *Biochem. J*, **413**, 261–268. 22

MIYAZAKI, K., SENGA, T., MATSUDA, S., TANAKA, M., MACHIDA, K., TAKENOUCHI, Y., NIMURA, Y. & HAMAGUCHI, M. (1999). Critical amino acid substitutions in the src sh3 domain that convert c-src to be oncogenic. *Biochemical and biophysical research communications*, **263**, 759–764. 32

MIYOSHI, T., TAKEUCHI, A., SIOMI, H. & SIOMI, M.C. (2010). A direct role for hsp90 in pre-risc formation in drosophila. *Nature structural & molecular biology*, **17**, 1024–1026. 27

MOLLAPOUR, M. & NECKERS, L. (2012). Post-translational modifications of hsp90 and their contributions to chaperone regulation. *Biochimica et Biophysica Acta (BBA)-Molecular Cell Research*, **1823**, 648–655. 25

MOLLAPOUR, M., TSUTSUMI, S., TRUMAN, A.W., XU, W., VAUGHAN, C.K., BEEBE, K., KONSTANTINOVA, A., VOURGANTI, S., PANARETOU, B., PIPER, P.W. *et al.* (2011). Threonine 22 phosphorylation attenuates hsp90 interaction with cochaperones and affects its chaperone activity. *Molecular cell*, **41**, 672–681. 128

MOLLAPOUR, M., BOURBOULIA, D., BEEBE, K., WOODFORD, M.R., POLIER, S., HOANG, A., CHELLURI, R., LI, Y., GUO, A., LEE, M.J. *et al.* (2014). Asymmetric hsp90 n domain sumoylation recruits aha1 and atp-competitive inhibitors. *Molecular cell*, **53**, 317–329. 26

MORISHIMA, Y., KANELAKIS, K.C., MURPHY, P.J., LOWE, E.R., JENKINS, G.J., OSAWA, Y., SUNAHARA, R.K. & PRATT, W.B. (2003). The hsp90 cochaperone p23 is the limiting component of the multiprotein hsp90/hsp70-based chaperone system in vivo where it acts to stabilize the client protein·hsp90 complex. *Journal of Biological Chemistry*, **278**, 48754–48763. 19

NELSON, C.C., HENDY, S.C., SHUKIN, R.J., CHENG, H., BRUCHOVSKY, N., KOOP, B.F. & RENNIE, P.S. (1999). Determinants of dna sequence specificity of the androgen, progesterone, and glucocorticoid receptors: evidence for differential steroid receptor response elements. *Molecular endocrinology*, **13**, 2090–2107. 80

NEUWALD, A.F., ARAVIND, L., SPOUGE, J.L. & KOONIN, E.V. (1999). Aaa+: A class of chaperone-like atpases associated with the assembly, operation, and disassembly of protein complexes. *Genome research*, **9**, 27–43. 7

NEWMAN, J.R., GHAEMMAGHAMI, S., IHMELS, J., BRESLOW, D.K., NOBLE, M., DERISI, J.L. & WEISSMAN, J.S. (2006). Single-cell proteomic analysis of s. cerevisiae reveals the architecture of biological noise. *Nature*, **441**, 840–846. 119, 122

NICOLET, C.M. & CRAIG, E.A. (1989). Isolation and characterization of sti1, a stress-inducible gene from saccharomyces cerevisiae. *Molecular and Cellular Biology*, **9**, 3638–3646. 17

OGI, H., SAKURABA, Y., KITAGAWA, R., XIAO, L., SHEN, C., CYNTHIA, M., OHTA, S., ARNOLD, M., RAMIREZ, N., HOUGHTON, P. *et al.* (2015). The oncogenic role of the cochaperone sgt1. *Oncogenesis*, **4**, e149. 17

OURA, J., TAMURA, Y., KAMIGUCHI, K., KUTOMI, G., SAHARA, H., TORIGOE, T., HIMI, T. & SATO, N. (2011). Extracellular heat shock protein 90 plays a role in translocating chaperoned antigen from endosome to proteasome for generating antigenic peptide to be cross-presented by dendritic cells. *International immunology*, dxq475. 13

OXELMARK, E., KNOBLAUCH, R., ARNAL, S., SU, L.F., SCHAPIRA, M. & GARABEDIAN, M.J. (2003). Genetic dissection of p23, an hsp90 cochaperone, reveals a distinct surface involved in estrogen receptor signaling. *Journal of Biological Chemistry*, **278**, 36547–36555. 27

OXELMARK, E., ROTH, J.M., BROOKS, P.C., BRAUNSTEIN, S.E., SCHNEIDER, R.J. & GARABEDIAN, M.J. (2006). The cochaperone p23 differentially regulates estrogen receptor target genes and promotes tumor cell adhesion and invasion. *Molecular and cellular biology*, **26**, 5205–5213. 20

PACI, A., LIU, X.H., HUANG, H., LIM, A., HOURY, W.A. & ZHAO, R. (2012). The stability of the small nucleolar ribonucleoprotein (snornp) assembly protein pih1 in saccharomyces cerevisiae is modulated by its c terminus. *Journal of Biological Chemistry*, **287**, 43205–43214. 124

PAL, M., MORGAN, M., PHELPS, S.E., ROE, S.M., PARRY-MORRIS, S., DOWNS, J.A., POLIER, S., PEARL, L.H. & PRODROMOU, C. (2014). Structural basis for phosphorylation-dependent recruitment of tel2 to hsp90 by pih1. *Structure*, **22**, 805–818. 22

PANARETOU, B., PRODROMOU, C., ROE, S.M., O'BRIEN, R., LADBURY, J.E., PIPER, P.W. & PEARL, L.H. (1998). Atp binding and hydrolysis are essential to the function of the hsp90 molecular chaperone in vivo. *The EMBO journal*, **17**, 4829–4836. 15

PANARETOU, B., SILIGARDI, G., MEYER, P., MALONEY, A., SULLIVAN, J.K., SINGH, S., MILLSON, S.H., CLARKE, P.A., NAABY-HANSEN, S., STEIN, R. *et al.* (2002). Activation of the atpase activity of hsp90 by the stress-regulated cochaperone aha1. *Molecular cell*, **10**, 1307–1318. 21, 28

PAUL, A., GARCIA, Y.A., ZIERER, B., PATWARDHAN, C., GUTIERREZ, O., HILDENBRAND, Z., HARRIS, D.C., BALSIGER, H.A., SIVILS, J.C., JOHNSON, J.L. *et al.* (2014). The cochaperone sgta (small

glutamine-rich tetratricopeptide repeat-containing protein alpha) demonstrates regulatory specificity for the androgen, glucocorticoid, and progesterone receptors. *Journal of Biological Chemistry*, **289**, 15297–15308. 27

PEISKER, K., CHIABUDINI, M. & ROSPERT, S. (2010). The ribosome-bound hsp70 homolog ssb of saccharomyces cerevisiae. *Biochimica et Biophysica Acta (BBA)-Molecular Cell Research*, **1803**, 662–672. 10

PENNISI, R., ASCENZI, P. & DI MASI, A. (2015). Hsp90: A new player in dna repair? *Biomolecules*, **5**, 2589–2618. 27

PESCHEK, J., BRAUN, N., ROHRBERG, J., BACK, K.C., KRIEHUBER, T., KASTENMÜLLER, A., WEINKAUF, S. & BUCHNER, J. (2013). Regulated structural transitions unleash the chaperone activity of αb-crystallin. *Proceedings of the National Academy of Sciences*, **110**, E3780–E3789. 6

PETREZSELYOVA, S., ZAHRADKA, J. & SYCHROVA, H. (2010). Saccharomyces cerevisiae by4741 and w303-1a laboratory strains differ in salt tolerance. *Fungal biology*, **114**, 144–150. 125

PICARD, D. (2015). Hsp90 interactors. 26

PICARD, D. & YAMAMOTO, K.R. (1987). Two signals mediate hormone-dependent nuclear localization of the glucocorticoid receptor. *The EMBO journal*, **6**, 3333. 29

PICARD, D., KHURSHEED, B., GARABEDIAN, M.J., FORTIN, M.G., LINDQUIST, S. & YAMAMOTO, K.R. (1990). Reduced levels of hsp90 compromise steroid receptor action in vivo. *Nature*. 26, 29

PIRKL, F. & BUCHNER, J. (2001). Functional analysis of the hsp90-associated human peptidyl prolyl cis/trans isomerases fkbp51, fkbp52 and cyp40. *Journal of molecular biology*, **308**, 795–806. 17

POLIER, S., DRAGOVIC, Z., HARTL, F.U. & BRACHER, A. (2008). Structural basis for the cooperation of hsp70 and hsp110 chaperones in protein folding. *Cell*, **133**, 1068–1079. 11

PRATT, W., MORISHIMA, Y., MURPHY, M. & HARRELL, M. (2006). Chaperoning of glucocorticoid receptors. In *Molecular Chaperones in Health and Disease*, 111–138, Springer. 26

PRATT, W. *et al.* (1993). The role of heat shock proteins in regulating the function, folding, and trafficking of the glucocorticoid receptor. *Journal of Biological Chemistry*, **268**, 21455–21455. 12

PRATT, W.B. (1990). Interaction of hsp90 with steroid receptors: organizing some diverse observations and presenting the newest concepts. *Molecular and cellular endocrinology*, **74**, C69–C76. 26

PRATT, W.B. (1992). Control of steroid receptor function and cytoplasmic-nuclear transport by heat shock proteins. *Bioessays*. 29

PRATT, W.B. & TOFT, D.O. (2003). Regulation of signaling protein function and trafficking by the hsp90/hsp70-based chaperone machinery. *Experimental Biology and Medicine*, **228**, 111–133. 30

PREISSLER, S. & DEUERLING, E. (2012). Ribosome-associated chaperones as key players in proteostasis. *Trends in biochemical sciences*, **37**, 274–283. 5

PROIA, D.A. & KAUFMANN, G.F. (2015). Targeting heat-shock protein 90 (hsp90) as a complementary strategy to immune checkpoint blockade for cancer therapy. *Cancer immunology research*. 27

RAO, J., LEE, P., BENZENO, S., CARDOZO, C., ALBERTUS, J., ROBINS, D.M. & CAPLAN, A.J. (2001). Functional interaction of human cdc37 with the androgen receptor but not with the glucocorticoid receptor. *Journal of Biological Chemistry*, **276**, 5814–5820. 27

RATAJCZAK, T., CLUNING, C. & WARD, B.K. (2015). Steroid receptor-associated immunophilins: A gateway to steroid signalling. *The Clinical Biochemist Reviews*, **36**, 31. 29, 30

RATZKE, C., MICKLER, M., HELLENKAMP, B., BUCHNER, J. & HUGEL, T. (2010). Dynamics of heat shock protein 90 c-terminal dimerization is an important part of its conformational cycle. *Proceed-*

ings of the National Academy of Sciences, **107**, 16101–16106. 15

RATZKE, C., NGUYEN, M.N., MAYER, M.P. & HUGEL, T. (2012). From a ratchet mechanism to random fluctuations evolution of hsp90's mechanochemical cycle. *Journal of molecular biology*, **423**, 462–471. 15

RAVIOL, H., SADLISH, H., RODRIGUEZ, F., MAYER, M.P. & BUKAU, B. (2006). Chaperone network in the yeast cytosol: Hsp110 is revealed as an hsp70 nucleotide exchange factor. *The EMBO journal*, **25**, 2510–2518. 11, 109

REHN, A.B. & BUCHNER, J. (2015). p23 and aha1. In *The Networking of Chaperones by Co-chaperones*, 113–131, Springer. 16, 17

RETZLAFF, M., STAHL, M., EBERL, H.C., LAGLEDER, S., BECK, J., KESSLER, H. & BUCHNER, J. (2009). Hsp90 is regulated by a switch point in the c-terminal domain. *EMBO reports*, **10**, 1147–1153. 26

RETZLAFF, M., HAGN, F., MITSCHKE, L., HESSLING, M., GUGEL, F., KESSLER, H., RICHTER, K. & BUCHNER, J. (2010). Asymmetric activation of the hsp90 dimer by its cochaperone aha1. *Molecular cell*, **37**, 344–354. 16, 21

REYNOLDS, A.B., VILA, J., LANSING, T., POTTS, W., WEBER, M. & PARSONS, J. (1987). Activation of the oncogenic potential of the avian cellular src protein by specific structural alteration of the carboxy terminus. *The EMBO journal*, **6**, 2359. 32

RICHTER, K. & BUCHNER, J. (2011). Closing in on the hsp90 chaperone-client relationship. *Structure*, **19**, 445–446. 15

RICHTER, K., MUSCHLER, P., HAINZL, O., REINSTEIN, J. & BUCHNER, J. (2003). Sti1 is a non-competitive inhibitor of the hsp90 atpase binding prevents the n-terminal dimerization reaction during the atpase cycle. *Journal of Biological Chemistry*, **278**, 10328–10333. 18

RICHTER, K., WALTER, S. & BUCHNER, J. (2004). The co-chaperone sba1 connects the atpase reaction of hsp90 to the progression of the chaperone cycle. *Journal of molecular biology*, **342**, 1403–1413. 17, 19

RICHTER, K., SOROKA, J., SKALNIAK, L., LESKOVAR, A., HESSLING, M., REINSTEIN, J. & BUCHNER, J. (2008). Conserved conformational changes in the atpase cycle of human hsp90. *Journal of Biological Chemistry*, **283**, 17757–17765. 13, 15

RICHTER, K., HASLBECK, M. & BUCHNER, J. (2010). The heat shock response: life on the verge of death. *Molecular cell*, **40**, 253–266. 3, 8

RIGGS, D.L., ROBERTS, P.J., CHIRILLO, S.C., CHEUNG-FLYNN, J., PRAPAPANICH, V., RATAJCZAK, T., GABER, R., PICARD, D. & SMITH, D.F. (2003). The hsp90-binding peptidylprolyl isomerase fkbp52 potentiates glucocorticoid signaling in vivo. *The EMBO journal*, **22**, 1158–1167. 30

RIGGS, D.L., COX, M.B., TARDIF, H.L., HESSLING, M., BUCHNER, J. & SMITH, D.F. (2007). Non-catalytic role of the fkbp52 peptidyl-prolyl isomerase domain in the regulation of steroid hormone signaling. *Molecular and cellular biology*, **27**, 8658–8669. 30

RODRIGUEZ, F., ARSÈNE-PLOETZE, F., RIST, W., RÜDIGER, S., SCHNEIDER-MERGENER, J., MAYER, M.P. & BUKAU, B. (2008). Molecular basis for regulation of the heat shock transcription factor σ 32 by the dnak and dnaj chaperones. *Molecular cell*, **32**, 347–358. 10

ROE, S.M., ALI, M.M., MEYER, P., VAUGHAN, C.K., PANARETOU, B., PIPER, P.W., PRODROMOU, C. & PEARL, L.H. (2004). The mechanism of hsp90 regulation by the protein kinase-specific cochaperone p50 cdc37. *Cell*, **116**, 87–98. 23

RÖHL, A., ROHRBERG, J. & BUCHNER, J. (2013). The chaperone Hsp90: Changing partners for de-

manding clients. *Trends in Biochemical Sciences*, **38**, 253–262. 15, 16

RÖHL, A., WENGLER, D., MADL, T., LAGLEDER, S., TIPPEL, F., HERRMANN, M., HENDRIX, J., RICHTER, K., HACK, G., SCHMID, A.B. *et al.* (2015). Hsp90 regulates the dynamics of its cochaperone sti1 and the transfer of hsp70 between modules. *Nature communications*, **6**. 16, 18, 135

ROUS, P. (1911). A sarcoma of the fowl transmissible by an agent separable from the tumor cells. *The Journal of experimental medicine*, **13**, 397–411. 31

RÜDIGER, S., GERMEROTH, L., SCHNEIDER-MERGENER, J. & BUKAU, B. (1997). Substrate specificity of the dnak chaperone determined by screening cellulose-bound peptide libraries. *The EMBO journal*, **16**, 1501–1507. 8

RUTHERFORD, S.L. & LINDQUIST, S. (1998). Hsp90 as a capacitor for morphological evolution. *Nature*, **396**, 336–342. 12

SANGSTER, T.A. & QUEITSCH, C. (2005). The hsp90 chaperone complex, an emerging force in plant development and phenotypic plasticity. *Current opinion in plant biology*, **8**, 86–92. 131

SCHERRER, L.C., HUTCHISON, K.A., SANCHEZ, E.R., RANDALL, S.K. & PRATT, W.B. (1992). A heat shock protein complex isolated from rabbit reticulocyte lysate can reconstitute a functional glucocorticoid receptor-hsp90 complex. *Biochemistry*, **31**, 7325–7329. 29

SCHEUFLER, C., BRINKER, A., BOURENKOV, G., PEGORARO, S., MORODER, L., BARTUNIK, H., HARTL, F.U. & MOAREFI, I. (2000). Structure of tpr domain–peptide complexes: critical elements in the assembly of the hsp70–hsp90 multichaperone machine. *Cell*, **101**, 199–210. 18

SCHIENE-FISCHER, C. (2014). Multidomain peptidyl prolyl cis/trans isomerases. *Biochimica et Biophysica Acta (BBA)-General Subjects*. 4

SCHMID, A.B., LAGLEDER, S., GRÄWERT, M.A., RÖHL, A., HAGN, F., WANDINGER, S.K., COX, M.B., DEMMER, O., RICHTER, K., GROLL, M. *et al.* (2012). The architecture of functional modules in the hsp90 co-chaperone sti1/hop. *The EMBO journal*, **31**, 1506–1517. 16, 18

SCHMIDPETER, P.A. & SCHMID, F.X. (2015). Prolyl isomerization and its catalysis in protein folding and protein function. *Journal of molecular biology*, **427**, 1609–1631. 4

SCHUERMANN, J.P., JIANG, J., CUELLAR, J., LLORCA, O., WANG, L., GIMENEZ, L.E., JIN, S., TAYLOR, A.B., DEMELER, B., MORANO, K.A. *et al.* (2008). Structure of the hsp110: Hsc70 nucleotide exchange machine. *Molecular cell*, **31**, 232–243. 11

SCHULDINER, M., COLLINS, S.R., THOMPSON, N.J., DENIC, V., BHAMIDIPATI, A., PUNNA, T., IHMELS, J., ANDREWS, B., BOONE, C., GREENBLATT, J.F. *et al.* (2005). Exploration of the function and organization of the yeast early secretory pathway through an epistatic miniarray profile. *Cell*, **123**, 507–519. 104

SCIOR, A. & DEUERLING, E. (2014). Functions of ribosome-associated chaperones and their interaction network. In *The Molecular Chaperones Interaction Networks in Protein Folding and Degradation*, 27–49, Springer. 6

SCROGGINS, B.T., ROBZYK, K., WANG, D., MARCU, M.G., TSUTSUMI, S., BEEBE, K., COTTER, R.J., FELTS, S., TOFT, D., KARNITZ, L. *et al.* (2007). An acetylation site in the middle domain of hsp90 regulates chaperone function. *Molecular cell*, **25**, 151–159. 26

SEITZ, T., THOMA, R., SCHOCH, G.A., STIHLE, M., BENZ, J., D'ARCY, B., WIGET, A., RUF, A., HENNIG, M. & STERNER, R. (2010). Enhancing the stability and solubility of the glucocorticoid receptor ligand-binding domain by high-throughput library screening. *Journal of molecular biology*, **403**, 562–577. 28, 98

SEYFFER, F., KUMMER, E., OGUCHI, Y., WINKLER, J., KUMAR, M., ZAHN, R., SOURJIK, V., BUKAU, B. & MOGK, A. (2012). Hsp70 proteins bind hsp100 regulatory m domains to activate aaa+ disaggregase at aggregate surfaces. *Nature structural & molecular biology*, **19**, 1347–1355. 8

SHANER, L., SOUSA, R. & MORANO, K.A. (2006). Characterization of hsp70 binding and nucleotide exchange by the yeast hsp110 chaperone sse1. *Biochemistry*, **45**, 15075–15084. 11

SHAO, J., GRAMMATIKAKIS, N., SCROGGINS, B.T., UMA, S., HUANG, W., CHEN, J.J., HARTSON, S.D. & MATTS, R.L. (2001). Hsp90 regulates p50 cdc37 function during the biogenesis of the active conformation of the heme-regulated eif2α kinase. *Journal of Biological Chemistry*, **276**, 206–214. 23

SHAO, J., PRINCE, T., HARTSON, S.D. & MATTS, R.L. (2003). Phosphorylation of serine 13 is required for the proper function of the hsp90 co-chaperone, cdc37. *Journal of Biological Chemistry*, **278**, 38117–38120. 23

SHARMA, D., MARTINEAU, C.N., LE DALL, M.T., REIDY, M., MASISON, D.C. & KABANI, M. (2009). Function of ssa subfamily of hsp70 within and across species varies widely in complementing saccharomyces cerevisiae cell growth and prion propagation. *PloS one*, **4**, e6644. 10

SILIGARDI, G., PANARETOU, B., MEYER, P., SINGH, S., WOOLFSON, D.N., PIPER, P.W., PEARL, L.H. & PRODROMOU, C. (2002). Regulation of hsp90 atpase activity by the co-chaperone cdc37p/p50 cdc37. *Journal of Biological Chemistry*, **277**, 20151–20159. 17, 23

SILIGARDI, G., HU, B., PANARETOU, B., PIPER, P.W., PEARL, L.H. & PRODROMOU, C. (2004). Co-chaperone regulation of conformational switching in the hsp90 atpase cycle. *Journal of Biological Chemistry*, **279**, 51989–51998. 23, 33

SKJAERVEN, L., MUGA, A., REUTER, N. & MARTINEZ, A. (2012). A dynamic model of long-range conformational adaptations triggered by nucleotide binding in groel-groes. *Proteins: Structure, Function, and Bioinformatics*, **80**, 2333–2346. 7

SKJÆRVEN, L., CUELLAR, J., MARTINEZ, A. & VALPUESTA, J.M. (2015). Dynamics, flexibility, and allostery in molecular chaperonins. *FEBS letters*, **589**, 2522–2532. 6

SMITH, D.F. (1993). Dynamics of heat shock protein 90-progesterone receptor binding and the disactivation loop model for steroid receptor complexes. *Molecular Endocrinology*, **7**, 1418–1429. 29

SMITH, D.F. (2004). Tetratricopeptide repeat cochaperones in steroid receptor complexes. *Cell stress & chaperones*, **9**, 109. 16

SMITH, D.F. & TOFT, D.O. (1992). Composition, assembly and activation of the avian progesterone receptor. *The Journal of steroid biochemistry and molecular biology*, **41**, 201–207. 27

SONDERMANN, H., HO, A.K., LISTENBERGER, L.L., SIEGERS, K., MOAREFI, I., WENTE, S.R., HARTL, F.U. & YOUNG, J.C. (2002). Prediction of novel bag-1 homologs based on structure/function analysis identifies snl1p as an hsp70 co-chaperone in saccharomyces cerevisiae. *Journal of Biological Chemistry*, **277**, 33220–33227. 11, 109

SOROKA, J., WANDINGER, S.K., MÄUSBACHER, N., SCHREIBER, T., RICHTER, K., DAUB, H. & BUCHNER, J. (2012). Conformational switching of the molecular chaperone hsp90 via regulated phosphorylation. *Molecular cell*, **45**, 517–528. 17, 19, 26

SOUTHWORTH, D.R. & AGARD, D.A. (2011). Client-loading conformation of the hsp90 molecular chaperone revealed in the cryo-em structure of the human hsp90: Hop complex. *Molecular cell*, **42**, 771–781. 15, 18, 29

STANCATO, L.F., CHOW, Y.H., OWENS-GRILLO, J.K., YEM, A.W., DEIBEL, M., JOVE, R. & PRATT, W.B.

(1994). The native v-raf. hsp90. p50 heterocomplex contains a novel immunophilin of the fk506 binding class. *Journal of Biological Chemistry*, **269**, 22157–22161. 32, 130

STÉHELIN, D. & GRAF, T. (1978). Avian myelocytomatosis and erythroblastosis viruses lack the transforming gene src of avian sarcoma viruses. *Cell*, **13**, 745–750. 31

STEPANOVA, L., LENG, X., PARKER, S.B. & HARPER, J.W. (1996). Mammalian p50cdc37 is a protein kinase-targeting subunit of hsp90 that binds and stabilizes cdk4. *Genes & development*, **10**, 1491–1502. 23, 32

STONE, D.E. & CRAIG, E.A. (1990). Self-regulation of 70-kilodalton heat shock proteins in saccharomyces cerevisiae. *Molecular and cellular biology*, **10**, 1622–1632. 9

STUTTMANN, J., PARKER, J.E. & NOËL, L.D. (2008). Staying in the fold: the sgt1/chaperone machinery in maintenance and evolution of leucine-rich repeat proteins. *Plant signaling & behavior*, **3**, 283–285. 25

SUN, L., PRINCE, T., MANJARREZ, J.R., SCROGGINS, B.T. & MATTS, R.L. (2012). Characterization of the interaction of aha1 with components of the hsp90 chaperone machine and client proteins. *Biochimica et Biophysica Acta (BBA)-Molecular Cell Research*, **1823**, 1092–1101. 27

TAHERIAN, A., KRONE, P.H. & OVSENEK, N. (2008). A comparison of hsp90 α and hsp90 β interactions with cochaperones and substrates. *Biochemistry and Cell Biology*, **86**, 37–45. 12

TAIPALE, M., JAROSZ, D.F. & LINDQUIST, S. (2010). Hsp90 at the hub of protein homeostasis: emerging mechanistic insights. *Nature reviews Molecular cell biology*, **11**, 515–528. 11

TAIPALE, M., KRYKBAEVA, I., KOEVA, M., KAYATEKIN, C., WESTOVER, K.D., KARRAS, G.I. & LINDQUIST, S. (2012). Quantitative analysis of hsp90-client interactions reveals principles of substrate recognition. *Cell*, **150**, 987–1001. 23, 27

TAKAHASHI, A., CASAIS, C., ICHIMURA, K. & SHIRASU, K. (2003). Hsp90 interacts with rar1 and sgt1 and is essential for rps2-mediated disease resistance in arabidopsis. *Proceedings of the National Academy of Sciences*, **100**, 11777–11782. 24

TAKEYA, T. & HANAFUSA, H. (1983). Structure and sequence of the cellular gene homologous to the rsv src gene and the mechanism for generating the transforming virus. *Cell*, **32**, 881–890. 32

TALDONE, T., OCHIANA, S.O., PATEL, P.D. & CHIOSIS, G. (2014). Selective targeting of the stress chaperome as a therapeutic strategy. *Trends in pharmacological sciences*, **35**, 592–603. 27, 34, 123

TENGE, V.R., ZUEHLKE, A.D., SHRESTHA, N. & JOHNSON, J.L. (2015). The hsp90 cochaperones cpr6, cpr7, and cns1 interact with the intact ribosome. *Eukaryotic cell*, **14**, 55–63. 17, 20, 21, 24

TESIC, M., MARSH, J.A., CULLINAN, S.B. & GABER, R.F. (2003). Functional interactions between hsp90 and the co-chaperones cns1 and cpr7 in saccharomyces cerevisiae. *Journal of Biological Chemistry*, **278**, 32692–32701. 17, 24, 74

TISSIÉRES, A., MITCHELL, H.K. & TRACY, U.M. (1974). Protein synthesis in salivary glands of drosophila melanogaster: relation to chromosome puffs. *Journal of molecular biology*, **84**, 389–398. 3

TRANGUCH, S., CHEUNG-FLYNN, J., DAIKOKU, T., PRAPAPANICH, V., COX, M.B., XIE, H., WANG, H., DAS, S.K., SMITH, D.F. & DEY, S.K. (2005). Cochaperone immunophilin fkbp52 is critical to uterine receptivity for embryo implantation. *Proceedings of the National Academy of Sciences of the United States of America*, **102**, 14326–14331. 30

TRIPATHI, V., DARNAUER, S., HARTWIG, N.R. & OBERMANN, W.M. (2014). Aha1 can act as an autonomous chaperone to prevent aggregation of stressed proteins. *Journal of Biological Chemistry*,

289, 36220–36228. 22

TRÖSCH, R., MÜHLHAUS, T., SCHRODA, M. & WILLMUND, F. (2015). Atp-dependent molecular chaperones in plastidsÃşmore complex than expected. *Biochimica et Biophysica Acta (BBA)-Bioenergetics*. 13

TURNBULL, E.L., MARTIN, I.V. & FANTES, P.A. (2005). Cdc37 maintains cellular viability in schizosaccharomyces pombe independently of interactions with heat-shock protein 90. *Febs Journal*, **272**, 4129–4140. 24

TYEDMERS, J., MOGK, A. & BUKAU, B. (2010). Cellular strategies for controlling protein aggregation. *Nature reviews Molecular cell biology*, **11**, 777–788. 8

VALPUESTA, J.M., MARTIÌĄN-BENITO, J., GÓMEZ-PUERTAS, P., CARRASCOSA, J.L. & WILLISON, K.R. (2002). Structure and function of a protein folding machine: the eukaryotic cytosolic chaperonin cct. *FEBS letters*, **529**, 11–16. 7

VAN MONTFORT, R.L., BASHA, E., FRIEDRICH, K.L., SLINGSBY, C. & VIERLING, E. (2001). Crystal structure and assembly of a eukaryotic small heat shock protein. *Nature Structural & Molecular Biology*, **8**, 1025–1030. 6

VAUGHAN, C.K., GOHLKE, U., SOBOTT, F., GOOD, V.M., ALI, M.M., PRODROMOU, C., ROBINSON, C.V., SAIBIL, H.R. & PEARL, L.H. (2006). Structure of an hsp90-cdc37-cdk4 complex. *Molecular cell*, **23**, 697–707. 23

VAUGHAN, C.K., MOLLAPOUR, M., SMITH, J.R., TRUMAN, A., HU, B., GOOD, V.M., PANARETOU, B., NECKERS, L., CLARKE, P.A., WORKMAN, P. *et al.* (2008). Hsp90-dependent activation of protein kinases is regulated by chaperone-targeted dephosphorylation of cdc37. *Molecular cell*, **31**, 886–895. 18, 32

VERGHESE, J. & MORANO, K.A. (2012). A lysine-rich region within fungal bag domain-containing proteins mediates a novel association with ribosomes. *Eukaryotic cell*, **11**, 1003–1011. 11

VERI, A. & COWEN, L.E. (2014). Progress and prospects for targeting hsp90 to treat fungal infections. *Parasitology*, **141**, 1127–1137. 27

WALERYCH, D., KUDLA, G., GUTKOWSKA, M., WAWRZYNOW, B., MULLER, L., KING, F.W., HELWAK, A., BOROS, J., ZYLICZ, A. & ZYLICZ, M. (2004). Hsp90 chaperones wild-type p53 tumor suppressor protein. *Journal of Biological Chemistry*, **279**, 48836–48845. 27

WALTER, S. & BUCHNER, J. (2002). Molecular chaperonesâĂŤcellular machines for protein folding. *Angewandte Chemie International Edition*, **41**, 1098–1113. 3

WANDINGER, S.K., SUHRE, M.H., WEGELE, H. & BUCHNER, J. (2006). The phosphatase ppt1 is a dedicated regulator of the molecular chaperone hsp90. *The EMBO journal*, **25**, 367–376. 17, 19, 128

WANDINGER, S.K., RICHTER, K. & BUCHNER, J. (2008). The hsp90 chaperone machinery. *Journal of Biological Chemistry*, **283**, 18473–18477. 12

WANG, C.C. & TSOU, C. (1993). Protein disulfide isomerase is both an enzyme and a chaperone. *The FASEB journal*, **7**, 1515–1517. 4

WANG, L., WANG, X. & WANG, C.C. (2015). Protein disulfide–isomerase, a folding catalyst and a redox-regulated chaperone. *Free Radical Biology and Medicine*, **83**, 305–313. 4, 24

WANG, X., VENABLE, J., LAPOINTE, P., HUTT, D.M., KOULOV, A.V., COPPINGER, J., GURKAN, C., KELLNER, W., MATTESON, J., PLUTNER, H. *et al.* (2006). Hsp90 cochaperone aha1 downregulation rescues misfolding of cftr in cystic fibrosis. *Cell*, **127**, 803–815. 22, 26, 128

WAYNE, N., MISHRA, P. & BOLON, D.N. (2011). Hsp90 and client protein maturation. In *Molecular Chaperones*, 33–44, Springer. 27

WEAVER, A.J., SULLIVAN, W.P., FELTS, S.J., OWEN, B.A. & TOFT, D.O. (2000). Crystal structure and activity of human p23, a heat shock protein 90 co-chaperone. *Journal of Biological Chemistry*, **275**, 23045–23052. 19

WEGELE, H., WANDINGER, S.K., SCHMID, A.B., REINSTEIN, J. & BUCHNER, J. (2006). Substrate transfer from the chaperone hsp70 to hsp90. *Journal of molecular biology*, **356**, 802–811. 10

WEIKL, T., ABELMANN, K. & BUCHNER, J. (1999). An unstructured c-terminal region of the hsp90 co-chaperone p23 is important for its chaperone function. *Journal of molecular biology*, **293**, 685–691. 19

WELCH, W.J. (1991). The role of heat-shock proteins as molecular chaperones. *Current opinion in cell biology*, **3**, 1033–1038. 5

WELCH, W.J. & FERAMISCO, J. (1982). Purification of the major mammalian heat shock proteins. *Journal of Biological Chemistry*, **257**, 14949–14959. 11

WERNER-WASHBURNE, M., STONE, D.E. & CRAIG, E.A. (1987). Complex interactions among members of an essential subfamily of hsp70 genes in saccharomyces cerevisiae. *Molecular and Cellular Biology*, **7**, 2568–2577. 9

WHITE, D.A., BUELL, A.K., KNOWLES, T.P.J., WELLAND, M.E. & DOBSON, C.M. (2010). Protein aggregation in crowded environments. *Journal of the American Chemical Society*, **132**, 5170–5175. 2

WHITESELL, L. & LIN, N.U. (2012). Hsp90 as a platform for the assembly of more effective cancer chemotherapy. *Biochimica et Biophysica Acta (BBA)-Molecular Cell Research*, **1823**, 756–766. 12

WHITESELL, L. & LINDQUIST, S. (2009). Inhibiting the transcription factor hsf1 as an anticancer strategy. *Expert Opinion on Therapeutic Targets*, **13**, 469–478. 12

WHITTIER, J.E., XIONG, Y., RECHSTEINER, M.C. & SQUIER, T.C. (2004). Hsp90 enhances degradation of oxidized calmodulin by the 20 s proteasome. *Journal of Biological Chemistry*, **279**, 46135–46142. 26

WINKLER, J., TYEDMERS, J., BUKAU, B. & MOGK, A. (2012). Hsp70 targets hsp100 chaperones to substrates for protein disaggregation and prion fragmentation. *The Journal of cell biology*, **198**, 387–404. 8

XU, W., MOLLAPOUR, M., PRODROMOU, C., WANG, S., SCROGGINS, B.T., PALCHICK, Z., BEEBE, K., SIDERIUS, M., LEE, M.J., COUVILLON, A. *et al.* (2012). Dynamic tyrosine phosphorylation modulates cycling of the hsp90-p50 cdc37-aha1 chaperone machine. *Molecular cell*, **47**, 434–443. 26

XU, Y. & LINDQUIST, S. (1993). Heat-shock protein hsp90 governs the activity of pp60v-src kinase. *Proceedings of the National Academy of Sciences*, **90**, 7074–7078. 27, 28, 31

XU, Y., SINGER, M.A. & LINDQUIST, S. (1999). Maturation of the tyrosine kinase c-src as a kinase and as a substrate depends on the molecular chaperone hsp90. *Proceedings of the National Academy of Sciences*, **96**, 109–114. 31

XU, Z., HORWICH, A.L. & SIGLER, P.B. (1997). The crystal structure of the asymmetric groel–groes–(adp) 7 chaperonin complex. *Nature*, **388**, 741–750. 7

YOUNG, J.C., HOOGENRAAD, N.J. & HARTL, F.U. (2003). Molecular chaperones hsp90 and hsp70 deliver preproteins to the mitochondrial import receptor tom70. *Cell*, **112**, 41–50. 26

ZHANG, J., BAKER, M.L., SCHRÖDER, G.F., DOUGLAS, N.R., REISSMANN, S., JAKANA, J., DOUGHERTY, M., FU, C.J., LEVITT, M., LUDTKE, S.J. *et al.* (2010a). Mechanism of folding chamber closure in a group ii chaperonin. *Nature*, **463**, 379–383. 7

ZHANG, M., BOTER, M., LI, K., KADOTA, Y., PANARETOU, B., PRODROMOU, C., SHIRASU, K. & PEARL, L.H. (2008). Structural and functional coupling of hsp90-and sgt1-centred multi-protein complexes. *The EMBO journal*, **27**, 2789–2798. 17, 24

ZHANG, M., KADOTA, Y., PRODROMOU, C., SHIRASU, K. & PEARL, L.H. (2010b). Structural basis for assembly of hsp90-sgt1-chord protein complexes: implications for chaperoning of nlr innate immunity receptors. *Molecular cell*, **39**, 269–281. 25

ZHAO, R., DAVEY, M., HSU, Y.C., KAPLANEK, P., TONG, A., PARSONS, A.B., KROGAN, N., CAGNEY, G., MAI, D., GREENBLATT, J. *et al.* (2005). Navigating the chaperone network: an integrative map of physical and genetic interactions mediated by the hsp90 chaperone. *Cell*, **120**, 715–727. 22

ZHAO, R., KAKIHARA, Y., GRIBUN, A., HUEN, J., YANG, G., KHANNA, M., COSTANZO, M., BROST, R.L., BOONE, C., HUGHES, T.R. *et al.* (2008). Molecular chaperone hsp90 stabilizes pih1/nop17 to maintain r2tp complex activity that regulates snorna accumulation. *The Journal of cell biology*, **180**, 563–578. 22, 27

ZHOU, Z., SAR, M., SIMENTAL, J.A., LANE, M.V. & WILSON, E.M. (1994). A ligand-dependent bipartite nuclear targeting signal in the human androgen receptor. requirement for the dna-binding domain and modulation by nh2-terminal and carboxyl-terminal sequences. *Journal of Biological Chemistry*, **269**, 13115–13123. 29

ZHU, X., ZHAO, X., BURKHOLDER, W.F., GRAGEROV, A., OGATA, C.M., GOTTESMAN, M.E. & HENDRICKSON, W.A. (1996). Structural analysis of substrate binding by the molecular chaperone dnak. *Science*, **272**, 1606–1614. 8

ZIEMIECKI, A., CATELLI, M.G., JOAB, I. & MONCHARMONT, B. (1986). Association of the heat shock protein hsp90 with steroid hormone receptors and tyrosine kinase oncogene products. *Biochemical and biophysical research communications*, **138**, 1298–1307. 27

ZIMMERMAN, S.B. & MINTON, A.P. (1993). Macromolecular crowding: biochemical, biophysical, and physiological consequences. *Annual review of biophysics and biomolecular structure*, **22**, 27–65. 2

ZIMMERMAN, S.B. & TRACH, S.O. (1991). Estimation of macromolecule concentrations and excluded volume effects for the cytoplasm of escherichia coli. *Journal of molecular biology*, **222**, 599–620. 1

ZOU, J., GUO, Y., GUETTOUCHE, T., SMITH, D.F. & VOELLMY, R. (1998). Repression of heat shock transcription factor hsf1 activation by hsp90 (hsp90 complex) that forms a stress-sensitive complex with hsf1. *Cell*, **94**, 471–480. 27

ZUEHLKE, A.D. & JOHNSON, J.L. (2012). Chaperoning the chaperone: a role for the co-chaperone cpr7 in modulating hsp90 function in saccharomyces cerevisiae. *Genetics*, **191**, 805–814. 21

ZUEHLKE, A.D., WREN, N., TENGE, V. & JOHNSON, J.L. (2013). Interaction of heat shock protein 90 and the co-chaperone cpr6 with ura2, a bifunctional enzyme required for pyrimidine biosynthesis. *Journal of Biological Chemistry*, **288**, 27406–27414. 20, 21

ZUEHLKE, A.D., BEEBE, K., NECKERS, L. & PRINCE, T. (2015). Regulation and function of the human hsp90aa1 gene. *Gene*, **570**, 8–16. 12

Declaration

I, Priyanka Sahasrabudhe, hereby declare that this thesis was prepared by me independently and using only the references and resources stated here. The work has so far not been submitted to any audit commission.

Hiermit erkläre ich, Priyanka Sahasrabudhe, dass ich die vorliegende Arbeit selbständig verfasst und keine anderen als die angegebenen Quellen und Hilfsmittel verwendet habe. Die Arbeit wurde bisher keiner Prüfungskommission vorgelegt.

Munich, December 2015